Exploring the Anticancer Potential of Niloticin and Prieurianin: Promising Phytochemicals from *Aphanamixis polystachya* (Wall.) R.Parker

By

ANUJA JOSEPH G.
10BB19J39005

A thesis submitted to the
Academy of Scientific & Innovative Research
for the award of the degree of

DOCTOR OF PHILOSOPHY
in
SCIENCE

Under the supervision of
Dr. K. V. Radhakrishnan

&

Dr. Kaustabh Kumar Maiti
(Co-supervisor)

CSIR – National Institute for Interdisciplinary Science and Technology (CSIR-NIIST), Thiruvananthapuram-695019

Academy of Scientific and Innovative Research
AcSIR Headquarters, CSIR-HRDC campus
Sector 19, Kamla Nehru Nagar,
Ghaziabad, U.P. – 201 002, India

January 2025

राष्ट्रीय अंतर्विषयी विज्ञान तथा प्रौद्योगिकी संस्थान
वैज्ञानिक तथा औद्योगिक अनुसंधान परिषद् | विज्ञान तथा प्रौद्योगिकी मंत्रालय, भारत सरकार
इंडस्ट्रियल इस्टेट पी.ओ., पाप्पनंकोड, तिरुवनंतपुरम, भारत-695 019

CSIR-NATIONAL INSTITUTE FOR INTERDISCIPLINARY SCIENCE AND TECHNOLOGY (CSIR-NIIST)
Council of Scientific & Industrial Research | Ministry of Science and Technology, Govt. of India
Industrial Estate P.O., Pappanamcode, Thiruvananthapuram, India-695 019

3rd January 2025

CERTIFICATE

This is to certify that the work incorporated in this Ph.D. thesis entitled, ***"Exploring the Anticancer Potential of Niloticin and Prieurianin: Promising Phytochemicals from Aphanamixis polystachya (Wall.) R.Parker"***, submitted by ***Ms. Anuja Joseph G.*** to the Academy of Scientific and Innovative Research (AcSIR) in fulfillment of the requirements for the award of the Degree of ***Doctor of Philosophy in Science***, embodies original research work carried out by the student. We further certify that this work has not been submitted to any other University or Institution in part or full for the award of any degree or diploma. Research materials obtained from other sources and used in this research work have been duly acknowledged in the thesis. Images, illustrations, figures, tables, etc., used in the thesis from other sources, have also been duly cited and acknowledged.

Anuja 03/01/25
Anuja Joseph G.

3/1/25
Dr. K. V. Radhakrishnan
(Supervisor)

Kaustabh Kumar Maiti 03/01/2025
Dr. Kaustabh Kumar Maiti
(Co-Supervisor)

Tel : 91 471 2515226 | 2515234 | E-mail : director@niist.res.in | Website : http://niist.res.in

STATEMENTS OF ACADEMIC INTEGRITY

I Anuja Joseph G., a Ph.D. student of the Academy of Scientific and Innovative Research (AcSIR) with Registration No. 10BB19J39005 hereby undertake that, the thesis entitled ***"Exploring the Anticancer Potential of Niloticin and Prieurianin: Promising Phytochemicals from Aphanamixis polystachya (Wall.) R.Parker"*** has been prepared by me and that the document reports original work carried out by me and is free of any plagiarism in compliance with the UGC Regulations on *"Promotion of Academic Integrity and Prevention of Plagiarism in Higher Educational Institutions (2018)"* andthe CSIR Guidelines for "*Ethics in Research and in Governance (2020)*".

03/01/25

January 3 2025

Anuja Joseph G.

Thiruvananthapuram

It is hereby certified that the work done by the student, under my supervision, is plagiarism-free in accordance with the UGC Regulations on *"Promotion of Academic Integrity and Prevention of Plagiarism in Higher Educational Institutions (2018)"* and the CSIR Guidelines for "*Ethics in Research and in Governance (2020)*".

Dr. K. V. Radhakrishnan

(Supervisor)

January 3 2025

Thiruvananthapuram

Kaustabh Maiti 03/01/2025

Dr. Kaustabh Kumar Maiti

(Co-supervisor)

January 3 2025

Thiruvananthapuram

ACKNOWLEDGEMENTS

I have immense pleasure in expressing my deep gratitude to Dr. K. V. Radhakrishnan and Dr. Kaustabh Kumar Maiti, my thesis supervisor and co-supervisor for all the support and encouragement provided during these years.

I wish to thank Dr. C. Anandharamakrishnan and Dr. A. Ajayaghosh, present and former Director of the CSIR-National Institute for Interdisciplinary Science and Technology, Thiruvananthapuram, for providing me with the necessary facilities for carrying out the work.

I would like extend my sincere thanks to:

- ✓ *Dr. P. Jayamurthy, Dr. V. Karunakaran, Dr. C. H. Suresh, and Dr. R. Luxmi Varma; present and former AcSIR co-ordinators.*
- ✓ *Dr. P. Jayamurthy, Dr. Rajeev K. Sukumaran and Dr. L. Ravishankar; Doctoral Advisory Committee members for their valuable suggestions and discussions during DAC meetings*
- ✓ *Dr.K V Radhakrishnan, Dr. P. Sujatha Devi, and Dr. R. Luxmi Varma, present and former Head of the Division, Chemical Sciences and Technology Division (CSTD).*
- ✓ *Dr. A. Kumaran, Dr. L. Ravishankar, Dr. B.S. Sasidhar, Dr. Sunil Varughese and Dr. Jubi John; Scientists in organic chemistry are greatly acknowledged*
- ✓ *Mrs. Saumini Matthew for NMR, Mrs. Viji S., for mass spectral analyses*
- ✓ *Dr. Vishnupriya Murali, Dr. Biji M for the support during whole research years*
- ✓ *Dr. Vishnu K. Omanakuttan, Priya, Sangeeth, Vidyalekshmi M S, Vimal, Dr. Shamjith for all the help.*
- ✓ *A special thanks to Ms. Alisha for being there for me every time since the beginning of Niist life*
- ✓ *Dr. Manu M. Joseph, Dr. Greeshma Gopalan, Dr. Prabha B., Dr. Sasikumar, Dr. Sharathna, Dr. Meenu M. T, Dr.Neethu, Dr. Santhi, Dr. Arya J.S, Dr. Varsha K. Karunankaran, Mr. Madhukrishnan, Dr. Hridhya, Dr. Aswathy, Dr. Rajimol, Shamna, Deepika, Chandana, Reshma, Kavya, Dr. Abeesh, Hari, Campbell, Arun, Shelton, Arathy, Athira, Ashiki, Aadithya, Dr. Deepa all other KVR and KKM group members for their love.*

- ✓ *Anusha, Aravind, Abhi, Jasim for all those good times in Niist*
- ✓ *SA 2020 members and Team CSTD (Throwball, cricket, badminton) for making my 5 years at NIIST wonderful.*
- ✓ *Most grateful to Mummy, Daddy, Chetan, Jojy, Appachan, Amma*
- ✓ *CSIR for the financial assistance*

Above all, I express my gratitude to the Almighty for the abundant blessings bestowed upon me.

ANUJA JOSEPH G.

TABLE OF CONTENTS

List of abbreviations

AGE	Agarose gel electrophoresis
Apaf	Apoptotic protease activating factor-1
ATCC	American type culture collection
Bax	BCL-2 associated X-protein
BCA assay	Bicinchoninic acid assay
Bcl-2	B-cell lymphoma-2
Bid	BH3 interacting domain death agonist
CD40	Cluster of differentiation 40
Cdc25c	Cell division cycle 25c
CDKs	Cyclin dependent kinases
Cyt c	Cytochrome c
DCM	DIchloromethane
DMEM	Dulbecco's modified eagle medium
DMSO	Dimethyl sulfoxide
ECM	Extracellular matrix

EMT	Epithelial mesenchymal transition
FBS	Fetal bovine serum
FITC	Fluorescein isothiocyanate
HBSS	Hanks' balanced salt solution
HIF-1α	Hypoxia inducible factor-1 alpha
HPLC	High performance liquid chromatography
HPV	Human papillomavirus
HRMS	High resolution mass spectroscopy
HSP 60	Heat shock protein 60
IAPs	Inhibitor of apoptosis proteins
IC_{50}	Half maximal inhibitory concentration
ICMR	Indian Council of Medical Research
IGF-2	Insulin like growth factor-2
JC-1	5,5,6,6′-Tetrachloro-1,1′,3,3′-tetraethylbenzimidazoylcarbocyanine iodide
JNK	c-Jun-N-terminal kinases
MAPK	Mitogen activated protein kinase

MDR	Multi Drug Resistance
MDS	Molecular dynamic simulation
MMP	Matrix metalloproteinase
MTT	3-[4,5-dimethylthiazol-2-yl]-2,5-diphenyltetrazolium
NF-κB	Nuclear factor kappa-light-chain-enhancer of activated B cells
NMR	Nuclear magnetic resonance
PAGE	Poly acrylamide gel electrophoresis
PARP	Poly ADP ribose polymerase
PBS	Phosphate buffer saline
PDI	Polydispersity index
PI	Propidium iodide
PS	Phosphatidyl serine
RBCs	Red blood cells
RhoB	Rhodamine B
RIPA buffer	Radio-immuno precipitation assay buffer
RMSD	Root mean square deviation
RMSF	Root mean square fluctuation

ROS	Reactive oxygen species
SD	Standard deviation
SERS	Surface enhanced raman spectroscopy
SMAC	Second mitochondria-derived activator of caspase
STAT	Signal transducer and activator of transcription
TGF-β	Transforming growth factor- beta
TLC	Thin layer chromatography
TME	Tumor microenvironment
TNBC	Triple negative breast cancer
TNF-α	Tumor necrosis factor- alpha
TP53	Tumor protein P53
TRAILR	TNF-related apoptosis-inducing ligand receptor
VEGF	Vascular endothelial growth factor
WBCs	White blood cell
XIAP	X-linked inhibitor of apoptosis protein

PREFACE

Cancer is a complex group of diseases characterized by uncontrolled cell growth and the ability to invade surrounding tissues and metastasize to distant organs. It remains a leading cause of mortality worldwide, necessitating innovative therapeutic approaches. Unlike conventional therapies, which often cause significant side effects, natural products tend to exhibit lower toxicity and greater selectivity toward cancer cells. Their potential for discovery of novel mechanisms of action makes them a valuable resource for developing safer and more effective anticancer drugs.

The introductory **chapter 1** provides a comprehensive introduction to natural products and their pivotal role in drug development, emphasizing their importance as a source of bioactive compounds. The chapter explores the pharmacological potential of Aphanamixis polystachya, a plant renowned for its diverse secondary metabolites with therapeutic applications. A detailed overview of cervical cancer is presented, highlighting its global prevalence and the limitations of existing treatments. The role of natural products in addressing these challenges is thoroughly discussed, showcasing their potential to offer safer and more effective alternatives. This foundation sets the stage for the subsequent exploration of phytomolecules with anticancer properties.

Chapter 2 explores the extraction, isolation, and characterization of bioactive phytomolecules from Aphanamixis polystachya, focusing on compounds with anticancer potential. Niloticin, one such compound, is evaluated for its apoptotic effects on HeLa cervical cancer cells. It exhibits selective toxicity, sparing non-cancerous cells. In-depth molecular studies reveal niloticin's interactions with apoptotic proteins, triggering both intrinsic and extrinsic apoptosis pathways. Additionally, its anti-metastatic properties are highlighted, showing inhibition of cancer cell proliferation and invasion. Through in silico docking, molecular dynamics simulations, and in vitro assays, niloticin demonstrates significant promise as a targeted anticancer therapy.

Chapter 3 shifts the focus to prieurianin, the second potent compound selected for in-depth evaluation, with an emphasis on its apoptotic efficacy in the SiHa cervical cancer cell line. With an IC50 value of 3.9 µM, prieurianin demonstrates strong anticancer activity, triggering programmed cell death. The chapter outlines various assays, including live/dead,

APOPercentage, and Annexin V assays, to assess the compound's apoptotic effects. Additionally, prieurianin's ability to activate the caspase cascade and induce cell cycle arrest is explored, highlighting its potential in halting cancer cell proliferation. Molecular analysis of apoptosis markers shows prieurianin's ability to engage both intrinsic and extrinsic apoptotic pathways. The chapter concludes with an exploration of prieurianin's anti-metastatic potential, demonstrated through scratch wound and colony formation assays, and its ability to downregulate the Ki-67 proliferation marker.

Chapter 4 focuses on the comparative evaluation of prieurianin and niloticin's anti-metastatic and anti-angiogenic properties in 4T1 triple-negative breast cancer cells and EaHy 926 endothelial cells. The chapter explores the apoptotic potential of both compounds in aggressive breast cancer cells using various assays, confirming their ability to induce apoptosis. It further investigates their anti-metastatic effects through colony formation, scratch wound, and invasion assays, demonstrating significant inhibition of cancer cell migration and invasion. Protein expression analysis reveals the downregulation of key metastatic markers, highlighting their potential to target metastatic pathways. By employing a range of assays and techniques, including molecular docking, this chapter underscores the therapeutic promise of prieurianin and niloticin as multi-target anticancer agents, with potential clinical applications in cancer treatment.

Chapter 1

An Overview of Plant-derived Compounds in Anti-cancer Potential: current perspectives of *Aphanamixis polystachya*

Abstract

Natural products have long been a source of medicinal compounds, playing a critical role in drug discovery and development. Their bioactive compounds offer valuable pharmacological properties for treating a range of diseases, including cancer. One such natural product is Apamanamixis polystachya, a plant known for its medicinal properties. Research into its pharmacology has shown promising effects against various diseases, including cervical cancer. This conclusion discusses the importance of natural products in drug development, the role of Apamanamixis polystachya in pharmacology, and its potential application in the treatment of cervical cancer, highlighting the broader significance of natural products in cancer therapies.

1.1 Introduction to Natural Products in Drug Discovery

Natural products have long served as a cornerstone in drug discovery, offering unparalleled chemical diversity and biological relevance. These compounds, derived from plants, microorganisms, and marine organisms, have provided the foundation for many life-saving drugs across a variety of therapeutic areas. Their complex and diverse structures, often rich in stereochemical and functional diversity, make natural products uniquely suited for interaction with biological targets. Despite shifts in the focus of pharmaceutical research and development, the role of natural products in addressing global health challenges, including cancer, infectious diseases, and metabolic disorders, remains irreplaceable (1). This introduction delves into the historical significance, ongoing challenges, technological advancements, and future potential of natural product-based drug discovery, reflecting the wealth of information already discovered.

1.1.1 Historical Significance of Natural Products

For centuries, natural products have played a significant role in the treatment of diseases. The discovery of penicillin in the early 20th century revolutionized modern medicine, marking the beginning of the antibiotic era and saving countless lives. Similarly, the identification of taxol from the Pacific yew tree (*Taxus brevifolia*) introduced a powerful chemotherapeutic agent that transformed cancer treatment (2). Another notable example is artemisinin, a compound derived from *Artemisia annua*, which remains a cornerstone in the fight against malaria. These breakthroughs underscore the transformative potential of natural products. Traditional medicine systems, such as Ayurveda and Traditional Chinese Medicine (TCM), have long relied on natural products for therapeutic purposes. Plants like *Catharanthus roseus*, the source of the anticancer agents vinblastine and vincristine, have been used for centuries in traditional remedies before their active compounds were isolated and validated through modern science. The sustained importance of natural products is reflected in their prevalence among FDA-approved drugs; over 50% of approved drugs can be traced back to natural sources or inspired by their molecular frameworks. This enduring legacy highlights nature's unmatched capacity to inspire therapeutic innovation. Natural products also hold historical importance in combating infectious diseases. For example, streptomycin, the first antibiotic effective against tuberculosis, was derived from the bacterium *Streptomyces griseus*. Similarly, tetracycline, erythromycin, and rifamycin were all derived from natural microbial sources (3). These discoveries not only saved lives but also revolutionized the field of microbiology by demonstrating the therapeutic potential of microorganisms.

1.1.2 Decline and Revival in Natural Product Research

The mid-20th century saw a surge in natural product-based drug discovery, driven by the success of antibiotics and other bioactive compounds. However, the subsequent rise of combinatorial chemistry and high-throughput screening led to a decline in natural product research. Pharmaceutical companies shifted focus toward synthetic libraries, attracted by the perceived simplicity of generating and optimizing synthetic molecules. Challenges in accessing, isolating, and characterizing natural compounds further contributed to this decline, alongside concerns about intellectual property rights and sustainable sourcing. Despite these challenges, the limitations of synthetic libraries became increasingly apparent. Synthetic

compounds often lack the structural complexity and bioactivity inherent to natural products, leading to a renewed interest in nature's chemical diversity (4).

The renewed interest in natural products is further fueled by the global health crisis posed by antibiotic resistance. The alarming rise of multidrug-resistant bacteria has highlighted the urgent need for new antimicrobial agents. Natural products, with their rich chemical diversity and unique mechanisms of action, offer a promising solution to this challenge. For instance, daptomycin, a lipopeptide antibiotic derived from *Streptomyces roseosporus*, has proven effective against multidrug-resistant Gram-positive bacteria, exemplifying the therapeutic potential of natural compounds.

1.1.3 The Role of Technology in Advancing Natural Product Research

Modern technologies have revolutionized the discovery and development of natural products, addressing many of the historical barriers to their utilization. High-throughput screening (HTS) methods now enable the rapid evaluation of complex natural product libraries, significantly accelerating the identification of bioactive compounds. Automated and miniaturized systems further enhance the efficiency of these processes, making them compatible with the demands of modern drug discovery pipelines. Advances in genomics and metagenomics have opened new frontiers in natural product research. By sequencing the genomes of microorganisms and other natural sources, researchers can identify biosynthetic gene clusters responsible for producing bioactive compounds. This approach has been particularly fruitful in uncovering novel metabolites from previously unculturable microbes. Metagenomic techniques allow scientists to explore the genetic material of entire microbial communities, revealing an untapped reservoir of chemical diversity.

In addition to genomics, transcriptomics, and proteomics play critical roles in identifying and characterizing natural products. These technologies enable researchers to study the expression of genes and proteins involved in natural product biosynthesis, providing insights into their regulation and optimization. Analytical technologies have also played a crucial role in advancing natural product research. Techniques such as nuclear magnetic resonance (NMR) spectroscopy, mass spectrometry, and X-ray crystallography enable the rapid and precise

characterization of complex natural compounds, even in minute quantities. These tools have streamlined the process of structural elucidation, allowing researchers to decode the intricate architectures of natural products with unprecedented accuracy. Moreover, advancements in imaging technologies, such as cryo-electron microscopy, are providing new ways to visualize the interactions between natural products and their biological targets (5).

1.1.4 Therapeutic Potential of Natural Products

Natural products have made indelible contributions to a wide range of therapeutic areas, cementing their status as indispensable resources in drug discovery. In oncology, compounds such as taxanes (e.g., paclitaxel), camptothecins, and anthracyclines have become cornerstones of cancer treatment, demonstrating potent efficacy against a variety of malignancies. These agents exemplify the unique ability of natural products to target complex biological pathways.

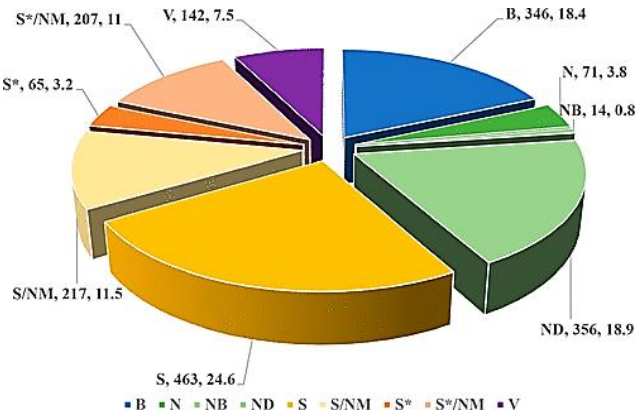

Table 1. Codes Used in Analyses

code	brief definition/year
B	biological macromolecule, 1997
N	unaltered natural product, 1997
NB	botanical drug (defined mixture), 2012
ND	natural product derivative, 1997
S	synthetic drug, 1997
S*	synthetic drug (NP pharmacophore), 1997
V	vaccine, 2003
/NM	mimic of natural product, 2003

Figure 1.1. Drugs Approved in Between 1981-2019 by FDA, *J. Nat. Prod.* 2020, 83, 770−803

The field of infectious diseases have also benefited immensely from natural products. Antibiotics such as penicillins, cephalosporins, and macrolides have transformed the treatment of bacterial infections, saving millions of lives worldwide. In recent years, the emergence of antibiotic resistance has reignited interest in exploring new natural sources, particularly marine and microbial environments, for novel antimicrobial agents.

Marine natural products have emerged as a particularly rich source of bioactive compounds. For example, trabectedin, derived from the sea squirt *Ecteinascidia turbinata*, has shown

remarkable efficacy as an anticancer agent. Similarly, ziconotide, a peptide isolated from the venom of cone snails, has been approved for the treatment of severe chronic pain, highlighting the therapeutic potential of marine-derived natural products. Cardiovascular medicine has been revolutionized by the discovery of statins, which are derived from fungal metabolites. These lipid-lowering agents have significantly reduced cardiovascular morbidity and mortality, underscoring the clinical impact of natural products. Similarly, immunosuppressants such as cyclosporine, tacrolimus, and rapamycin, all derived from natural sources, have enabled groundbreaking advances in organ transplantation and autoimmune disease management. Natural products are also being explored for their potential in emerging therapeutic areas, such as neurodegenerative diseases and metabolic disorders. For instance, resveratrol, a polyphenol found in grapes, has shown promise in preclinical studies for its neuroprotective and anti-inflammatory effects. Similarly, berberine, an alkaloid derived from various plants, is being investigated for its potential to treat type 2 diabetes and hyperlipidemia (1).

1.1.5 Challenges and Emerging Opportunities of Natural Product Research

While the potential of natural products is immense, their development is not without challenges. One major issue is the sustainable sourcing of bioactive compounds. Overharvesting of medicinal plants and marine organisms poses a significant threat to biodiversity, necessitating the implementation of sustainable cultivation and collection practices. Synthetic biology and combinatorial biosynthesis offer promising solutions to these challenges, enabling the production of natural products in laboratory settings while reducing environmental impact.

Intellectual property rights and benefit-sharing agreements present additional hurdles. The equitable sharing of benefits derived from natural resources, particularly those sourced from indigenous communities, is essential to ensure ethical research practices. Frameworks such as the Nagoya Protocol provide guidelines for addressing these issues, but their implementation remains inconsistent across different regions.

Regulatory challenges also complicate the development of natural products. The complexity of their structures often necessitates rigorous characterization and standardization, which can

delay the approval process. However, advances in analytical techniques and quality control methods are helping to streamline these efforts, paving the way for more efficient regulatory pathways (6).

The future of natural product research lies in the integration of traditional knowledge with cutting-edge scientific approaches. Omics technologies, including genomics, proteomics, and metabolomics, are providing new insights into the mechanisms of action and synergistic effects of natural compounds. Systems biology approaches, which emphasize the holistic understanding of biological networks, are further enhancing our ability to elucidate the multifaceted effects of natural products.

Collaborative efforts between academia, industry, and government agencies are essential to overcoming resource and knowledge gaps. By fostering interdisciplinary partnerships, researchers can leverage the strengths of different fields to accelerate the discovery and development of natural products. Emerging fields such as organ-on-chip models, quantum computing, and precision medicine are expected to play a pivotal role in advancing natural product-based therapeutics (7).

Marine ecosystems represent a particularly promising frontier for natural product discovery. With their unique biodiversity and chemical environments, marine organisms have already yielded groundbreaking compounds. For example, salinosporamide A, derived from marine actinomycetes, has demonstrated significant anticancer properties. Similarly, eribulin mesylate, a synthetic analog of the natural product halichondrin B, derived from marine sponges, has shown efficacy in treating metastatic breast cancer. These examples underscore the untapped potential of marine ecosystems as reservoirs of novel bioactive compounds (1). Recent advances in synthetic biology have further enhanced the ability to harness natural products from marine sources. By engineering biosynthetic pathways in microbial hosts, researchers can replicate the complex structures of marine-derived compounds in a sustainable and scalable manner. This approach not only addresses challenges related to sourcing but also facilitates the generation of novel analogs with improved pharmacological properties.

Plant-derived natural products continue to play a vital role in drug discovery. The field of oncology has particularly benefited from plant-based compounds. Vinblastine and vincristine, alkaloids derived from the Madagascar periwinkle, remain essential chemotherapeutic agents. Podophyllotoxin, extracted from the rhizomes of Podophyllum species, serves as the precursor for etoposide and teniposide, two drugs widely used in cancer treatment. Similarly, camptothecin, a natural product isolated from the Chinese tree *Camptotheca acuminata*, has inspired the development of topotecan and irinotecan, which are crucial in treating various malignancies.s

The exploration of ethnomedicinal plants has provided valuable insights into the therapeutic potential of natural products. Indigenous knowledge systems have guided the identification of bioactive compounds, leading to the development of modern drugs. For example, aspirin was developed from salicin, a compound found in willow bark that was historically used in traditional medicine to treat pain and fever. Similarly, quinine, derived from the bark of the cinchona tree, was a cornerstone in malaria treatment for centuries. These examples highlight the importance of preserving and integrating traditional knowledge into contemporary drug discovery efforts (8).

1.1.6 Expanding Therapeutic Horizons and Future Directions and Innovations

Beyond their established roles in treating infectious diseases and cancer, natural products are being increasingly investigated for their potential to address emerging health challenges. The rise of neurodegenerative disorders, such as Alzheimer's and Parkinson's diseases, has spurred interest in natural compounds with neuroprotective properties. For instance, galantamine, an alkaloid derived from the bulbs of *Galanthus species* (snowdrops), is used to manage cognitive symptoms in Alzheimer's disease. Similarly, curcumin, a polyphenol found in turmeric, is being studied for its anti-inflammatory and antioxidant effects in neurodegenerative conditions.

Metabolic disorders, including diabetes and obesity, represent another area where natural products show promise. Berberine, an alkaloid extracted from various plants, has demonstrated hypoglycemic effects in clinical studies, making it a potential candidate for managing type 2

diabetes. Similarly, compounds such as mangiferin, found in mango leaves, and resveratrol, present in grapes, are being explored for their roles in modulating metabolic pathways and reducing the risk of cardiovascular diseases.

The immunomodulatory properties of natural products have also garnered significant attention. With the advent of immunotherapy, natural compounds that enhance or regulate immune responses are being actively investigated. For example, polysaccharides derived from medicinal mushrooms, such as *Ganoderma lucidum* (reishi) and *Lentinula edodes* (shiitake), have shown potential as adjuvants in cancer immunotherapy. These compounds stimulate the activity of natural killer cells and enhance the body's immune surveillance mechanisms (9).

The future of natural product research is poised to be shaped by interdisciplinary collaborations and technological advancements. The integration of omics technologies—genomics, proteomics, metabolomics, and transcriptomics—is enabling a deeper understanding of the biosynthetic pathways and mechanisms of action of natural products. These insights are facilitating the rational design and optimization of natural product-based therapeutics.

Advances in artificial intelligence (AI) and machine learning are revolutionizing the discovery process by predicting the bioactivity of natural compounds and identifying potential drug targets. These tools are accelerating the screening of vast natural product libraries and uncovering novel structure-activity relationships. Furthermore, quantum computing holds promise in simulating complex molecular interactions, paving the way for precision drug design.

The emergence of precision medicine is aligning with the potential of natural products to offer personalized therapeutic solutions. By integrating genetic, epigenetic, and environmental data, researchers can identify patient-specific natural product interventions. For example, studies on the gut microbiome have revealed that microbial metabolites, many of which are natural products, play a crucial role in modulating host health. Leveraging these insights, microbiome-based therapies are being developed to address conditions ranging from inflammatory bowel disease to mental health disorders (10).

1.2 Applications of Natural products in Cancer Research

Natural products have long been a cornerstone in cancer research, offering a diverse array of bioactive compounds that have led to significant therapeutic advancements. Their multifaceted mechanisms of action make them invaluable in addressing complex challenges in oncology, including epigenetic modulation, targeting cancer stem cells (CSCs), overcoming drug resistance, immunomodulation, and the discovery of novel anticancer agents.

- **Epigenetic Modulation**

Epigenetic alterations, such as DNA methylation and histone modification, play a pivotal role in cancer development and progression. Natural compounds have demonstrated the ability to modulate these epigenetic mechanisms, thereby influencing gene expression and tumor behavior. For instance, certain natural products can interfere with the cellular epigenetic machinery, affecting gene expression and DNA repair mechanisms. Additionally, some natural compounds have been shown to modulate antitumor immunity through epigenetic changes, enhancing the body's immune response against cancer cells (11).

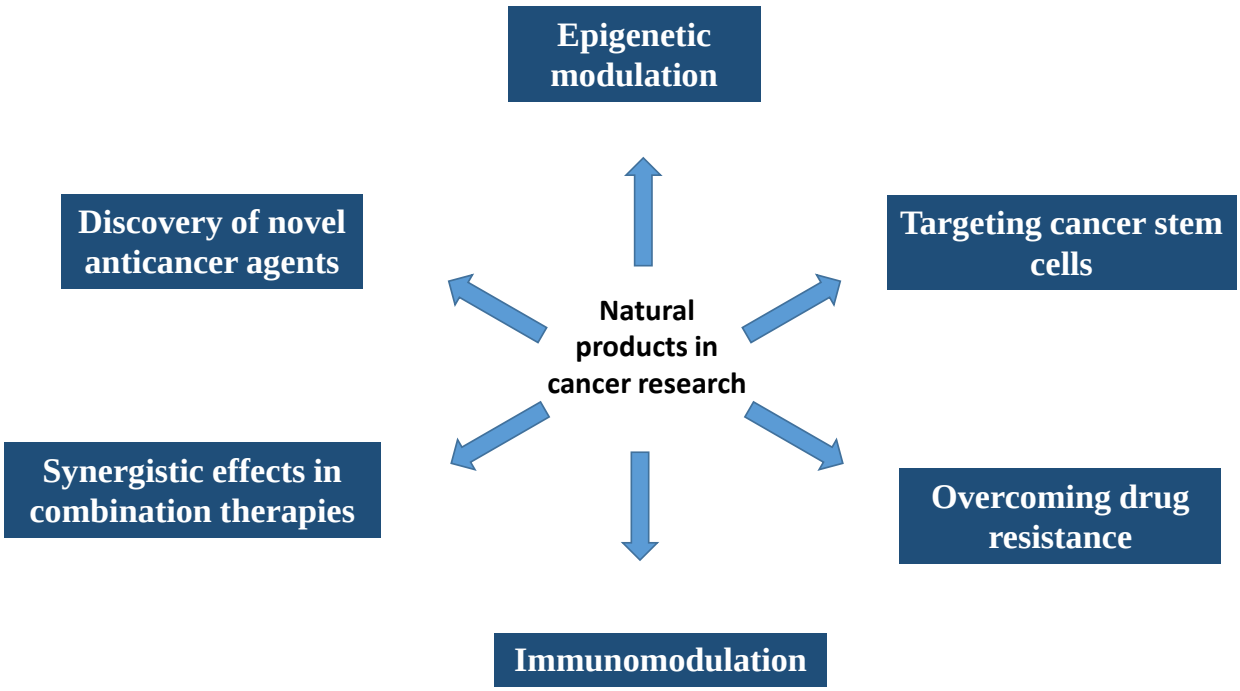

Figure 1.2. Applications of natural products in cancer research

- **Targeting Cancer Stem Cells**

CSCs are a subpopulation of tumor cells with self-renewal capabilities, contributing to tumor recurrence and resistance to conventional therapies. Natural products have shown promise in targeting CSCs by inducing differentiation, sensitizing them to chemotherapy, or directly triggering apoptosis. For example, certain natural compounds have been found to induce cell death in CSCs, cause CSCs to differentiate, or sensitize CSCs to conventional chemotherapy treatments. This approach holds the potential to prevent metastasis and improve long-term treatment outcomes (12).

- **Overcoming Drug Resistance**

Drug resistance remains a significant hurdle in effective cancer treatment. Natural products offer alternative mechanisms to circumvent resistance, either by modulating drug efflux pumps, altering apoptotic pathways, or enhancing the efficacy of existing chemotherapeutic agents. For instance, epigenetic drugs (epidrugs) are a group of promising target therapies for cancer treatment acting as coadjuvants to reverse drug resistance in various cancers. Additionally, natural compounds have been shown to enhance chemotherapy by generating intracellular signals that lead to cancer cell death (13).

- **Immunomodulation**

The tumor microenvironment plays a crucial role in cancer progression, with immune cells being key components. Natural products can modulate the immune system, enhancing antitumor immunity or alleviating immunosuppression within the tumor microenvironment. Research has highlighted the potential of natural products in regulating immune responses against cancer, offering avenues for novel immunotherapeutic strategies (14).

- **Discovery of Novel Anticancer Agents**

The structural diversity of natural products provides a vast reservoir for the discovery of new anticancer agents. Compounds such as honokiol have exhibited pro-apoptotic effects across various cancer cell lines, including melanoma, sarcoma, myeloma, leukemia, bladder, lung, prostate, and colon cancers. Honokiol inhibits pathways like Akt and MAPK, regulates NF-κB activation, and induces caspase-dependent apoptosis, showcasing its potential as a multifaceted anticancer agent.

One of the most compelling attributes of natural products is their ability to modulate multiple oncogenic pathways simultaneously. Unlike synthetic drugs that typically target a single molecular mechanism, natural products can interact with diverse biological targets, thereby exerting a broad spectrum of anticancer effects. This multi-targeted approach is particularly advantageous in combating drug-resistant cancers, which often exploit redundant signaling pathways to evade therapeutic intervention. For example, curcumin, a polyphenol derived from turmeric (*Curcuma longa*), has demonstrated the ability to inhibit the PI3K/AKT/mTOR, NF-κB, and Wnt/β-catenin pathways, all of which are implicated in cancer progression and metastasis. Additionally, curcumin modulates the expression of pro-apoptotic and anti-apoptotic proteins, thereby promoting cell death in cancer cells while sparing normal tissues. Such pleiotropic effects make natural products uniquely suited for addressing the complexity of cancer biology.

The immunomodulatory properties of natural products further enhance their appeal as anticancer agents. Cancer immunotherapy, which aims to harness the immune system to combat tumors, has emerged as a groundbreaking approach in oncology. However, its efficacy is often limited by the immunosuppressive tumor microenvironment (TME), which inhibits immune cell activation and facilitates tumor escape. Natural products have shown promise in overcoming this barrier by modulating the TME and enhancing immune responses. For instance, polysaccharides extracted from medicinal mushrooms such as *Ganoderma lucidum* have been found to stimulate dendritic cell maturation and promote T-cell activation, thereby enhancing antitumor immunity. Similarly, saponins from *Panax ginseng* have demonstrated the ability to inhibit the proliferation of myeloid-derived suppressor cells (MDSCs) and regulatory T cells (Tregs), both of which contribute to immunosuppression in the TME. These findings underscore the potential of natural products to serve as adjuncts to existing immunotherapeutic strategies, such as immune checkpoint inhibitors and cancer vaccines (1).

The advent of nanotechnology has further expanded the therapeutic potential of natural products. Nanoparticle-based delivery systems have been developed to address the limitations associated with the poor solubility, stability, and bioavailability of many natural compounds. These systems enable targeted delivery of natural products to tumor sites, thereby minimizing systemic toxicity and enhancing therapeutic efficacy. For example, liposomal formulations of

curcumin and paclitaxel have demonstrated improved pharmacokinetic profiles and increased accumulation in tumor tissues, resulting in enhanced anticancer activity. Additionally, the use of antibody-drug conjugates (ADCs) that incorporate natural product-derived cytotoxins has emerged as a promising approach for achieving precision oncology. By coupling these cytotoxins with tumor-specific antibodies, ADCs can deliver potent anticancer agents directly to malignant cells while sparing normal tissues. Such innovations exemplify the synergy between natural products and cutting-edge technologies in advancing cancer therapy.

Despite their immense potential, the development of natural products as anticancer agents is not without challenges. The complex and often labor-intensive processes involved in their isolation, structural characterization, and large-scale production pose significant barriers to their clinical translation. Furthermore, the variability in natural sources and the lack of standardized protocols for evaluating their efficacy complicate the drug development pipeline. To address these challenges, interdisciplinary approaches that integrate advanced analytical techniques, high-throughput screening, and computational modeling are being increasingly employed. The use of omics technologies, such as genomics, proteomics, and metabolomics, has also facilitated a deeper understanding of the molecular mechanisms underlying the anticancer effects of natural products. These advancements have paved the way for the rational design and optimization of natural product-based therapies, thereby accelerating their journey from bench to bedside.

The integration of natural products into combinatorial treatment regimens represents another promising avenue for enhancing cancer therapy. By leveraging their complementary mechanisms of action, natural products can synergize with conventional chemotherapeutic agents to overcome resistance and improve clinical outcomes. For instance, resveratrol, a polyphenol found in grapes and berries, has been shown to sensitize cancer cells to doxorubicin by modulating the expression of MDR-related genes and enhancing oxidative stress. Similarly, berberine, an alkaloid derived from Berberis species, has been found to enhance the efficacy of cisplatin and paclitaxel in various cancer models. Such combinatorial approaches not only enhance therapeutic efficacy but also reduce the doses of chemotherapeutic agents required, thereby mitigating their associated side effects. The advent of cancer immunotherapy marks a transformative milestone in oncology, establishing it as a pivotal addition to traditional

modalities such as surgery, radiotherapy, and chemotherapy. Distinguished by its ability to harness and amplify the body's immune system to target malignancies, cancer immunotherapy offers promising therapeutic efficacy with comparatively lower systemic side effects. Despite these advancements, its application is predominantly effective in immunologically active ("hot") tumors, such as metastatic melanoma and urothelial carcinoma, while facing substantial limitations in treating poorly immunogenic ("cold") tumors like triple-negative breast cancer and colorectal cancer. The primary obstacle in expanding its efficacy lies in the tumor's immunosuppressive microenvironment, which enables cancer cells to evade immune detection and orchestrates mechanisms that resist immunotherapeutic interventions

The use of natural products in cancer therapy has emerged as a promising avenue to overcome these challenges. Derived from diverse biological sources such as plants, microbes, and marine organisms, natural products possess a broad spectrum of bioactive properties and have historically contributed to a significant portion of anticancer drugs, including paclitaxel, camptothecin, and vinblastine. These compounds exhibit multifaceted mechanisms of action, influencing key oncogenic pathways and immune responses while maintaining a favorable safety profile. Recent advancements in the understanding of tumor biology and immune modulation have further underscored the potential of natural products as adjuvants in cancer immunotherapy.

Despite these promising developments, the integration of natural products into mainstream cancer immunotherapy faces challenges. These include the complex nature of their isolation, structural characterization, and large-scale production. Furthermore, the inherent variability in biological sources and the lack of standardized protocols for evaluating their efficacy pose significant barriers to their clinical p0translation. Addressing these challenges requires a multidisciplinary approach involving advanced analytical techniques, high-throughput screening, and innovative pharmacological models. The recent resurgence of interest in natural product research, driven by technological advancements and a deeper understanding of their mechanistic roles, offers renewed optimism for their application in cancer therapy (15).

- **Natural products in Anti-cancer potential**

The utilization of natural products in medicine has a long and illustrious history, particularly in the realm of cancer treatment. Natural products have played a pivotal role as sources of

anticancer agents, either through direct application or as templates for the development of synthetic derivatives. They have contributed significantly to the advancement of modern oncology, addressing the limitations of traditional therapies such as surgery, radiation, and chemotherapy. Despite the advent of sophisticated medical technologies, cancer remains one of the leading causes of mortality worldwide, accounting for over 10 million deaths in 2020 alone. This alarming statistic underscores the need for innovative and effective treatment options. Natural products, characterized by their structural diversity and biofunctional properties, offer a promising alternative for combating this global health challenge.

Cancer is a complex and heterogeneous disease, comprising over 277 distinct types, each with unique genetic and molecular profiles. Its pathogenesis involves multiple stages, including initiation, promotion, and progression, during which normal cells acquire genetic mutations that lead to uncontrolled growth and, in many cases, metastasis. Conventional treatments such as chemotherapy and radiotherapy, although effective in targeting rapidly dividing cells, are often accompanied by severe side effects, including myelosuppression, mucositis, and multi-drug resistance (MDR). Furthermore, these treatments frequently lack specificity, leading to damage to healthy tissues and organs. This has catalyzed a shift towards more targeted therapies, including small molecule inhibitors and immunotherapeutics. However, even these advanced approaches are not without limitations, as they too are susceptible to drug resistance and off-target effects. Against this backdrop, the exploration of natural products as sources of novel anticancer agents has gained renewed momentum (16,17).

1.3 *Aphanamixis polystachya*

Aphanamixis polystachya, a member of the Meliaceae family, is a well-known medicinal plant distributed throughout tropical regions of Asia, including India, Malaysia, Indonesia, and southern China (18,19,20). It has various vernacular names for different regions such as Pithraj, Tiktaraj, Roina, Badhiraj (Bengali); Rohituka (English); Harin-hara, Harin khana (Hindi) and Shan lian (Chinese) (21). Within the genus Aphanamixis, *A. polystachya* is the most prevalent species in India. This plant is a tall, evergreen timber tree, reaching heights of 20–30 meters with a girth of 1.5–1.8 meters. Its leaves are 30–60 cm long, arranged in either odd or even-pinnate formations. The flowers, which are polygamo-dioecious, measure 0.6–0.7 cm in diameter and typically feature five sepals. The fruits are characterized by their bitterness and

have three valves that open to reveal numerous seeds surrounded by an orange or red aril (22). *Aphanamixis polystachya* contains various bioactive compounds, including alkaloids, flavonoids, terpenoids, and limonoids, which hold significant pharmacological importance (23,24,25). The scientific classification of *Aphanamixis polystachya* is provided in Table 1.

Figure 1.3. *A. polystachya* tree, fruits and bark

Traditionally, various parts of the *A. polystachya* plant have been utilized to address a range of health issues. The oil derived from its seeds is applied topically as a stimulating liniment for rheumatism, as well as to treat blood disorders and as a healing agent for wounds. Additionally, the seed oil is specifically favored for its efficacy in managing skin conditions (22). Notably, the plant exhibits repellent and toxic properties against *Tribolium castaneum*, a common pest. Furthermore, the dried seed powder, when consumed with water or milk, is ingested to alleviate liver ailments and promote blood purification (26). The roots and flowers of *A. polystachya*, often combined with coriander, are believed to aid in weight reduction (27).

Kingdom	Plantae
Division	Magnoliophyta
Class	Magnoliatae
Subclass	Rosidae
Order	Sapindales

Family	Meliaceae
Genus	*Aphanamixis*
Species	*Aphanamixis polystachya*

Table 1.1: Scientific classification of *Aphanamixis polystachya*

Moreover, the bark is a strong astringent and is traditionally used to treat spleen and liver diseases, as well as cardiac and hepatic disorders. Additionally, the hepatoprotective action of the ethanol extract of its leaves has been demonstrated against carbon tetrachloride-induced liver injury in rats. In Ayurveda, the traditional Indian medicinal system, Amoora rohituka is revered for its therapeutic properties in managing various health issues such as blood disorders, eye ailments, helminthiasis, ulcers, liver disorders, and splenomegaly (28). In specific regions like the West and South districts of Tripura, India, ethnic communities utilize the bark and leaves of *A. polystachya* to alleviate stomach pain and treat various skin-related conditions (29). This widespread utilization of different parts of the plant underscores its importance in traditional medicine across diverse cultures.

1.3.1 Phytochemistry of *A. polystachya*

The first phytochemical investigation of *A. polystachya* was carried out by Kundu *et al.* in 1967 resulting in the isolation of a tetranortriterpenes Aphanamixinin (30). Alessandra *et al*. isolated two mexicanolide type and three polyoxyphragmalin type limonoids, along with two known andirobin-type limonoids and three phenolic derivatives from the leaves and also checked their interaction with chaperone protein Hsp90 (31). Recently Xiao *et al*. isolated a rare C-24 appendage 5/6/5 fused-ring limonoid Aphananoid A. Other reported limonoids from various parts of the plant are Aphanalide A-H, Aphanamolide A, Rohituka 1-14, kihadalactone A, Amoorinin, and Aphanamixoid A-P. Aphanaperoxide E-H, novel diterpenes having rare five-membered peroxide ring were isolated from the ethanolic extract of stem bark by Wu *et.al* in 2013 (32-40). Xiapo *et al*. described the isolation of six new acyclic diterpenoids Aphanamixins A-F and two known compounds nemoralisin and nemoralisin C. They evaluated the absolute configurations of all stereogenic carbon centres by using auxiliary chiral α-methoxy-α-(trifluoromethyl) phenylacetic acid (MTPA) derivatives and circular dichroism (CD). Two nemoralisin diterpenoids Aphapolins A, containing a 4/5 fused ring system and

Aphapolins B, possessing a benzofuran moiety were isolated from the stem and leaves of *A. polystachya*. They also isolated a synthetic intermediate, in the total synthesis of Aphadilactones A-D, as a natural product for the first time. In 2020 Zhen *et al*. reported two novel heptanornemoralisin-type diterpenoids nornemoralisins A and B along with two known compounds nemoralisin and nemoralisin A (41). Recently, Shang Xue *et al*. isolated three acyclic diterpenes Aphanamoxene A-C and one norsesquediterpene Aphanamoxene D from the ethanolic extract of seeds of *A. polystachya* (42). Only five sesquiterpenoids have been reported from *A. polystachya* (43). Two novel guaiane-derived sesquiterpenoids, 6b,7b-epoxyguai-4-en-3-one and 6b,7b-epoxy-4b,5-dihydroxyguaiane from the stem bark and 15-hydroxy-*α*-cadinol, *1S,4S,5S,10R*-4,10- guaianediol and 4(15)-eudesmene-1*β*, 6*α*-diol from the leaves and twigs (44,45). Harmon *et al*. in 1979 discovered a chromone alkaloid Rohitukine (the first alkaloid from Meliaceae) from *A. polystachya* by acid-base workup of ethanol extract. They also isolated a known flavonoid noreugenin from the alkaloidal extract (46). A new lignin compound polystachyol, two lignin glycosides, lyoniside and nudiposide were isolated from the methanolic extract of dried stem bark of *A. polystachya* by Sadhu *et al*. in 2006. From the roots of *A. polystachya* Srivastava *et al*. isolated two flavone glycosides 8-methyl-7, 2', 4'-tri-*O*-methyl flavanone-5-*O*-*α*-L-rhamnopyranosyl-(1→4)-*β*-D-glucopyranosyl-(1→6)-*β*-D glucopyranoside and 8-C-methyl-5, 7, 3', 4'- tetrahydroxy-flavone-3-*O*-*α*-L-arabinopyranoside (47). In 1985 Anjali *et al*. isolated another flavone glycoside 8-C-methyl-quercetin-3-0-*β*-D-xylopyranoside, from the roots of *A. polystachya* (48).

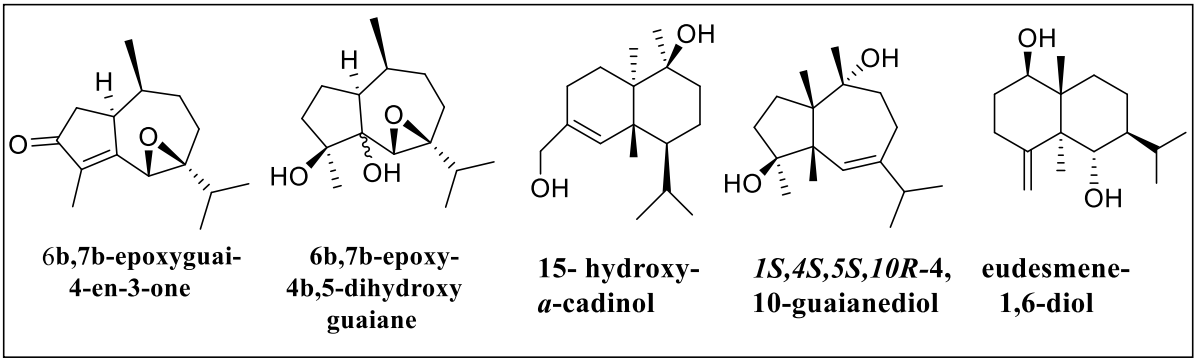

6b,7b-epoxyguai-4-en-3-one | **6b,7b-epoxy-4b,5-dihydroxy guaiane** | **15- hydroxy-*a*-cadinol** | ***1S,4S,5S,10R*-4, 10-guaianediol** | **eudesmene-1,6-diol**

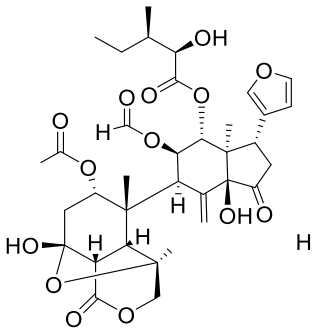

Aphanamolide A

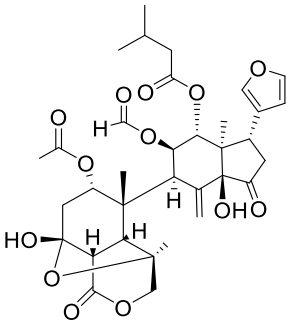

Aphanamolide B

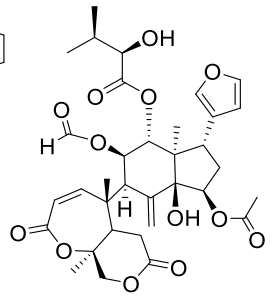

Dregenana-1

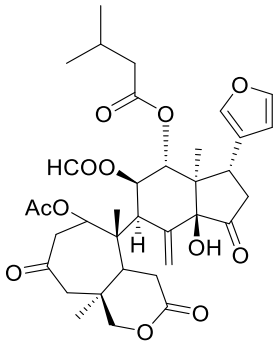

Rohitukine

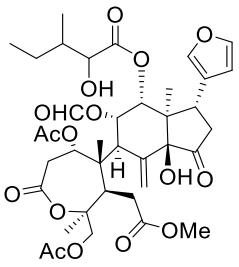

Prieurianin

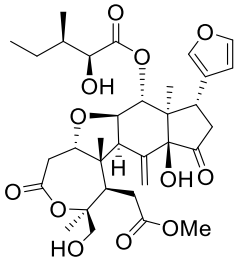

Aphapolynins A

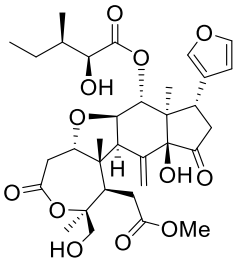

Aphapolynins B

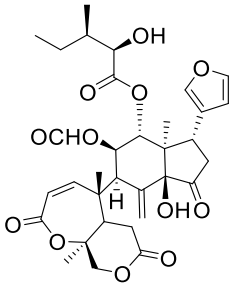

Aphapolynins C

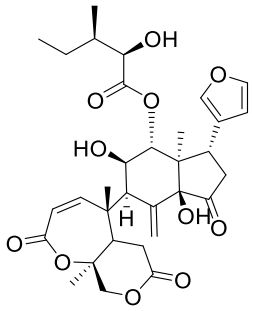

Aphapolynins D

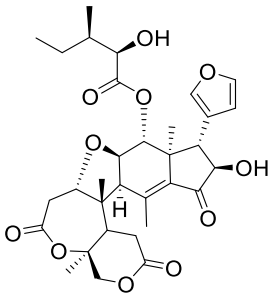

Aphapolynins E

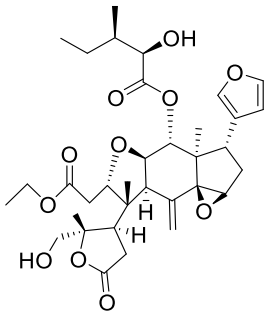

Aphapolynins F

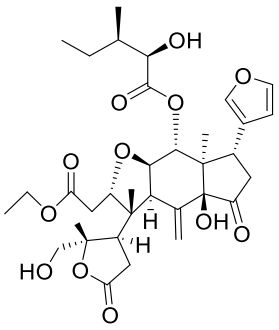

Aphapolynins G

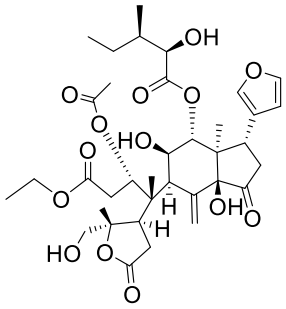

Aphapolynins H

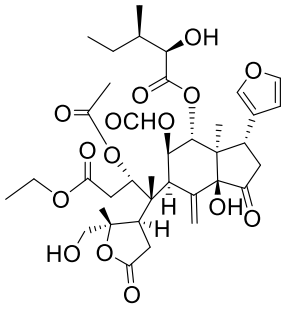

Aphapolynins I

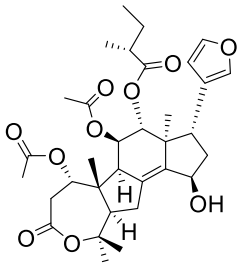

Aphananoid A

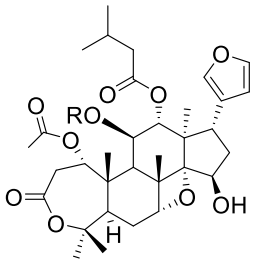

R=HCO **Aphanalides A**
R=H **Aphanalides B**

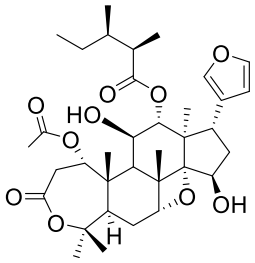

Aphanalides C

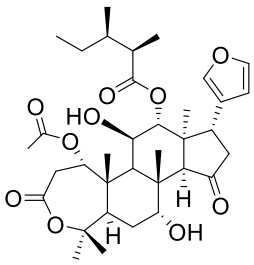

Aphanalides D

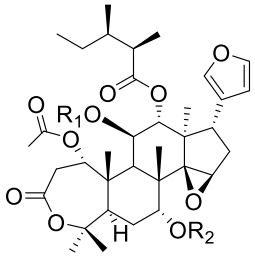

R_1=H, R_2=H **Aphanalides E**
R_1=H, R_2=Ac **Aphanalides F**
R_1=HCO, R_2=H **Aphanalides G**

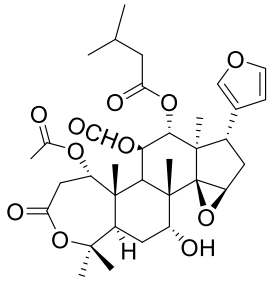

Aphanalides H

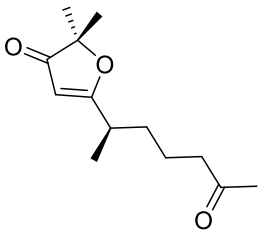

Nornemoralisin A

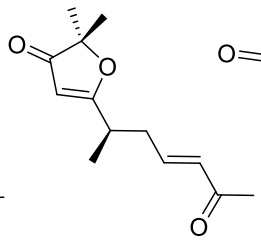

Nornemoralisin B

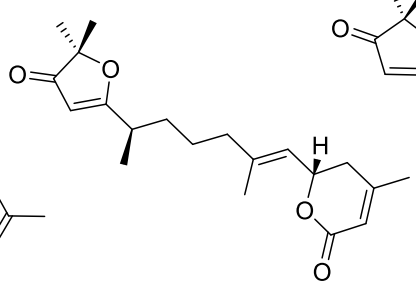

Nemoralisin A

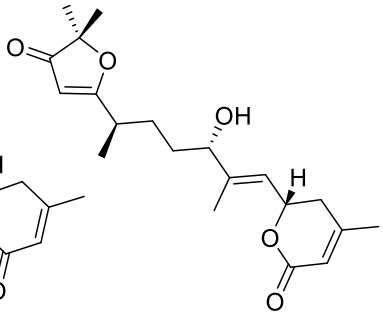

Nemoralisin B

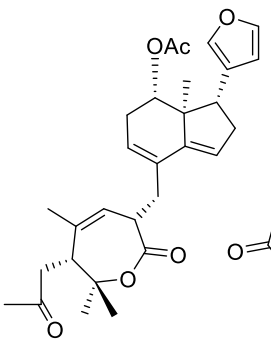

Aphanamixoid A

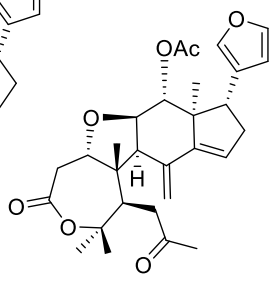

Aphanamixoid B

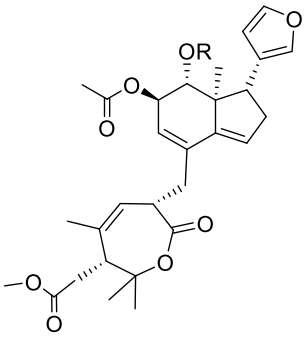

R=Ac **Aphanamixoid C**
R=A **Aphanamixoid D**
R=B **Aphanamixoid E**

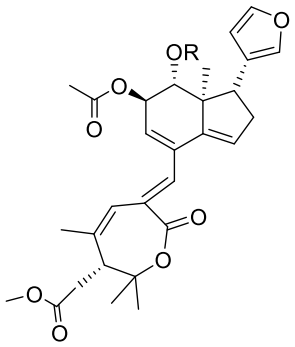

R=Ac **Aphanamixoid F**
R=A **Aphanamixoid G**

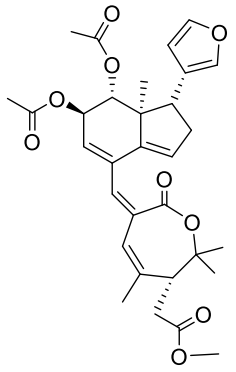

Aphanamixoid H

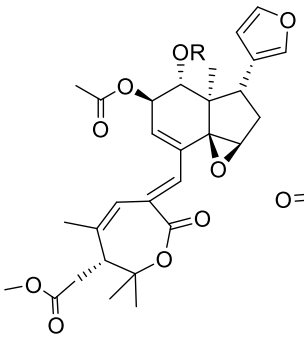

R=Ac **Aphanamixoid I**
R=A **Aphanamixoid J**

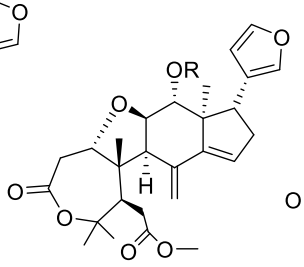

R=A **Aphanamixoid K**
R=B **Aphanamixoid L**
R=C **Aphanamixoid M**

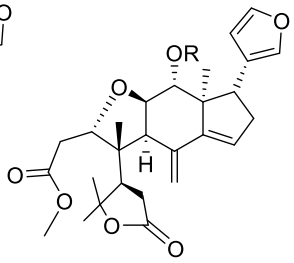

R=A **Aphanamixoid N**
R=B **Aphanamixoid O**
R=C **Aphanamixoid P**

A = 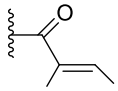

B = 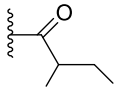

C = 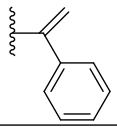

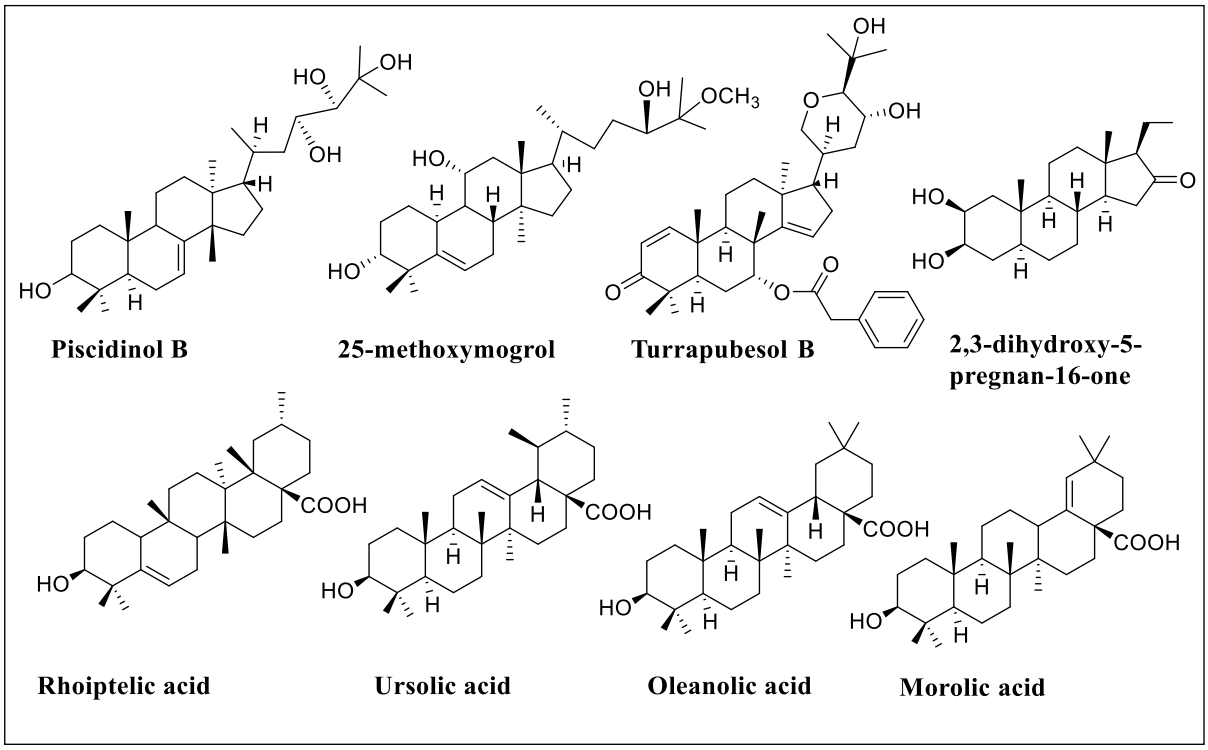

Figure 1.4. Reported compounds from *A. polystachya*

A. polystachya is known to possess a variety of pharmacological activities like anti-tumour, anti- insecticidal, anti-microbial, anti-malarial, anti- inflammatory and antifeedant, etc. In the year 1995, Rabi *et al*. studied the anticancer activity of ethyl acetate extract of the stem bark of *A. polystachya* on mice inoculated with Dalton's lymphoma ascites cells (DLA) with an IC_{50} value of 9 μg/ml. Later in 2002, the same group also reported the cytotoxicity study of a triterpene acid amoorarin and its methyl ester derivative on MCF-7 and HeLa cell lines. They also reported that amoorarin induces apoptosis in human breast carcinoma cell MDA-468 via the caspase activation pathway. In addition, this triterpene overcomes multidrug resistance in human leukemia CEM and colon carcinoma SW620 cell lines. In 2013, Kong and coworkers isolated 7 new prieurianin type limonoids and evaluated their insecticidal activity against four pest species (S. avenae, P. xylostella, D. balteata, and C. elegans). From the result, they found that molecules possessing α, β- unsaturated moiety showed good activity. Anti-bacterial and anti-fungal properties of the methanolic extract of the stem bark of A. polystachya were carried out by Chawdhary et al., by disc diffusion method and poisoned food technique respectively. In 1997, MacKinnon et al., evaluated the ethanolic extract of the stem bark of *A. polystachya*

for anti-malarial activity. In 2013 He et al., isolated new Aphanamixoid type compounds from the leaves and checked their antifeedant activity. Among them Aphanamixoid A, having a new carbon skeleton showed significant antifeedant activity against the larvae of two generalist insects, *Spodoptera exigua* (0.052 μmol/cm2), and *Helicoverpa armigera* (0.015 μmol/cm2. Lampronti and co-workers found that, a low concentration of ethanolic extract of stem bark is effective in inhibited NF-kB/DNA interactions.

1.3.2 Pharmacological Relevance of *A. polystachya*

Anti-oxidant activity

Recent research has highlighted the detrimental effects of oxidative stress, which arises from the damaging activities of free radicals within cells where antioxidants counteract this damage (49). *In vivo* studies have revealed the remarkable antioxidant potential of polyphenolics found in the ethanol extract of *Aphanamixis polystachya* leaf. When administered to mice models intoxicated with CCl_4, this leaf extract significantly reduced and normalized levels of oxidative stress markers such as thiobarbituric acid reactive substances (TBARS), nitric oxide (NO), and advanced protein oxidation products (APOP) ($P < 0.05$). Moreover, this treatment notably enhanced the activities of two natural antioxidant enzymes, catalase and superoxide dismutase (SOD), in rats intoxicated with CCl4 (50). Further experiments on the *A. polystachya* fraction (AP-110/82C) in rats, at doses of 50 and 100 mg/kg body weight, demonstrated a dose-dependent improvement in oxidative stress. Hepatic glutathione and catalase levels increased, while hepatic malondialdehyde levels decreased, indicating significant therapeutic potential (51).

In vitro investigations on the antioxidant properties of ethanol acetate extracts from *A. polystachya* fruit revealed robust free-radical scavenging activity against DPPH (2,2-Diphenyl-1-picrylhydrazyl) and nitric oxide (NO) (52). Additionally, both carbon tetrachloride and methanolic extracts from *A. polystachya* bark and leaf exhibited substantial DPPH (1,1-diphenyl-2-picrylhydrazyl) free radical scavenging activity (53). Moreover, the study determined IC_{50} values for various antioxidant assays, suggesting the crude methanol extract of A. rohituka as a rich source of natural antioxidants (54). Notably, *A. polystachya* bark extract displayed nearly twice the efficacy of vitamin C in ABTS free radical scavenging activity and ferric reducing antioxidant power (FRAP). The methanol and water, as well as aqueous

methanol bark extracts, exhibited potent superoxide free radical scavenging activity, approximately 16 times more efficient than vitamin C, as evidenced by their lower IC_{50} values of 7–8.3 μg/mL compared to vitamin C's IC_{50} of 125 μg/mL.

Anti-inflammatory activity

The body's immune system response can cause inflammation through the overproduction of nitric oxide (NO) (55). However, extracts from various parts of the *Aphanamixis polystachya* plant have exhibited significant anti-inflammatory properties by reducing NO production. In a macrophage cell line, RAW264.7, nitric oxide (NO) generation induced by lipopolysaccharide (LPS) was notably inhibited by aphamine and aphanamoxenes, which are acyclic diterpenes and norsesquiterpenes found in the seed extracts of *A. polystachya*. The inhibition was observed at concentrations of up to 50 μM, with IC50 values ranging from 6.71 to 17.6 μmol/L (56,57). Additionally, Aphananoid A, a limonoid present in the leaf and twig extracts of *A. polystachya*, also demonstrated a significant NO inhibitory effect in the RAW264.7 cell line (22). Furthermore, the acyclic diterpenes present in rohituka were found to decrease the levels of inducible nitric oxide synthase (iNOS) protein, further emphasizing the potential anti-inflammatory properties of *A. polystachya* extracts (58).

In a study evaluating the anti-inflammatory potential of various plant extracts, it was found that hydroalcoholic extracts of Amoora rohituka stem bark resulted in a significant 53.3% inhibition of carrageenan-induced rat paw edema at an oral dose of 100 mg/kg (59). Additionally, triterpenoids and limonoids derived from rohituka root extracts exhibited high anti-inflammatory activity in human neutrophils. Specifically, the production of superoxide anion and secretion of elastase were inhibited by up to 86.65% and 78.36%, respectively, at a concentration of 10 μg/mL in the presence of FMLP/CB. Furthermore, *Aphanamixis polystachya* leaf extract was assessed in an anti-inflammatory study involving twenty-four rats with acute paw edema. The results demonstrated decisive anti-inflammatory action, with liposomal administration of the leaf extract increasing its potent anti-inflammatory efficacy nearly twofold (60,61).

Antimalarial activity

Plasmodium falciparum, the deadliest parasite responsible for malaria-induced anemia, poses a significant global health threat (62,63). In combating this disease, research has explored natural sources for potential antimalarial agents. One such source is Amoora rohituka, from which an ethanolic wood extract displayed promising antimalarial activity with IC_{50} values of 16.8 μg/mL *in vitro* (64). Additionally, rohitukine, a chromane alkaloid isolated from the leaves and stems of Amoora rohituka, has been investigated for its potential as an antimalarial agent. In an *in silico* study, rohitukine was assessed as a ligand targeting *Plasmodium falciparum* enoyl-acyl carrier protein reductase (PfENR), a key enzyme involved in the parasite's fatty acid biosynthesis pathway. The study revealed that rohitukine exhibited a potential inhibitory effect against PfENR, as evidenced by a binding energy of -7.04 kcal/mol (65). These findings suggest that rohitukine holds promise as a prospective antimalarial agent, warranting further exploration in experimental settings.

Antiulcer activity

In the investigation of Amoora rohituka's potential as an antiulcer agent, both aqueous (AEAP) and methanolic (MEAP) stem bark extracts were evaluated using various ulcer models in rats at an oral dose of 200 mg/kg. The study encompassed indomethacin-induced ulcers, pylorus ligation-induced ulcers, and stress ulcers induced by cold-water immersion. The results revealed significant antiulcer efficacy for both extracts. MEAP and AEAP markedly reduced the volume of free acidity, total acidity, and pH of gastric juice, indicative of their antiulcer properties. Specifically, MEAP and AEAP exhibited substantial protection against pylorus ligation-induced ulcers, reducing the ulcer index from 45.16 to 6.42 and 7.77, respectively, with protection rates of 56.68% and 47.57%. Similarly, they demonstrated significant protection against indomethacin-induced ulcers, with reductions in ulcer index from 16.43 to 7.12 and 8.2, respectively, and protection rates of 56.67% and 50.1%. Additionally, both extracts provided protection against cold stress-induced ulcers, reducing the ulcer index from 13.7 to 6.32 and 7.58, respectively, with protection rates of 53.9% and 44.7% (66).

Moreover, a compound isolated from *Aphanamixis polystachya* demonstrated noteworthy protective effects against various types of induced gastric ulcers in mice. Specifically, it provided significant protection against ethanol, cold restraint, and pyloric ligation-induced gastric ulcers, with protection rates of 82.0%, 74.97%, and 50%, respectively. In ethanol-

induced gastric ulcers in rats, rohitukine, a compound found in Amoora rohituka, exhibited remarkable efficacy in preventing erosion formation and increasing prostaglandin E2 (PGE2) levels, surpassing the reference medication sucralfate. Furthermore, the study demonstrated that rohitukine could block gastric microsomal H+/K+ ATPase activity, indicating its potential as an effective therapeutic agent for peptic ulcer disease.

Anthelmintic activity

Anthelmintic treatment primarily leads to flaccid paralysis in worms, rendering them immobile (67). *Aphanamixis polystachya*'s seed and bark extracts have demonstrated noteworthy anthelmintic activity in a dose-dependent manner (68,69). Recent research highlights the potency of the n-hexane seed extract, exhibiting a stronger anthelmintic activity with an LC50 value of 0.10 mg/ml compared to the standard albendazole, which had an LC_{50} value of 0.15 mg/ml. Additionally, both chloroform and methanol extracts of seeds showed significant anthelmintic activity, with an LC_{50} value of 0.156 mg/ml against Haemonchus contortus. In studies targeting *Pheritima posthuma* earthworms, the methanolic extract of *A. polystachya* bark demonstrated anthelmintic effects (70). The paralysis time for *Pheritima posthuma* was notably reduced with increasing concentrations of the methanolic extract, with times ranging from 35.66 to 25.66 minutes, and death times ranging from 52.33 to 38.33 minutes at concentrations of 10, 20, 40, and 60 mg/ml, respectively. In comparison, the standard drug albendazole induced paralysis and death at 56.20 and 77.40 minutes, respectively, at a concentration of 10 mg/ml. These findings underscore the potential of *A. polystachya* extracts as effective anthelmintic agents.

Anti-diabetic activity

Diabetes mellitus, a chronic condition characterized by elevated blood sugar levels (hyperglycemia), is often associated with organ damage and various complications (71). One such complication is dyslipidemia, marked by an increase in serum total cholesterol (TC), triglycerides (TG), and low-density lipoproteins (LDL), alongside a decrease in high-density lipoproteins (HDL) (72,73). In addressing these issues, research has explored the potential of *Aphanamixis polystachya* leaves. A methanolic extract of these leaves, administered at doses of 100 mg/kg and 200 mg/kg, demonstrated significant efficacy ($P < 0.05$) in reducing serum glucose levels in streptozotocin (STZ)-induced diabetic rats. Moreover, this extract effectively

modulated dyslipidemia by reducing TC, TG, and LDL levels, while increasing HDL levels in diabetic rats at the same doses. The observed antidiabetic effects of *A. polystachya* may be attributed to the presence of various bioactive compounds such as tannins, flavonoids, saponins, and sterols in the methanolic leaf extract. These compounds are believed to facilitate pancreatic β-cell regeneration and contribute to the reduction of blood sugar levels, thus highlighting the potential therapeutic benefits of *A. polystachya* in managing diabetes and its associated complications.

Laxative effect

Traditionally, *Aphanamixis polystachya* has been utilized as a remedy for constipation due to its purported laxative properties (74). Recent investigations have delved into the efficacy of various extracts from the stem bark of *A. polystachya* in this regard. At different dose levels ranging from 250 to 400 mg/kg body weight, petroleum ether, dichloromethane, and methanol extracts of *A. polystachya* stem bark have exhibited significant laxative effects in mice, as evidenced by marked improvements in gastrointestinal motility ($P < 0.01$ and $P < 0.001$). Furthermore, crude extracts of *A. polystachya* demonstrated a noteworthy enhancement in gastrointestinal motility at a dose of 100 mg/kg ($P < 0.05$) (75). Despite these promising findings, the precise mechanism underlying the laxative effect of *A. polystachya* extracts remains elusive. Therefore, further research endeavors are imperative to elucidate and validate *A. polystachya*'s potential as a therapeutic laxative agent.

Antibacterial activity

Aphanamixis polystachya boasts a diverse array of bioactive compounds, including limonoids, lignans, and phenolics, which endow it with substantial antibacterial properties (76). These compounds operate through various mechanisms, such as inhibiting the signaling of auto-inducer peptides (AIPs), and crucial quorum sensing (QS) mediators in Gram-positive bacteria (77). Phenolics and limonoids, in particular, exhibit bactericidal effects and impede cell-cell adhesion necessary for biofilm formation, a pivotal aspect of pathogenic bacteria's virulence (78). In combating biofilm-related infections, leaf extracts from *A. polystachya* have shown remarkable efficacy in preventing and disintegrating biofilms produced by Methicillin-resistant *Staphylococcus aureus* (MRSA) strains, even at low concentrations. Moreover, *A. polystachya*'s antimicrobial prowess extends beyond biofilm disruption (79). Stem bark

extracts of *A. polystachya* have been subjected to rigorous testing against 19 different bacteria strains, showcasing significant antibacterial activity. The extracts exhibited substantial inhibition zones against various pathogens, with diameters ranging from 7 to 30 mm, depending on the bacterial strain and the extract used.

Furthermore, comparative studies have highlighted the varying efficacy of different parts of *A. polystachya*. Bark extracts, particularly the methanolic variant, demonstrated superior antibacterial activity against *Escherichia coli*, Pseudomonas sp., and Staphylococcus sp. compared to leaf extracts. The disparity in effectiveness underscores the importance of selecting the appropriate plant part for specific antimicrobial applications. In assessing the minimum inhibitory concentrations (MICs), a critical metric for evaluating antimicrobial efficacy, *A. polystachya* extracts exhibited potent activity against various bacterial strains. Notably, the methanolic extracts from both leaves and bark demonstrated remarkably low MIC values against E. coli, Pseudomonas sp., and Staphylococcus sp., underscoring their potent antibacterial properties. Overall, these findings underscore the significant potential of *Aphanamixis polystachya* as a valuable source of antimicrobial agents, paving the way for further exploration and development of novel antibacterial therapeutics (80-86).

Anti-fungal activity

Fungi, omnipresent in diverse environments including indoors, outdoors, and even on our skin and within our bodies, pose significant health risks by causing various diseases. *Aphanamixis polystachya*, renowned for its rich repertoire of bioactive compounds, has emerged as a promising source of antifungal agents. In particular, the fruits of *A. polystachya* harbor several potent antifungal limonoids. Isolated compounds such as Chisocheton compound G, Chisocheton compound E, and 6α-Acetoxyepoxyazadiradione VI have been scrutinized for their efficacy against nine phytopathogenic fungi. Notably, compound 3 exhibited remarkable antifungal activity, particularly against *Sclerotium rolfsii*, *Fusarium oxysporum*, and *Magnaporthe oryzae*, showcasing its potential as an effective agent against various phytopathogens. Further exploration into *A. polystachya*'s fruit-derived limonoids uncovered additional compounds like Aphapolynin and rohituka-15, demonstrating robust antifungal activity against specific fungi strains such as *Uromyces viciae*-fabae and *P. dissimile* (87,88). Additionally, the presence of amoorinin-3-O-α-L-rhamnopyranosyl-(1–6)-ß-D-

glucopyranoside in *A. polystachya* has shown inhibitory effects against *Aspergillus niger* and *Candida albicans*, further expanding the spectrum of its antifungal arsenal. Moreover, investigations into *A. polystachya*'s bark extract have revealed moderate fungicidal properties against several fungi strains, including *Candida albicans* and *Aspergillus alliaceus*. Similarly, evaluations of *A. polystachya*'s seed oil and alkaloid solution have unveiled varying degrees of antifungal efficacy. The seed oil, for instance, exhibited notable effects against strains like *D. oryzae*, while the alkaloid solution demonstrated potent inhibition against *M. phaseolina* (89,90). Overall, the diverse array of antifungal compounds present in *Aphanamixis polystachya* underscores its potential as a valuable source of novel antifungal agents, warranting further exploration and development in the field of fungal disease management.

Thrombolytic effect

Thrombolysis, the process of dissolving blood clots using thrombolytic agents, is vital in managing conditions like thrombosis. *Aphanamixis polystachya*, enriched with alkaloids, flavonoids, tannins, and terpenoids, exhibits noteworthy thrombolytic properties. In particular, studies have highlighted the potent thrombolytic effects of *A. polystachya* extracts. The methanolic extract of *A. polystachya* demonstrated remarkable thrombolytic activity, achieving a clot lysis of 23.49%, surpassing the control group's efficacy. Similarly, the n-hexane extract exhibited moderate thrombolytic capabilities, with an 18.84% clot lysis rate. Furthermore, investigations into *A. polystachya* seed extracts revealed their efficacy as thrombolytic agents, particularly at a concentration of 10 mg/ml, where the methanolic extract achieved a clot lysis of 23.49%. Additionally, *A. polystachya* fruit extracts displayed significant thrombolytic activity at a concentration of 100 mg/ml, further underscoring the plant's potential in thrombolytic therapy. Notably, the petroleum ether bark extract of *A. polystachya* exhibited substantial thrombolytic activity across various concentrations, with clot lysis rates of 19.01%, 13.81%, and 9.83% at 20, 10, and 5 mg/ml, respectively. These findings were statistically significant compared to the negative control group (91,92). Overall, the robust thrombolytic properties of *Aphanamixis polystachya* extracts highlight their potential as effective agents in managing thrombotic disorders, warranting further exploration and development in therapeutic applications.

Insecticidal activity

Derived from the fruits of *Aphanamixis polystachya*, preurainin-type limonoids such as Aphapolynin C-1, C-2, C-4, dregenana-1, and aphanalides (E-H) exhibit promising insecticidal properties against various pest species, including *S. avenae, P. xylostella, D. balteata*, and *C. elegans*. These compounds feature α, β-unsaturated lactone and 14,15-epoxy moieties, contributing to their efficacy. Aphapolynin C-1 and Aphanalides H have demonstrated notable inhibition of nicotine response, with IC_{50} values of 3.13 ppm and 1.59 ppm, respectively. Moreover, Aphanalides H exhibited inhibition of GABA response with an IC_{50} value of 8.00 ppm. The seed extract of *A. polystachya* displays moderate inhibition against *Sitophilus zeamais*, with a 27% inhibition rate. Additionally, it exhibits significant toxic effects on T. castaneum, resulting in 42–55% mortality within 72 hours at a dose of 100 μg/insect. Against the pulse beetle *Callosobruchus chinensis*, the seed extract of *A. polystachya* demonstrates substantial mortality rates, characterized by low LD_{50} values (10 μg/insect) and the shortest LT_{50} values (50hr/insect). Similarly, it exhibits high toxicity (37%) against rice weevils (*Sitophilus oryzae*) at a dose of 100 μg/insect within 72 hours. Furthermore, the leaf, bark, and seed powders hinder oviposition by weevils by 29.2%, 20.3%, and 29.6%, respectively, and reduce egg survivorship. Seed extract of *A. polystachya* also displays significant toxic effects on red flour beetles (*Tribolium castaneum*), causing mortality rates of 79.1% at a dose of 100 μg/insect, with the lowest LD50 values (32 μg/insect) among all insects studied (93,94).

Antifeedent activity

Aphanamixya polystachya extract yields limonoids such as Aphanamixoid C, Aphanamixoid F, and Aphanamixoid G, characterized by a high olefinic bond spanning from C-2 to C-30, rendering them effective antifeedants. Their EC_{50} values are notably low: 0.017 μmol/cm2 for Aphanamixoid C, 0.008 μmol/cm2 for Aphanamixoid F, and 0.012 μmol/cm2 for Aphanamixoid G. In addition to these, Aphanamixoid A, found in leaf and twig extracts, demonstrates antifeedant activity against the larvae of two generalist insects: beet armyworm (*Spodoptera exigua*) and cotton bollworm (*Helicoverpa armigera*), with respective EC_{50} values of 0.052 μmol/cm2 and 0.015 μmol/cm2. The seed extract of *A. polystachya* exhibits moderate-feeding deterrent activity, inhibiting the feeding behavior of red flour beetles (*Tribolium castaneum*) by 69.9%. Moreover, it demonstrates a moderate inhibition rate against

Sitophilus zeamais (27%), as reported by Haque et al. (2000). Interestingly, it exerts a potent effect (159.50) on feeding deterrence against rice weevils (*Sitophilus oryzae*) (95,96).

Hepatoprotective effect

Investigations have unveiled that liver fibrosis is primarily triggered by lipid peroxidation. Under elevated oxygen partial pressure, trichloromethylperoxy radicals emerge, instigating lipid peroxidation and reacting with aldehydes, notably monoaldehyde (MDA), detectable as TBARS. *A. polystachya* leaf extract showcases a remarkable capacity to alleviate oxidative stress, substantially reducing TBARS ($p<0.005$), NO ($p<0.005$), APOP ($P<0.05$), and the inflammatory marker MPO ($P<0.05$). Additionally, it elevates the levels of endogenous antioxidant enzymes such as catalase and SOD to nearly normal values ($P<0.05$). Catechin hydrate, found in *A. polystachya* extract, demonstrates a remarkable capability to reverse liver fibrosis. Moreover, *A. polystachya* leaf extract significantly reduces iron deposition, crucial as iron accumulation in liver cirrhosis catalyzes free radical production. Furthermore, the extract diminishes plasma levels of ASAT, ALAT, LDH, ALP, ACP, and bilirubin concentration ($P<0.05$). Notably, the plasma enzyme levels and total bilirubin concentration are substantially lowered, with ALP at 89.175, ALAT at 88.667, ACP at 81.264, ASAT at 75.432, LDH at 80.992, total bilirubin at 76.176, and total albumin at 71.524 (97-99).

CNS depressant

Inflammation plays a pivotal role in degenerative CNS disorders, such as Alzheimer's disease, often exacerbating disease progression and outcome, leading to cognitive impairment and, ultimately, dementia. Studies conducted on mice with dementia have highlighted the remarkable efficacy of *A. polystachya* liposomal formulation of leaf extract in ameliorating locomotor activity and ambulatory behavior ($P \leq 0.001$). Demonstrating robust anti-inflammatory activity (evaluated against acute edema, $P \leq 0.001$), the leaf extract also significantly enhances spatial learning ($p \leq 0.001$). Beta-elemene, found in *A. polystachya* leaf extract, boasts potent antioxidant and anti-inflammatory properties, effectively ameliorating traumatic brain injury in rats by mitigating inflammation. Moreover, *A. polystachya* is rich in ketone bodies, long recognized for their ability to enhance cognitive function in CNS pathologies, including stroke. Furthermore, crude extract of *A. polystachya* has been shown to extend the duration of thiopental sodium-induced sleeping time ($p<0.001$) (100-102).

Analgesic activity

The synthesis of eicosanoids, including Prostaglandin-E and prostacyclin (PGI2), from arachidonic acid via the cyclooxygenase pathway is a key contributor to the sensation of pain. Through its ability to inhibit prostaglandin synthesis, the methanolic extract of *A. polystachya* leaf and bark effectively reduces the number of writhing responses, indicative of its analgesic properties. Notably, *A. polystachya* leaf extract demonstrates significant analgesic activity in both the tail immersion test ($p<0.001$) and the hot plate method ($p<0.05–0.001$). Oral administration of *A. polystachya* leaf extract results in remarkable inhibition ($p<0.001$) of the writhing response. Moreover, *A. polystachya* bark extract exhibits dose-dependent analgesic effects, with a 250 mg/kg body weight dose in mice demonstrating 40.69% writhing inhibition ($P<0.001$), while a 500 mg/kg body weight dose leads to 62.07% writhing inhibition ($P<0.001$) induced by acetic acid (103-104).

Repellent activity

Insect repellents serve as a barrier against insects and arthropods, preventing them from settling on surfaces and biting or causing discomfort to individuals. These repellents offer an alternative to insecticides and can be applied to the skin, clothing, or various surfaces. The acetone seed extract of *A. polystachya* demonstrates remarkable repellency, particularly against the red flour beetle (*Tribolium castaneum*), achieving 100% effectiveness. Even at concentrations as low as 0.5% and 1.0%, the acetone seed extract exhibits significant repellency, with rates of 88% and 93%, respectively. Moreover, the seed extract displays a repellency effect of 44% against the pulse beetle (*Callosobruchus chinensis*). When evaluated using the filter paper repellency method at doses ranging from 0 to 31 mg/cm2, *A. polystachya* seed extract demonstrates fair repellency, reaching 67% effectiveness against rice weevils (*Sitophilus oryzae*) (105).

Allelopathic effect

The allelopathic effect, where specific plant species accumulate allelochemicals in the soil, significantly impacts the growth and germination of neighboring plants. *A. polystachya* demonstrates notable allelopathic properties on various crops, including jute, mung bean, mustard, radish, tomato, rice, and wheat. Both leaf and twig extracts of *A. polystachya* exhibit

potent allelopathic activity. Leaf extract inhibits root growth by 90% in jute and significantly affects the growth of mung bean, mustard, radish, tomato, rice, and wheat at varying concentrations. Meanwhile, twig extract suppresses shoot growth in jute and significantly impacts mustard, radish, tomato, rice, and wheat growth at different concentrations. For instance, at 1:20 (w/v) concentration, leaf extract inhibits root growth by 90% in jute, while twig extract at 1:2 (w/v) concentration suppresses shoot growth by 90% in the same crop. Additionally, both extracts affect the growth of other crops like mustard, radish, tomato, rice, and wheat, demonstrating varying levels of inhibition. Interestingly, Rohituka root extracts show a positive effect on wheat shoot growth, increasing it by 45% at the same concentration. These findings underscore the significant role of *A. polystachya* in influencing the growth patterns of neighboring plant species through allelopathic interactions (106-108).

Anticancer activity

Aphanamixis polystachya exhibits remarkable potential as a natural anticancer agent due to its selective cytotoxic effects against various cancer cell lines. In recent studies, the leaf extract of *A. polystachya* in ethyl acetate has demonstrated anticancer activity against human breast adenocarcinoma (MCF-7) and mouse undifferentiated carcinoma (EAC) cell lines, while exhibiting relative safety for L929 cells. Significant anticancer effects, including cell toxicity and apoptosis induction, were observed in MCF-7 cells with an IC_{50} value of 9.81 µg/ml. Additionally, *A. polystachya* leaf extract has shown cytotoxic activity against Huh-7 (human hepatocellular carcinoma), DU-145 (human prostate cancer), and MCF-7 cell lines with IC_{50} values of 3 µg/ml, 3.5 µg/ml, and 13.4 µg/ml, respectively, in another study. Moreover, recent identification of two novel cycloartane triterpenoids from the leaves and twigs of *A. polystachya*, namely (24 R)-cycloartane-3,24,25,30-tetrol and (24 R)-24,25,30-trihydroxy-9,19-cycloartane-3-one, has shown cytotoxic activity against various human cancer cell lines. Furthermore, compounds isolated from the fruit and stem bark extract of *A. polystachya*, including β-sitosterol, piscidinol A, and others, exhibited potent anticancer activity against SKOV3 (ovarian cancer), MDA-MB-231 (breast cancer), and DU145 (prostate cancer) cell lines. These compounds, such as polystanin and aphanamixin A, induced cell cycle arrest and necrosis in DU145 cells in a concentration-dependent manner (109-114).

Amooranin (AMR), a triterpene acid found in Amoora rohituka stem bark extract, demonstrated cytotoxicity against various cancer cell lines, including MCF-7 and HeLa cells. Additionally, AMR exhibited a chemo-sensitizing effect on doxorubicin hydrochloride (DOX) cytotoxicity against multidrug-resistant leukemia and colon carcinoma cell lines by reversing DOX resistance characteristics. Moreover, AMR was identified as a competitive inhibitor of P-glycoprotein (P-gp) mediated DOX efflux, thus enhancing the cytotoxic effect of DOX. *In vivo* and *in vitro* investigations further support the potential of AMR as a novel anticancer drug, particularly for colon cancer. The ethyl acetate extract derived from stem barks has displayed both *in vitro* (IC_{50}: 9 μg/ml) and *in vivo* anticancer effects against Dalton's lymphoma ascites tumor. Further investigation into the anticancer potential led to the identification of the methyl derivative of amooranin, known as Methyl-25 hydroxy-3-oxoolean-12-en-28-oate (AMR-Me), which has shown significant efficacy as an anticancer agent. To evaluate the *in vivo* anticancer efficacy of AMR-Me, mice were inoculated with Dalton's lymphoma ascites tumor cells. Administration of AMR-Me at doses of 1 and 3 mg/kg resulted in enhanced survival rates of 121% and 133%, respectively. Additionally, *in vitro* studies demonstrated that treatment with AMR-Me at concentrations ranging from 0.5 to 4 μM suppressed the expression of the hTERT gene, induced apoptosis via the activation of the caspase-3 cascade, and arrested the G2+M phase in human lymphoblastic leukemia CEM cells, thereby inhibiting their proliferation. Moreover, AMR-Me was found to modulate intracellular signaling pathways implicated in cancer progression. Specifically, it stimulated the p38 mitogen-activated protein kinase (MAPK) and c-Jun NH2-terminal kinase (JNK) pathways while inhibiting the PI3K/Akt signaling pathway, leading to apoptosis of MCF-7 cells. These findings underscore the potential of AMR-Me as a promising therapeutic agent for cancer treatment.

Pancreatic carcinomas are notorious for their high frequency of mutations in the K-Ras gene, with over 90% of cases exhibiting such mutations. In the realm of natural compounds, a novel triterpenoid called aphanin, isolated from Amoora rohituka, has shown promising potential in inhibiting K-Ras mutant activity. Acting on pancreatic cancer HPAF-II (ΔKRASG12D) cell lines, aphanin not only inhibits K-Ras mutant activity but also disrupts Akt signaling and c-Myc, while activating STAT3 phosphorylation and the caspase cascade, ultimately leading to apoptosis. Meanwhile, the bark extract of *Aphanamixis polystachya*, particularly in ethyl

acetate form, has demonstrated remarkable abilities in mitigating radiation-induced chromosomal damage in mice. Moreover, methanolic bark extracts from the same plant have served as radio-sensitizing agents for mice bearing Ehrlich ascites carcinoma (EAC), enhancing the radiation effect and inhibiting tumor growth. Interestingly, administering the bark extract in split doses of 0.5 g/kg has proven more effective in increasing the survival rate of mice compared to a single dose of 1 g/kg. However, it's noteworthy that the dichloromethane extract exhibited superior anticancer activity compared to the ethyl acetate extract in EAC-affected mice. Another noteworthy compound is the protolimonoid isolated from the root of Amoora rohituka, which has shown promising anticancer activity against various cancer cell lines, including HEp-2 (laryngeal carcinoma), Hep-G2 (hepatocellular carcinoma), A549 (lung carcinoma), and MCF-7 (breast adenocarcinoma). Furthermore, rohitukine, a chromane alkaloid originally isolated from the leaves and stems of Amoora rohituka, stands out as a potent natural anticancer agent. It exhibits cytotoxicity against multiple human carcinoma cell lines, particularly leukemia HL-60 and Molt-4, with concentrations of 10 μmol/L and 12 μmol/L causing 50% cell growth inhibition (115-118). These findings collectively highlight the diverse potential of natural compounds in the fight against cancer.

1.4 Cervical cancer

Cervical cancer remains one of the most pressing gynecological health concerns worldwide, ranking as the fourth most common malignancy in women. This condition is a significant public health challenge, particularly in low- and middle-income countries (LMICs), where it is also the fourth leading cause of cancer-related mortality. The prevalence of cervical cancer is alarming, with approximately 18.1 million new cancer cases reported globally in 2018. The burden is disproportionately higher in LMICs due to limited access to effective prevention, screening, and treatment strategies. Early detection is crucial for successful management, yet the lack of adequate screening programs in these regions often leads to delayed diagnosis and poor outcomes. Sociocultural, economic, and systemic barriers further complicate the implementation of widespread screening initiatives, highlighting the need for innovative and scalable solutions to improve access to preventive care. A key driver of cervical cancer is persistent infection with high-risk human papillomavirus (HPV) types, particularly HPV-16 and HPV-18. These oncogenic strains play a central role in the development of cervical cancer,

with progression influenced by various biological and environmental factors. Dysregulation of apoptotic pathways, such as the overexpression of Inhibitor of Apoptotic Proteins (IAPs) and increased Vascular Endothelial Growth Factor (VEGF) levels, contributes significantly to tumor growth and metastasis. Lifestyle factors, including smoking, exacerbate the risk by impairing the immune response and promoting chronic inflammation. Additionally, immune dysfunction, driven by genetic predispositions or external factors, allows cervical cancer to evade immune surveillance. These insights into the disease's pathogenesis have paved the way for targeted therapies and immunotherapies aimed at restoring immune function and inhibiting key molecular pathways. Despite advances in understanding cervical cancer's underlying mechanisms, current treatment options remain limited to surgery, radiation therapy, and chemotherapy. While effective in some cases, these treatments are often associated with significant side effects and limited efficacy in advanced stages. Consequently, there is an urgent need for novel therapeutic strategies to improve outcomes while minimizing toxicity. Emerging pipeline drugs and investigational therapies are reshaping the treatment landscape by targeting specific molecular pathways. Clinical trials play a vital role in evaluating the safety and efficacy of these new treatments, offering patients access to promising therapies not yet widely available (119).

Research into dysregulated apoptotic pathways offers significant potential for advancing cervical cancer treatment. Caspases, enzymes central to programmed cell death, are often inhibited in cervical cancer, allowing cancer cells to survive and proliferate. Strategies to restore caspase activity or inhibit anti-apoptotic proteins, such as IAPs, have shown promise in preclinical studies. VEGF, a key regulator of angiogenesis, is another critical target. Overexpression of VEGF promotes tumor growth and metastasis by encouraging the formation of new blood vessels. Anti-angiogenic therapies, including VEGF inhibitors like bevacizumab, have demonstrated efficacy in advanced cervical cancer, and research continues to explore similar agents.

Immunotherapy represents a groundbreaking approach to treating cervical cancer by harnessing the body's immune system to combat the disease. Immune checkpoint inhibitors, such as pembrolizumab, have shown promise in clinical trials. These agents block inhibitory signals that prevent immune cells from attacking cancer cells. Combining immune checkpoint

inhibitors with chemotherapy or radiotherapy is being explored to enhance their effectiveness. Additionally, HPV vaccines, such as Gardasil and Cervarix, have proven effective in preventing high-risk HPV infections. While vaccination programs have significantly reduced HPV infection rates in high-income countries, challenges related to cost, infrastructure, and awareness hinder their implementation in LMICs. Expanding vaccine access and integrating them into national immunization programs could drastically reduce the global burden of cervical cancer. Combination therapies are a promising avenue for improving outcomes. By integrating targeted therapies, immunotherapies, and traditional treatments, these approaches can enhance efficacy and reduce resistance. For example, combining VEGF inhibitors with immune checkpoint inhibitors has shown potential in preclinical studies and is currently being evaluated in clinical trials. Advances in genomics and bioinformatics have enabled the identification of novel therapeutic targets, facilitating the development of precision medicine approaches. However, challenges such as high costs, limited access to clinical trials, and healthcare disparities must be addressed to ensure equitable access to these innovations. Collaborative efforts among governments, healthcare organizations, and the pharmaceutical industry are essential to overcoming these barriers (120).

1.4.1 Natural Products in Cervical Cancer Research

Cervical cancer is the fourth most common cancer among women globally, responsible for significant morbidity and mortality. Advances in therapeutics and prevention, including vaccines and screening programs, have contributed to reductions in incidence and mortality. However, challenges persist, particularly for advanced and recurrent stages where survival rates remain alarmingly low. Researchers are investigating novel therapeutic agents and strategies, including apoptosis inducers, immune checkpoint inhibitors, and natural compounds, which offer promising new avenues for treatment.

Natural products derived from plants and microorganisms have garnered attention for their anticancer properties. These compounds offer several advantages, including low toxicity and the ability to target multiple pathways.

Plant-Derived Compounds

Curcumin, extracted from *Curcuma longa*, and thymoquinone from *Nigella sativa* have demonstrated significant anticancer activity. Curcumin promotes apoptosis through reactive oxygen species (ROS)-mediated mitochondrial pathways, while thymoquinone inhibits migration and invasion of cervical cancer cells by modulating epithelial-to-mesenchymal transition (EMT)-related pathways. Other notable plant-derived agents include tanshinone IIA from *Danshen*, which induces apoptosis via a p53-dependent pathway; carnosic acid from rosemary, which exerts antioxidant and anticancer effects by modulating mitochondrial signaling; and protodioscin, a saponin from *Dioscorea* species, which triggers apoptosis through ROS-mediated ER stress (121).

Microbial-Derived Compounds

Secondary metabolites from microorganisms exhibit potent anticancer properties. Gliotoxin, a product of marine fungi, and rosoloactone from endophytic fungi induce apoptosis via intrinsic pathways. These findings highlight the potential of microbial products as a rich source of novel anticancer agents (122).

1.4.2 Pharmacological Mechanisms and Preclinical Advances

Drug Discovery and Development

The preclinical pipeline for cervical cancer therapy includes small molecules, biologics, and synthetic derivatives targeting specific molecular pathways. Structural modifications of natural products, such as curcumin analogs (MS17) and resveratrol derivatives (MPDB), enhance bioavailability and anticancer efficacy. Novel small molecules, including biphenylurea derivatives and quinazoline compounds, exhibit potent antitumor activity by inducing apoptosis and disrupting cell cycle progression.

Mechanisms Under Investigation

Preclinical studies have identified several mechanisms of action for emerging drugs. For example, nelfinavir induces ER stress, leading to apoptosis via the unfolded protein response. Protodioscin targets mitochondrial pathways and promotes cancer cell death by disrupting

mitochondrial membrane potential. Additionally, compounds that suppress E6 and E7 oncoproteins restore p53 function and enable apoptosis, addressing the primary drivers of HPV-associated cervical cancers.

Combination Therapies in Preclinical Models

Combining therapeutic agents is a key strategy to overcome resistance and enhance efficacy. Preclinical models show that combining cisplatin with VEGF inhibitors or PI3K/Akt inhibitors results in synergistic effects. Similarly, immune checkpoint inhibitors combined with radiation therapy amplify immune responses while directly damaging tumor cells.

Challenges and Future Directions

Despite promising advances, several challenges remain in developing and implementing novel therapies for cervical cancer:

1. **High Cost and Accessibility**: Many new treatments are prohibitively expensive, limiting their availability in low- and middle-income countries (LMICs), where the burden of cervical cancer is highest.
2. **Toxicity and Side Effects**: Although targeted therapies often have fewer side effects than conventional treatments, some novel agents still pose significant toxicity concerns.
3. **Clinical Trial Participation**: Enrollment in clinical trials remains low, particularly in LMICs, due to lack of awareness, infrastructure, and accessibility.
4. **Toxicity and Safety in Preclinical Studies**: Many promising agents fail to advance due to unacceptable toxicity profiles.
5. **Drug Resistance**: Tumors often develop resistance through compensatory activation of alternative pathways, presenting a major hurdle in treatment efficacy.

1.5 Conclusion

Natural products have been integral to the development of modern pharmaceuticals, offering a wealth of bioactive compounds with diverse pharmacological activities. Historically, many drugs derived from plants, animals, and microorganisms have formed the foundation of treatment for a wide array of diseases, including cancer, cardiovascular conditions, and

infectious diseases. These naturally occurring compounds have been studied for their ability to interact with biological targets, providing novel mechanisms of action. The discovery of natural products continues to be crucial in the search for new therapies, especially when synthetic options are limited or less effective. In drug development, natural products play a crucial role as sources of lead compounds that can be further modified or synthesized for therapeutic purposes. Their unique chemical structures often present opportunities for the development of drugs with fewer side effects and more specific actions. Moreover, the chemical diversity inherent in natural products provides an extensive pool of compounds to explore for novel drug development, particularly in areas like cancer research, where existing therapies may fail to address all aspects of disease progression. The pharmacology of *Apamanamixis polystachya*, a plant indigenous to certain regions, has shown promising potential in various studies. This plant is recognized for its diverse bioactive compounds, including alkaloids, flavonoids, and terpenoids, which have demonstrated significant pharmacological activities. Research indicates that these compounds may exert anti-inflammatory, antioxidant, and anticancer effects, making *Apamanamixis polystachya* a candidate for further exploration in drug development. The plant's role in oncology, particularly in the treatment of cervical cancer, is being actively studied, with preliminary results suggesting its efficacy in inhibiting the growth of cancer cells, enhancing apoptosis, and possibly sensitizing tumor cells to other chemotherapeutic agents. Cervical cancer remains a significant public health concern, being one of the most common types of cancer in women worldwide. Despite advances in prevention and early detection through screening and vaccination, treatment options for advanced stages of cervical cancer remain limited. Traditional treatments such as surgery, radiation, and chemotherapy have been used, but they are often associated with severe side effects and limited effectiveness in certain cases. This has spurred interest in alternative and complementary therapies, with natural products emerging as promising candidates. The role of natural products in cervical cancer therapy is particularly noteworthy. Many natural compounds have been found to possess anticancer properties that can selectively target tumor cells while minimizing damage to healthy tissues. These properties are crucial in overcoming the challenges posed by conventional treatments, which often result in debilitating side effects. *Apamanamixis polystachya* is one such natural product that holds potential in cervical cancer treatment, with studies suggesting its ability to inhibit tumor

growth, reduce metastasis, and improve the overall therapeutic outcome when used in combination with other treatments. In conclusion, natural products continue to serve as an invaluable resource in drug development, particularly in the realm of oncology. The pharmacological potential of plants like *Apamanamixis polystachya* offers hope for the development of new and more effective therapies for challenging diseases such as cervical cancer. Future research and clinical trials are essential to unlock the full potential of these natural compounds, paving the way for more targeted and less toxic cancer treatments.

1.6 Objectives of current investigation

The main focus of the current study is to explore the anti-cancer potential phytomolecules that is isolated from *Aphanamixis polystachya*, a pharmacologically relevant species. The objectives of the research work includes:

- Isolation and Cytotoxicity Evaluation: Isolate phytomolecules from *Aphanamixis polystachya* and assess their cytotoxic effects on various cancer cells to identify promising compounds for cancer treatment.
- Anticancer Potential of Niloticin in HeLa Cells: Investigate the anticancer efficacy of niloticin in the HeLa cervical cancer cell line by analyzing cell viability and apoptosis.
- Anticancer Potential of Prieurianin in SiHa Cells: Evaluate prieurianin's potential against SiHa cervical cancer cells, focusing on its growth-inhibitory and apoptotic effects.
- Antimetastatic and Antiangiogenic Evaluation: Examine the ability of niloticin and prieurianin to inhibit metastasis and angiogenesis in 4T1 triple-negative cancer cells and Ea.hy 926 endothelial cells.

Through these objectives, the research aims to provides a deeper understanding of relevance of niloticin and prieurianin for its anticancer activities, and giving a preliminary insights into its anti-metastatic and anti-angiogenic activities through *in vitro* systems.

1.7 References

1. Newman DJ, Cragg GM. Natural products as sources of new drugs over the 30 years from 1981 to 2010. J Nat Prod. 2012;75(3):311-335.

2. Wani MC, Taylor HL, Wall ME, Coggon P, McPhail AT. Plant antitumor agents. VI. The isolation and structure of taxol, a novel antileukemic and antitumor agent from Taxus brevifolia. J Am Chem Soc. 1971;93(9):2325-2327.

3. Tu YY. Artemisinin—a gift from traditional Chinese medicine to the world (Nobel Lecture). Angew Chem Int Ed. 2016;55(35):10210-10226.

4. Wright GD. Unlocking the potential of natural products in drug discovery. Microb Biotechnol. 2017;10(5):1004-1007.

5. Ziemert N, Alanjary M, Weber T. The evolution of genome mining in microbes—a review. Nat Prod Rep. 2016;33(8):988-1005.

6. Harvey AL, Edrada-Ebel R, Quinn RJ. The re-emergence of natural products for drug discovery in the genomics era. Nat Rev Drug Discov. 2015;14(2):111-129.

7. Atanasov AG, Waltenberger B, Pferschy-Wenzig EM, et al. Discovery and resupply of pharmacologically active plant-derived natural products: A review. Biotechnol Adv. 2015;33(8):1582-1614.

8. Dias DA, Urban S, Roessner U. A historical overview of natural products in drug discovery. Metabolites. 2012;2(4):303-336.

9. Atanasov AG, Zotchev SB, Dirsch VM, et al. Natural products in drug discovery: Advances and opportunities. Nat Rev Drug Discov. 2021;20(3):200-216

10. Harvey AL, Edrada-Ebel R, Quinn RJ. The re-emergence of natural products for drug discovery in the genomics era. Nat Rev Drug Discov. 2015;14(2):111-129.

11. Jones PA, Ohtani H, Chakravarthy A, De Carvalho DD. Epigenetic therapy in immune-oncology. Nat Rev Cancer. 2019;19(3):151-161.

12. Phi LTH, Sari IN, Yang YG, et al. Cancer stem cells (CSCs) in drug resistance and their therapeutic implications in cancer treatment. Stem Cells Int. 2018;2018:5416923.

13. Piro G, Carbone C, Cataldo I, et al. An overview of cancer drug resistance: mechanisms, treatments, and strategies. Front Oncol. 2022;12:809322.

14. Gabrilovich DI, Nagaraj S. Myeloid-derived suppressor cells as regulators of the immune system. Nat Rev Immunol. 2009;9(3):162-174.

15. Aggarwal BB, Gupta SC, Sung B. Curcumin: an orally bioavailable blocker of TNF and other pro-inflammatory biomarkers. Br J Pharmacol. 2013;169(8):1672-1692.

16. Atanasov AG, Waltenberger B, Pferschy-Wenzig EM, et al. Discovery and resupply of pharmacologically active plant-derived natural products: a review. Biotechnol Adv. 2015;33(8):1582-1614.

17. Demain AL, Vaishnav P. Natural products for cancer chemotherapy. Microb Biotechnol. 2011;4(6):687-699.

18. Hua, P., Edmonds, J.M., 2008. Toona (Endlicher) M. Roemer. Fam. Nat. Syn. Monogr. 1(131), 1846. Flora of China 11, 125.

19. Cai, J.Y., Zhang, Y., Luo, S.H., Chen, D.Z., Tang, G.H., Yuan, C.M., Di, Y.T., Li, S.H., Hao, X.J., He, H.P., 2012. Aphanamixoid A, a potent defensive limonoid, with a new carbon skeleton from Aphanamixis polystachya. Org. Lett. 14, 2524–2527.

20. Ghani, A., 1998. Medicinal Plants of Bangladesh: Chemical Constituents and Uses. Asiat.Soc. Bangladesh. Rahman, M.M., Khan, M.A., 2013. Anti-cancer potential of South Asian plants. Nat. Products Bioprospect.

21. Rahmatullah, M., Rahman, L., Rehana, F., Kalpana, M.A., Khatun, M.A., Jahan, R., Taufiq-ur-Rahman, M., Bashar, A.A., Azad, A., 2010. A scientific evaluation of medicinal plants used in the folk medicinal system of five villages in Narsinghdi District Mohammed Rahmatullah: a scientific evaluation of medicinal plants used in the folk medicinal system of five villages in narsinghdi distri. Bangladesh Am.- Eurasian J. Sustain. Agric. 4, 55–64.

22. Sanyal, M., Datta, P.C., 1981. Pharmacognosy of Aphanamixis polystachya stem bark. Q. J. Crude Drug Res. 19, 113–126.

23. Harmon, A.D., Weiss, U., Silverton, J.V., 1979. The structure of rohitukine, the main alkaloid of Amoora rohituka (Syn. Aphanamixis polystachya) (meliaceae).

24. Lin, C.J., Lo, I.W., Lin, Y.C., Chen, S.Y., Chien, C.Te, Kuo, Y.H., Hwang, T.L., Liou, S.S., Shen, Y.C., 2016. Tetranortriterpenes and limonoids from the roots of aphanamixis polystachya. Molecules 21.

25. Valan, M.F., 2014. Isolation and characterisation of the active principle from the bark of Aphanamixis polystachya. Asian J. Pharm. Res. 4, 19–23.

26. Sajeeb, B.K., Uddin, M.Z., Bachar, R., Bachar, S.C., 2022. Ethnobotanical Study on Medicinal Plants Used by the Ethnic People of Khagrachhari District, Bangladesh. Dhaka Univ. J. Pharm. Sci. 21, 217–230.

27. Rahmatullah, M., Ferdausi, D., Mollik, M.A.H., Kabidul, M.N., Taufiq-Ur-Rahman, M., Jahan, R., 2009a. Ethnomedicinal Survey of Bheramara Area in Kushtia District, Bangladesh. J. Sustain. Agric. 3, 534–541.

28. Singh, R.K., Ranjan, A., Srivastava, A.K., Singh, M., Shukla, A.K., Atri, N., Mishra, A., Singh, A.K., Singh, S.K., 2020. Cytotoxic and apoptotic inducing activity of Amoora rohituka leaf extracts in human breast cancer cells. J. Ayurveda Integr. Med. 11, 383–390.

29. Sen, S., Chakraborty, R., De, B., Devanna, N., 2011. An ethnobotanical survey of medicinal plants used by ethnic people in West and South district of Tripura. India. J. For. Res. 22, 417–426.

30. Kundu AB, Ray S, Chatterjee A. A novel sesquiterpene from Curcuma longa. *Phytochemistry.* 1985;24(9):2123–5.

31. Chen DH, Li SG, Peng S, et al. Natural products targeting epigenetic modulation in cancer. *Phytochemistry.* 2020;177:112449.

32. Yu BJ, Feng SR, Chen JY, et al. Structural elucidation of anticancer compounds. *J Org Chem.* 2020;85(13):8597–602.

33. Wang JS, Zhang Y, Wang XB, et al. Targeting cancer stem cells with natural products. *Tetrahedron.* 2012;68(2):3963–71.

34. Yang SP, Chen HD, Liao SG. Discovery of natural epigenetic modifiers. *Org Lett.* 2011;13(2):150–3.

35. Brown DA, Taylor DAH. Phytochemical investigations of anticancer agents. *Phytochemistry.* 1978;17(8):1995–9.

36. Kishi K, Yoshikawa K, Arihara S. Bioactive constituents from natural sources. *Phytochemistry.* 1992;31(5):1335–8.

37. Agnihotri VK, Srivastava SD, Srivastava SK. A review of chemopreventive natural products. *Curr Sci.* 1987;56(15):770–1.

38. Cai JY, Zhang Y, Luo SH. Marine-derived anticancer compounds. *Org Lett.* 2012;14(11):2524–7.

39. Chen JY, Cao DZ, Li SH, et al. Immunomodulatory properties of medicinal plants. *J Nat Prod.* 2014;77(3):472–82.

40. Wang HF, Zhang XP, Wang Y, et al. Overcoming drug resistance using natural compounds. *Fitoterapia.* 2013;90:126–31.

41. Wang XZ, Feng FH, He WJ, et al. Nanotechnology-enhanced natural products. *Fitoterapia.* 2020;140:104431.

42. Lee JH, Kakuda N, Iwasaki T, et al. Structure-function relationships in anticancer natural products. *Chem Pharm Bull.* 2007;55(8):1151–6.

43. Nishizawa M, Inoue A, Hayashi Y. Advances in organic synthesis of natural compounds. *J Org Chem.* 1984;49(20):3660–2.

44. Chowdhury R, Hasan CM, Rashid MA. Potential anticancer agents from medicinal plants. *Phytochemistry.* 2003;62(8):1213–6.

45. Talukder FA, Howse PE. Pesticidal and anticancer activities of plant products. *J Plant Dis Prot.* 2000;107(5):498–504.

46. Harmon AD, Weiss U, Silverton JV. Synthesis and activity of anticancer sesquiterpenes. *Tetrahedron Lett.* 1979;8:721–4.

47. Srivastava SK, Agnihotri VK. Mechanistic insights into cancer therapy using natural products. *Curr Sci.* 1985;54(1):38–40.

48. Srivastava SK, Srivastava SD, Srivastava S. Alkaloids in cancer chemoprevention. *Indian J Chem B.* 2003;42(12):3155–8.

49. Albano, E., 2006. Alcohol, oxidative stress and free radical damage. Proc. Nutr. Soc. 65, 278–290.

50. Rahman, M.M., Shahab, N.B., Miah, P., Rahaman, M.M., Kabir, A.U., Subhan, N., Khan, A.A., Afroze, M., Khan, M., Ahmed, K.S., Hossain, H., Haque, M.A., Alam, M. A., 2021.

Polyphenol-rich leaf of Aphanamixis polystachya averts liver inflammation, fibrogenesis and oxidative stress in ovariectomized Long-Evans rats. Biomed. Pharmacother. 138

51. Krishnaraju, A.V., Rao, C.V., Rao, T.V.N., Reddy, K.N., Trimurtulu, G., 2009. *In vitro* and *in vivo* antioxidant activity of aphanamixis polystachya bark. Am. J. Infect. Dis. 5, 60–67.

52. Apu, A.S., Chowdhury, F.A., Khatun, F., Jamaluddin, A.T.M., Pathan, A.H., Pal, A., 2013. Phytochemical screening and *in vitro* evaluation of pharmacological activities of Aphanamixis polystachya (Wall) Parker fruit extracts. Trop. J. Pharm. Res. 12, 111–116.

53. Baruah, G., Kalita, D.J., Goswami, A.K., Baishya, D.J., Deka, N., 2016. Free radical scavenging potential and antibacterial activity of leaves of aphanamixis polystachya (WALL.) RN Parker. Eur. J. Biomed. 3, 309–313.

54. Umesh, M.K., Sanjeevkumar, C.B., Londonkar, R.L., 2016. Evaluation of phenolics content and *in vitro* antioxidant activities of methanolic extract of Amoora rohituka Bark. Int. J. Curr. Microbiol. Appl. Sci. 5, 225–235.

55. Sharma, J.N., Al-Omran, A., Parvathy, S.S., 2007. Role of nitric oxide in inflammatory diseases. Inflammopharmacology 15, 252–259.

56. Xue, S., Zhang, P., Tang, P., Wang, C., Kong, L., Luo, J., 2020. Acyclic diterpene and norsesquiterpene from the seed of Aphanamixis polystachya. Fitoterapia 142.

57. Zhang, P., Xue, S., Tang, P., Cui, Z., Wang, Z., Luo, J., Kong, L., 2021. Aphamines A–C, dimeric acyclic diterpene enantiomers from Aphanamixis polystachya. Chin. Chem. Lett. 32, 1480–1484.

58. Yang, B.J., Fan, S.R., Cai, J.Y., Wang, Y.T., Jing, C.X., Guo, J.J., Chen, D.Z., Hao, X.J., 2020. Aphananoid A is an anti-inflammatory limonoid with a new 5/6/5 fused ring featuring a C24Carbon skeleton from aphanamixis polystachya. J. Org. Chem. 85, 8597–8602.

59. Maioli, N.A., Zarpelon, A.C., Mizokami, S.S., Calixto-Campos, C., Guazelli, C.F.S., Hohmann, M.S.N., Pinho-Ribeiro, F.A., Carvalho, T.T., Manchope, M.F., Ferraz, C.R., Casagrande, R., Verri, W.A., 2015. The superoxide anion donor, potassium superoxide, induces pain and inflammation in mice through production of reactive oxygen species and cyclooxygenase-2. Braz. J. Med. Biol. Res. 48, 321–331.

60. Shariare, M.H., Rahman, M., Lubna, S.R., Roy, R.S., Abedin, J., Marzan, A.L., Altamimi, M.A., Ahamad, S.R., Ahmad, A., Alanazi, F.K., Kazi, M., 2020. Liposomal drug delivery of Aphanamixis polystachya leaf extracts and its neurobehavioral activity in mice model. Sci. Rep. 10, 1–16.

61. Yadav, R., Kashaw, V., 2018. Evaluation of anti-inflammatory activity of alcoholic, hydroalcoholic and aqueous extract of Amoora Rohituka and Soymida Febrifuga in albino rats. Asian J. Pharm. Pharmacol. 4, 908–913.

62. Phillips, R.E., Pasvol, G., 1992. Anaemia of Plasmodium falciparum malaria. Baillieres. Clin. Haematol. 5, 315–330.

63. White, N.J., 2018. Anaemia and malaria 11 medical and health sciences 1108 medical microbiology 11 medical and health sciences 1103 clinical sciences. Malar. J.

64. MacKinnon, S., Durst, T., Arnason, J.T., Angerhofer, C., Pezzuto, J., Sanchez-Vindas, P.E., Poveda, L.J., Gbeassor, M., 1997. Antimalarial activity of tropical Meliaceae extracts and gedunin derivatives. J. Nat. Prod. 60, 336–341.

65. Narayanaswamy, R., Wai, L.K., Ismail, I.S., 2017. Natural compounds as inhibitors of plasmodium falciparum enoyl-acyl carrier protein reductase (PfENR): an *in silico* study. J. Chosun Nat. Sci. 10, 1–6.

66. Nagar, H., Tiwari, P., Jain, D.K., Chandel, H.S., 2012. Evaluation of Anti-ulcer activity of stem bark extract of Aphanmixis polystachya in experimental rats. Ind. J. Pharm. Educ. Res. 46, 222–227.

67. Martin, R.J., 1997. Modes of action of anthelmintic drugs. Vet. J. 154, 11–34. https://doi.org/10.1016/S1090-0233(05)80005-X.

68. Haque, M.E., M.M.R.-, undefined 2020, 2020. Evaluation of in vitro anthelmintic and antifungal activity of different organic extracts of the seeds of aphanamixis polystachya (Wall.). pharmacologyonline.silae.it 2, 281–292.

69. Tanveer, R.K., Palash, K., Rana, B., Mafruhi, S.M., Das, A., 2013. Evaluation of cytotoxic and anthelmintic activities of bark extract of aphanamixis polystachya (WALL.). Int. Res. J. Pharm. 4, 126–129.

70. Amin, M.N., Majumder, M.S., Moghal, M.M.R., Banik, S., Kar, A., Hossain, M.M., 2014. Anthelmintic and cytotoxic activities of two medicinal plants: polygonum viscosum and Aphanamixis polystachya growing in Bangladesh. J. Sci. Res. 6, 339–345.

71. Alam, U., Asghar, O., Azmi, S., Malik, R.A., 2014. General aspects of diabetes mellitus. Handb. Clin. Neurol.

72. Tiwari, P., Loksh, K.R., Yadav, R., 2019. Antihyperglycemic effect of methanolic extract of aphanamixis polystachya leaves on streptozotocin-induced diabetic rats. J. Drug Deliv. Ther. 9, 783–787.

73. Andallu, B., Kumar, A.V., Varadacharyulu, N., 2009. Lipid abnormalities in streptozotocin-diabetes: amelioration by morus indica L. cv Suguna leaves. Int. J. Diabetes Dev. Ctries. 29, 123–128.

74. Akter, K.M., Sajib, N.H., Kang, D.M., Ahn, M.J., Uddin, S.B., 2021. Ethnomedicinal study of plants in Begumganj, Noakhali, Bangladesh. Nat. Prod. Sci.

75. Chowdhury, R., Rashid, R.B., 2003. Effect of the crude extracts of Amoora rohituka stem bark on gastrointestinal transit in mice. Indian J. Pharmacol. 35, 304–307.

76. Zhang, L., Ismail, M.M., Rocchetti, G., Fayek, N.M., Lucini, L., Saber, F.R., 2022. The untargeted phytochemical profile of three meliaceae species related to *in vitro* cytotoxicity and anti-virulence activity against MRSA isolates. Molecules 27.

77. Lu, L., Hu, W., Tian, Z., Yuan, D., Yi, G., Zhou, Y., Cheng, Q., Zhu, J., Li, M., 2019. Developing natural products as potential anti-biofilm agents. Chin. Med. (United Kingdom).

78. Quelemes, P.V., Perfeito, M.L.G., Guimar˜aes, M.A., Santos, R.C.Dos, Lima, D.F., Nascimento, C., Silva, M.P.N., Soares, M.J.D.S., Ropke, C.D., Eaton, P., Moraes, J.De, Leite, J.R.S.A., 2015. Effect of neem (Azadirachta indica A. Juss) leaf extract on resistant Staphylococcus aureus biofilm formation and Schistosoma mansoni worms. J. Ethnopharmacol. 175, 287–294.

79. Mohamed, J.A., Huang, D.B., 2007. Biofilm formation by enterococci. J. Med. Microbiol.

80. Saklani, S., Mishra, A.P., Sati, B., Sati, H., 2012. Pharmacognostic, phytochemical and antimicrobial screening of Aphanamixis polystachya, an endangered medicinal tree. Int. J. Pharm. Pharm. Sci. 4, 235–240.

81. Chowdhury, R., Hasan, C.M., Rashid, M.A., 2003b. Antimicrobial activity of Toona ciliata and Amoora rohituka. Fitoterapia 74, 155–158.

82. Paul, G.K., Mahmud, S., Hasan, M.M., Zaman, S., Uddin, M.S., Saleh, M.A., 2021. Biochemical and in silico study of leaf and bark extracts from Aphanamixis polystachya against common pathogenic bacteria. Saudi J. Biol. Sci. 28, 6592–6605.

83. Shadid, H.M., Snigdha, H., Ali, R., Das, D.K., Wadud, M.A., 2016. Biological evaluation of ethanolic extract of Aphanamixis polystachya (Wall.) Parker leaf. Int. J. Adv. Multidiscip. Res. 3, 13–21.

84. Aboutabl, E.A., El-Sakhawy, F.S., Fathy, M.M., Megid, R.M.A., 2000. Composition and antimicrobial activity of the leaf and fruit oils from amoora rohituka wigth. Et arn. J. Essent. Oil Res. 12, 635–638.

85. Andrews, J.M., 2001. Determination of minimum inhibitory concentrations. J. Antimicrob. Chemother. 48, 5–16.

86. Rahman, M., Ahad, A., Saha, S.K., Hong, J., Kim, K.-.H., 2017. Antibacterial and phytochemical properties of Aphanamixis polystachya essential oil.

87. Tan, T.N., Trung, H.T., Dang, Q.Le, Thi, H.V., Vu, H.D., Ngoc, T.N., Do, H.T.T., Nguyen, T.H., Quang, D.N., Dinh, T.T., 2021. Characterization and antifungal activity of limonoid constituents isolated from Meliaceae Plants Melia dubia, Aphanamixis polystachya, and Swietenia macrophylla against plant pathogenic fungi *in vitro*. J. Chem. 2021, 1–12.

88. Zhang, Y., Wang, J.S., Wang, X.B., Gu, Y.C., Wei, D.D., Guo, C., Yang, M.H., Kong, L.Y., 2013b. Limonoids from the fruits of Aphanamixis polystachya (meliaceae) and their biological activities. J. Agric. Food Chem. 61, 2171–2182.

89. Srivastava, S.K., Srivastava, So, Srivastava, Soumya, 2003. Note New biologically active limonoids and fla-vonoids from Aphanamixis polystachya. Indian J. Chem. 42, 3155–3158.

90. Majumder, M.S., Hossain, D.M.S., Amin, M.N., Moghal, M.M.R., Banik, S., Hossain, M.M., 2014. Charactarization of chemical groups and study of antioxidant, antimicrobial and thrombolytic activities of aphanamixis polystachya (stem bark). World J. Pharm. Pharm. Sci. 3, 58–72.

91. Bhuyan, M.A.K., Begum, J., Chowdhury, J.U., Ahmed, K., Anwar, M.N., 2000. Antimicrobial activity of oil and crude alkaloids from seeds of Aphanamixis polystachya (Wall.) RN Parker. Bangladesh J. Bot. 29, 1–5.

92. Adibhatla, R.M., Hatcher, J.F., 2008. Tissue plasminogen activator (tPA) and matrix metalloproteinases in the pathogenesis of stroke: therapeutic strategies. CNS Neurol. Disord. Targets (Formerly Curr. Drug Targets-CNS Neurol. Disord. 7, 243–253.

93. Banik, S.K., Iftekhar, S., Rahman, A., Bari, M.L., Islam, M.S., 2021. Bioactive potential of Aphanamixis polystachya seed extracts. Bangladesh J. Sci. Ind. Res. 56, 75–86.

94. Koul, O., Daniewski, W.M., Multani, J.S., Gumulka, M., Singh, G., 2003. Antifeedant Effects of the Limonoids from Entandrophragma candolei (Meliaceae) on the Gram Pod Borer, Helicoverpa armigera (Lepidoptera: noctuidae). J. Agric. Food Chem. 51, 7271–7275.

95. Talukder, F.A., Howse, P.E., 1995. Evaluation of Aphanamixis polystachya as a source of repellents, antifeedants, toxicants and protectants in storage against Tribolium castaneum (Herbst). J. Stored Prod. Res. 31, 55–61.

96. Cai, J.Y., Chen, D.Z., Luo, S.H., Kong, N.C., Zhang, Y., Di, Y.T., Zhang, Q., Hua, J., Jing, S. X., Li, S.L., Li, S.H., Hao, X.J., He, H.P., 2014. Limonoids from Aphanamixis polystachya and their antifeedant activity. J. Nat. Prod. 77, 472–482.

97. Parola, M., Leonarduzzi, G., Robino, G., Albano, E., Poli, G., Dianzani, M.U., 1996. On the role of lipid peroxidation in the pathogenesis of liver damage induced by long-standing cholestasis. Free Radic. Biol. Med. 20, 351–359.

98. Boll, M., Lutz, W.D., Becker, E., Stampfl, A., 2001. Mechanism of carbon tetrachloride-induced hepatotoxicity. Hepatocellular damage by reactive carbon tetrachloride metabolites. Z. Naturforsch. C 56, 649–659.

99. Gole, M.K., Dasgupta, S., 2002. Role of plant metabolites in toxic liver injury. Asia Pac. J. Clin. Nutr. 11, 48–50.

100. Kinney, J.W., Bemiller, S.M., Murtishaw, A.S., Leisgang, A.M., Salazar, A.M., Lamb, B.T., 2018. Inflammation as a central mechanism in Alzheimer's disease. Alzheimer's Dement. Transl. Res. Clin. Interv.

101. Meng, X., Li, N., Zhang, Y., Fan, D., Yang, C., Li, H., Guo, D., Pan, S., 2018. Beneficial effect of b-elemene alone and in combination with hyperbaric oxygen in traumatic brain injury by inflammatory pathway. Transl. Neurosci. 9, 33–37.

102. Hossain, M.M., Biva, J., Jahangir, R., Mynol, M., Vhuiyan, I., 2009. Central nervous system depressant and analgesic activity of Aphanamixis polystachya (Wall.) parker leaf extract in mice. Afr. J. Pharm. Pharmacol. 3, 282–286.

103. Ali, R., Snigdha, H.M.S.H., Ali, M.A., 2016. Comparative preliminary phytochemical and analgesic activity on methanolic extract of leaf and bark of Aphanamixis polystachya (Wall.) Parker International Journal of Advanced Multidisciplinary Research (IJAMR) comparative preliminary phytochemical and an. Int. J. Adv. Multidiscip. Res. 3, 1–5.

104. Uddin, S.J., Shilpi, J.A., Rouf, R., Ferdous, M.M., Nahar, L., Sarker, S.D., 2006. Antinociceptive activity of some Bangladeshi medicinal plant extracts. Adv. Tradit. Med. 6, 96–101.

105. Rodil, R., Moeder, M., 2008. Stir bar sorptive extraction coupled to thermodesorption-gas chromatography-mass spectrometry for the determination of insect repelling substances in water samples. J. Chromatogr. A 1178, 9–16.

106. Mallik, A.U., 1998. Allelopathy and competition in coniferous forests. Environ. For. Sci. Proc. IUFRO Div. 8 Conf. Environ. For. Sci. https://doi.org/10.1007/978-94-011- 5324-9_33 held 19–23 Oct. 1998, Kyoto Univ. Japan.

107. Bhowmik, O., Yeasmin, S., Islam, A.K.M., Anwar, M., Juraimi, A.S., 2020. Assessment of allelopathic potential of Aphanamixis polystachya on selected field crops. J. Hortic. Postharvest Res. 3, 257–268.

108. Talukder, F.A., Howse, P.E., 1994b. Laboratory evaluation of toxic and repellent properties of the pithraj tree, aphanamixis polystachya wall and parker, against sitophilus oryzae (L). Int. J. Pest Manag. 40, 274–279.

109. Zhang, L., Ismail, M.M., Rocchetti, G., Fayek, N.M., Lucini, L., Saber, F.R., 2022. The untargeted phytochemical profile of three meliaceae species related to *in vitro* cytotoxicity and anti-virulence activity against MRSA isolates. Molecules 27.

110. Ting Wang, Y., rui Fan, S., yun Cai, J., jing Guo, J., fang Zhang, X., juan Yang, B., jiang Hao, X., zhi Chen, D., 2022. Two new cytotoxic cycloartane triterpenoids from Aphanamixis polystachya (Wall.) R. N. Parker. Nat. Prod. Res. 36, 2473–2478.

111. Kumari, G.S., Siva, B., Sambyal, S., Gourishetti, K., Kumar, H.M.S., Balaji, A.S., Ramalingam, V., Babu, K.S., Swarna Kumari, G., Siva, B., Sambyal, S., Gourishetti, K., Sampath Kumar, H.M., Sai Balaji, A., Ramalingam, V., Suresh Babu, K., 2022. Identification of phytoconstituents from the aerial parts of Aphanamixis polystachya and evaluation of their anticancer activities. Phytomedicine Plus 2.

112. Rabi, T., Ramachandran, C., Fonseca, H.B., Nair, R.P.K., Alamo, A., Melnick, S.J., Escalon, E., 2003. Novel drug amooranin induces apoptosis through caspase activity in human breast carcinoma cell lines. Breast Cancer Res. Treat. 80, 321–330.

113. Rabi, T., Karunagaran, D., Nair, M.K., Bhattathiri, V.N., 2002. Cytotoxic activity of amooranin and its derivatives. Phyther. Res. 16

114. Ramachandran, C., Nair, P.K.R., Alamo, A., Cochrane, C.B., Escalon, E., Melnick, S.J., 2006. Anticancer effects of amooranin in human colon carcinoma cell line in vitro and in nude mice xenografts. Int. J. Cancer 119, 2443–2454.

115. Rabi, T., Gupta, R.C., 1995. Antitumor and cytotoxic investigation of Amoora Rohituka. Int. J. Pharmacogn. 33, 359–361. https://doi.org/10.3109/13880209509065396. Rabi, T., Huwiler, A., Zangemeister-Wittke, U., 2014. AMR-Me inhibits PI3K/Akt

116. Rabi, T., Banerjee, S., 2009. Novel semisynthetic triterpenoid AMR-Me inhibits telomerase activity in human leukemic CEM cells and exhibits in vivo antitumor activity against Dalton's lymphoma ascites tumor. Cancer Lett. 278, 156–163.

117. Rabi, T., Huwiler, A., Zangemeister-Wittke, U., 2014. AMR-Me inhibits PI3K/Akt signaling in hormone-dependent MCF-7 breast cancer cells and inactivates NF-$κ$B in hormone-independent MDA-MB-231 cells. Mol. Carcinog. 53, 578–588.

118. Rabi, T., Banerjee, S., 2008. Novel synthetic triterpenoid methyl 25-hydroxy-3-oxoolean-12-en-28-oate induces apoptosis through JNK and p38 MAPK pathways in human breast adenocarcinoma MCF-7 cells. Mol. Carcinog. 47, 415–423.

119. Arbyn M, Anttila A, Jordan J, et al. European guidelines for quality assurance in cervical cancer screening. Second edition–summary document. Ann Oncol. 2010;21(3):448-458.

120. Vaccarella S, Lortet-Tieulent J, Plummer M, et al. Worldwide trends in cervical cancer incidence: impact of screening against changes in disease risk factors. Eur J Cancer. 2013;49(15):3262-3273.

121. Zandi K, Shaterian M, Marzbali MH, et al. Curcumin and its anticancer effects: a review of the molecular mechanisms. J Cancer Res Ther. 2018;14(3):431-439.

122. Rajagopal P, Malathi P, Sundararajan V, et al. Gliotoxin, a potent fungal secondary metabolite, induces apoptosis through intrinsic and extrinsic pathways in human cervical cancer cells. Appl Microbiol Biotechnol. 2015;99(7):3059-3069.

Chapter 2

Exploring the anti-cancer potential of phytomolecules isolated from *Aphanamixis polystachya* and apoptotic evaluation of niloticin in cervical cancer cells

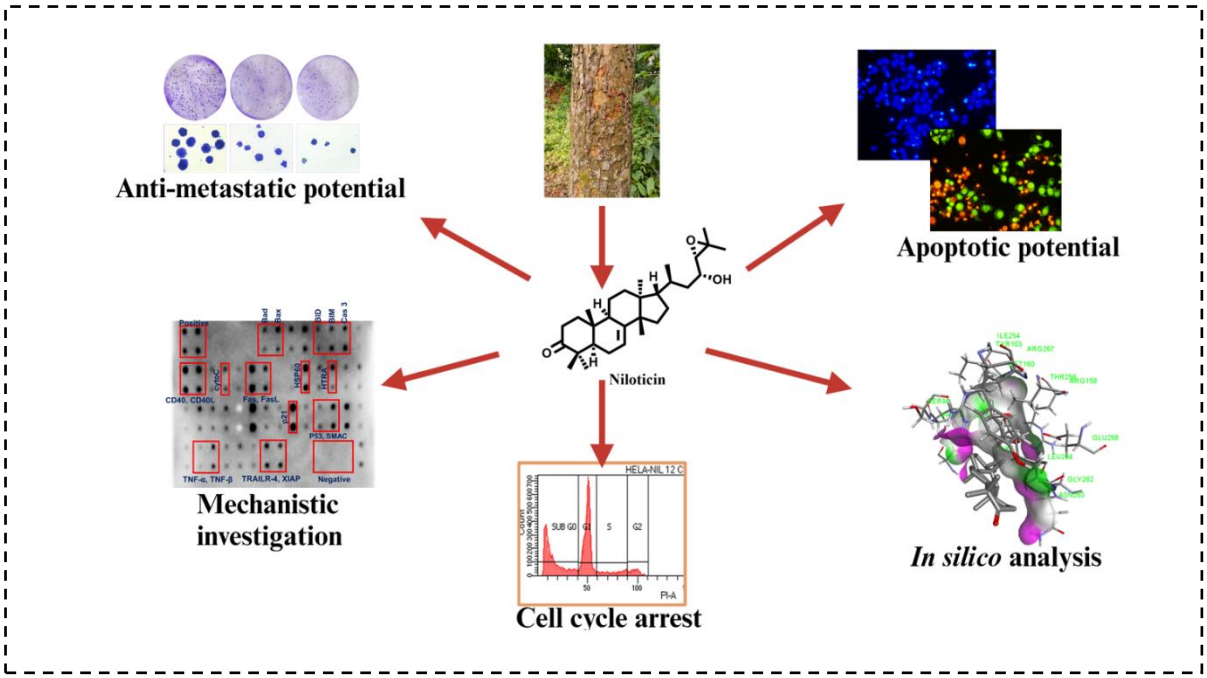

Abstract

Pharmacologically active small organic molecules derived from natural resources are prominent drug candidates due to their inherent structural diversity. Herein, one such bioactive molecule, niloticin was explored, which is a tirucallane-type triterpenoid isolated from the stem barks of Aphanamixis polystachya (Wall.) Parker. After initial screening with other isolated compounds from the same plant, niloticin demonstrated selective cytotoxicity against cervical cancer cells (HeLa) with an IC_{50} value of 11.64 μM. Whereas the compound exhibited minimal cytotoxicity in normal epithelial cell line MCF-10A, with an IC_{50} value of 83.31 μM. Subsequently, in silico molecular docking studies of niloticin based on key apoptotic proteins such as p53, Fas, FasL, and TNF β revealed striking binding affinity, reflecting docking scores of −7.2, −7.1, −6.8, and −7.2. Thus, the binding stability was evaluated through molecular dynamic simulation. In a downstream in vitro process,

the apoptotic capability of niloticin was effectively validated through fluorimetric assays, encompassing nuclear fragmentation. Additionally, an insightful approach involving surface-enhanced Raman spectroscopy (SERS) re-establishes the occurrence of DNA cleavage during cellular apoptosis. Furthermore, niloticin was observed to induce apoptosis through both intrinsic and extrinsic pathways. This was evidenced by the upregulation of upstream regulatory molecules such as CD40 and TNF, which facilitate the activation of caspase 8. Concurrently, niloticin-induced p53 activation augmented the expression of proapoptotic proteins Bax and Bcl-2 and downregulation of IAPs, leading to the release of cytochrome C and subsequent activation of caspase 9. Therefore, the reflection of mitochondrial-mediated apoptosis is in good agreement with molecular docking studies. Furthermore, the anti-metastatic potential was evidenced by wound area closure and Ki67 expression patterns. This pivotal in vitro assessment confirms the possibility of niloticin being a potent anti-cancer drug candidate, and it is evidenced as the first comprehensive anticancer assessment of niloticin in HeLa cells.

2.1 Introduction

Nature has long served as a cornerstone of therapeutic innovation, offering a vast array of bioactive compounds that address a multitude of chronic diseases. Medicinal plants, in particular, have been integral to healthcare resource worldwide, from traditional remedies to modern medicine. Their efficacy, safety, and affordability make them indispensable, even in the era of synthetic drugs. Natural products exhibit unique physicochemical properties, such as high bioactivity, biocompatibility, and bioavailability, which sustain their relevance in drug discovery (1,2). Despite advancements in medical interventions, cancer remains a leading global cause of mortality, with current treatments like chemotherapy, radiation, and surgery often causing collateral damage to healthy cells and tissues. Moreover, the emergence of chemoresistance further complicates cancer management, underscoring the need for novel, effective, and minimally invasive therapies (3-5). Among the various cancers, cervical cancer ranks fourth in incidence and is a major cause of death among women (6). Intensive research seeks to identify compounds that can target cancer cells while minimizing side effects. Natural products are gaining attention for their ability to modulate multiple signaling pathways, regulate cell growth and apoptosis, and activate the immune system, ultimately leading to tumor suppression (7-10). Within this domain, *Aphanamixis polystachya* (Wall.) Parker, commonly known as Amoora rohituka, stands out due to its extensive medicinal properties (11). This plant, a member of

the Meliaceae family, has been traditionally used to treat ailments such as liver and spleen diseases, tumors, abdominal issues, rheumatoid arthritis, and jaundice (12,13). Pharmacologically, it exhibits antibacterial, antifungal, insecticidal, CNS depressant, analgesic, and clot-lysis activities (14,15). Additionally, its ethyl acetate fraction has shown protective effects against gamma radiation-induced chromosomal abnormalities in bone marrow cells, hinting at potential applications in radiation therapy for cancer (16). Niloticin, a tirucallane-type triterpenoid derived from *A. polystachya*, has emerged as a compound of interest due to its diverse biological activities. It inhibits osteoclastogenesis by suppressing RANKL-induced activation of the AKT, MAPK, and NF-κB signaling pathways and functions as an MD-2 antagonist with anti-inflammatory properties (17,18). Niloticin also demonstrates antiplasmodial, anti-respiratory syncytial virus (RSV), and insecticidal activities (19,20). It exhibits cytotoxic effects against various cancer cell lines, including gastric, liver, breast, prostate, fibrosarcoma, and hepatoma cells (21-24). However, its anticancer potential in cervical cancer, specifically HeLa cell proliferation, has not been extensively studied, which formed the basis of the present investigation.

The study focused on isolating and characterizing bioactive compounds from the stem bark of *A. polystachya* to explore their anticancer potential. Initial evaluations of acetone extracts in HeLa cells revealed significant antiproliferative activity. Subsequent isolation yielded five tirucallane-type triterpenoids, characteristic of the Meliaceae family, with niloticin emerging as the most potent compound. Comprehensive anticancer profiling of niloticin revealed its mechanisms of action against cervical cancer cells. *In silico* screening demonstrated niloticin's high binding affinity with key apoptotic pathway proteins, such as p53, Fas receptor, Fas ligand, Bax, CDK2, BCL2, and TNF-β. Complementing these findings, *in vitro* assays elucidated the compound's apoptotic mechanisms. DNA fragmentation analysis by agarose gel electrophoresis, supported by surface-enhanced Raman scattering (SERS), confirmed its apoptotic effects. Niloticin induced sub-G0 cell cycle arrest, corroborated by cell cycle assays and expression analysis of regulatory proteins. Further, fluorometric assays highlighted niloticin's dual-mode apoptosis induction via both intrinsic and extrinsic pathways, validated by molecular docking and protein expression studies. The study also assessed niloticin's anti-metastatic potential through wound healing assays and clonogenic inhibition tests. Immunofluorescence analysis of Ki67 expression further substantiated its ability to suppress cancer cell proliferation. Detailed evaluations of signaling proteins involved in apoptotic pathways

confirmed niloticin's mode of action, positioning it as a promising candidate for further exploration in cervical cancer therapy. This investigation represents the first detailed study of niloticin's anticancer activity in cervical cancer using the HeLa cell line. By demonstrating its ability to modulate key cellular pathways, induce apoptosis, and inhibit metastasis, niloticin emerges as a compelling phytomolecule for potential clinical applications (Scheme 2.1). These findings pave the way for further research into its therapeutic utility, emphasizing its role as a natural product-based approach to cervical cancer treatment.

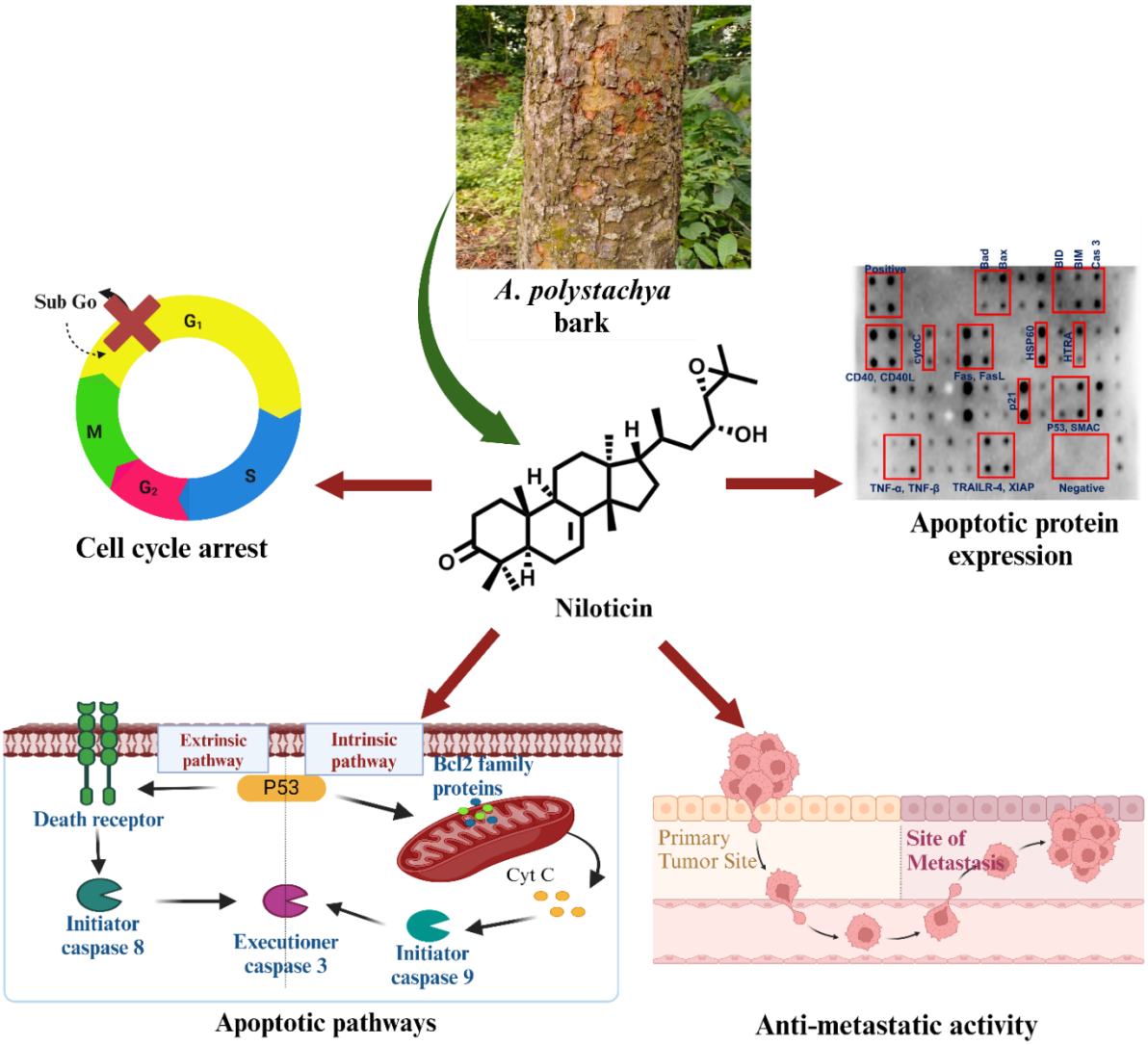

Scheme 2.1: Cell death induced by niloticin through intrinsic and extrinsic modes of apoptosis

2.2 Results and Discussion

2.2.1 Plant material collection and extraction of *A. polystachya* stembark

The stem bark of *Aphanamixis polystachya* was collected in April 2017 from Parassala, Kerala, India, geographically located at 8.3478° N latitude and 77.1410° E longitude. The plant material was authenticated and deposited in the herbarium of the Department of Botany, University of Kerala, Thiruvananthapuram, under the voucher number 2018-06-05. Approximately 1.0 kg of the collected stem bark was air-dried to remove moisture and subsequently ground into a fine powder using a mechanical grinder. The powdered material was subjected to sequential solvent extraction using different solvents based on their polarity. Initially, the powdered bark was extracted with hexane, a non-polar solvent, at room temperature. This process involved soaking the material in 3 liters of hexane for three consecutive days, with gentle stirring to ensure effective extraction. After the extraction period, the mixture was filtered to separate the liquid extract from the plant residue. The filtrate was then concentrated under reduced pressure using a rotary evaporator, resulting in a concentrated hexane extract weighing approximately 5 grams. The remaining plant residue was dried and subsequently subjected to extraction with acetone, a moderately polar solvent. Similar to the hexane extraction, the residue was soaked in 3 liters of acetone for three days at room temperature. The acetone extract was filtered and concentrated under reduced pressure, yielding approximately 20 grams. The next step involved extracting the residue with ethanol, a polar organic solvent. The process was carried out at room temperature with the same solvent volume (3 liters) and duration (3days). This yielded about 30 grams of ethanol extract after filtration and concentration. Finally, the remaining residue underwent extraction using water, a highly polar solvent. Following the same protocol, the water extract was obtained, yielding approximately 16 grams. Each extract - hexane, acetone, ethanol, and water was analyzed to evaluate its cytotoxic properties in preliminary studies. This sequential extraction method, using solvents of increasing polarity, ensured the comprehensive recovery of a wide range of phytochemicals from the stem bark of *A. polystachya*, facilitating further biological evaluation.

2.2.2 Isolation and characterization of compounds from *A. polystachya*

To explore the chemical constituents present in stembarks of *A. polystachya,* each extract underwent detailed purification processes. Thin Layer Chromatography (TLC) was initially employed to analyze the chemical profiles of the extracts and guide the subsequent fractionation process. Based on these observations, the extracts were subjected to column chromatography (CC) using silica gel with a particle size of 100–200 mesh as the stationary

phase. For the hexane extract, column elution commenced with 100% hexane as the mobile phase. Gradual increases in polarity were achieved by incrementally adding ethyl acetate. For the acetone and ethanol extracts, the final stage of elution was carried out using a mixture of 10% methanol in ethyl acetate to ensure the effective separation of polar compounds. A total of 150 fractions, each approximately 200 mL in volume, were collected across all three extracts during the column chromatography process. Based on similarities observed in their TLC profiles, the fractions were pooled into distinct groups. The hexane extract yielded three major fraction pools (FrA.1 to FrA.3), the acetone extract was divided into 19 fraction pools, and the ethanol extract resulted in 12 fraction pools. To further purify the chemical constituents, the pooled fractions underwent repeated column chromatographic separation. A schematic representation summarizing the entire extraction, fractionation, and isolation procedure is provided in Figure 2.1. This iterative process led to the successful isolation of several bioactive compounds, which were subsequently characterized for their structural and biological properties (Figure 2.2). This workflow highlights the systematic approach undertaken to isolate and identify the key bioactive molecules present in *A. polystachya*.

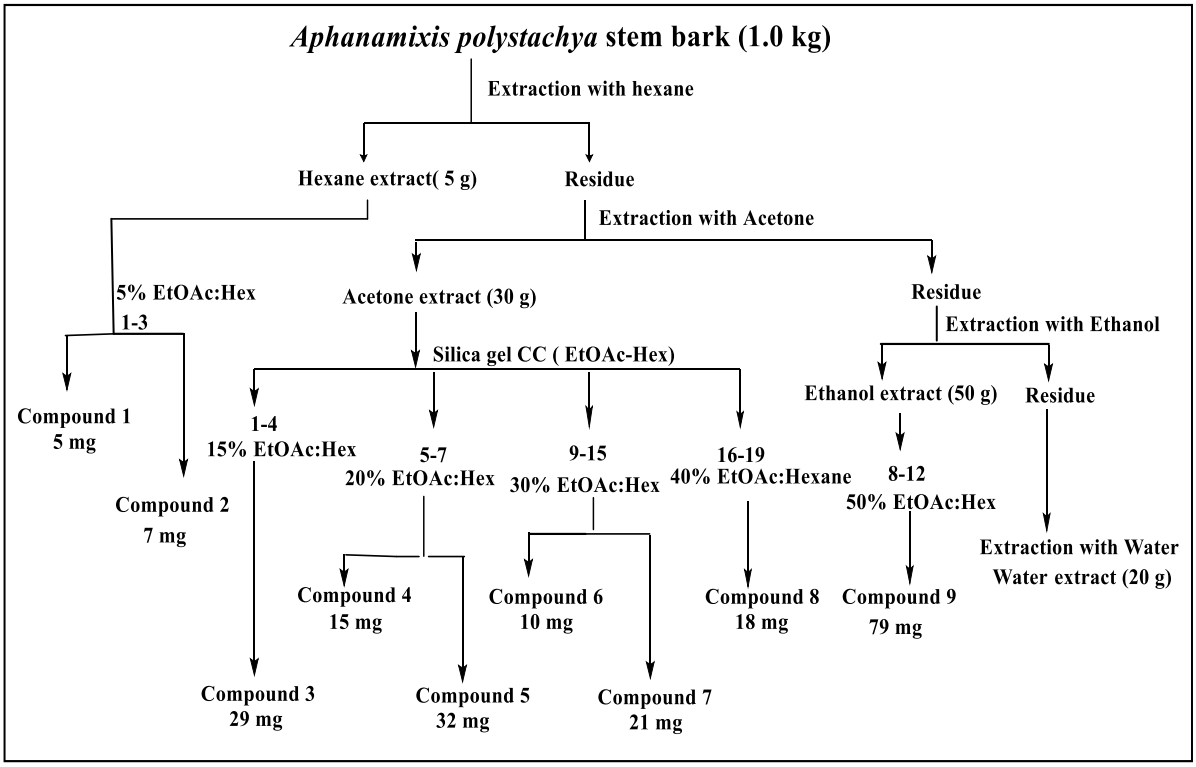

Figure 2.1: Schematic representation of extraction and isolation procedure

2.2.3 Characterisation of isolated molecules

The hexane extract fractions on CC on silica gel (100-200 mesh) using EtOAc: Hexane polarity as eluent afforded compounds **1** and **2**. These two compounds were isolated as UV active colorless liquid after CC separation of fraction pool 1-3 using 5% EtOAc: Hexane. Compound **3** was isolated in 29 mg as a white crystalline solid after the CC of fraction pool 1-4 using 15% EtOAc: Hexane. While doing CC of fraction pool 5-7 with 20% EtOAc: Hexane, compounds **4** and **5** were obtained as colorless crystals with 15 and 32 mg, respectively. After repeated CC of fraction pool 5-7, compound **5** was obtained as a white crystalline solid. Compound **5** possessed a molecular formula $C_{30}H_{48}NaO_3$, as obtained by its HRMS data at *m/z* 479.3501 $[M+Na]^+$ (Calcd. for $C_{30}H_{48}NaO_3$, 479.3496). Fraction pool 9-15 of acetone extract showed the presence of a UV inactive spot. The TLC turned into a green colour on charring in Enhollm yellow solution. The fraction on CC separation using 30% EtOAc-Hexane, resulted in the isolation of compounds **6** and **7** as white crystalline solids. Compound **8** was also isolated as a crystalline solid from fraction pool 16-19 by eluting with 40% EtOAc-Hexane polarity. Next, we carried out the CC separation of the ethanol extract. About 50 g of the ethanol extract was subjected to silica gel CC (100-200 mesh) afforded compound **9** (79 mg) as an amorphous solid (Figure 2.3-2.20). All the molecules were characterized by 1D NMR, 2D NMR, and HRMS, which were in accordance with the reported data (25–28).

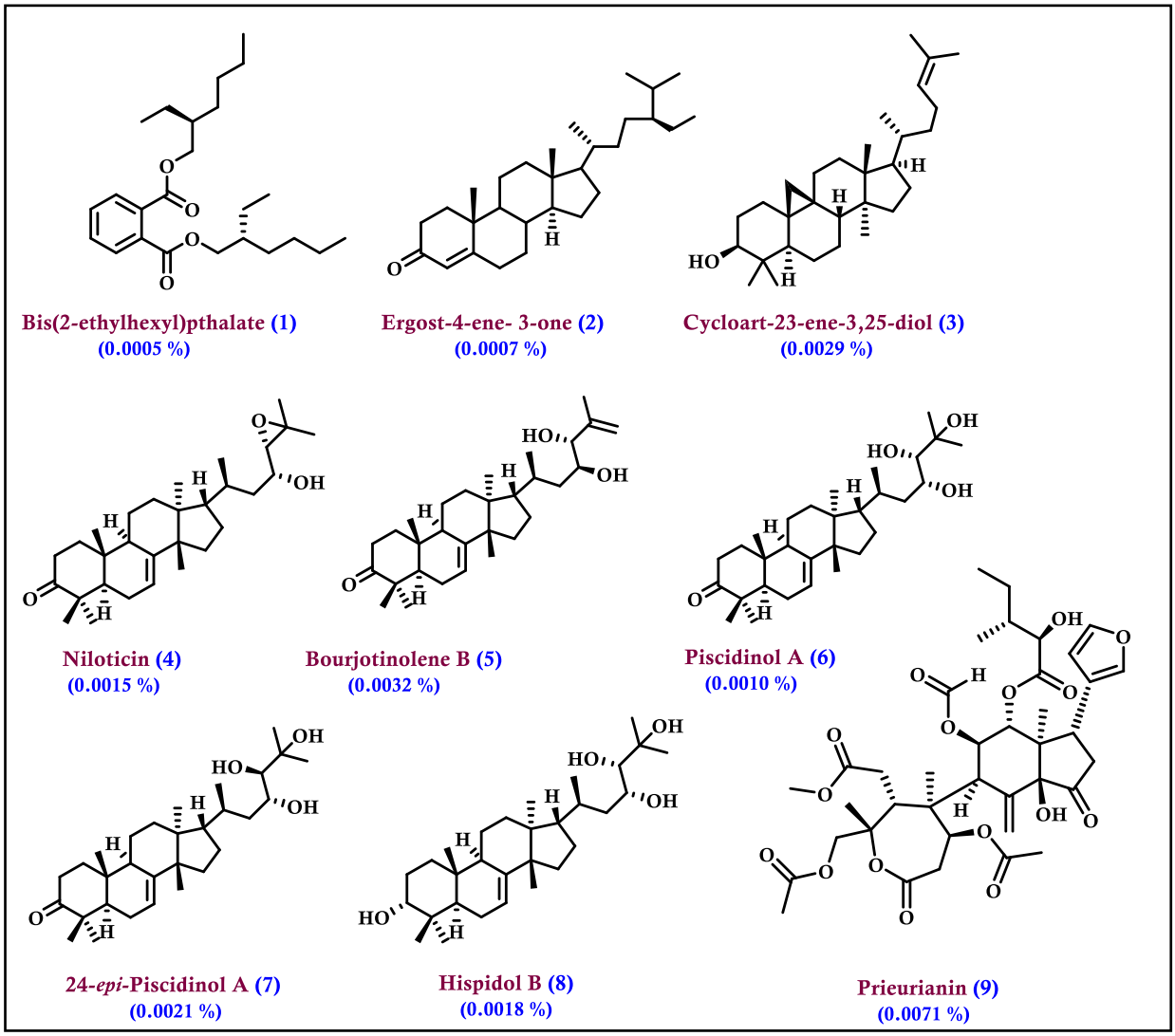

Fig 2.2: Molecules isolated from *Aphanamixis polystachya*

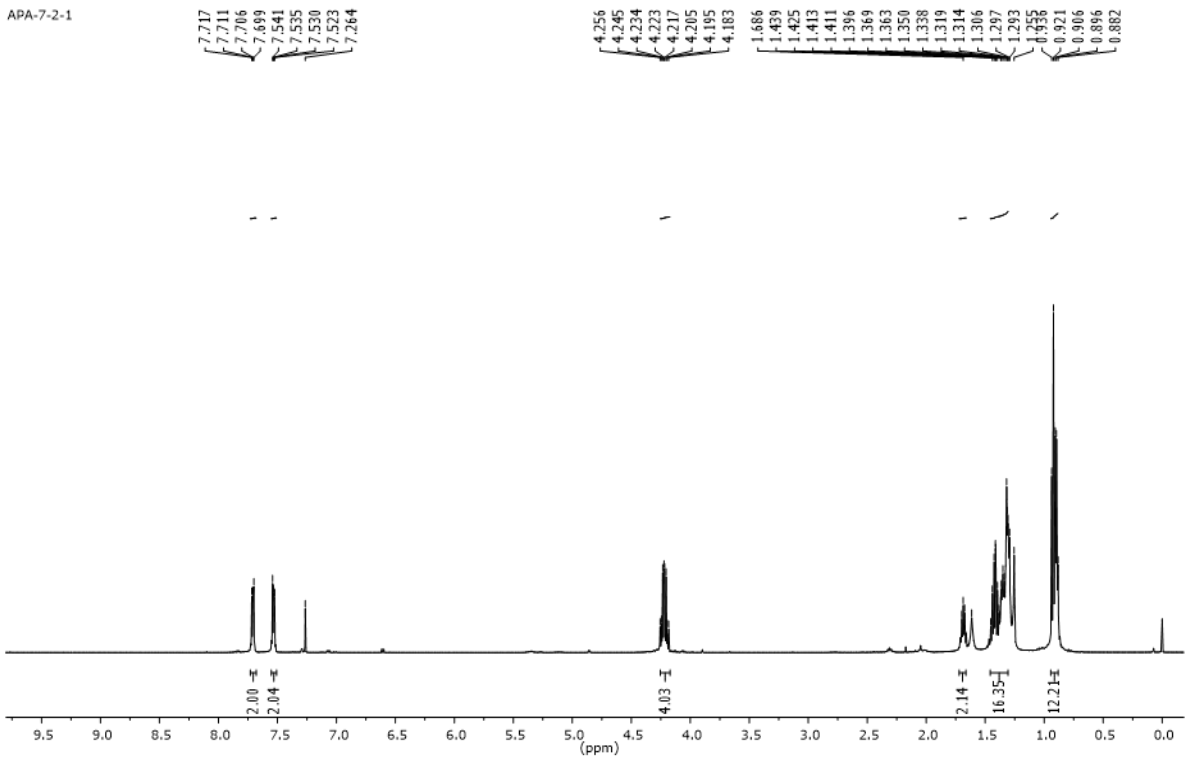

Fig. 2.3. ^{1}H NMR spectrum of Bis (2-ethylhexyl) phthalate (1) in $CDCl_3$

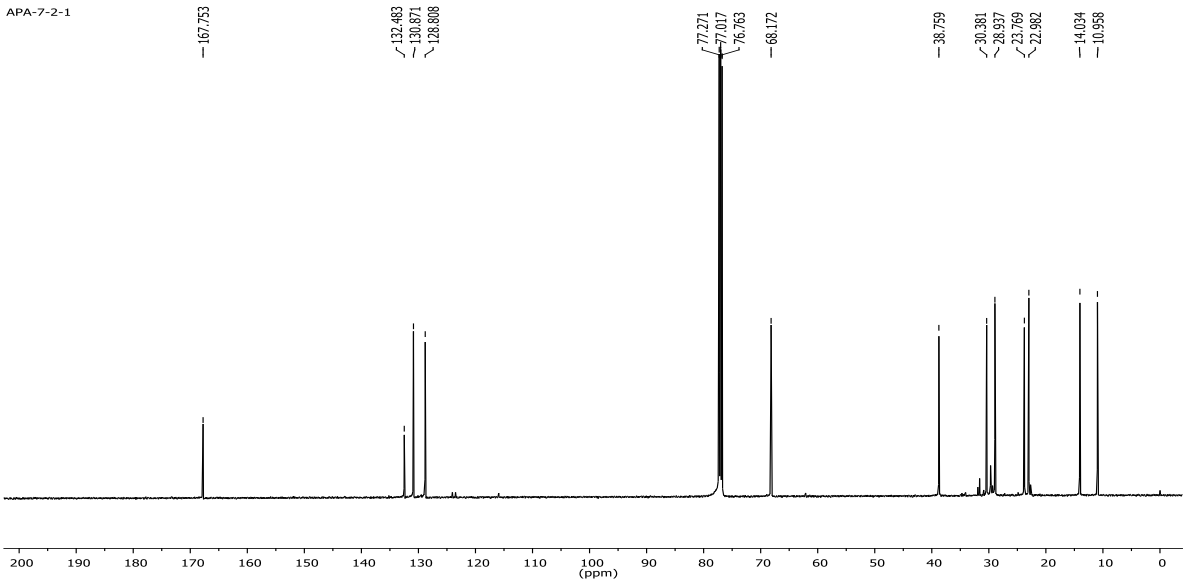

Fig. 2.4. ^{13}C NMR spectrum of Bis (2-ethylhexyl) phthalate (1) in $CDCl_3$

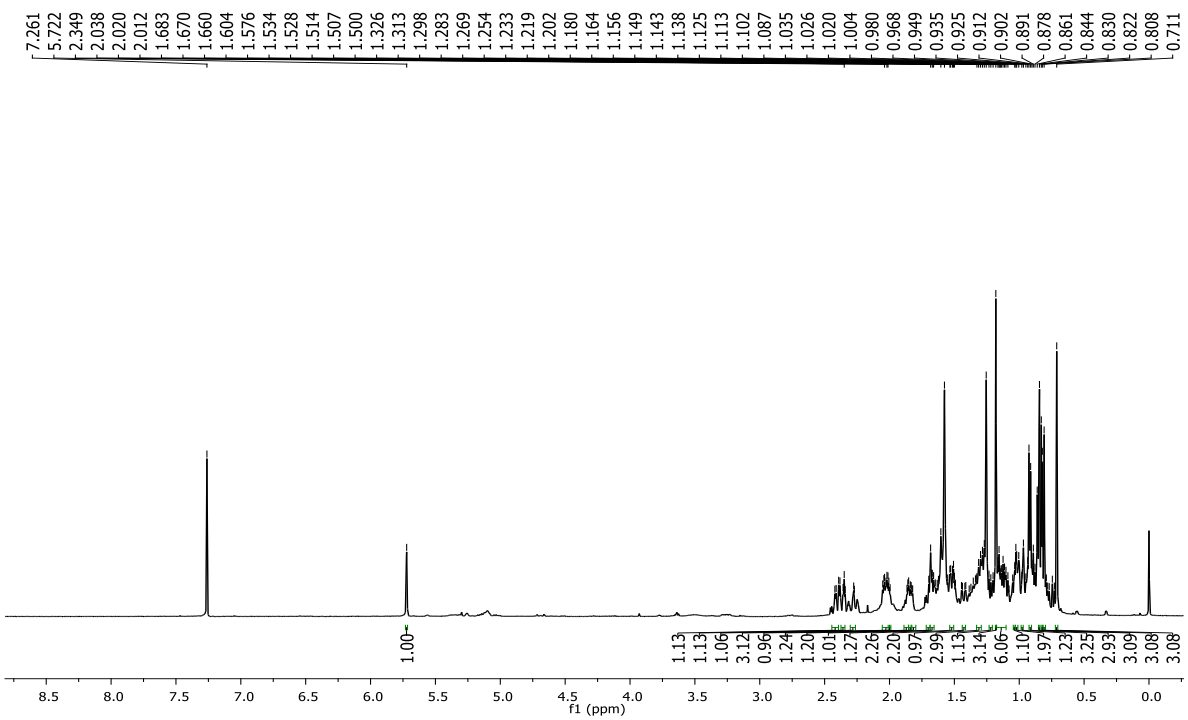

Fig. 2.5. ^{1}H NMR spectrum of Ergost- 4- ene-3- one (2) in $CDCl_3$

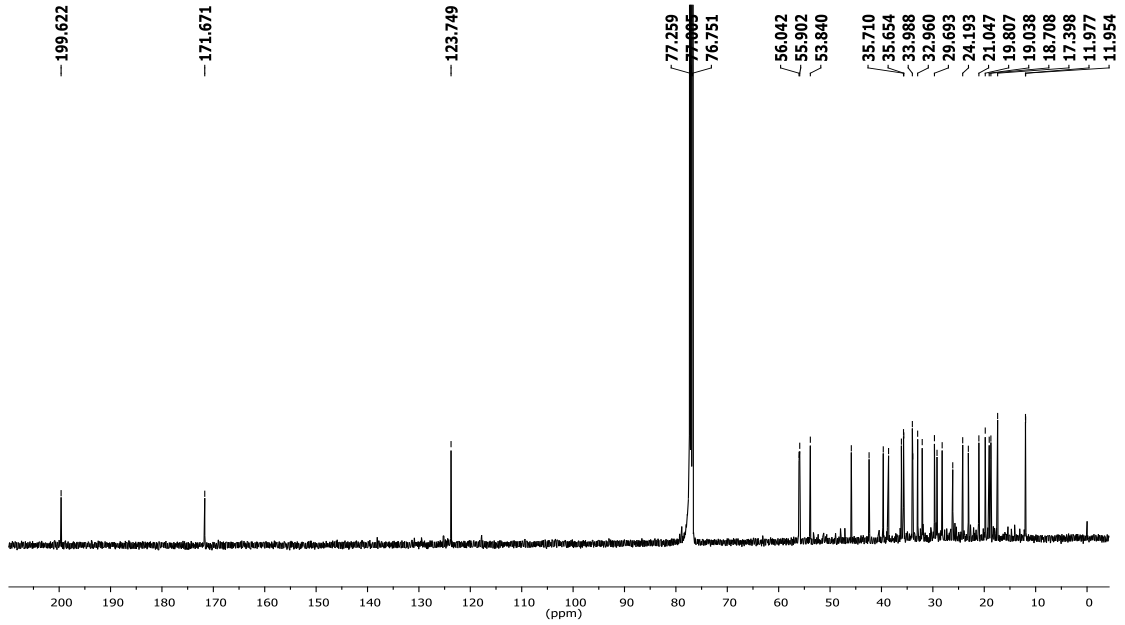

Fig. 2.6. ^{13}C NMR spectrum of Ergost- 4- ene-3- one (2) in $CDCl_3$

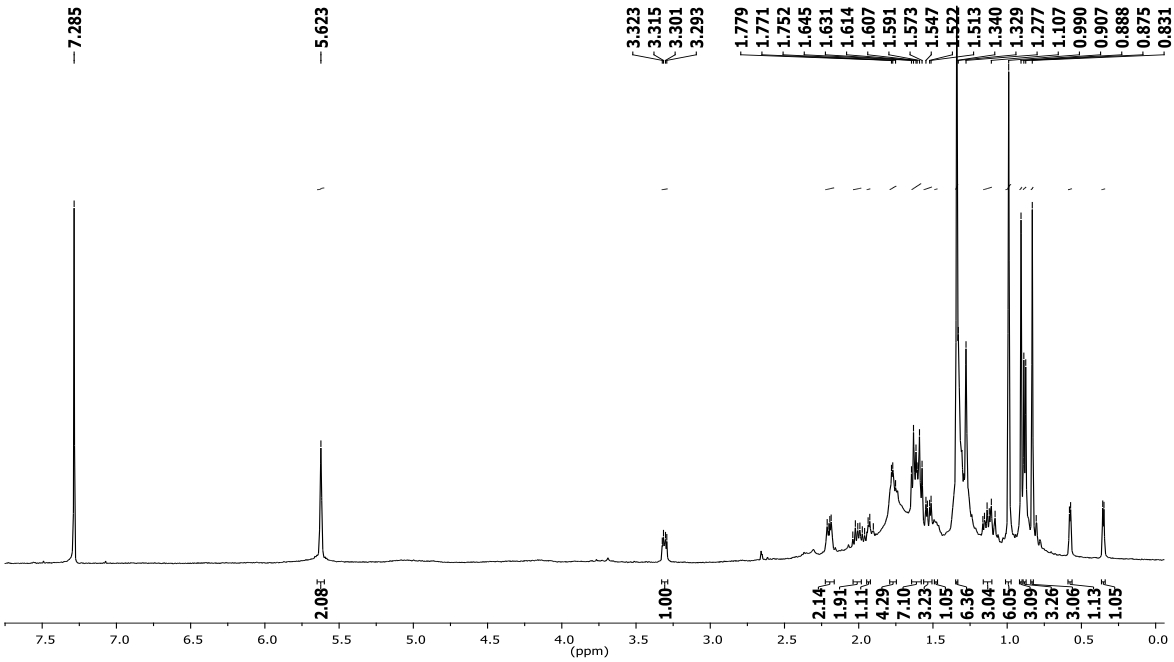

Fig. 2.7 ^{1}H NMR spectrum of Cycloart-23-ene-3,25-diol (3) in $CDCl_3$

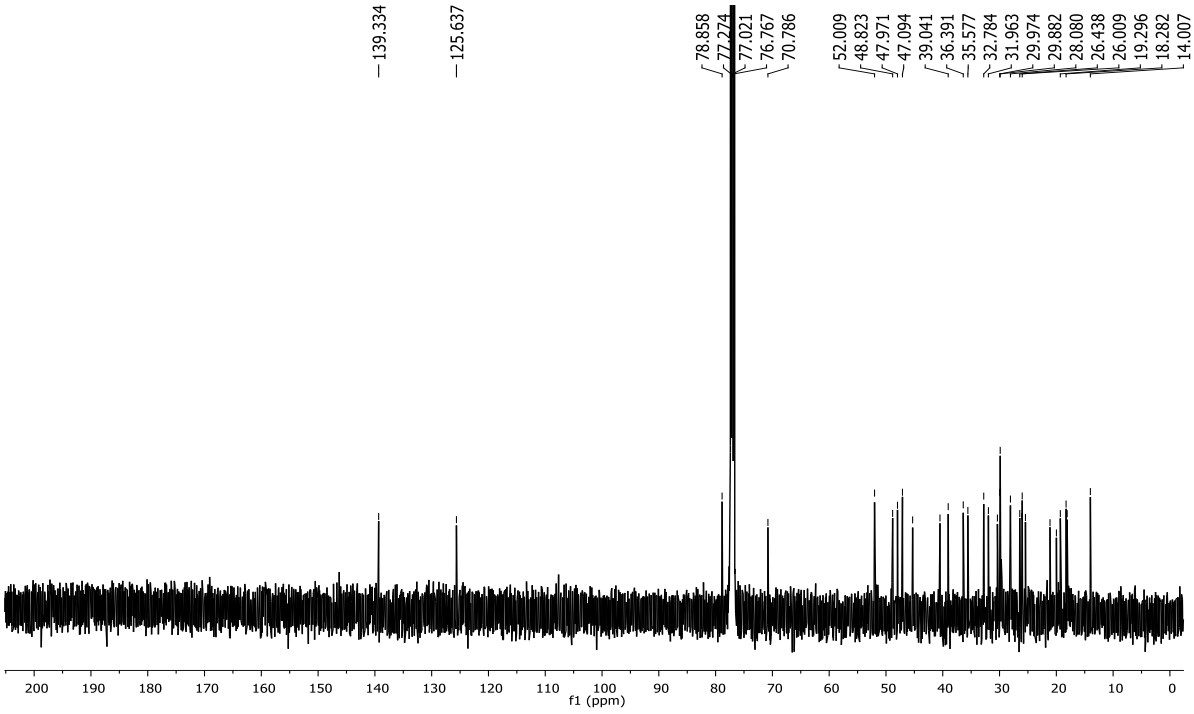

Fig. 2.8. ^{13}C NMR spectrum of Cycloart-23-ene-3,25-diol (3) in $CDCl_3$

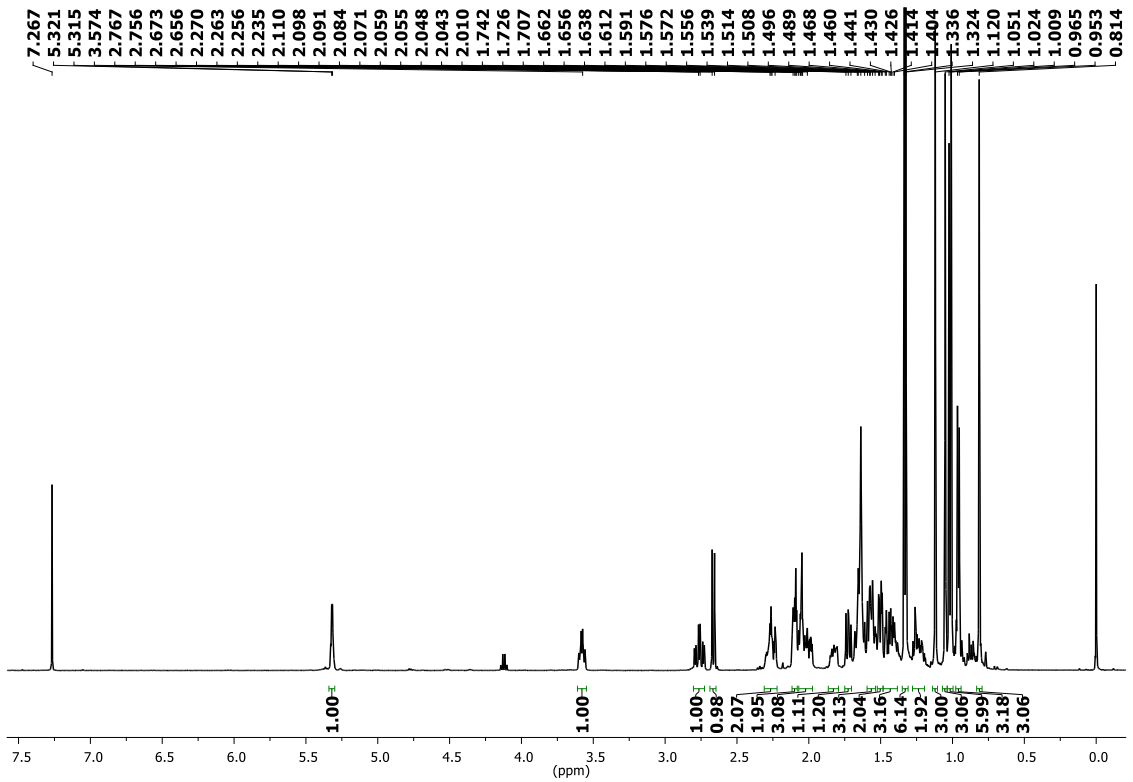

Fig. 2.9. ^{1}H NMR spectrum of Niloticin (4) in $CDCl_3$

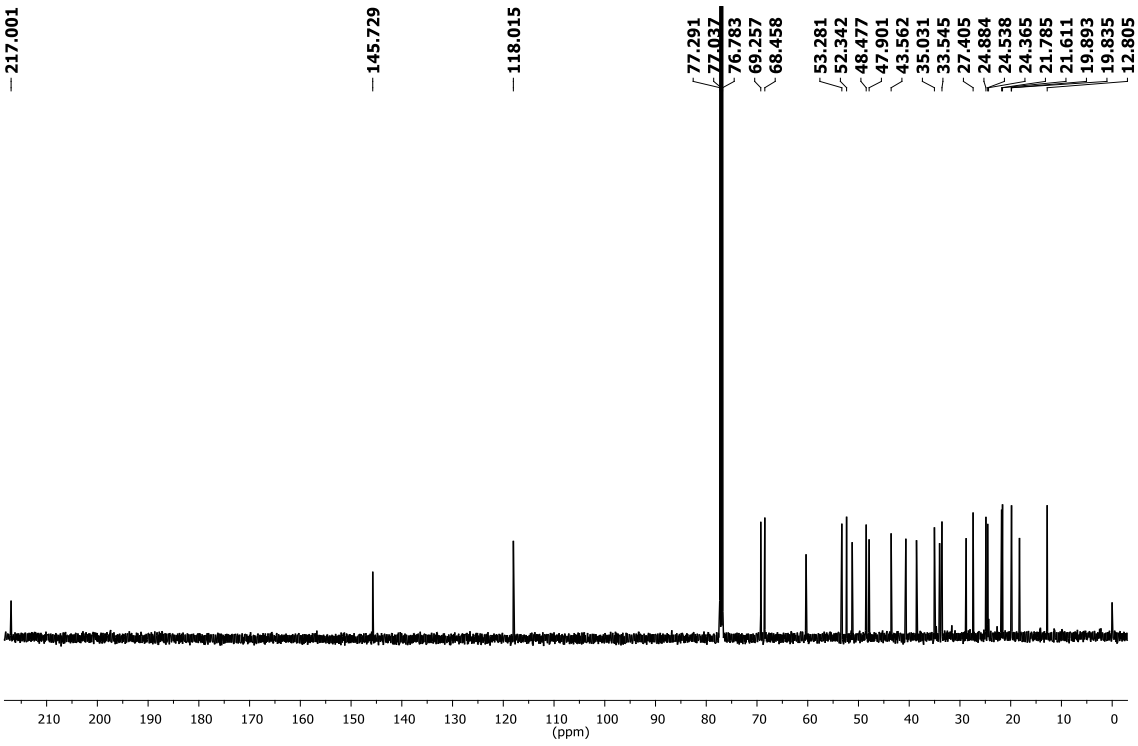

Fig. 2.10 ^{13}C NMR spectrum of Niloticin (4) in $CDCl_3$

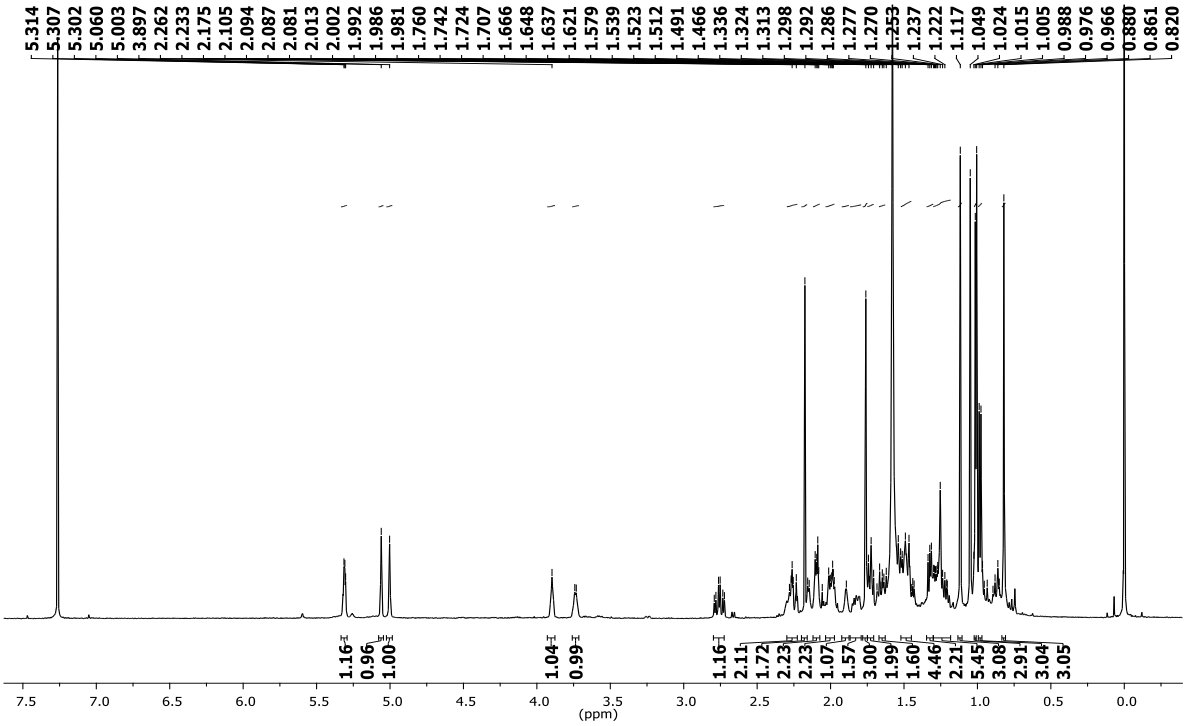

Fig. 2.11 ^{1}H NMR spectrum of Bourjotinolone B (5) in $CDCl_3$

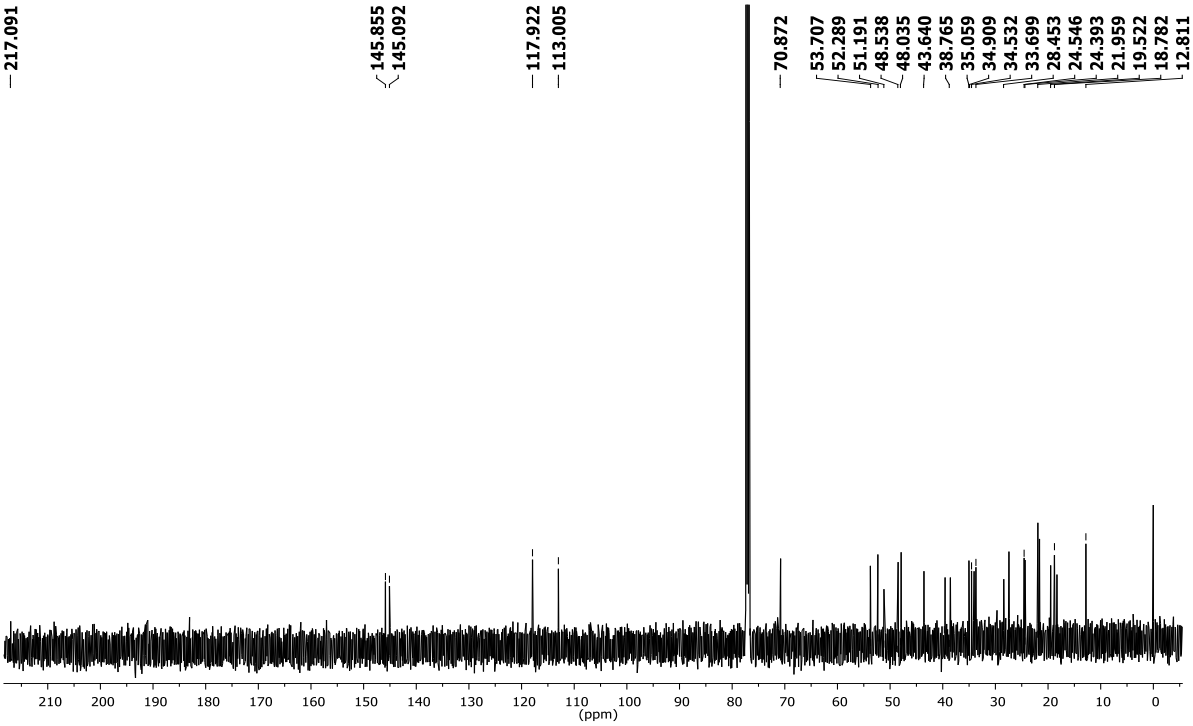

Fig. 2.12 ^{13}C NMR spectrum of Bourjotinolone B (5) in $CDCl_3$

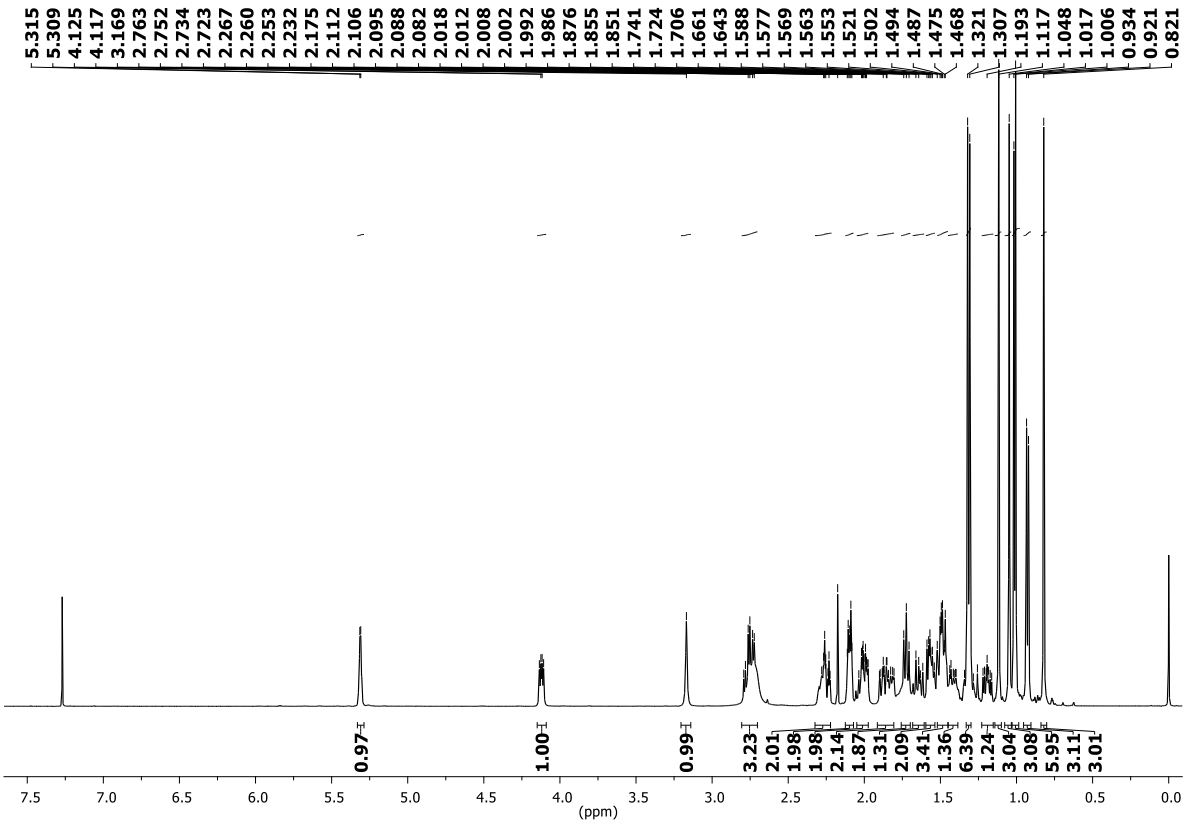

Fig. 2.13 ^{1}H NMR spectrum of Piscidinol A (6) in $CDCl_3$

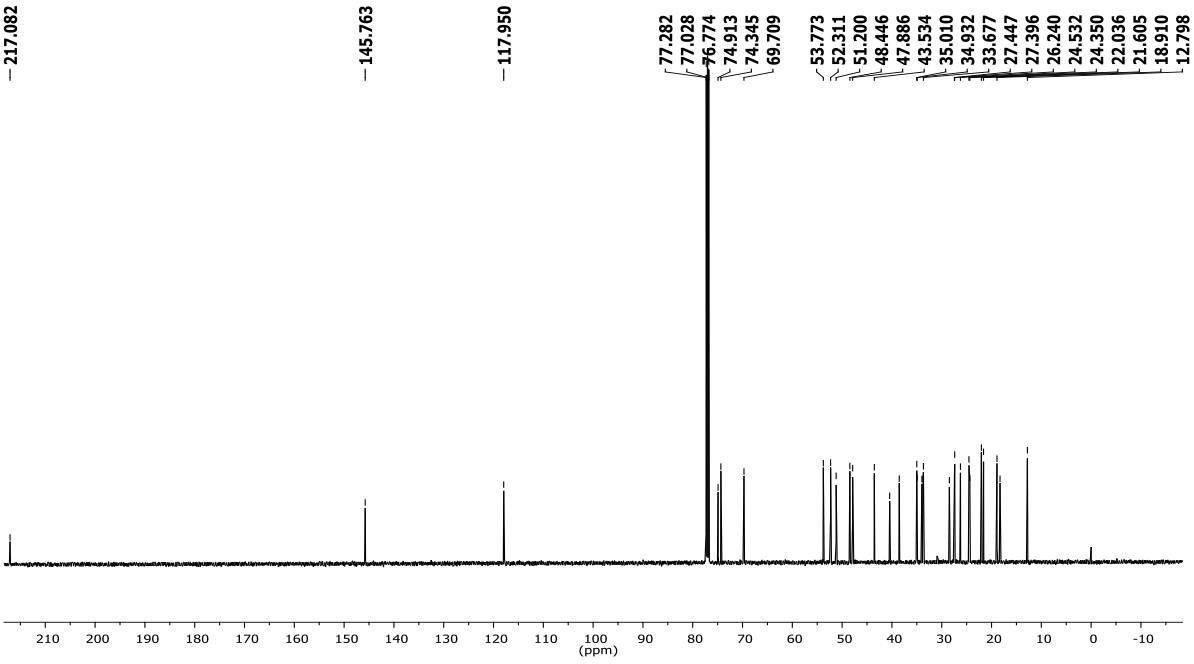

Fig. 2.14 ^{13}C NMR spectrum of Piscidinol A (6) in $CDCl_3$

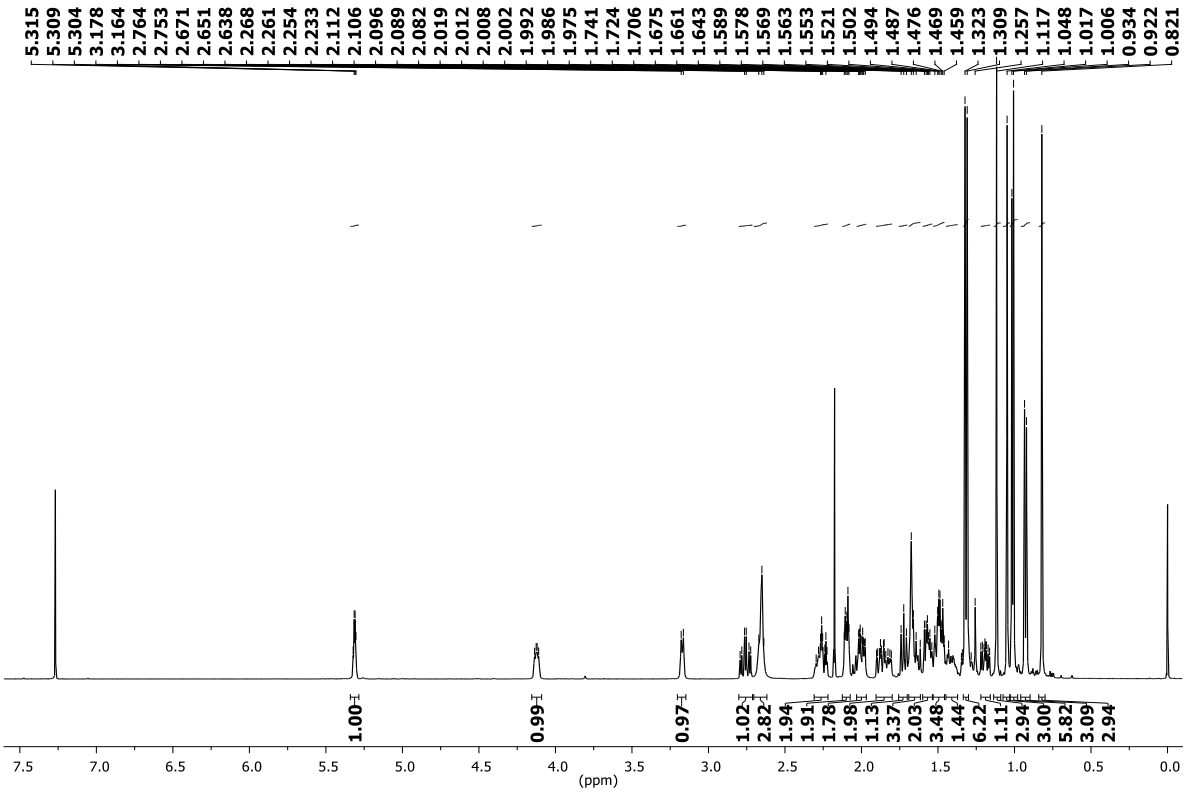

Fig. 2.15 ^{1}H NMR spectrum of 24-*epi*-Piscidinol A (7) in $CDCl_3$

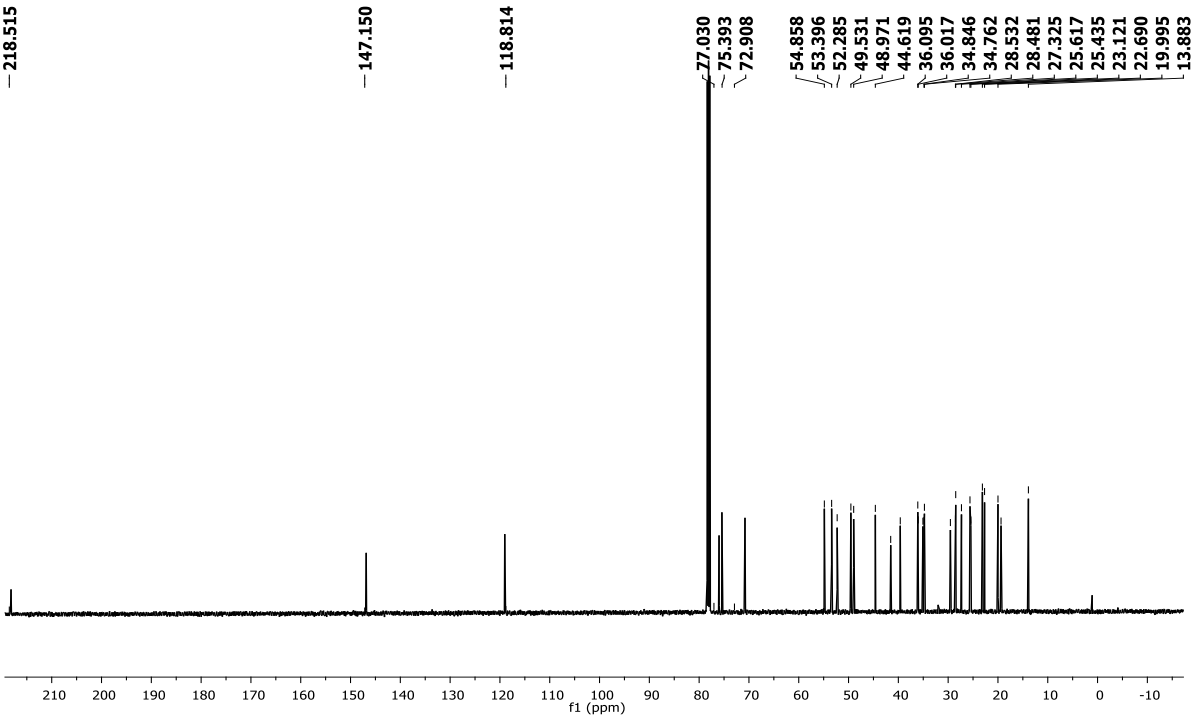

Fig. 2.16 ^{13}C NMR spectrum of 24-*epi*-Piscidinol A (7) in $CDCl_3$

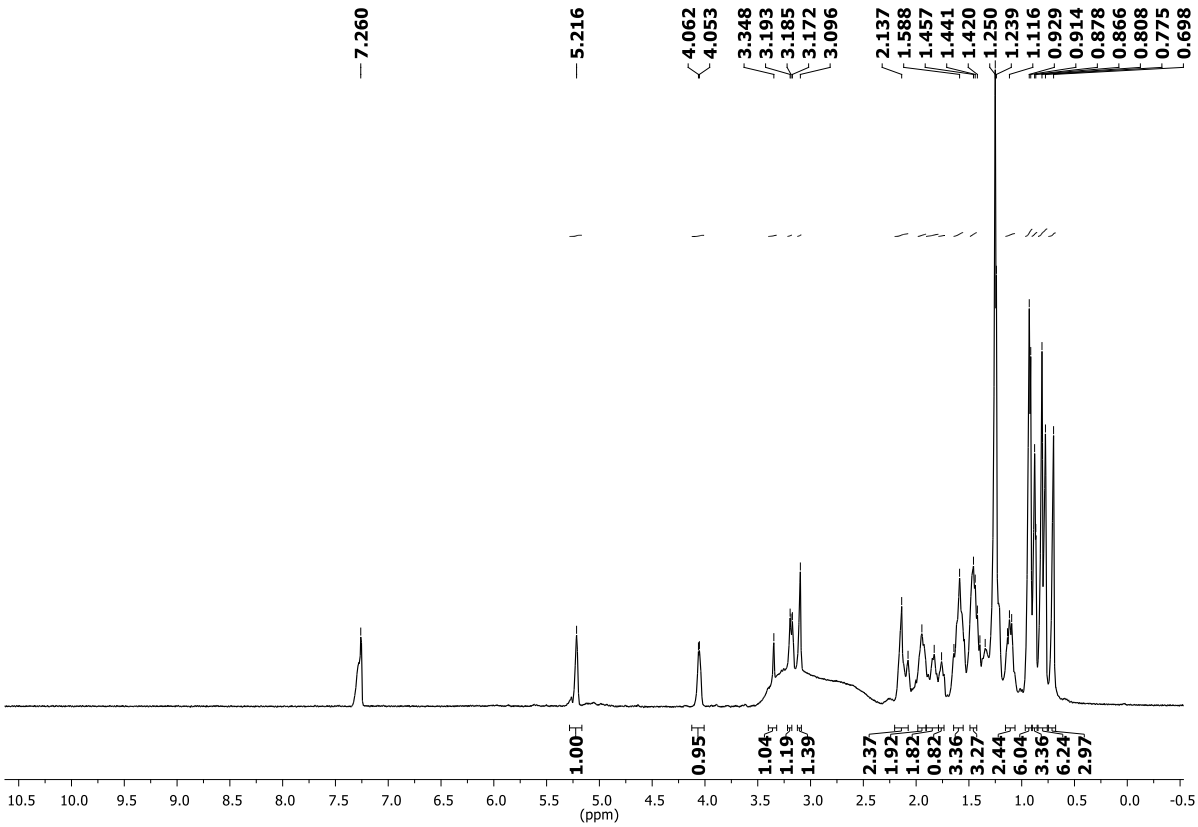

Fig. 2.17 ^{1}H NMR spectrum of Hispidol B (8) in $CDCl_3$ + MeOD

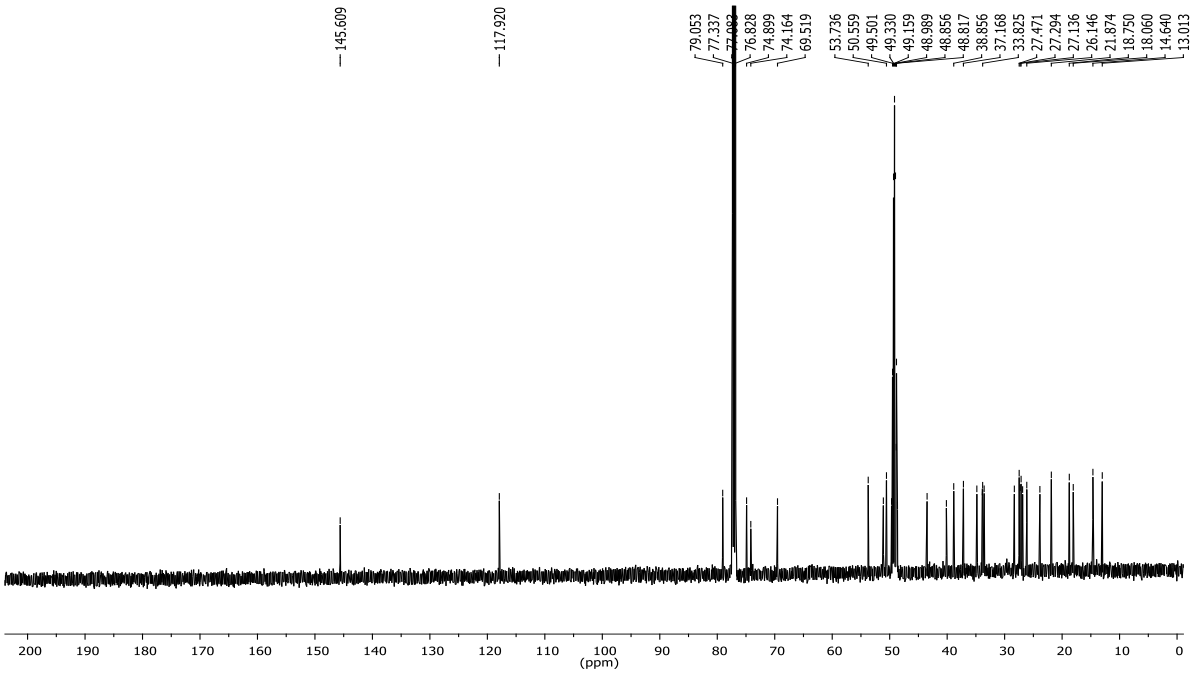

Fig. 2.18 ^{13}C NMR spectrum of Hispidol B (8) in $CDCl_3$ + MeOD

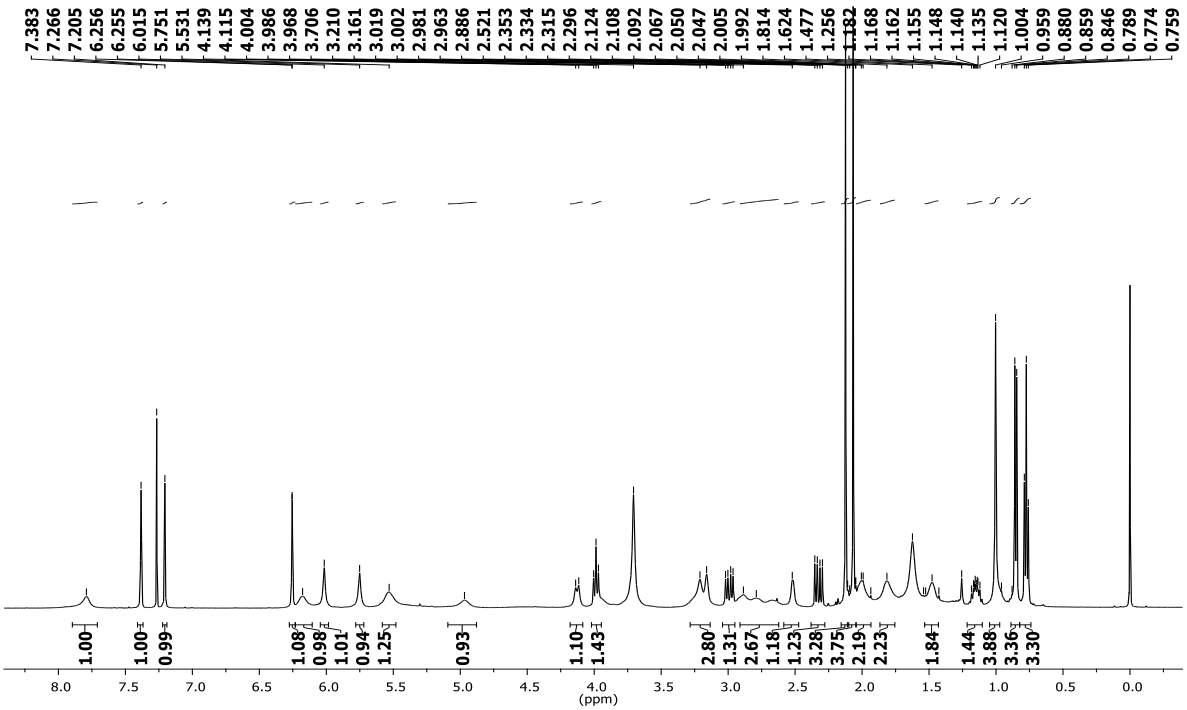

Fig. 2.19 ^{1}H NMR spectrum of Prieurianin (9) in $CDCl_3$

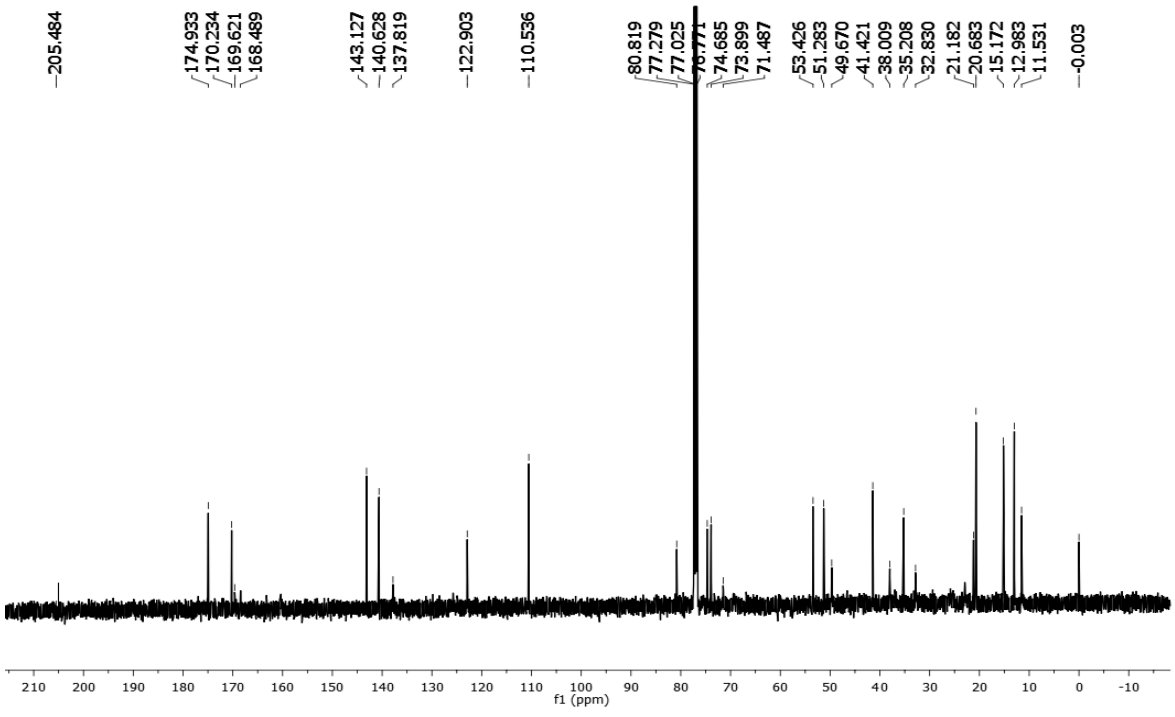

Fig. 2.20 ^{13}C NMR spectrum of Prieurianin (9) in $CDCl_3$

2.2.4. Screening of phytomolecules isolated from *Aphanamixis polystachya*

Preliminary cytotoxicity analysis was done for 6 molecules isolated from barks of *Aphanamixis polystachya* by MTT ((3-(4,5-dimethylthiazol-2-yl)-2,5-diphenyltetrazolium bromide) assay. This assay works on the principle of conversion of MTT into formazan crystals by living cells, whereas dead cells could not carry out this process. The assay was done in MDA-MB-231 breast cancer and HeLa cervical cancer cell lines (Table 2.1). Among the molecules, niloticin and prieurianin exhibited reasonable cytotoxicity in HeLa cells at 11 µM and 13 µM for 24 and 48 hours of incubation for niloticin and 5 µM at 48 hours of incubation for prieurianin. With the screening results, niloticin and prieurianin were selected for further in-depth exploration of its anticancer potential.

2.2.5. Evaluation of the anticancer potential of niloticin

To evaluate the anticancer potential of niloticin in different cancer cell types, we performed an MTT assay on A549 (lung cancer), PANC-1 (pancreatic cancer), and MDA-MB-231 (breast cancer) cell lines, using the same concentrations applied to HeLa cells. The study revealed that the minimal inhibitory concentration (IC_{50}) of niloticin at 24 hours of incubation was 30.6 µM for A549, 16.5 µM for PANC-1, and 23.9 µM for MDA-MB-231 (Figure 2.21).

Compounds	MDA-MB-231 IC50 (µM)		HeLa IC50 (µM)	
	24 hr	48 hr	24 hr	48 hr
Prieurianin	>100	83.6	27.8	5
Piscidinol A	>100	>100	>100	>100
Bourjotinolone B	>100	>100	>100	>100
Niloticin	23.9	30.2	11.65	13.68
Hispidol B	>100	>100	>100	>100
24-epi-piscidinol A	>100	>100	51.85	44.27

Table 2.1: IC_{50} values of molecules screened for its cytotoxic potential

(a)

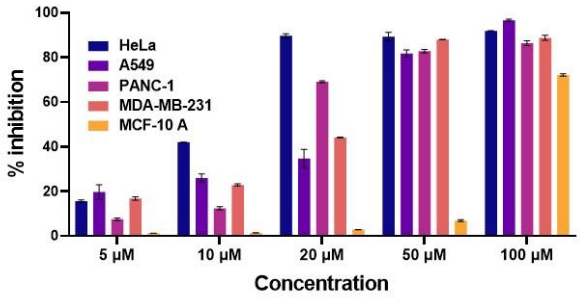

(b)

No.	Cell line	IC_{50} (in µM)
1	MCF-10A	83.31
2	HeLa	11.65
3	A549	30.6
4	PANC-1	16.5
5	MDA-MB-231	23.9

Fig 2.21: a) Comparative study of percentage inhibition of niloticin in different cancer cell lines b) and their IC_{50} values using MTT assay.

These results indicate that niloticin demonstrates the highest activity against cervical cancer cells, specifically the HeLa cell line. Given the strong cytotoxic effect on HeLa cells, evaluation of cytotoxicity in SiHa cells was done, and a model for cervical squamous cell carcinoma, and found an IC_{50} value of 16.23 µM. This further confirmed the anti-proliferative efficacy of niloticin in cervical cancer. To assess its selectivity, niloticin was also tested on MCF 10A, a non-tumorigenic epithelial cell line, where it exhibited a much higher IC_{50} value of approximately 83.31 µM. These findings underscore the selective anticancer activity of niloticin, particularly against cervical cancer cells, and provide a strong rationale for further investigation into its apoptotic effects in HeLa cells.

2.2.6 Computational screening of niloticin

In the investigation of niloticin's pharmacokinetic properties, the compound displayed highly favorable attributes, underscoring its potential as a therapeutic agent. Initial assessments revealed that niloticin exhibited excellent human intestinal absorption, an essential factor for efficient oral bioavailability. Additionally, it demonstrated favorable lipophilicity, with an iLOGP value of 4.58, indicative of optimal membrane permeability. A critical advantage of niloticin was its lack of pan-assay interference compounds (PAINS), ensuring that its observed biological effects were not the result of nonspecific or artifactual interactions. These findings laid the groundwork for a deeper exploration of its molecular mechanisms and interactions with key apoptotic proteins involved in cervical cancer. To elucidate niloticin's potential mechanisms of action, molecular docking studies were conducted to examine its interactions with pivotal proteins within the apoptotic pathways of cervical cancer. Seven proteins were selected for this analysis based on their critical roles in apoptosis and cancer progression: p53, Fas receptor, Fas ligand, Bax, CDK2, BCL2, and TNF-β. These simulations consistently demonstrated robust binding affinities, as evidenced

by docking scores ranging from −6.8 to −9.0 kcal/mol. Niloticin exhibited strong binding to p53, a tumor suppressor protein central to apoptosis and cell cycle regulation, through hydrogen bonds and hydrophobic interactions with residues such as ASN 263, GLY 262, and GLU 258, resulting in a docking score of −7.2 kcal/mol. Similar binding affinities were observed with the Fas receptor and Fas ligand, key mediators of the extrinsic apoptotic pathway, involving interactions with residues like GLY 247, PHE 248, and ARG 144. These interactions underscore niloticin's potential to modulate death receptor-mediated signaling. The pro-apoptotic protein Bax, which promotes mitochondrial membrane permeabilization, displayed a docking score of −7.7 kcal/mol, suggesting a strong interaction that could enhance apoptotic processes. Niloticin also showed a notable affinity for CDK2, a cell cycle regulatory kinase, with a docking score of −7.2 kcal/mol, indicating its capacity to induce cell cycle arrest and suppress tumor proliferation. The most significant interaction was observed with BCL2, an anti-apoptotic protein that inhibits cell death, where niloticin exhibited a docking score of −9.0 kcal/mol, suggesting its potential to neutralize BCL2's protective effects on cancer cells. Furthermore, niloticin demonstrated a strong affinity for TNF-β, a cytokine involved in inflammation and apoptosis, with a docking score of −7.2 kcal/mol, indicating its ability to modulate the tumor microenvironment (Table 2.2). Moreover, niloticin demonstrated high affinity for proteins like Bax (PDB ID: 6EB6), CDK2 (PDB ID: 2UZE), BCL2 (PDB ID: 6O0K), and TNF β (PDB ID: 1TNR), with docking scores of -7.7, -7.2, -9.0, and -7.2 kcal/mol, respectively (29–34). The docking simulations provided detailed insights into niloticin's binding interactions, characterized by a combination of hydrogen bonds and hydrophobic contacts with key residues in each protein. These findings suggest that niloticin can target multiple regulatory and apoptotic pathways, potentially disrupting the survival mechanisms of cervical cancer cells. This comprehensive molecular profiling highlights niloticin's potential as a therapeutic agent with the ability to modulate complex biological processes underlying cancer progression.

Entry	**PDB ID**	**Docking Score**	**Interacting Residues**
1	1TUP	-7.2	ASN 263, GLY 262, GLU 258, LUE 264, THR 256, TYR103, ARG 267, ILE 254, THR 256, SER 99, PRO 98, SER 95, MET 160, ARG 158
2	3EZQ	-7.1	GLN 244, GLY247, PHE 248, LYS 251, ASN 252, GLU 289, ASP 292, THR 293, LYS 296, ASP 297, LYS 300, ALA 301

3	5L19	-6.8	ARG 144, VAL 146, ALA 147, HIS 148, LEU 168, LEU 170, TYR 192, PHE 275, Leu 278, TYR 279, LEU 278
4	6EB6	-7.7	ARG 89, PHE 92, PHE 93, ALA 96, ALA 97, PHE 100, SER 101, ALA 139, ASP 142, PHE 143, GLU 146, ARG 147
5	2UZE	-7.2	PHE 152, GLY 153, VAL 154, PRO 155, VAL 156, GLU 172, CYS 177, TYR 179, SER 181, THR 182, Met 233, GLY 229, TRP 227, PRO 228, ASP 270, PRO 271, ASN 272
6	6O0K	-9.0	PHE 104, SER 105, TYR 108, ASP 111, MET 115, VAL 133, LEU 137, ASN 143, GLY 145 ARG 146, ALA 149, PHE 150, GLU 152, PHE 153, VAL 156
7	1TNR	-7.2	HIS 32, PHE 74, TYR 76, TYR 134, PRO 161, SER 162, PHE 165, PHE 169, LEU 171

Table 2.2. Docking scores and interacting residues of selected proteins in apoptotic pathway with niloticin

2.2.7 Molecular dynamics simulation of protein-niloticin complex

The investigation into niloticin's interactions with the selected apoptotic pathway proteins was further advanced through comprehensive molecular dynamics simulations. These simulations, conducted using the OPLS-2005 force field over a rigorous 100-nanosecond time frame, provided in-depth insights into the stability and dynamics of the protein-niloticin complexes. A key analytical tool in this phase was the root mean square deviation (RMSD) plot, which offered a detailed understanding of the structural dynamics and stability of both the individual proteins and their complexes with niloticin. The RMSD analysis revealed that the protein-niloticin complexes maintained exceptional structural integrity throughout the simulation period, with maximum deviations not exceeding 3.5 Å (Fig. 2.22h). This minimal fluctuation highlighted the robustness and stability of the binding interactions. The consistency in RMSD values underscored the resilience of these complexes, reflecting the sustained nature of the molecular bonds formed between niloticin and the apoptotic proteins. These findings emphasize that niloticin's impact is not limited to strong binding affinities but extends to significantly enhancing the structural stability of its target proteins. This enduring interaction suggests a profound influence on the proteins' functionality, reinforcing niloticin's potential role in inducing apoptosis in human cervical cancer cells.

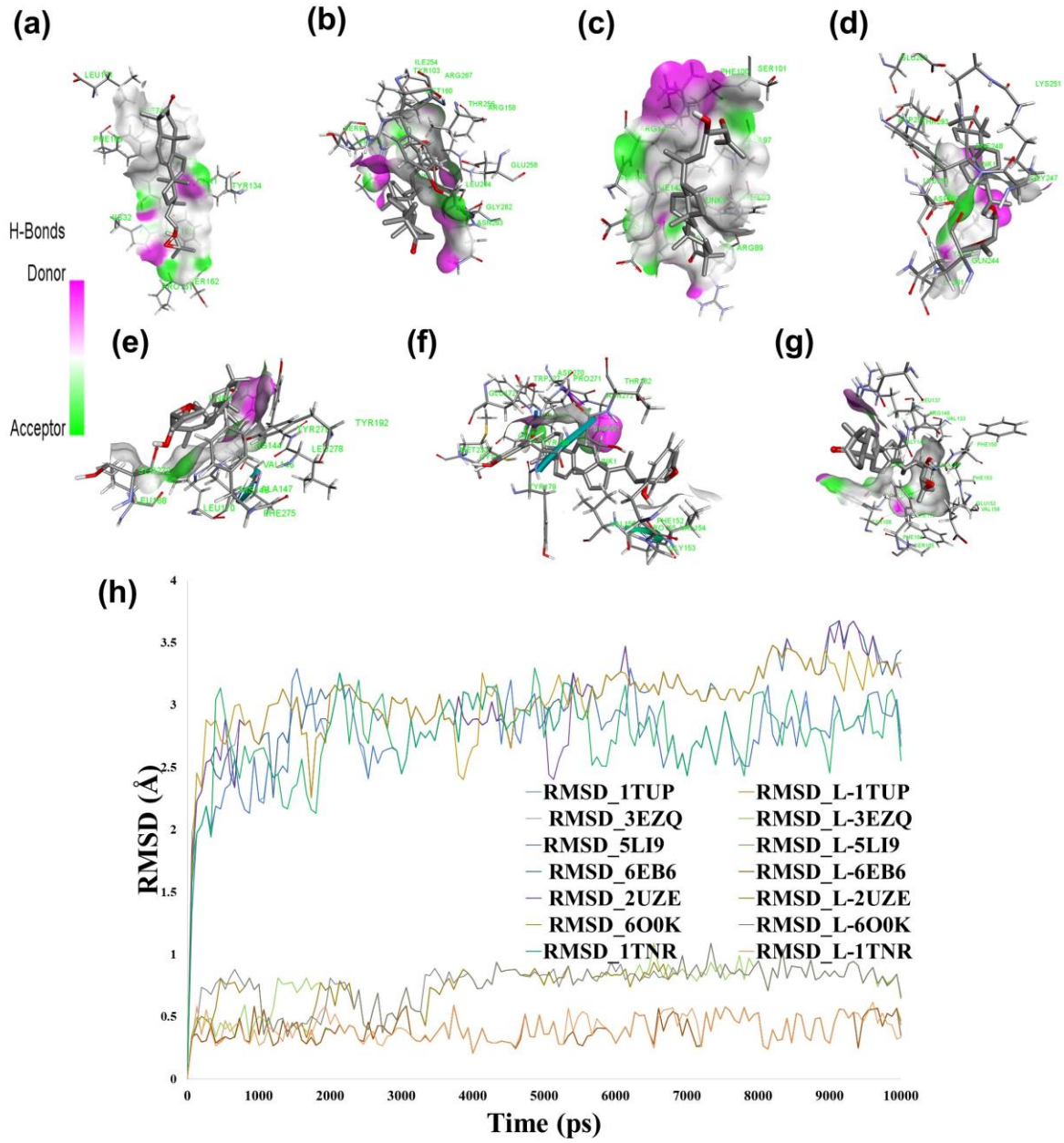

Figure 2.22. 3-D interaction of niloticin with a) TNF β b) P53 c) Bax d) Fas receptor e) FasL f) CDK2 g) BCL2 h) RMSD plot of niloticin with different proteins

2.2.8. Apoptotic evaluation of niloticin

The mechanisms of cell death triggered by niloticin in HeLa cells were thoroughly investigated using multiple assays, which provided detailed insights into its apoptotic potential. The initial assessment involved the use of acridine orange (AO) and ethidium bromide (EB) dual staining to differentiate between viable and apoptotic cells. AO, a membrane-permeable DNA-binding dye, stains viable cells green, as it can penetrate intact cell membranes, whereas EB, a membrane-impermeant dye, stains the DNA of cells with compromised membranes, emitting a reddish-orange fluorescence indicative of apoptosis.

Fluorescence microscopy with a FITC filter was employed to visualize these staining patterns. Niloticin at different concentrations (7 μM and 11 μM) were treated and the cells displayed a reddish-orange fluorescence, in stark contrast to the untreated control cells, which remained green, confirming apoptotic membrane disruption in niloticin-treated cells (Fig. 2.23a). To further validate these findings and analyze membrane integrity changes during apoptosis, the APOPercentage assay was utilized. This method relies on a dye that selectively enters cells with compromised membranes, staining apoptotic cells pink, while non-apoptotic cells remain unstained (35). Consistent with the fluorescence microscopy results, niloticin-treated cells exhibited intense pink staining, with the color intensity directly correlating with the concentration of niloticin. Control cells, lacking any treatment, remained unstained, further reinforcing niloticin's capacity to disrupt membrane integrity and induce apoptosis (Fig. 2.23b). Additionally, the externalization of phosphatidylserine, a hallmark of early apoptosis, was examined using the annexin V apoptosis assay. Annexin V specifically binds to phosphatidylserine exposed on the outer leaflet of the plasma membrane during apoptosis, and when coupled with propidium iodide (PI), it enables the differentiation of cells at various stages of apoptosis or necrosis. Flow cytometry analysis quantified cells across different quadrants: Q3 (annexin V-negative/PI-negative, viable cells), Q4 (annexin V-positive/PI-negative, early apoptotic cells), Q2 (annexin V-positive/PI-positive, late apoptotic), and Q1 (annexin V-negative/PI-positive, necrotic cells). The untreated control group showed 77.7% of cells in Q3, reflecting a predominance of live cells. However, niloticin treatment at 7 μM and 11 μM significantly reduced the viable cell population to 38.3% and 29.6%, respectively. Notably, the percentage of cells in Q4, indicative of early apoptosis, increased substantially to 50.9% in the 7 μM treatment group, emphasizing the activation of apoptotic pathways. Furthermore, the population of annexin V-FITC and PI-positive cells in Q2, representing late apoptotic stages, increased from 14.5% in the control to 49.2% in niloticin-treated groups, demonstrating a pronounced progression of apoptosis. In contrast, the necrotic population (Q1) remained minimal, with only 0.7% and 4.5% of cells in the 7 μM and 11 μM treatment groups, respectively, suggesting that necrosis was not a significant mode of cell death in this context. Collectively, these findings, corroborated by fluorescence microscopy, the APOPercentage assay, and flow cytometry data, highlight the potent apoptotic activity of niloticin in HeLa cells. The data show that niloticin induces apoptosis in a concentration-dependent manner, driving cells through early to late apoptotic stages while maintaining minimal necrotic cell

death. This comprehensive analysis underscores niloticin's efficacy in targeting cervical cancer cells through apoptosis, as illustrated in Fig. 2.23c.

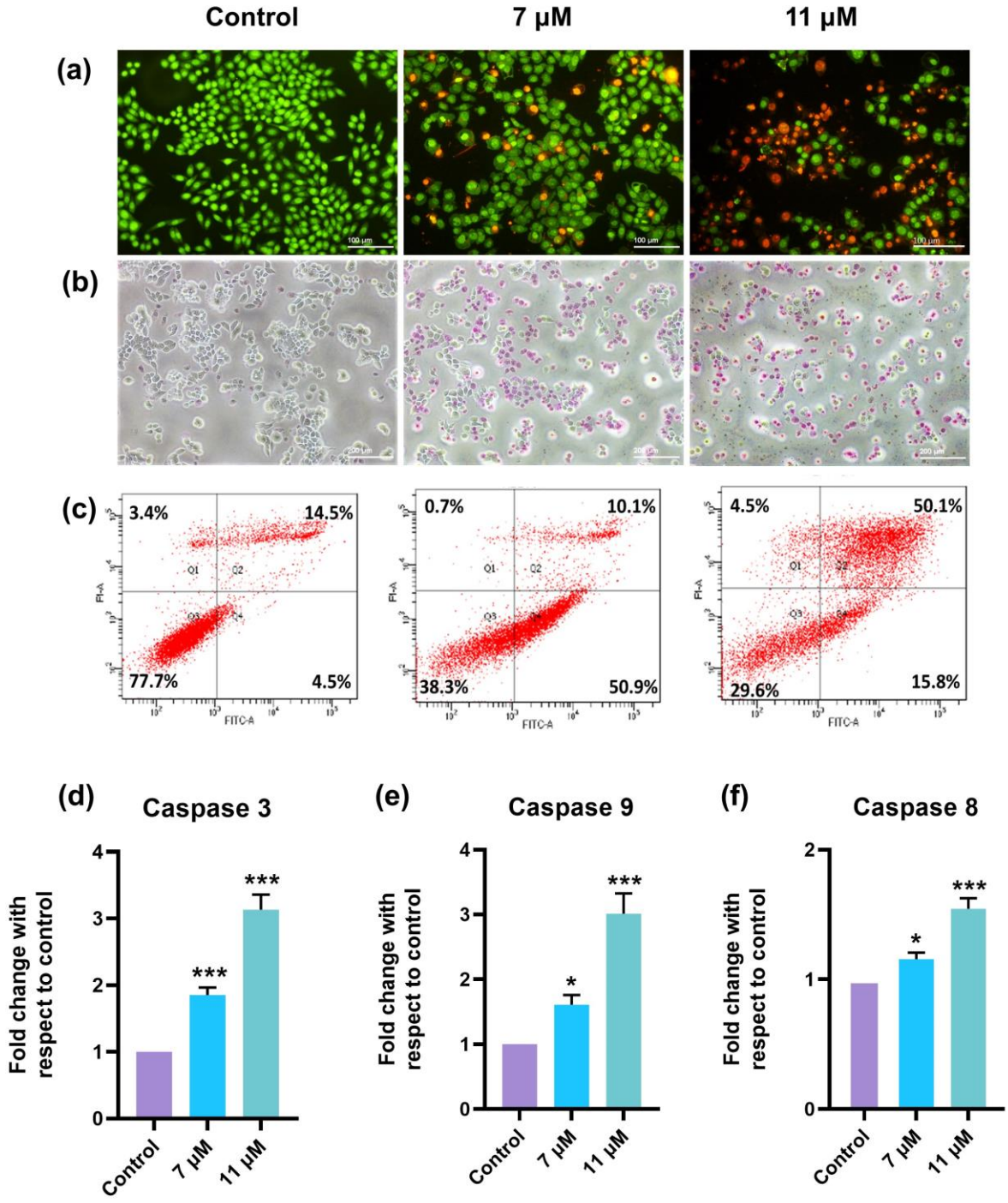

Figure 2.23. Induction of apoptosis in HeLa cells by niloticin analysed in different concentrations of 7 and 11 µM by a) Acidine orange ethidium bromide dual staining method. Green channel: emission wavelength (λ_{ex} = 450-490 nm), excitation wavelength (λ_{ex} = 520 nm) b) APOP assay c) Annexin V apoptosis assay by FACS c) Caspase expression analysis by flurometric method. Major caspases such as caspase-3, caspase-9 and caspase-8 involved in apoptotic pathways were checked and it is observed that all the 3 caspases show a fold increase in its fluorescence intensity with respect to control. Results are represented as mean ± SD, *p < 0.05, **p < 0.01, ***p < 0.001 compared to control.

2.2.9. Investigation of caspase-mediated apoptosis

Programmed cell death, or apoptosis, is a tightly regulated process largely governed by the activity of caspases, a specialized family of cysteine proteases. These enzymes are synthesized as inactive precursors, known as zymogens, and are activated through a cascade of proteolytic events during apoptosis (36). The activation of caspases serves as a hallmark of apoptosis and provides insight into the underlying pathway through which cell death is mediated. To elucidate the involvement of caspases in niloticin-induced apoptosis, a fluorescence-based assay was employed. This method quantifies the activation of various caspases by measuring fluorescence intensity, which correlates with the expression levels of these proteases. Apoptosis can be initiated via two primary pathways: the extrinsic (death receptor-mediated) pathway and the intrinsic (mitochondria-mediated) pathway. These pathways are distinguished by the activation of specific initiator caspases. In this study, the expression of caspase 3 was analyzed, a crucial executioner caspase that acts as a convergence point for both apoptotic pathways, executing the final stages of cell death. HeLa cells treated with niloticin at concentrations of 7 μM and 11 μM exhibited a substantial threefold increase in caspase 3 activation compared to untreated control cells. This marked elevation confirms that niloticin robustly induces apoptosis by engaging key components of the apoptotic machinery (Fig. 2.23d). To further dissect the apoptotic mechanisms triggered by niloticin, the activation of caspase 8 and caspase 9, which are key initiators of the extrinsic and intrinsic apoptotic pathways, respectively was investigated. The extrinsic pathway is typically activated by external signals binding to death receptors, such as Fas or TNF receptors, leading to the activation of caspase 8. Conversely, the intrinsic pathway is regulated by mitochondrial signals, culminating in the activation of caspase 9. Remarkably, the findings revealed that niloticin treatment significantly upregulated the expression of both caspase 8 and caspase 9, indicating that the compound activates both apoptotic pathways simultaneously (Fig. 2.23e and f). This dual activation underscores niloticin's multifaceted approach to inducing apoptosis in HeLa cells, enhancing its therapeutic potential against cervical cancer. The activation of both apoptotic pathways by niloticin is consistent with the behaviour of certain natural compounds belonging to the terpenoid family, as observed in the scientific literature. For instance, nimbolide, a terpenoid extracted from neem, induces apoptosis through both pathways in MCF-7 breast cancer cells. Similarly, hyperforin, a compound derived from *Hypericum*

perforatum (St. John's wort), triggers both apoptotic pathways in glioblastoma cells, while carnosic acid, found in rosemary, exhibits a dual-pathway activation in PC-3 prostate carcinoma cells. These examples demonstrate a shared mechanism among terpenoids in leveraging both intrinsic and extrinsic apoptotic pathways to exert their anticancer effects (37-39). The findings from this study establish that niloticin, akin to other terpenoids, employs a dual-pathway strategy to drive apoptosis. By simultaneously activating caspase 8 and caspase 9, niloticin ensures comprehensive apoptotic signaling, culminating in the activation of caspase 3 and the execution of cell death. This multifaceted mechanism not only enhances its efficacy against cancer cells but also aligns with the emerging therapeutic paradigm of targeting multiple apoptotic pathways to overcome resistance mechanisms often observed in cancer treatment. Consequently, niloticin's ability to orchestrate both apoptotic pathways highlights its potential as a powerful agent in the fight against cervical cancer, meriting further exploration in preclinical and clinical settings.

2.2.10. Evaluation of apoptosis by nuclear condensation and DNA fragmentation using fluorometric and SERS analysis

A defining characteristic of apoptosis is the condensation of DNA, which serves as a reliable marker to identify and analyze apoptotic events. In healthy cells, the nuclei maintain a spherical structure with evenly distributed DNA, whereas apoptotic cells exhibit condensed chromatin and fragmented DNA. This transformation can be visualized using DNA-binding dyes. One such dye, Hoechst 33342, is widely employed for its ability to permeate both live and apoptotic cells. It specifically binds to adenine-thymine-rich regions in the DNA minor groove, making it highly effective in identifying changes in nuclear morphology (40). Hoechst 33342 staining produces fluorescence detectable in both normal and condensed DNA; however, the fluorescence intensity is notably higher in condensed chromatin, which is a hallmark of apoptosis. In this experiment, HeLa cells were treated with niloticin at concentrations of 7 μM and 11 μM and subsequently stained with Hoechst 33342 to assess nuclear changes indicative of apoptosis. Under fluorescent microscopy, untreated control cells displayed intact nuclei with a uniform spherical appearance. In contrast, niloticin-treated cells showed a pronounced increase in nuclear condensation, as evidenced by the heightened fluorescence intensity of condensed DNA (Fig. 2.24a). This observation demonstrates niloticin's ability to induce chromatin condensation, validating its apoptotic potential.

Another critical feature of apoptosis is DNA fragmentation, characterized by internucleosomal cleavage of chromosomal DNA (41). This fragmentation is mediated by activated endonucleases, which cleave the DNA at regular intervals, producing fragments that appear as a distinctive "laddering" pattern when visualized using agarose gel electrophoresis. To investigate DNA fragmentation induced by niloticin, HeLa cells were treated with 7 μM and 11 μM concentrations of the compound. DNA was isolated from both control and treated cells and subjected to electrophoresis on a 0.8% agarose gel. Following staining with ethidium bromide, fragmented DNA from niloticin-treated cells exhibited a clear laddering pattern, which was absent in the control samples (Fig. 2.24b). This result further corroborates the strong apoptotic effect of niloticin.

To complement the gel electrophoresis findings and gain deeper insights into DNA fragmentation, surface-enhanced Raman spectroscopic (SERS) analysis was conducted. This advanced technique provides a detailed molecular fingerprint of DNA, offering precise insights into structural and compositional changes. Using a 633 nm laser on a confocal Raman microscope and colloidal gold nanoparticles (40–45 nm) as the SERS substrate, we analyzed DNA samples from both control and niloticin-treated HeLa cells. The Raman spectra of the treated cells showed significant alterations compared to the controls, particularly diminished peaks corresponding to the phosphodiester linkage (785 cm^{-1}) and O–P–O stretching vibrations (1093 cm^{-1}). Additionally, peaks associated with cytosine and guanine bases, as well as the DNA ring breathing mode (1178 cm^{-1} and 1316 cm^{-1}, respectively), were markedly reduced in intensity in the treated samples. Interestingly, the spectra also revealed an enhanced peak in the 1420–1440 cm^{-1} range, indicative of CH-deformation, alongside a less intense peak associated with deoxyribose vibrations (1460–1465 cm^{-1}). These spectral changes provide strong evidence of the structural disruption and fragmentation of DNA in niloticin-treated cells, further highlighting the compound's apoptotic potential (Fig. 2.24c). The combination of Hoechst staining, DNA laddering, and SERS analysis offers a comprehensive perspective on niloticin-induced DNA damage (42). The results conclusively demonstrate that niloticin triggers chromatin condensation and DNA fragmentation, key markers of apoptosis, through mechanisms that significantly alter the structural integrity of DNA. This multi-modal analysis underscores niloticin's robust capability to induce apoptosis in cervical cancer cells, emphasizing its potential as a promising therapeutic agent.

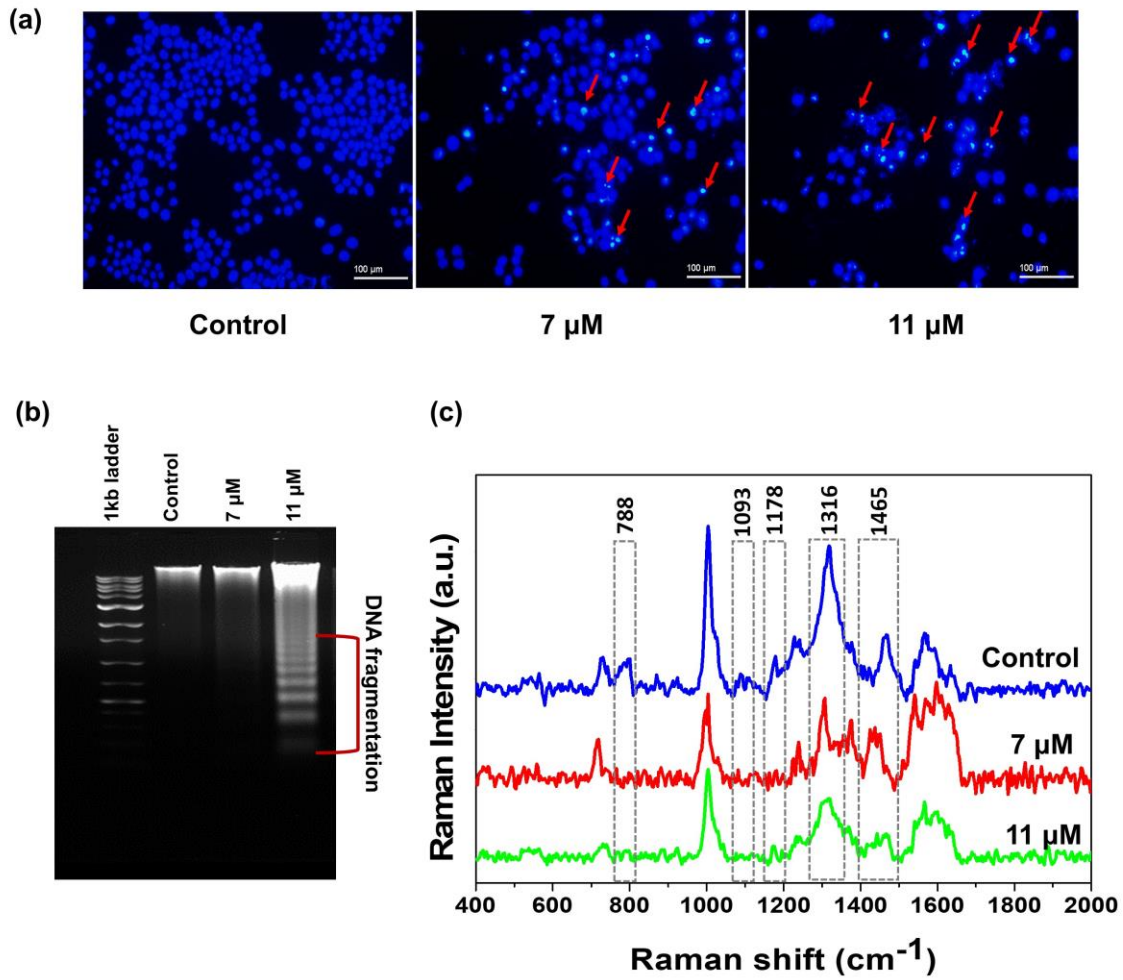

Figure 2.24. Nucleic acid condensation in HeLa cells upon treatment with niloticin is proved by a) Hoescht staining method where condensed DNA will give intense colouration comparing the untreated. Blue channel: emission wavelength (λ_{ex} = 361-389 nm), excitation wavelength (λ_{ex} = 430-490 nm) b) analysing DNA laddering pattern in both control and treated cells in which exonucleases act on niloticin treated cells giving a laddering pattern analysed by agarose gel electrophoresis c) SERS analysis of DNA laddering

2.2.11. Apoptotic assessment based on cell cycle regulation

Cancer is fundamentally driven by genomic mutations that disrupt the tightly regulated mechanisms governing the cell cycle (43). These mutations often compromise the cellular checkpoints that ensure orderly cell division, allowing uncontrolled proliferation and the escape of cells from normal regulatory controls. One key strategy for effective cancer therapy is to counteract this dysregulation by reestablishing cell cycle control or directing aberrant cells toward apoptosis. To elucidate the impact of niloticin on the cell cycle in HeLa cells, a cell cycle assay using flow cytometry was performed. This technique provides a precise evaluation of the cell cycle phases and apoptotic events by measuring DNA content in individual cells. In this study, the fluorescent nucleic acid dye propidium iodide

(PI) was used. PI selectively stains DNA and can permeate cells undergoing apoptosis or in late apoptotic stages, allowing for the differentiation of cell populations across various phases of the cell cycle. The untreated control group revealed a majority of cells distributed in the S and G2/M phases, indicative of ongoing cell proliferation. However, upon treatment with niloticin, a significant shift was observed, with a substantial portion of cells accumulating in the sub-G0 phase - a hallmark of apoptotic cell death. The quantitative analysis highlighted this shift clearly: in untreated cells, the sub-G0 population was limited to 7.6%, reflecting basal apoptosis levels. In contrast, treatment with niloticin at concentrations of 7 μM and 11 μM caused a marked increase in sub-G0 phase cells, rising to 25.6% and 39.5%, respectively (Fig. 2.25a). Concurrently, the proportion of cells in the G0/G1, S, and G2/M phases decreased significantly, illustrating a blockage in cell cycle progression and the induction of cell cycle arrest at the sub-G0 phase by niloticin.

The molecular basis of this arrest was further investigated through the analysis of critical cell cycle regulatory proteins using Western blotting. Cyclin-dependent kinase 2 (Cdk2), a pivotal regulator of cell cycle transitions at both the G1/S and G2/M checkpoints, emerged as a key target of niloticin (44). Cdk2 functions in concert with cyclins, particularly cyclin A2 and cyclin B1. Cyclin A2 facilitates the activation of Cdk2 during the G1/S checkpoint, enabling DNA replication, while cyclin B1 partners with Cdk2 to drive the cell into mitosis by phosphorylating numerous target proteins essential for progression through the mitotic phase. The data revealed that treatment with niloticin caused a pronounced downregulation of these proteins. Cyclin A2 and cyclin B1 levels were significantly reduced, aligning with the observed arrest in cell cycle progression (45-46). Moreover, the activity of Cdc25, a phosphatase that dephosphorylates and activates Cdks to promote cell cycle advancement, was similarly diminished following niloticin treatment. This reduction in Cdc25 activity further corroborates the blockage of cell cycle transitions (Fig. 2.24b–f). The coordinated downregulation of these regulatory proteins confirms the mechanism of niloticin-induced cell cycle arrest. By targeting key proteins such as Cdk2, cyclin A2, cyclin B1, and Cdc25, niloticin disrupts the regulatory networks necessary for the progression of the cell cycle, halting the division of cancer cells and redirecting them toward apoptosis. This dual action - impairing cell cycle progression while promoting cell death - underscores the therapeutic potential of niloticin in combating cervical cancer.

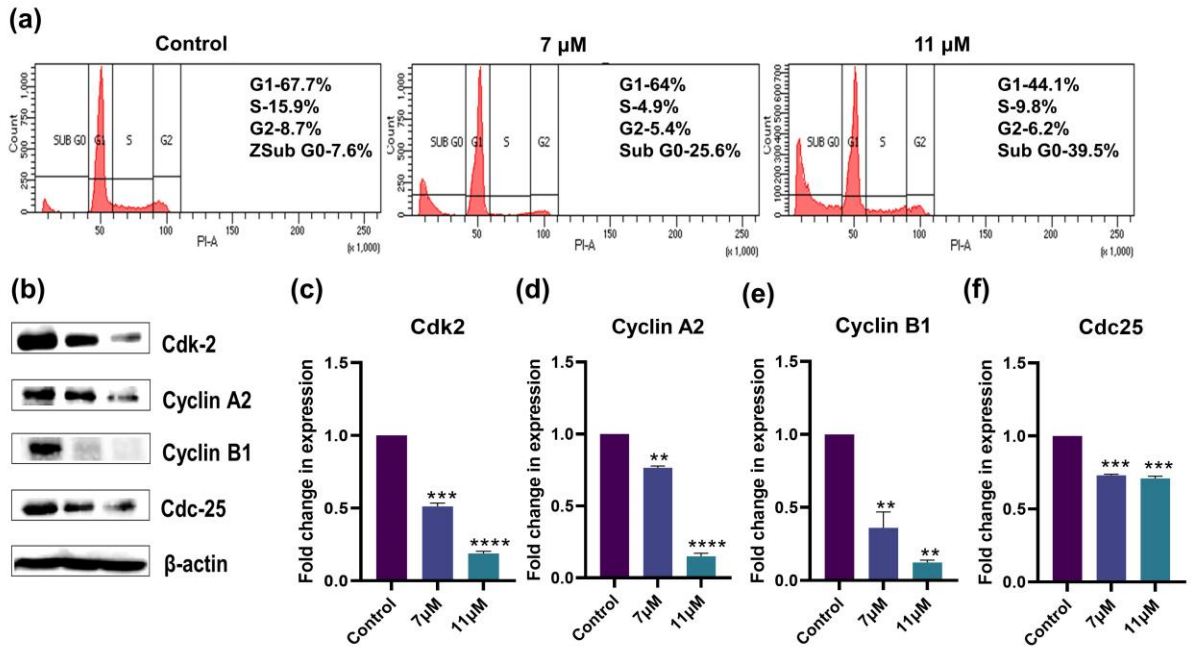

Figure 2.24. Cell cycle pattern change analysis and study of expression change in cell cycle regulatory proteins upon induction by niloticin in HeLa cells by a) Western blot of Cdk-2, cyclin A2, cyclin B1, cdc-25, some of the major proteins in cell cycle regulation. b) Graph representing fold change in expression of Cdk-2 c) Cyclin A2 d) Cyclin B1 e) Cdc25 in comparison with β-actin f) Cell cycle assay using PI staining done by FACS which confirms the sub-G0 phase arrest with higher number of cell population. Results are represented as mean ± SD, **p < 0.01, ***p < 0.001 compared to control.

2.2.12. Apoptotic induction through mitochondrial membrane potential

The maintenance of a stable mitochondrial membrane potential (ΔΨm) is a cornerstone of cellular homeostasis and essential for normal physiological processes. Disruption of this transmembrane potential can have catastrophic consequences for cellular viability, as mitochondria play a central role in energy production, signaling, and regulation of apoptotic pathways. Loss of mitochondrial membrane potential is a key event in the intrinsic (mitochondrial-mediated) pathway of apoptosis, wherein permeabilized mitochondria release pro-apoptotic factors and activate downstream caspases, culminating in programmed cell death. The depolarization of the mitochondrial membrane disrupts electron transport, leading to bioenergetic failure and triggering apoptotic cascades. To investigate the impact of niloticin on mitochondrial membrane potential, the study employed JC-1 dye, a well-established indicator for assessing ΔΨm. JC-1 is a lipophilic, cationic dye capable of penetrating mitochondria, where it forms reversible J-aggregates in cells with intact membrane potential. These aggregates emit red fluorescence, signifying healthy mitochondria with stable ΔΨm. However, in cells undergoing apoptosis, where the transmembrane potential is compromised, the JC-1 dye fails to form aggregates due to

decreased membrane negativity. Instead, the dye remains in its monomeric form, emitting green fluorescence - a hallmark of mitochondrial depolarization. In this experiment, HeLa cells were treated with niloticin for 24 hours to evaluate its impact on mitochondrial stability. Following incubation, JC-1 dye was added to the cell cultures. In untreated control cells with intact mitochondrial function, the dye predominantly formed J-aggregates, resulting in robust red fluorescence. However, in cells treated with niloticin, a notable shift was observed, with the dye primarily existing in its monomeric form, exhibiting green fluorescence. This transition highlights a loss of mitochondrial membrane potential in response to niloticin treatment (Fig. 2.25a). The data clearly demonstrate an increase in green fluorescence intensity in niloticin-treated cells compared to controls. This shift serves as direct evidence of mitochondrial dysfunction induced by the compound. The depolarization of the mitochondrial membrane underscores the involvement of niloticin in initiating the intrinsic apoptotic pathway. By disrupting ΔΨm, niloticin triggers a cascade of mitochondrial events, including the release of cytochrome c and activation of caspases, driving cells toward apoptosis. These findings provide compelling insights into the mechanistic action of niloticin as a pro-apoptotic agent. The ability of niloticin to target mitochondrial integrity not only confirms its role in promoting intrinsic apoptosis but also highlights its therapeutic potential in selectively inducing cell death in cancer cells while sparing normal cellular functions. The study underscores the importance of mitochondrial dynamics in cancer therapy and establishes niloticin as a promising candidate for mitochondrial-targeted therapeutic interventions.

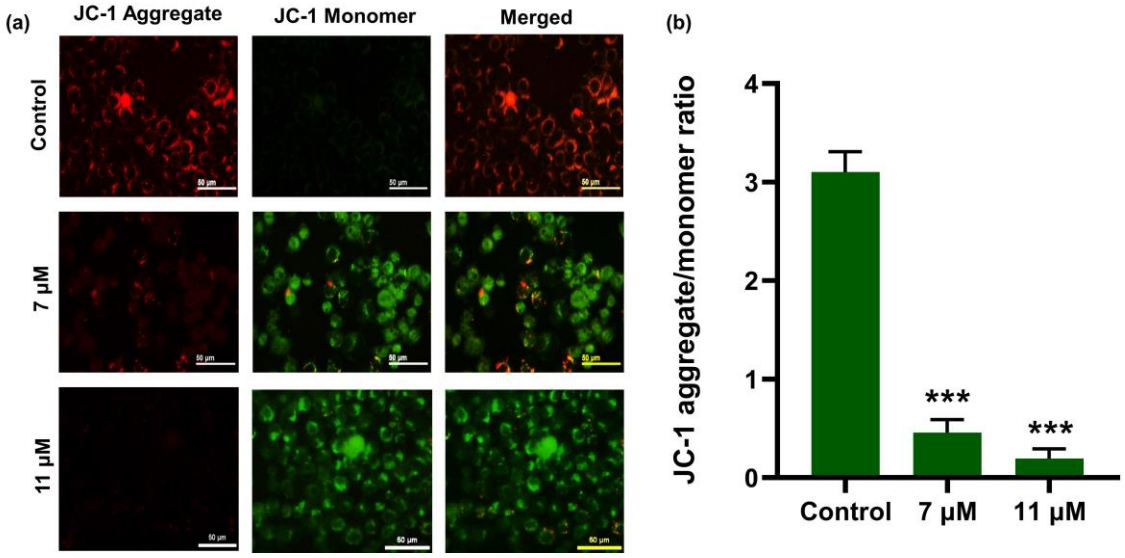

Figure 2.25. a) Analysis of change in mitochondrial membrane potential is done by JC-1 assay in HeLa cells after inducing with Niloticin b) graph showing decrease in JC-1 aggregate to monomer ratio with respect to control. Green channel: emission wavelength (λ_{ex} = 450-490 nm),

excitation wavelength (λ_{ex} = 520 nm), red channel: emission wavelength (λ_{ex} = 510-560 nm), excitation wavelength (λ_{ex} = 590 nm). Results are represented as mean ± SD, ***$p < 0.001$ is considered to be significant as compared to control. Scale bar corresponds to 50 μm.

2.2.13. Assessment of metastatic potential by niloticin

The clonogenic potential of cancer cells, which refers to their ability to survive, proliferate, and form colonies, serves as a critical marker for their reproductive viability and aggressiveness. In this study, the inhibitory effect of niloticin on the clonogenic capacity of HeLa cells was assessed using a standard colony formation assay. This assay evaluates the potential of individual cells to undergo unrestricted division and develop into colonies, reflecting their long-term survival and resilience (47). The experiment was conducted by treating HeLa cells with niloticin at concentrations of 3 μM and 6 μM. Following treatment, the surviving colonies were stained and quantified using ImageJ software. The results revealed a clear, dose-dependent suppression of colony formation in niloticin-treated cells. In untreated control cells, the total number of colonies was recorded as 639. This number significantly declined to 424 colonies in cells treated with 3 μM niloticin and further to 397 colonies at a 6 μM concentration (Fig. 2.26a). These findings highlight the potent inhibitory effect of niloticin on the clonogenic potential of HeLa cells, suggesting its capability to hinder their capacity for sustained growth and reproduction.

The ability of cancer cells to migrate and establish themselves at secondary sites, a fundamental process in metastasis, was also examined in this study using a scratch wound assay. This assay simulates a wound by creating an artificial gap in a confluent monolayer of cells and monitors the cells' ability to migrate and close the wound over time. The assay serves as a robust method to investigate the migratory behavior of cells, which is critical for their metastatic potential. In the current experiment, HeLa cells were treated with niloticin at concentrations of 3 μM and 6 μM, and their wound closure ability was observed at 0-, 24-, and 48-hours post-treatment. The percentage of wound closure was quantified using ImageJ software. The data showed a significant reduction in the migratory capacity of niloticin-treated cells compared to the untreated controls. In control cells, the wound closure percentage was markedly higher, indicating robust migratory behavior. In contrast, niloticin-treated cells displayed a noticeable delay in wound closure, with reduced migration at both concentrations tested (Fig. 2.26c and d). These findings collectively underscore the dual action of niloticin in targeting two critical aspects of cancer cell behavior—colony formation and migration. By impairing the clonogenic potential,

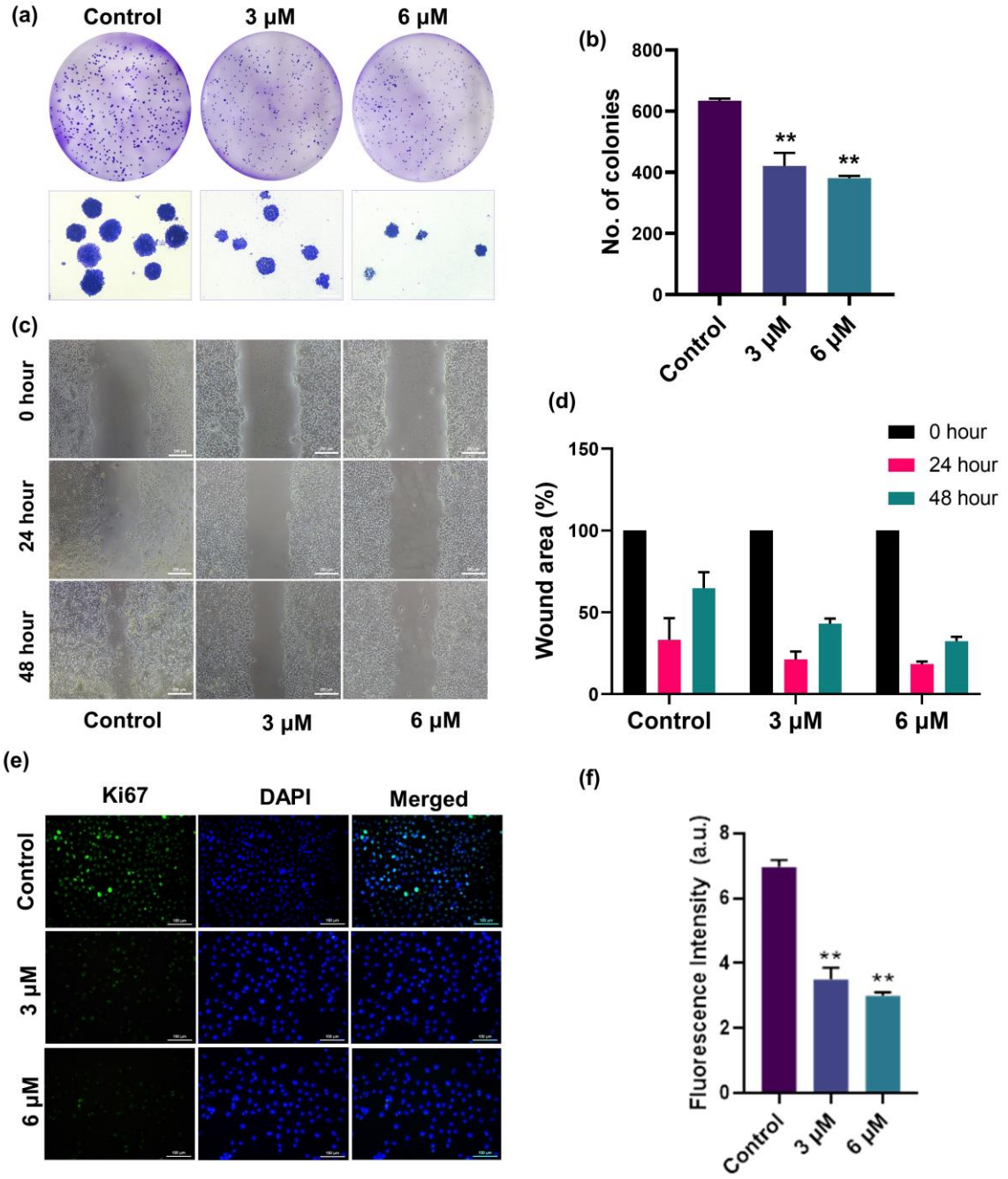

Figure 2.26. a) Inhibition of clonogenic potential of HeLa cells by niloticin treatment at 3 µM and 6 µM b) graph showing decrease in number of colonies with niloticin treatment compared to control c) Inhibtion of migratory potential of HeLa cells by niloticin treatment d) graph representing wound area percentage at different time points e) Analysis of Ki67 expression in HeLa cells at 3 µM and 6 µM niloticin treatment f) graph showing fluroscent intensity of Ki67 expression of niloticin treated cells compared to control. Blue channel: emission wavelength (λex = 361-389 nm), excitation wavelength (λex = 430-490 nm). Results are represented as mean ± SD, **p < 0.01 as compared to control.

niloticin restricts the ability of cancer cells to sustain their proliferative lineage. Concurrently, its inhibition of cell migration diminishes the metastatic potential, which is vital for cancer progression and dissemination to distant organs. This dual inhibition

positions niloticin as a promising candidate for therapeutic interventions aimed at suppressing both primary tumor growth and metastatic spread, crucial goals in the management of aggressive cancers such as cervical carcinoma.

2.2.14. Assessment of proliferative activity by immunofluorescence assay of Ki67

Ki67, a well-known proliferation marker, is commonly used in cancer diagnostics to assess the proliferative activity of tumor cells (48). Its expression is closely associated with cell division, and its presence is typically elevated in actively proliferating cells, making it an important indicator of tumor growth and aggressiveness. In this study, the anti-metastatic potential of niloticin was investigated by evaluating its effect on Ki67 expression in HeLa cells using an immunofluorescence assay. HeLa cells were treated with niloticin at two different concentrations, and the expression of Ki67 was analysed after staining with DAPI, which labels the nuclei of all cells. The treated cells were then examined under a fluorescence microscope. The results revealed a noticeable downregulation of Ki67 expression in the niloticin-treated cells in a dose-dependent manner. As the concentration of niloticin increased, the expression of Ki67 decreased significantly, indicating a reduction in the proliferative activity of the treated cells. This suggests that niloticin effectively suppresses cell division and proliferation, which is a key characteristic of its anti-metastatic potential. In contrast, the control cells, which were not treated with niloticin, displayed a high expression of Ki67, consistent with their active proliferative state. These cells showed a significantly higher level of Ki67 staining, confirming their robust cell division and growth (Fig. 2.26e). The observed decrease in Ki67 expression in niloticin-treated cells correlates with the compound's ability to inhibit cell proliferation, a crucial aspect in preventing the spread and metastasis of cancer cells. This downregulation of Ki67 expression further supports the notion that niloticin has a potent effect on curbing the growth and metastatic potential of cancer cells, highlighting its potential as a therapeutic agent for targeting tumor progression and metastasis. By suppressing the proliferative capacity of HeLa cells, niloticin may effectively hinder the ability of the tumor to expand and invade surrounding tissues, making it a promising candidate for further clinical exploration.

2.2.15. Modulation of various protein expressions involved in apoptosis

Understanding the underlying mechanisms of action of phytochemicals is crucial for identifying molecular targets that could be leveraged to develop effective therapeutic agents. Niloticin's mechanism of action in HeLa cells likely involves the activation of various apoptotic signaling pathways, as revealed by the analysis of key proteins involved in apoptosis. To explore this, a human apoptotic array membrane, encompassing 43 critical apoptotic proteins, was used to assess the expression of these markers (Fig. 2.27a–c). Heat shock protein 60 (HSP60) plays a significant role in the induction of apoptosis by accumulating in the cytosol, triggering signals that can lead to either cell death or survival. In the context of apoptosis, HSP60 facilitates the maturation and activation of caspase-3 (49). Another pivotal protein, p53, is known for its pro-apoptotic functions, which are activated in response to cellular stress. Upon activation, p53 exerts its influence on a range of pro-apoptotic pathways. Niloticin treatment led to increased expression of p53, which is known to regulate multiple apoptotic signals, including those that trigger cell cycle arrest and DNA repair or direct cells toward apoptosis (50). Additionally, CD40, a member of the TNF receptor family, also played a crucial role. Niloticin induced the binding of CD40 to its ligand, CD40L, which subsequently activated the enzymatic maturation of caspases 8 and 3, initiating the extrinsic apoptotic pathway (51). TNF, a potent pro-inflammatory cytokine, can activate both cell survival and death mechanisms. Niloticin facilitated the activation of TNF through the CD40/CD40L signaling axis, leading to apoptosis via the TNF receptor. The extrinsic apoptotic pathway is further executed by the death receptor TRAILR, which, upon activation, triggers caspase activation. The interplay between p53 activation and the upregulation of Fas receptor and FasL further enhances apoptosis by activating caspase-8, a key initiator of the extrinsic pathway.

Niloticin also triggered the expression of pro-apoptotic proteins such as Bad and Bax, which activate Bid, a Bcl-2 family protein. Bid in its truncated form, tBid, stimulates the release of Smac, a mitochondrial protein that counteracts inhibitors of apoptosis proteins (IAPs), thereby promoting apoptosis. The release of cytochrome c from mitochondria into the cytosol is another hallmark of apoptosis, activating Apaf-1 and initiating caspase-9 activation, a central component of the intrinsic apoptotic pathway (52). The expression of cytochrome c and caspase-9 further supports the involvement of the intrinsic pathway in niloticin's action. Moreover, the activation of p53 triggers caspase-8 and caspase-9, leading to the proteolytic activation of caspase-3, the executioner caspase that ultimately drives the cell toward its death phase. Additionally, p53 activates p21, a key regulator of the cell cycle,

which interacts with cyclin–cdk complexes to induce cell cycle arrest in niloticin-treated cells. This detailed expression analysis of apoptotic proteins provides strong evidence for the involvement of both the extrinsic and intrinsic apoptotic pathways in the action of niloticin, positioning it as a promising candidate for development as an effective anticancer agent (Fig. 2.28).

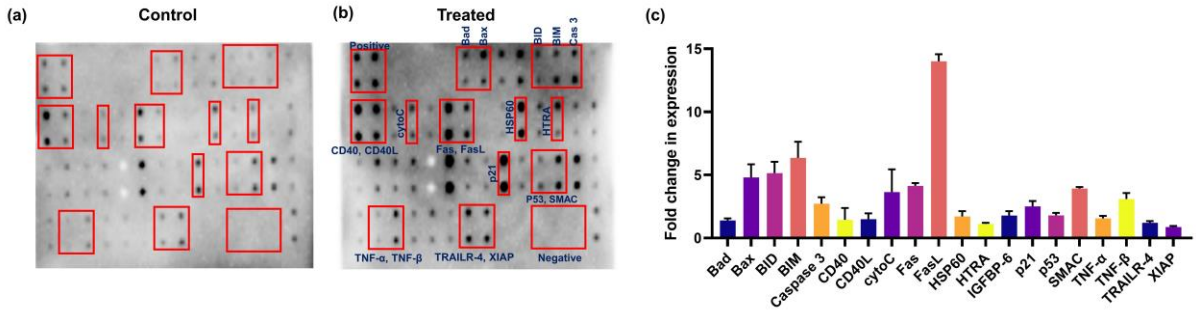

Figure 2.27. Apoptotic protein expression study in HeLa cells a) with and b) without treatment were analyzed using antibody array kit. c) Comparison of expression change in major proteins in niloticin-treated cells with respect to control

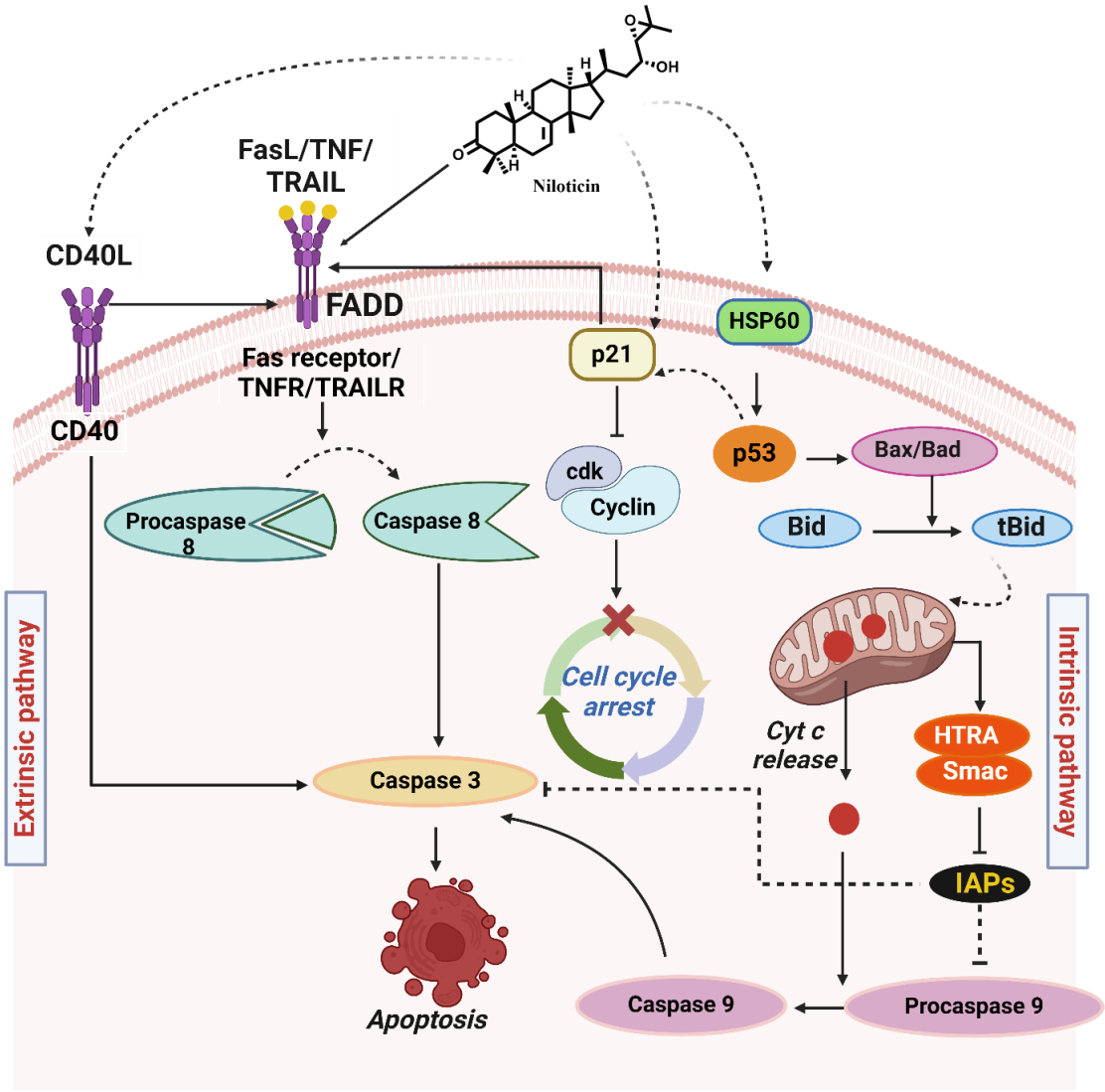

Figure 2.28. Proposed mechanism of action of Niloticin

2.3 Materials and Methods

2.3.1. General Experimental Procedures and Chemicals

The solvents used in all experiments were of the highest available grade and did not undergo further purification. Column chromatography was carried out using silica gel (100–200 mesh; Merck, Darmstadt, Germany). Thin-layer chromatography (TLC) was performed on Merck 60 F254 silica gel plates, and phytomolecules were detected either under UV light or after heating, following the application of a p-anisaldehyde–sulfuric acid spray. Nuclear magnetic resonance (NMR) spectra were recorded using a Bruker Avance 500 MHz spectrometer, with $CDCl_3$ and CD_3OD as solvents. Chemical shifts are expressed in δ (ppm) relative to tetramethylsilane (TMS). High-resolution electrospray ionization

mass spectrometry (HR-ESI-MS) data were obtained on a Thermo Scientific Exactive mass spectrometer, operating at 60,000 revolutions per minute (RPM). The purity of the tirucallane-type triterpenoids was determined using a Waters Arc analytical high-performance liquid chromatography (HPLC) system.

2.3.2. Plant Material Collection

The stem barks of *Aphanamixis polystachya* were collected in April 2017 from Parassala, Kerala, India (latitude 8.34780° N, longitude 77.1410° E). The plant specimen was deposited at the Department of Botany, University of Kerala, Thiruvananthapuram, and assigned voucher number 2018-06-05.

2.3.3. Isolation and Characterization of Compounds from *A. polystachya*

Approximately 1.0 kg of dried stem bark was mechanically powdered and extracted with acetone at room temperature (3 L × 3 days). The extract was filtered and concentrated under reduced pressure using a rotary evaporator, yielding approximately 20 g of the acetone extract. The extract was then subjected to column chromatography using silica gel, eluted with a gradient of petroleum ether/ethyl acetate (100:0 v/v to 0:100 v/v). A total of 22 fractions were collected. Fractions 5–7 were further purified by re-chromatography on silica gel, eluting with a mixture of petroleum ether/ethyl acetate (9:1 to 4:1 v/v), yielding compounds 1 (15 mg) and 2 (32 mg). Similarly, compounds 3 (10 mg) and 4 (21 mg) were isolated from fractions 8–15 using a petroleum ether/ethyl acetate gradient (4:1 to 7:3 v/v). Further purification of fractions 16–19 yielded compound 5 (18 mg) using a gradient of petroleum ether/ethyl acetate (7:3 to 3:2 v/v). The structures of the compounds were determined by 1D and 2D NMR, HR-ESI-MS, and comparison with literature data.

2.3.4. Cell Culture Methods

The following cell lines were used for biological assays: HeLa (human cervical cancer), MDA-MB-231 (triple-negative human breast cancer), A549 (human non-small cell lung cancer), and PANC-1 (human pancreatic cancer). These were obtained from the American Type Culture Collection (ATCC, USA) and National Centre for Cell Science (India), respectively. MCF-10A cells were purchased from Elabscience, USA. Cells were cultured in Dulbecco's Modified Eagle Medium (DMEM, Sigma) supplemented with 10% fetal

bovine serum (FBS, Himedia) and 1% antibiotic antimycotic solution (Himedia). The cells were maintained at 37°C in a 5% CO_2 atmosphere.

2.3.5. Cell Proliferation Assay

Cells were seeded at a density of 8×10^3 per 100 µL of DMEM in 96-well plates for 24 and 48 hours. Niloticin was added at various concentrations (5, 10, 20, 50, and 100 µM) 24 hours after seeding. After incubation for 24 and 48 hours, 100 µL of MTT solution (0.5 mg/mL) was added to each well, followed by incubation for 2–4 hours at 37°C. The MTT solution was removed, and the wells were washed with PBS. To dissolve the formazan crystals, 100 µL of dimethyl sulfoxide (DMSO) was added to each well, and the absorbance was measured at 570 nm using a Synergy H1 multimode plate reader (Biotek).

2.3.6. Molecular Simulations

The pharmacokinetic properties of niloticin were evaluated using the SwissADME online tool, which provides insights into drug-likeness, human intestinal absorption, and lipophilicity. Molecular docking studies were performed to explore the interactions between niloticin and key proteins involved in the apoptotic pathway. AutoDock Vina was used for docking simulations, utilizing crystal structures of p53 (1TUP), Fas receptor (3EZQ), FasL (5L19), Bax (6EB6), CDK2 (2UZE), BCL2 (6O0K), and TNF-β (1TNR) from the RCSB Protein Data Bank (PDB) (54). Docking scores were used to assess the binding interactions, and the results were analyzed using UCSF Chimera version 1.16 (55). Molecular dynamics simulations were conducted using Desmond, part of the Schrödinger suite, for 100 ns to examine the stability and dynamic behavior of the protein–niloticin complexes (56). The root means square deviation (RMSD) was calculated to evaluate the structural stability.

2.3.7. Apoptotic Assays

The apoptotic potential of niloticin was assessed through several assays. Live/dead cell staining was performed using the ethidium bromide-acridine orange dual-staining method, followed by imaging using a Nikon TS100 inverted microscope. The annexin V apoptosis assay was conducted using the FITC Annexin V apoptosis detection kit (BD Pharmingen),

as per the manufacturer's protocol, with cells stained with annexin V and propidium iodide, and apoptosis quantified via flow cytometry.

2.3.8. Caspase Fluorometric Assay

Caspase activity, a hallmark of apoptosis, was evaluated using the fluorometric assay for caspases 3, 8, and 9. HeLa cells were seeded at 3×10^6 density on 6-well plates and treated with niloticin at varying concentrations. Caspase activation was monitored according to the manufacturer's protocol (Abcam), with fluorescence intensity measured using a multimode plate reader (Synergy H1, Biotek) at an excitation wavelength of 400 nm and emission at 505 nm.

2.3.9. Nucleic Acid Degradation and DNA Fragmentation Studies

DNA condensation was visualized using Hoechst 33258 staining. HeLa cells were seeded at 7×10^3 per well in 96-well plates, treated with niloticin, and stained with Hoechst (1 μg/mL). DNA fragmentation was analyzed by agarose gel electrophoresis after DNA isolation using the Geneaid genomic DNA mini kit (Geneaid, cat. no. GB100). DNA concentration was measured using a Nanodrop spectrophotometer. DNA fragmentation patterns were analyzed by Raman spectroscopy using gold nanoparticles (40–45 nm) as the SERS substrate, with analysis performed on a WITec Raman microscope (WITec, Germany).

2.3.10. Cell Cycle Analysis

Cell cycle arrest induced by niloticin was studied using flow cytometry with the BD Cycle Test Plus DNA kit (BD Pharmingen, cat. no. 340242). Cells were stained with propidium iodide, and the distribution across different cell cycle phases was analyzed. Protein expression related to cell cycle regulation was assessed by Western blotting. Proteins were extracted from HeLa cells and quantified using the Pierce BCA Assay Kit (Pierce, cat. no. 23225). SDS-PAGE and Western blotting were carried out to analyze the expression of Cdk-2, cyclin A2, cyclin B1, Cdc-25, with β-actin used as a loading control.

2.3.11. Mitochondrial Membrane Potential Analysis

Mitochondrial membrane potential changes were assessed by the JC-1 assay (Sigma-Aldrich), which uses the JC-1 dye, which fluoresces green in healthy cells and red in cells undergoing apoptosis. Imaging was done using the Nikon TS100 inverted microscope.

2.3.12. Anti-Metastatic Studies

Niloticin's potential to inhibit metastasis was evaluated using clonogenic and scratch wound assays. For clonogenic assays, cells (1×10^3 per well) were treated with niloticin at 3 and 6 µM, incubated for 9 days, and stained with 0.3% crystal violet. For the scratch wound assay, cells were scratched after 24 hours of incubation, treated with niloticin, and monitored for wound closure at 0, 24, and 48 hours. Wound closure was quantified using ImageJ software.

2.3.13. Immunofluorescence Assay for Ki67 Expression

Ki67 expression was analyzed in niloticin-treated cells via immunofluorescence. Cells were seeded at 7×10^3 per well in 96-well plates, treated with niloticin, and stained for Ki67 after fixation and permeabilization. Secondary antibody staining and DAPI staining were performed, followed by imaging using the Nikon TS100 inverted fluorescent microscope.

2.3.14. Apoptotic Protein Expression

Expression of key apoptotic proteins was assessed by Western blot analysis. Proteins including p53, Bax, Bcl-2, and cleaved caspase-3 were extracted from HeLa cells after treatment with niloticin. The protein bands were detected using enhanced chemiluminescence (ECL) and quantified with ImageJ.

2.3.15. Statistical Analysis

Data are presented as mean ± standard deviation (SD) from three independent experiments. Statistical significance was determined using one-way analysis of variance (ANOVA), followed by post hoc Tukey's test. A value of $p < 0.05$ was considered statistically significant. Statistical analyses were performed using GraphPad Prism software version 8.0.

2.4. Conclusion

In summary, a detailed anticancer profiling of the tirucallane-type triterpenoid, niloticin evaluated which exhibited the highest anticancer properties among the other four isolated triterpenoids from the stem barks of *Aphanamixis polystachya* against cervical cancer cells. The primary cytotoxicity assessment of niloticin was carried out in various cancer cell lines. The cervical cancer HeLa cells turned out to have an impressive IC_{50} value of 11 μM after 24 hours of treatment, which was adequate for apoptotic induction in HeLa cells. Molecular docking studies with major protein targets (such as TNF, Fas, p53, and caspases) exhibit reasonably high binding affinity with niloticin, as evidenced by docking scores ranging from −6.8 to −9.0 kcal mol−1. The binding stability was further evaluated through molecular dynamic simulation. To complement the *in-silico* studies, downstream *in vitro* cell-based assays were employed including annexin V assay by flow cytometric analysis for validating the apoptotic potential of niloticin. In a subsequent apoptotic evaluation, DNA condensation was evident by Hoechst staining and DNA laddering supported the apoptotic potential of niloticin in HeLa cells. The SERS fingerprint analysis in the treated cells enabled the tracking of cellular DNA breakage as a complementary assessment, which was fully complemented by the DNA laddering experiment. The cell cycle analysis indicated the arrest at the sub-G0 phase. The halt in cell cycle progression was determined by the analysis of the proteins involved, which finally takes the cell into apoptosis. Another interesting fact is the involvement of both extrinsic and intrinsic modes of apoptosis induced by niloticin, analyzed by the substantial expression of caspase 3, 9, and 8. The expression of major regulatory proteins involved in the apoptosis cascade is evident in the protein dot-blot assay. Finally, the modulation in the signaling pathways involved in the cancer was studied by analyzing the different proteins involved. The activation of p53 by the induction of niloticin was the key step. p53 induced the binding of FasL to the Fas receptor, resulting in the activation of the initiator caspase 8, a prominent factor of the extrinsic pathway of apoptosis. The activation of p53 also upregulates the expression of proapoptotic proteins Bad/Bax and further activates Bid, SMAC and HTRA, which results in the export of cytochrome c from the nucleus to cytosol. Cytochrome c then activates Apaf-1, which is a requisite for the activation of caspase 9, the key factor in the intrinsic pathway of apoptosis. Both the extrinsic and intrinsic modes finally conclude in the catalytic activation of caspase-3, taking the cell to its demolition phase. Further evaluation of niloticin in its ability to inhibit colony formation and wound healing property reflected

its anti-metastatic potential. Niloticin exerting its effect in the downregulation of the proliferative marker Ki67 by immunofluorescence assay further proves its capability as an anti-metastatic potential agent. Therefore, it is envisaged that the naturally occurring phytomolecule niloticin would become a successful blueprint to generate a potential anticancer hit compound for pre-clinical studies against the efficacious management of cervical cancer.

2.5. References

(1) Halim, C. E.; Xinjing, S. L.; Fan, L.; Bailey Vitarbo, J.; Arfuso, F.; Tan, C. H.; Narula, A. S.; Kumar, A. P.; Sethi, G.; Ahn, K. S. Anti-Cancer Effects of Oxymatrine Are Mediated through Multiple Molecular Mechanism(s) in Tumor Models. Pharmacological Research. 2019.

(2) Rahmani, A. H.; Al Zohairy, M. A.; Aly, S. M.; Khan, M. A. Curcumin: A Potential Candidate in Prevention of Cancer via Modulation of Molecular Pathways. Biomed Res Int 2014, 2014.

(3) Sailo, B. L.; Banik, K.; Girisa, S.; Bordoloi, D.; Fan, L.; Halim, C. E.; Wang, H.; Kumar, A. P.; Zheng, D.; Mao, X.; Sethi, G.; Kunnumakkara, A. B. FBXW7 in Cancer: What Has Been Unraveled Thus Far? Cancers. 2019.

(4) Banik, K.; Ranaware, A. M.; Deshpande, V.; Nalawade, S. P.; Padmavathi, G.; Bordoloi, D.; Sailo, B. L.; Shanmugam, M. K.; Fan, L.; Arfuso, F.; Sethi, G.; Kunnumakkara, A. B. Honokiol for Cancer Therapeutics: A Traditional Medicine That Can Modulate Multiple Oncogenic Targets. Pharmacological Research. 2019.

(5) Zaimy, M. A.; Saffarzadeh, N.; Mohammadi, A.; Pourghadamyari, H.; Izadi, P.; Sarli, A.; Moghaddam, L. K.; Paschepari, S. R.; Azizi, H.; Torkamandi, S.; Tavakkoly-Bazzaz, J. New Methods in the Diagnosis of Cancer and Gene Therapy of Cancer Based on Nanoparticles. Cancer Gene Therapy. 2017.

(6) Valsan, A.; Meenu, M. T.; Murali, V. P.; Malgija, B.; Joseph, A. G.; Nisha, P.; Radhakrishnan, K. V.; Maiti, K. K. Exploration of Phaeanthine: A Bisbenzylisoquinoline Alkaloid Induces Anticancer Effect in Cervical Cancer Cells Involving Mitochondria-Mediated Apoptosis. ACS Omega 2023, 8 (16), 14799–14813.

(7) Ong, S. K. L.; Shanmugam, M. K.; Fan, L.; Fraser, S. E.; Arfuso, F.; Ahn, K. S.; Sethi, G.; Bishayee, A. Focus on Formononetin: Anticancer Potential and Molecular Targets. Cancers (Basel) 2019, 11 (5).

(8) Hashem, S.; Ali, T. A.; Akhtar, S.; Nisar, S.; Sageena, G.; Ali, S.; Al-Mannai, S.; Therachiyil, L.; Mir, R.; Elfaki, I.; Mir, M. M.; Jamal, F.; Masoodi, T.; Uddin, S.; Singh, M.; Haris, M.; Macha, M.; Bhat, A. A. Targeting Cancer Signaling Pathways by Natural Products: Exploring Promising Anti-Cancer Agents. Biomedicine and Pharmacotherapy. 2022.

(9) Nuzzo, G.; Senese, G.; Gallo, C.; Albiani, F.; Romano, L.; D'ippolito, G.; Manzo, E.; Fontana, A. Antitumor Potential of Immunomodulatory Natural Products. Marine Drugs. MDPI June 1, 2022.

(10) Mohamed, S. I. A.; Jantan, I.; Haque, M. A. Naturally Occurring Immunomodulators with Antitumor Activity: An Insight on Their Mechanisms of Action. International Immunopharmacology. Elsevier B.V. September 1, 2017, pp 291–304.

(11) Krishnaraju, A. V.; Rao, C. V.; Rao, T. V. N.; Reddy, K. N.; Trimurtulu, G. In Vitro and In Vivo Antioxidant Activity of Aphanamixis Polystachya Bark. Am J Infect Dis 2009, 5 (2).

(12) Sadhu, S. K.; Phattanawasin, P.; Choudhuri, M. S. K.; Ohtsuki, T.; Ishibashi, M. A New Lignan from Aphanamixis Polystachya. J Nat Med 2006, 60 (3).

(13) Mishra, A. P.; Saklani, S.; Chandra, S.; Mathur, A.; Milella, L.; Tiwari, P. Aphanamixis Polystachya (Wall.) Parker, Phytochemistry, Pharmacological Properties and Medicinal Uses: An Overview. World J Pharm Pharm Sci 2014, 3 (6).

(14) Hossain, M. S.; Islam, M.; Jahan, I.; Hasan, M. K. Aphanamixis Polystachya: Pharmacological Benefits, Health Benefits and Other Potential Benefits. Phytomedicine Plus. 2023.

(15) Hossain, M. M.; Biva, J.; Jahangir, R.; Mynol, M.; Vhuiyan, I. Central Nervous System Depressant and Analgesic Activity of Aphanamixis Polystachya (Wall.) Parker Leaf Extract in Mice. Afr J Pharm Pharmacol 2009, 3 (5), 282–286.

(16) Jagetia, G. C.; Venkatesha, V. A. Treatment of Mice with Stem Bark Extract of Aphanamixis Polystachya Reduces Radiation-Induced Chromosome Damage. Int J Radiat Biol 2006, 82 (3).

(17) Xu, H.; Jia, Y.; Li, J.; Huang, X.; Jiang, L.; Xiang, T.; Xie, Y.; Yang, X.; Liu, T.; Xiang, Z.; Sheng, J. Niloticin Inhibits Osteoclastogenesis by Blocking RANKL–RANK Interaction and Suppressing the AKT, MAPK, and NF-KB Signaling Pathways. Biomedicine and Pharmacotherapy 2022, 149.

(18) Chen, G.; Liu, C.; Zhang, M.; Wang, X.; Xu, Y. Niloticin Binds to MD-2 to Promote Anti-Inflammatory Pathway Activation in Macrophage Cells. Int J Immunopathol Pharmacol 2022, 36.

(19) Reegan, A. D.; Stalin, A.; Paulraj, M. G.; Balakrishna, K.; Ignacimuthu, S.; Al-Dhabi, N. A. In Silico Molecular Docking of Niloticin with Acetylcholinesterase 1 (AChE1) of Aedes Aegypti L. (Diptera: Culicidae): A Promising Molecular Target. Medicinal Chemistry Research 2016, 25 (7).

(20) Reegan, A. D.; Gandhi, M. R.; Paulraj, M. G.; Balakrishna, K.; Ignacimuthu, S. Effect of Niloticin, a Protolimonoid Isolated from Limonia Acidissima L. (Rutaceae) on the Immature Stages of Dengue Vector Aedes Aegypti L. (Diptera: Culicidae). Acta Trop 2014, 139.

(21) Hong, Z. L.; Xiong, J.; Wu, S. B.; Zhu, J. J.; Hong, J. L.; Zhao, Y.; Xia, G.; Hu, J. F. Tetracyclic Triterpenoids and Terpenylated Coumarins from the Bark of Ailanthus Altissima ("Tree of Heaven"). Phytochemistry 2013, 86.

(22) Yan, C.; Zhang, Y. D.; Wang, X. H.; Geng, S. D.; Wang, T. Y.; Sun, M.; Liang, W.; Zhang, W. Q.; Zhang, X. D.; Luo, H. Tirucallane-Type Triterpenoids from the Fruits of Phellodendron Chinense Schneid and Their Cytotoxic Activities. Fitoterapia 2016, 113.

(23) Zhao, W. Y.; Chen, J. J.; Zou, C. X.; Zhang, Y. Y.; Yao, G. D.; Wang, X. B.; Huang, X. X.; Lin, B.; Song, S. J. New Tirucallane Triterpenoids from Picrasma Quassioides with Their Potential Antiproliferative Activities on Hepatoma Cells. Bioorg Chem 2019, 84.

(24) Miyake, K.; Tezuka, Y.; Awale, S.; Li, F.; Kadota, S. Canthin-6-One Alkaloids and a Tirucallanoid from Eurycoma Longifolia and Their Cytotoxic Activity against a Human HT-1080 Fibrosarcoma Cell Line. Nat Prod Commun 2010, 5 (1).

(25) Su Ronghui; Kim Mujo; Kawaguchi Hitoshi; Yamamoto Takehiko; Goto Katsumi; Taga Tooru; Miwa Yoshihisa; Kozuka Mutsuo; Takahashi Shozo. Triterpenoids from the Fruits of Phellodendron Chinese SCHNEID.: The Stereostructure of Niloticin. Chemical and Pharmaceutical Bulletin 1990, 38 (6), 1616–1619.

(26) Wang, X.-N.; Fan, C.-Q.; Yin, S.; Lin, L.-P.; Ding, J.; Yue, J.-M. Cytotoxic Terpenoids from Turraea Pubescens; 2008.

(27) Mcchesney, J. D.; Dou, J.; Sindelar, R. D.; Goins, D. K.; Walker, L. A.; Rogers, R. D. Tirucallane-Type Triterpenoids: Nmr and X-Ray Diffraction Analyses of 24-Epi-Piscidinol A and Piscidinol A; 1997; Vol. 27.

(28) Jolad Shivanand D; Hoffmann Joseph J; Schram H Karl; Cole Jack R. Constituents of Trichilia Hispida (Meliaceae). 4. Hispidols A and B, Two New Tirucallane Triterpenoids. J. Org. Chem 1981, 46, 4085–4088.

(29) Mahdizadeh, S. J.; Thomas, M.; Eriksson, L. A. Reconstruction of the Fas-Based Death-Inducing Signaling Complex (DISC) Using a Protein-Protein Docking Meta-Approach. J Chem Inf Model 2021, 61 (7), 3543–3558.

(30) Khatal, T. K.; Chaturbhuj, G. U. Computational Analysis of the Binding Site(s) of TNF β-TNFR1 Complex: Implications for Designing Novel Anticancer Agents. Clin Cancer Drugs 2018, 5 (2), 94–104.

(31) Dengler, M. A.; Robin, A. Y.; Gibson, L.; Li, M. X.; Sandow, J. J.; Iyer, S.; Webb, A. I.; Westphal, D.; Dewson, G.; Adams, J. M. BAX Activation: Mutations Near Its Proposed Non-Canonical BH3 Binding Site Reveal Allosteric Changes Controlling Mitochondrial Association. Cell Rep 2019, 27 (2), 359-373.e6.

(32) Tondar, A.; Sánchez-Herrero, S.; Bepari, A. K.; Bahmani, A.; Calvet Liñán, L.; Hervás-Marín, D. Virtual Screening of Small Molecules Targeting BCL2 with Machine Learning, Molecular Docking, and MD Simulation. Biomolecules 2024, 14 (5).

(33) Liu, W.; Ramagopal, U.; Cheng, H.; Bonanno, J. B.; Toro, R.; Bhosle, R.; Zhan, C.; Almo, S. C. Crystal Structure of the Complex of Human FasL and Its Decoy Receptor DcR3. Structure 2016, 24 (11), 2016–2023.

(34) Nurhayati, A. P. D.; Rihandoko, A.; Fadlan, A.; Ghaissani, S. S.; Jadid, N.; Setiawan, E. Anti-Cancer Potency by Induced Apoptosis by Molecular Docking P53, Caspase, Cyclin D1, Cytotoxicity Analysis and Phagocytosis Activity of Trisindoline 1,3 and 4. Saudi Pharmaceutical Journal 2022, 30 (9), 1345–1359.

(35) Li, G. Y.; Fan, B.; Zheng, Y. C. Calcium Overload Is a Critical Step in Programmed Necrosis of ARPE-19 Cells Induced by High-Concentration H2O2. Biomedical and Environmental Sciences 2010, 23 (5).

(36) Shi, Y. Caspase Activation, Inhibition, and Reactivation: A Mechanistic View. Protein Science 2004, 13 (8).

(37) Elumalai, P.; Gunadharini, D. N.; Senthilkumar, K.; Banudevi, S.; Arunkumar, R.; Benson, C. S.; Sharmila, G.; Arunakaran, J. Induction of Apoptosis in Human Breast Cancer Cells by Nimbolide through Extrinsic and Intrinsic Pathway. Toxicol Lett 2012, 215 (2).

(38) Hsu, F. T.; Chen, W. T.; Wu, C. Te; Chung, J. G. Hyperforin Induces Apoptosis through Extrinsic/Intrinsic Pathways and Inhibits EGFR/ERK/NF-KB-Mediated Anti-Apoptotic Potential in Glioblastoma. Environ Toxicol 2020, 35 (10).

(39) Kar, S.; Palit, S.; Ball, W. B.; Das, P. K. Carnosic Acid Modulates Akt/IKK/NF-KB Signaling by PP2A and Induces Intrinsic and Extrinsic Pathway Mediated Apoptosis in Human Prostate Carcinoma PC-3 Cells. Apoptosis 2012, 17 (7).

(40) Crowley, L. C.; Marfell, B. J.; Waterhouse, N. J. Analyzing Cell Death by Nuclear Staining with Hoechst 33342. Cold Spring Harb Protoc 2016, 2016 (9).

(41) Majtnerová, P.; Roušar, T. An Overview of Apoptosis Assays Detecting DNA Fragmentation. Molecular Biology Reports. Springer Netherlands October 1, 2018, pp 1469–1478.

(42) Movasaghi, Z.; Rehman, S.; Rehman, I. U. Raman Spectroscopy of Biological Tissues. Applied Spectroscopy Reviews. September 2007, pp 493–541.

(43) Matthews, H. K.; Bertoli, C.; de Bruin, R. A. M. Cell Cycle Control in Cancer. Nature Reviews Molecular Cell Biology. Nature Research January 1, 2022, pp 74–88.

(44) Bačević, K.; Lossaint, G.; Achour, T. N.; Georget, V.; Fisher, D.; Dulić, V. Cdk2 Strengthens the Intra-S Checkpoint and Counteracts Cell Cycle Exit Induced by DNA Damage. Sci Rep 2017, 7 (1).

(45) Loukil, A. Cyclin A2: At the Crossroads of Cell Cycle and Cell Invasion. World J Biol Chem 2015, 6 (4), 346.

(46) Strauss, B.; Harrison, A.; Coelho, P. A.; Yata, K.; Zernicka-Goetz, M.; Pines, J. Cyclin B1 Is Essential for Mitosis in Mouse Embryos, and Its Nuclear Export Sets the Time for Mitosis. Journal of Cell Biology 2018, 217 (1).

(47) Franken, N. A. P.; Rodermond, H. M.; Stap, J.; Haveman, J.; van Bree, C. Clonogenic Assay of Cells in Vitro. Nat Protoc 2006, 1 (5), 2315–2319.

(48) Li, L. T.; Jiang, G.; Chen, Q.; Zheng, J. N. Predic Ki67 Is a Promising Molecular Target in the Diagnosis of Cancer (Review). Molecular Medicine Reports. Spandidos Publications March 1, 2015, pp 1566–1572.

(49) Chandra, D.; Choy, G.; Tang, D. G. Cytosolic Accumulation of HSP60 during Apoptosis with or without Apparent Mitochondrial Release: Evidence That Its pro-Apoptotic or pro-Survival Functions Involve Differential Interactions with Caspase-3. Journal of Biological Chemistry 2007, 282 (43).

(50) Shen, Y.; White, E. P53-Dependent Apoptosis Pathways; 2001.

(51) Arya, J. S.; Joseph, M. M.; Sherin, D. R.; Nair, J. B.; Manojkumar, T. K.; Maiti, K. K. Exploring Mitochondria-Mediated Intrinsic Apoptosis by New Phytochemical Entities: An Explicit Observation of Cytochrome c Dynamics on Lung and Melanoma Cancer Cells. J Med Chem 2019, 62 (17), 8311–8329.

(52) Van Loo, G.; Saelens, X.; Van Gurp, M.; MacFarlane, M.; Martin, S. J.; Vandenabeele, P. The Role of Mitochondrial Factors in Apoptosis: A Russian Roulette with More than One Bullet. Cell Death and Differentiation. 2002.

(53) Daina, A.; Michielin, O.; Zoete, V. SwissADME: A Free Web Tool to Evaluate Pharmacokinetics, Drug-Likeness and Medicinal Chemistry Friendliness of Small Molecules. Sci Rep 2017, 7.

(54) Trott, O.; Olson, A. J. AutoDock Vina: Improving the Speed and Accuracy of Docking with a New Scoring Function, Efficient Optimization, and Multithreading. J Comput Chem 2010, 31 (2), 455–461.

(55) Pettersen, E. F.; Goddard, T. D.; Huang, C. C.; Couch, G. S.; Greenblatt, D. M.; Meng, E. C.; Ferrin, T. E. UCSF Chimera - A Visualization System for Exploratory Research and Analysis. J Comput Chem 2004, 25 (13), 1605–1612.

(56) Bowers Kevin J; Chow Edmond; Xu Huafeng; Dror Ron O; Eastwood Michael P; Gregersen Brent A; Klepeis John L; Kolossvary Istvan; Moraes Mark A; D Federico; Sacerdoti; Salmon John K; Shan Yibing; Shaw David E. Scalable Algorithms for Molecular Dynamics Simulations on Commodity Clusters. IEEE 2007.

Chapter 3

Comprehensive apoptotic evaluation and mechanistic insights of prieurianin in cervical cancer cells

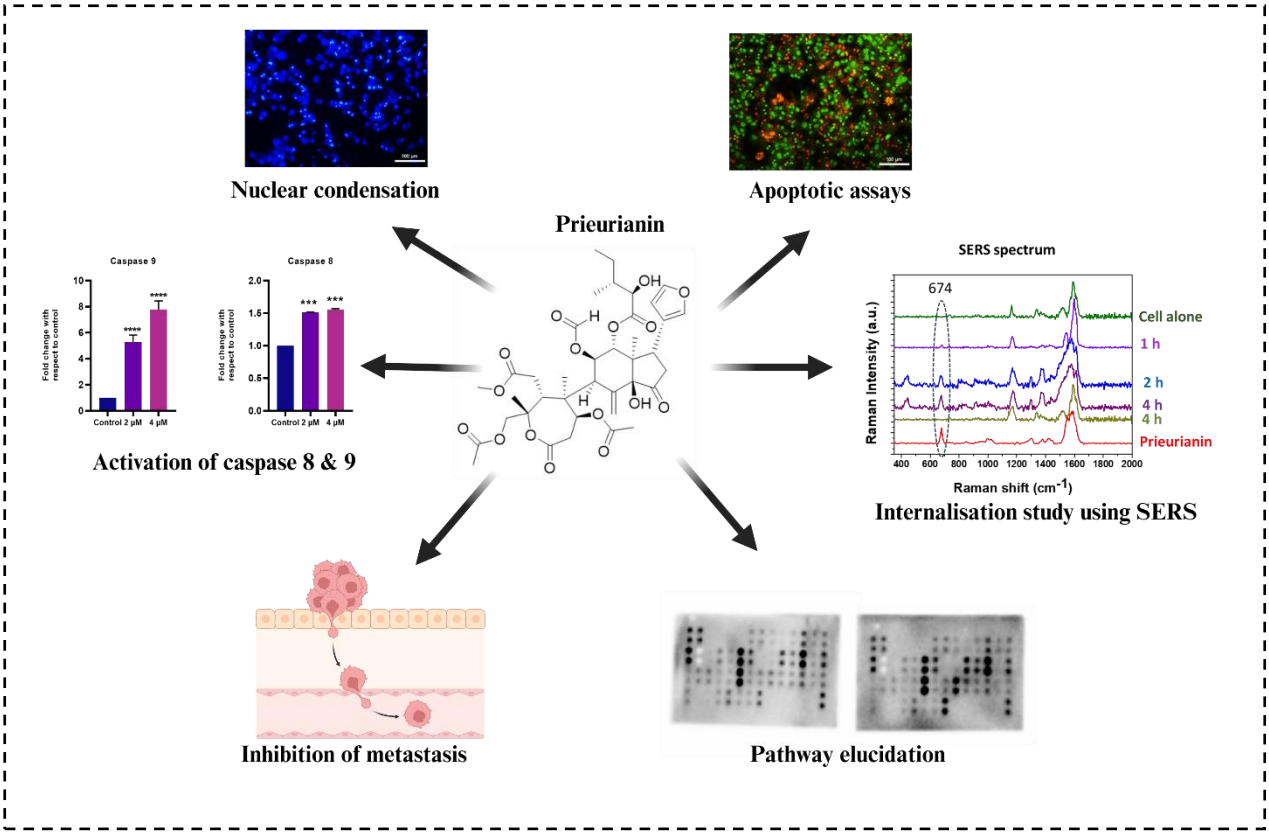

Abstract

Prieurianin, a limonoid isolated from the Meliaceae family, has been investigated for its paramacological capabilities. This study explores the apoptotic and mechanistic insights of prieurianin's action in SiHa (cervical cancer) cells. The compound exhibited significant cytotoxicity, with an IC_{50} of 3.9 µM at 48 hours, selectively targeting cancer cells over normal cells (IC_{50} = 43.58 µM). The study highlights the internalization of prieurianin in the cells explored through SERS modality. The detailed apoptotic evaluation revealed that prieurianin induces cell death via the mitochondrial-dependent intrinsic and extrinsic pathways. Flow cytometry analysis using annexin V/PI staining demonstrated significant early and late apoptosis, with minimal necrosis. Caspase activation assays showed a robust increase in caspase 3, 8, and 9, confirming the dual activation of both apoptotic pathways.

Moreover, Hoechst staining indicated chromatin condensation, a hallmark of apoptosis, and cell cycle analysis revealed a marked accumulation of cells in the sub-G0 phase, signifying apoptosis induction. Mitochondrial membrane potential studies with JC-1 dye further confirmed prieurianin's impact on mitochondrial dysfunction, leading to the release of pro-apoptotic factors. Additionally, prieurianin inhibited cancer cell clonogenic potential and migration, impairing cell proliferation and metastatic potential. Protein expression studies revealed prieurianin's ability to upregulate pro-apoptotic proteins (Bax, Bad), generate reactive oxygen species (ROS), and activate key apoptotic mediators such as caspase 9 and caspase 3, while inducing cell cycle arrest through p21 expression. These findings highlight prieurianin's multifaceted anticancer effects and its potential as a therapeutic agent for targeting cervical cancer. Further preclinical and clinical studies are warranted to explore its full pharmacological profile and therapeutic efficacy.

3.1 Introduction

Limonoids are a group of highly oxygenated triterpenoids primarily found in plants belonging to the Rutaceae and Meliaceae families (1). They are also referred to as tetranotriterpenoids due to the oxidative loss of four carbon atoms from the triterpenoid side chain, forming a unique α-substituted furyl ring. These compounds possess a characteristic 4,4,8-trimethyl-17-furyl steroidal skeleton, which serves as a precursor to structurally diverse limonoid derivatives. Limonoids are classified into subcategories based on structural modifications, including ring-intact limonoids, ring-seco limonoids, degraded limonoids, and highly oxidatively modified limonoids(2,3). Such diversity in their structure contributes to their wide spectrum of biological activities, such as cytotoxic, antioxidant, anti-inflammatory, neuroprotective, antiviral, antimicrobial, antimalarial, and antiprotozoal properties (4,5). Among these biological effects, limonoids have garnered significant attention for their anticancer potential. Their complex molecular frameworks, including furan rings and rearranged triterpenoid backbones, enable multi-targeted therapeutic effects in cancer treatment. Limonoids exert their anticancer activity by inducing apoptosis through the intrinsic mitochondrial-dependent pathway. This involves the activation of caspases (caspase-3, -7, and -9) and regulation of apoptotic proteins such as Bax (pro-apoptotic) and Bcl-2 (anti-apoptotic). These changes disrupt the mitochondrial membrane potential, triggering programmed cell death. Additionally, limonoids inhibit tumor progression by suppressing critical signaling pathways such as NF-κB, PI3K/Akt, and

MAPK, thereby reducing the expression of inflammatory cytokines, angiogenic factors, and cell survival proteins. Limonoids also exhibit anti-angiogenic effects, which hinder the formation of blood vessels essential for tumor growth and metastasis(6–8) . Compounds like nimbolide and gedunin have shown significant efficacy against cancers including breast, colon, prostate, liver, and leukemia cell lines. Their selective targeting of cancer cells while sparing healthy tissues highlights their potential as safer alternatives to conventional chemotherapies (9).

Prieurianin, a limonoid predominantly isolated from plants of the Meliaceae family, has emerged as a bioactive compound of interest for its diverse biological and pharmacological activities. Its structurally unique oxidized triterpenoid framework and furan-based rings endow it with notable therapeutic potential. Prieurianin displays potent anti-inflammatory activity by targeting the nuclear factor kappa B (NF-κB) signaling pathway, a master regulator of inflammation. By downregulating the expression of inflammatory cytokines like TNF-α, IL-1β, and IL-6, prieurianin effectively mitigates chronic inflammatory diseases such as arthritis and colitis. Moreover, its antioxidant properties contribute to reducing reactive oxygen species (ROS), protecting cellular components from oxidative damage. This makes prieurianin relevant for managing oxidative stress-related conditions, including neurodegenerative disorders like Alzheimer's and Parkinson's diseases, as well as cardiovascular diseases and diabetes. Prieurianin also exhibits significant anti-parasitic activity, particularly against Plasmodium species (malaria) and protozoan parasites responsible for leishmaniasis and trypanosomiasis. By interfering with parasitic cell metabolism and DNA replication, prieurianin has shown potential as a natural alternative to existing antiparasitic therapies. Additionally, its antimicrobial properties have been reported, with inhibitory effects against various bacterial and fungal strains, expanding its potential for infectious disease management (10,11) . While prieurianin's pharmacological potential is well established *in vitro*, further *in vivo* studies, pharmacokinetic evaluations, and clinical investigations are necessary to assess its safety, bioavailability, and therapeutic efficacy in humans. Future research efforts should also focus on optimizing prieurianin-based derivatives and formulations to enhance their pharmacological properties. Overall, prieurianin represents a promising therapeutic candidate for treating cancer, inflammatory diseases, oxidative stress disorders, and parasitic infections, making it a valuable molecule in natural product-based drug discovery. Herein, the anticancer properties of prieurianin has been investigated which was isolated from barks of *A. polystachya*. The study begins

with the cytotoxicity evaluation of prieurianin in different cancer cells, where a good activity was observed in SiHa cervical cancer cells with an IC_{50} of 3.9 µM at 48 hours of incubation. Internalization of prieurianin into SiHa cells was assessed using the surface-enhanced Raman spectroscopy (SERS), where internalization was observed after 2 and 4 hours after prieurianin treatment. Then, apoptotic effects of prieurianin were studied using live dead assay, APOPercentage assay, Annexin V assay using flow cytometric analysis. Cell cycle analysis revealed the cell cycle arrest upon prieurianin treatment in SiHa cells, leading to the apoptosis. Capase flurometric studies exposed the involvement of both extrinsic and intrinsic modes of apoptosis. Further detailed protein expression studies were done, proving prieurianin a efficient phytomolecule that could be developed into a promising anticancer agent. To the best of our knowledge, this is the first detailed evaluation of prieurainin in cancer cells.

3.2 Results and discussion

3.2.1 Evaluation of cytotoxicity of prieurianin

Preliminary cytotoxicity evaluation of prieurianin is conducted using MTT assay in various cancer cell lines HeLa, SiHa (cervical cancer), MDA-MB-231 (breast cancer), and PANC-1 (pancreatic cancer) cell lines (12). Comparing the IC_{50} values exhibited by these cell lines, prieurianin in SiHa, the cervical cancer cell line turned out to be the efficient one with an IC_{50} value of 3.9 µM at 48 hours of incubation time (Figure 3.1). In order the check the effect of prieurianin in normal cells, the assay was also conducted in WI-38 lung cells, where the IC_{50} was found to be 43.58 µM at 48 hours of incubation. With these findings, further experiments for analyzing anticancer potential of prieurianin proceeded in SiHa cell line.

(a)

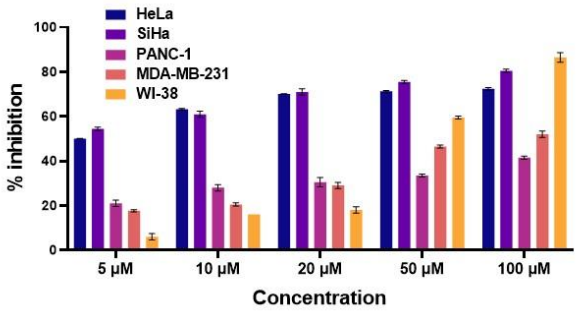

(b)

Cell line	IC_{50} (µM)
HeLa	5
SiHa	3.9
MDA-MB-231	83.6
PANC-1	<100
WI-38	43.58

Figure 3.1: a) Comparative study of percentage inhibition of prieurianin in different cancer cell lines and b) their IC_{50} values using MTT assay.

3.2.2. Internalisation studies of prieurianin using surface-enhanced Raman spectroscopy (SERS)

SERS analysis of prieurianin showed distinct Raman peaks with the gold nanoparticles. The major peaks observed were the acetate ester vibrations (O-C=O in-plane deformation) at 674 cm^{-1}, aromatic ring vibrations at 990–1100 cm^{-1}, C-CH3 vibrations at 1335-1385 cm^{-1}, CH2 vibrations at 1405–1455 cm^{-1}, and Aromatic/hetero ring vibration at 1550–1610 cm^{-1} as shown in figure 3.2a(13). Out of these, upon incubation with the cells, only the acetate ester vibrations of the compound at 674 cm^{-1} were found to not interfere with the SERS peak of the cells alone. For this, the SERS peaks from the untreated cells were collected and aligned with the compound-treated cells (Figure 3.2e). From the time-dependent internalisation study, it was found that the prieurianin-specific peak was visible from 1 h of the treatment itself which was more prominent in 2nd hour and 4th hour. SERS spectra collected after 8 hours of incubation showed no observable peak at 674 cm^{-1} , most probably due to its metabolic alterations within the cells. Figure 3.2c depicts the SERS images corresponding to 674 cm^{-1} position collected from the prieurianin treated (2 h) and untreated cells. The images demonstrated the bright yellow regions, especially from the cytoplasmic area of the compound-treated cells, where there is no such image was formed with the untreated cells when it was mapped for the 674 cm^{-1} Raman peak position.

3.2.3. Apoptotic evaluation of prieurianin in SiHa cells

After initial cytotoxicity assessment, to analyze effect in membrane disintegration imparted by prieurianin as a result of cell death, various assays were employed. Initially, a live dead assay using the acridine orange-ethidium bromide dual staining method was done. Prieurianin was treated in different concentrations (2 µM and 4 µM) around the minimal inhibitory concentration. The assay progresses in such a way of labeling control cells as green and membrane compromised cells as orange-reddish color, which is based on the principle that acridine orange has the potential of entering into cells with intact membrane, which will be seen as green and ethidium bromide could surpass only cells with a disrupted membrane which exhibits red coloration (14) . This assay proves the disintegration of the cell membrane as a result of prieurianin treatment as observed in the results given (Figure 3.3a). To assess the effects of prieurianin on membrane integrity during apoptosis, the

APOPercentage assay was employed. The results confirmed the observations from the live dead assay. Cells treated with prieurianin displayed prominent pink staining, with the intensity of the coloration increasing proportionally with the prieurianin concentration. In contrast, untreated control cells remained unstained, providing additional evidence of prieurianin's ability to disrupt membrane integrity and induce apoptosis (Figure 3.3a).

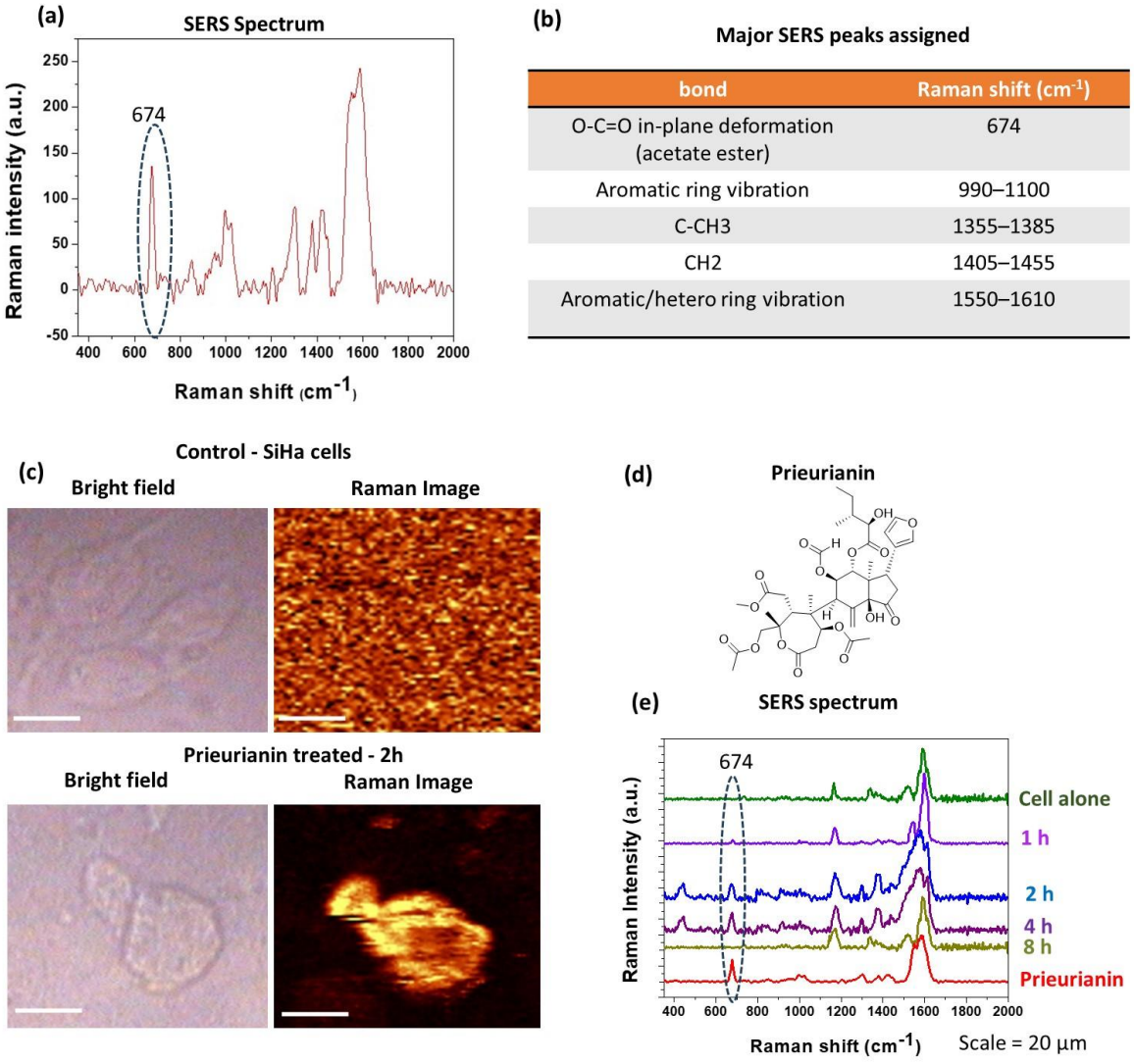

bond	Raman shift (cm^{-1})
O-C=O in-plane deformation (acetate ester)	674
Aromatic ring vibration	990–1100
C-CH3	1355–1385
CH2	1405–1455
Aromatic/hetero ring vibration	1550–1610

Figure 3.2. a) SERS spectrum of prieurianin b) assignmnet of major peaks c) bright field and Raman image of control and prieurianin treated SiHa cells d) structure of prieurianin e) SERS spectrum after prieurianin treatemnt in SiHa cells for analysing internalisation

The annexin V apoptosis assay was also performed to evaluate phosphatidylserine externalization, a key marker of early apoptosis. Annexin V binds specifically to phosphatidylserine on the outer surface of the plasma membrane during apoptosis. Combined with propidium iodide (PI), this assay distinguishes between viable, apoptotic,

and necrotic cells (15). Flow cytometry data were analyzed across four quadrants: Q3 (annexin V-negative/PI-negative, viable cells), Q4 (annexin V-positive/PI-negative, early apoptotic cells), Q2 (annexin V-positive/PI-positive, late apoptotic cells), and Q1 (annexin V-negative/PI-positive, necrotic cells).

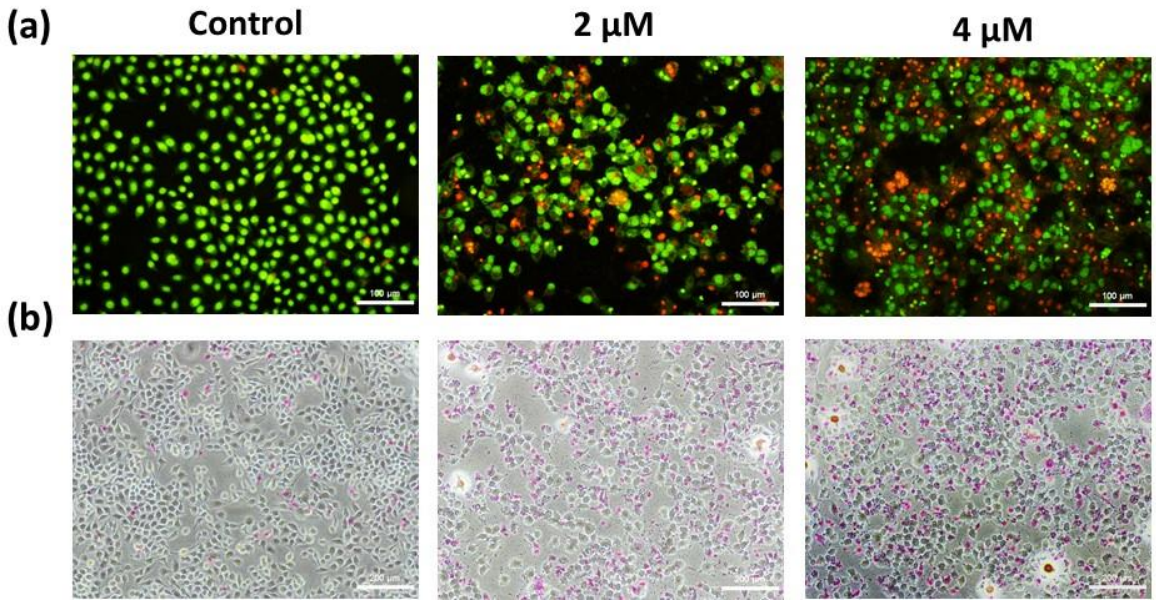

Figure 3.3. Induction of apoptosis in SiHa cells by prieurianin analysed in different concentrations of 7 and 11 µM by a) Acidine orange ethidium bromide dual staining method. Green channel: emission wavelength (λex = 450-490 nm), excitation wavelength (λex = 520 nm) b) APOP assay

The untreated control group had 90.5% of cells in Q3, representing mostly viable cells. However, treatment with 2 µM and 4 µM prieurianin significantly decreased the viable cell population to 25.8% and 10.6%, respectively. Moreover, the population of cells in Q2, indicative of late apoptosis, rose from 5.8% in the control group to 57.6% 2 µM prieurianin treatment and further to 75.5% in 4 µM concentration illustrating a strong progression through apoptotic stages. Necrotic cells in Q1, however, remained a minor population, with only 11.1% and 10.3% observed in the 2 µM and 4 µM treatment groups, respectively, indicating that necrosis was not the primary mechanism of cell death in this context (Figure 3.4a). These results, supported by fluorescence microscopy, the APOPercentage assay, and flow cytometry analysis, clearly demonstrate the pro-apoptotic effects of prieurianin in SiHa cells. Prieurianin induces apoptosis in a concentration-dependent manner, driving cells from early to late apoptotic stages while maintaining minimal necrotic cell death.

3.2.4. Caspase flurometric assays

Caspase activation serves as a hallmark of apoptosis, providing critical insights into the pathways driving cell death and apoptosis is a highly regulated process predominantly controlled by caspases. To investigate the role of caspases in prieurianin-induced apoptosis, a fluorescence-based assay was utilized to quantify the activation of specific caspases. The pathways (extrinsic or intrinsic), through which apoptosis occurs are distinguished by the involvement of distinct initiator caspases. In this study, the activation of caspase 3, a central executioner caspase common to both pathways, was analyzed. Caspase 3 executes the final stages of apoptosis, marking it as a key indicator of apoptotic progression. SiHa cells treated with prieurianin at 2 µM and 4 µM showed a six to nine-fold increase in caspase 3 activation compared to untreated controls, demonstrating that prieurianin robustly initiates apoptotic cell death (Fig. 3.4b).

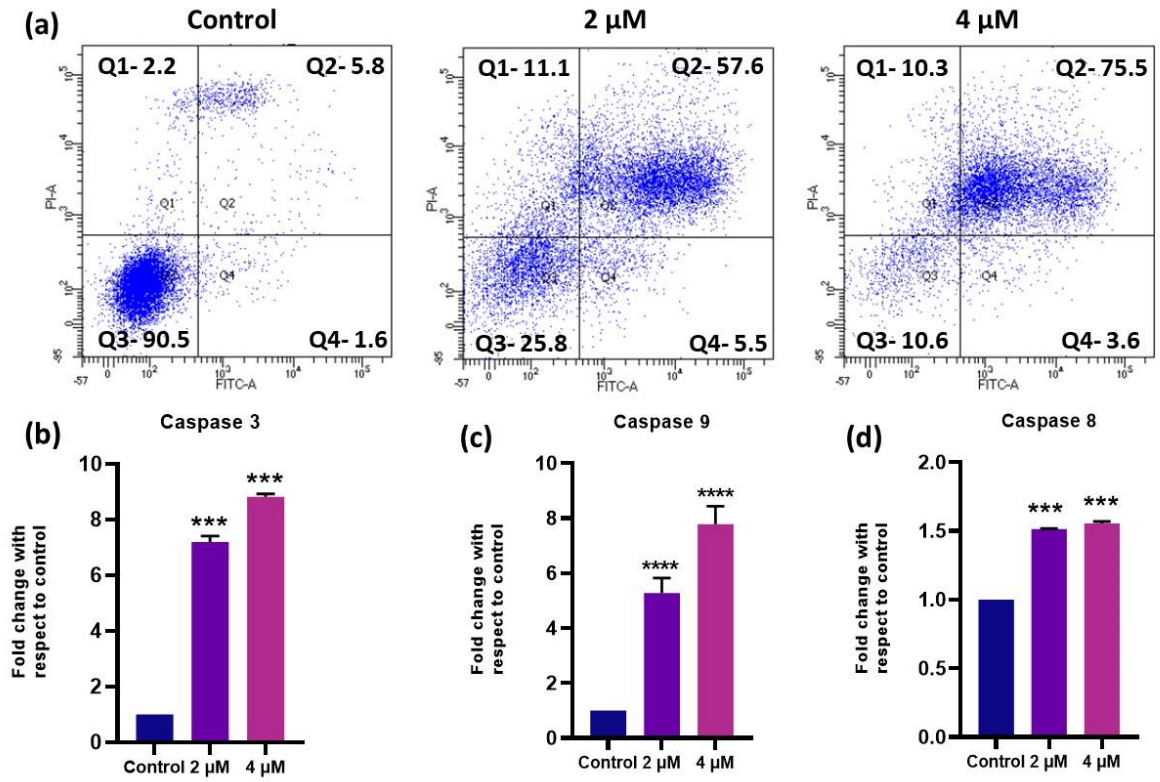

Figure 3.4: a) Annexin V apoptosis assay by FACS. Caspase expression analysis by flurometric method. Major caspases such as b) caspase-3, b) caspase-9 and d) caspase-8 involved in apoptotic pathways were checked and it is observed that all the 3 caspases show a fold increase in its fluorescence intensity with respect to control. Results are represented as mean ± SD, *p < 0.05, **p < 0.01, ***p < 0.001 compared to control.

To further delineate the apoptotic mechanisms activated by prieurianin, the involvement of caspase 8 and caspase 9, the initiator caspases for the extrinsic and intrinsic pathways, respectively, was examined(16). Prieurianin treatment significantly elevated the activation

levels of both caspase 8 and caspase 9 where caspase 9 showed around 5 to 7-fold increase and caspase 8 around 2 fold increase indicating that it simultaneously triggers both apoptotic pathways (Figure. 3.3c and d). The current study establishes that prieurianin, like other terpenoids, employs a dual-pathway strategy to drive apoptosis. By concurrently activating caspase 8 and caspase 9, prieurianin ensures robust apoptotic signaling, culminating in caspase 3 activation and cell death. This multifaceted mechanism not only amplifies its anticancer potential but also aligns with the emerging therapeutic paradigm of targeting multiple apoptotic pathways to counteract resistance mechanisms often encountered in cancer therapy. These findings underscore the promise of prieurianin as a potent agent against cervical cancer, warranting further preclinical and clinical investigations.

3.2.5 Hoescht staining for DNA condensation studies

DNA condensation is a hallmark of apoptosis and serves as a reliable indicator for identifying and studying apoptotic processes. In healthy cells, nuclei exhibit a spherical shape with uniformly distributed DNA, while apoptotic cells are characterized by chromatin condensation and DNA fragmentation. These changes are effectively visualized using DNA-binding dyes. Hoechst 33342, a DNA-binding dye, permeates both live and apoptotic cells and binds specifically to adenine-thymine-rich regions in the DNA minor groove. While Hoechst 33342 staining produces fluorescence in both normal and condensed DNA, the fluorescence intensity is significantly higher in regions of chromatin condensation, a signature of apoptosis (17). In this study, SiHa cells were treated with prieurianin at concentrations of 2 μM and 4 μM and subsequently stained with Hoechst 33342 to evaluate nuclear changes associated with apoptosis. Fluorescence microscopy revealed that untreated control cells displayed nuclei with an intact, spherical structure and evenly distributed DNA. In contrast, cells exposed to prieurianin exhibited significant chromatin condensation, as indicated by the increased fluorescence intensity of the condensed DNA (figure 3.5a). These findings provide clear evidence that prieurianin induces chromatin condensation, reinforcing its role in promoting apoptotic processes.

3.2.6. Cell cycle analysis by FACS

The mutations arise in cancer often impair critical cellular checkpoints, enabling unregulated cell division and the escape of normal growth control mechanisms. A central

approach ineffective cancer therapy addresses this dysregulation by either restoring cell cycle regulation or triggering apoptosis in abnormal cells. To investigate the effects of prieurianin on the cell cycle in SiHA cells, a flow cytometry-based cell cycle assay was conducted. This method allows for precise analysis of cell cycle distribution and apoptotic events by quantifying DNA content in individual cells. In this study, propidium iodide (PI), a DNA-binding fluorescent dye, was utilized. PI specifically stains DNA and penetrates cells in late apoptosis or apoptotic stages, enabling the identification of distinct cell cycle phases and apoptotic populations. Analysis of the untreated control group showed the majority of cells were in the S and G2/M phases, indicative of active cell proliferation. In contrast, prieurianin-treated cells displayed a significant accumulation in the sub-G0 phase, a recognized marker of apoptotic cell death. Quantitative analysis revealed a stark contrast, in control cells, only 12.9% were detected in the sub-G0 phase, representing baseline apoptosis levels. However, treatment with prieurianin at concentrations of 2 µM and 4 µM resulted in a notable increase in sub-G0 phase cells, rising to 19.5% and 24.6%, respectively (Figure 3.5b). Concurrently, a reduction in the G1 phase population was observed, indicating disrupted cell cycle progression and arrest at the sub-G0 phase. These findings demonstrate that prieurianin effectively induces apoptosis and halts cell cycle progression in SiHa cells.

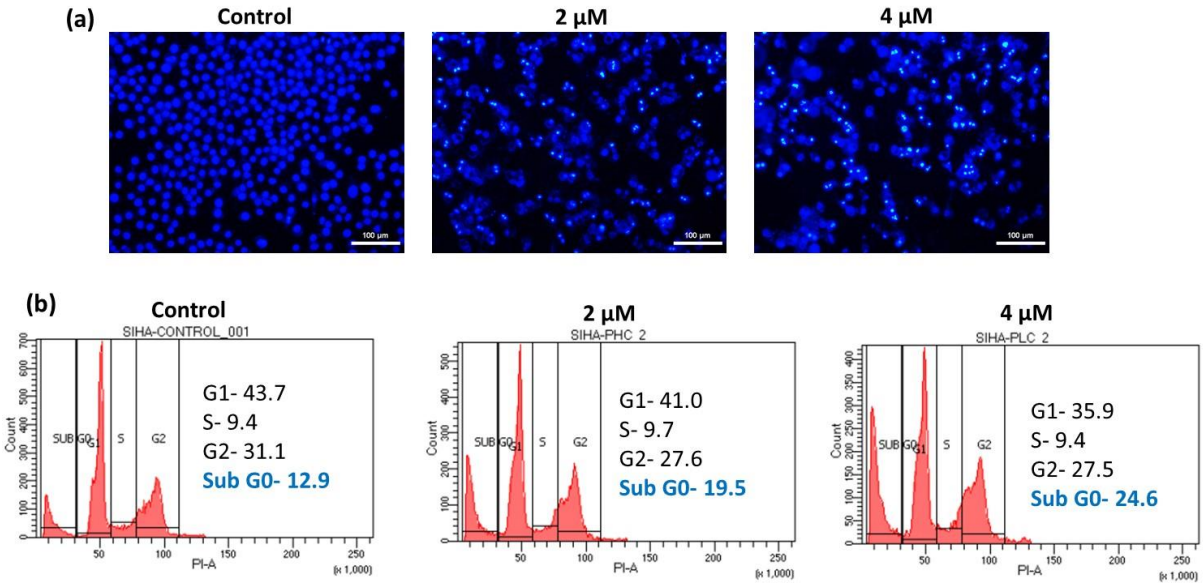

Figure 3.5: a) Nucleic acid condensation in SiHa cells upon treatment with prieurianin is proved by Hoescht staining method where condensed DNA will give intense colouration comparing the untreated. Blue channel: emission wavelength (λ_{ex} = 361-389 nm), excitation wavelength (λ_{ex} = 430-490 nm) b) Cell cycle assay using PI staining done by FACS which shows a cell accumulation in sub-G0 phase.

3.2.7. Assessment of mitochondrial membrane depolarisation by JC1 assay

A loss of mitochondrial membrane potential is a critical step in the intrinsic (mitochondria-mediated) apoptotic pathway, where mitochondrial permeabilization leads to the release of pro-apoptotic factors and activation of downstream caspases, ultimately driving programmed cell death (18,19). To assess the impact of prieurianin on mitochondrial membrane potential, the study utilized JC-1 dye that accumulates in mitochondria based on their membrane potential. In healthy mitochondria with an intact ΔΨm, JC-1 aggregates, producing red fluorescence. Conversely, in apoptotic cells with compromised ΔΨm, the dye remains in its monomeric form, emitting green fluorescence, a characteristic marker of mitochondrial depolarization. In this experiment, SiHa cells were treated with prieurianin for 48 hours, followed by staining with JC-1 dye. In untreated control cells, where the mitochondrial function was preserved, JC-1 predominantly formed red-fluorescent J-aggregates, indicating stable ΔΨm. In contrast, prieurianin-treated cells exhibited a marked increase in green fluorescence, reflecting a shift toward the monomeric form of the dye and signaling mitochondrial depolarization (Fig. 3.6a). This change demonstrates the loss of mitochondrial membrane potential in response to prieurianin treatment. The observed increase in green fluorescence intensity in prieurianin-treated cells compared to controls provides direct evidence of mitochondrial dysfunction. This disruption of ΔΨm indicates that prieurianin actively engages the intrinsic apoptotic pathway. By compromising mitochondrial integrity, prieurianin triggers a cascade of events, including cytochrome c release and caspase activation, leading to cell death. These findings highlight the pro-apoptotic mechanism of prieurianin and its ability to selectively target mitochondrial stability in cancer cells.

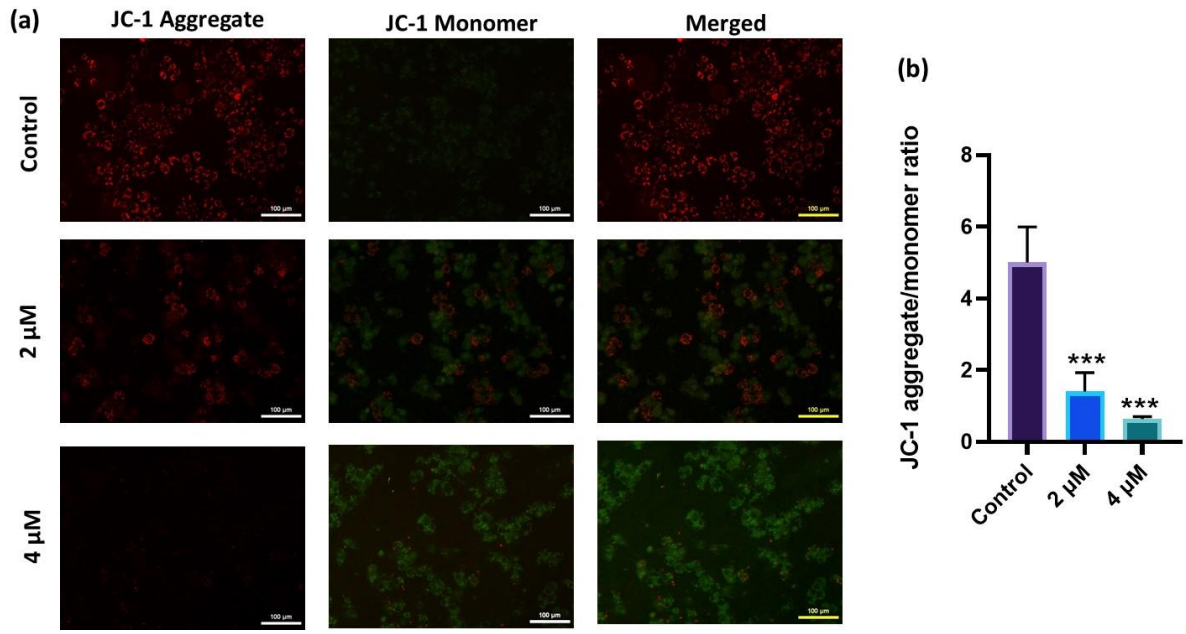

Figure 3.6: a) Analysis of change in mitochondrial membrane potential is done by JC-1 assay in SiHa cells after inducing with prieurianin. Green channel: emission wavelength (λ_{ex} = 450-490 nm), excitation wavelength (λ_{ex} = 520 nm), red channel: emission wavelength (λ_{ex} = 510-560 nm), excitation wavelength (λ_{ex} = 590 nm). b) graph showing decrease in JC-1 aggregate to monomer ratio with respect to control. Results are represented as mean ± SD, ***$p < 0.001$ is considered to be significant as compared to control.

By inducing intrinsic apoptosis, prieurianin demonstrates significant therapeutic potential, as it effectively promotes cancer cell death while sparing normal cellular processes. This study emphasizes the crucial role of mitochondrial dynamics in cancer therapy and positions prieurianin as a promising candidate for mitochondrial-targeted treatments.

3.2.8 Anti-metastatic studies of prieurianin

The ability of cancer cells to survive, multiply, and form colonies, known as their clonogenic potential, is a crucial indicator of their reproductive viability and aggressive behavior. This study evaluated the impact of prieurianin on the clonogenic capacity of SiHa cells using a standard colony formation assay. This assay measures the ability of single cells to undergo division and develop into colonies, reflecting their long-term survival and proliferation potential. SiHa cells were treated with prieurianin at concentrations of 0.5 µM and 1 µM, and surviving colonies were stained and quantified using ImageJ software (20). The results demonstrated a significant, dose-dependent reduction in colony formation. Untreated control cells formed a total of around 900 colonies, while cells treated with 0.5 µM prieurianin produced around 800 colonies, and those treated with 1 µM formed only

around 600 colonies (Fig. 3.7a-c). These findings emphasize the strong inhibitory effect of prieurianin on the clonogenic capacity of SiHa cells, indicating its ability to suppress their potential for sustained growth and reproduction.

In addition to clonogenicity, the study also examined the migratory behavior of SiHa cells, which is a fundamental process in cancer metastasis. A scratch wound assay was employed to simulate a wound by creating an artificial gap in a confluent monolayer of cells, allowing the observation of cell migration and wound closure over time. This assay provides a robust method for evaluating the migratory potential of cells, which is critical for their metastatic capability. SiHa cells were treated with prieurianin at 0.5 µM and 1 µM, and wound closure was monitored at 0, 24, and 48 hours post-treatment. The percentage of wound closure was quantified using ImageJ software. The results revealed that prieurianin-treated cells exhibited a significant reduction in migration compared to untreated controls. While control cells showed a high percentage of wound closure, indicative of strong migratory behavior, prieurianin-treated cells demonstrated a clear delay in wound closure at both tested concentrations (Fig. 3.7d-f). These findings highlight the dual action of prieurianin in targeting two essential characteristics of cancer cells - clonogenic potential and migration. By impairing clonogenic capacity, prieurianin limits the ability of cancer cells to maintain their proliferative lineage. Simultaneously, its suppression of cell migration diminishes the metastatic potential, a critical factor in cancer progression and the spread to secondary sites. This dual inhibitory effect positions prieurianin as a promising therapeutic candidate capable of addressing both primary tumor growth and metastatic dissemination, making it a valuable agent in the treatment of aggressive cancers such as cervical carcinoma.

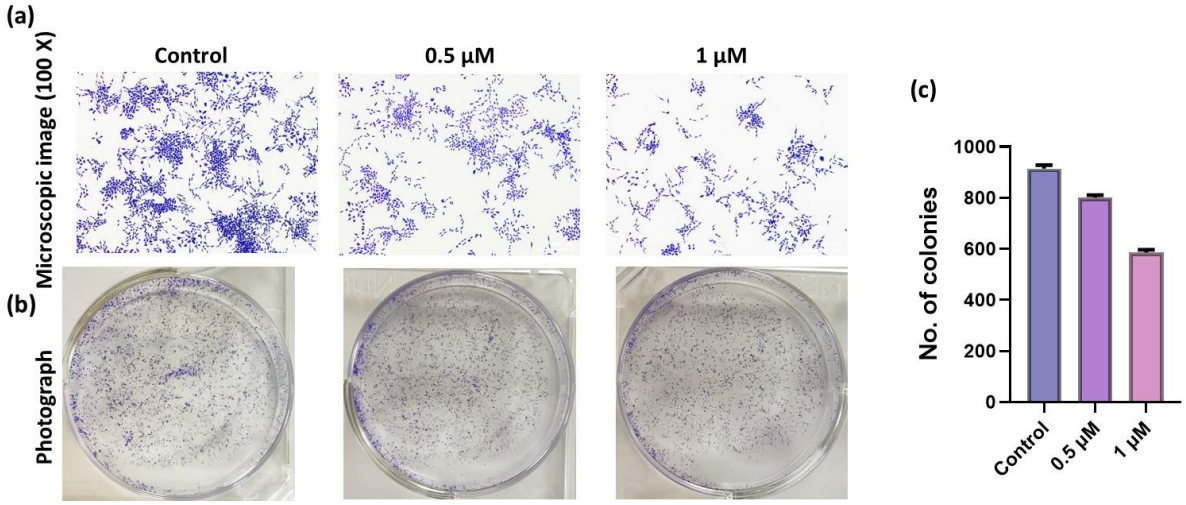

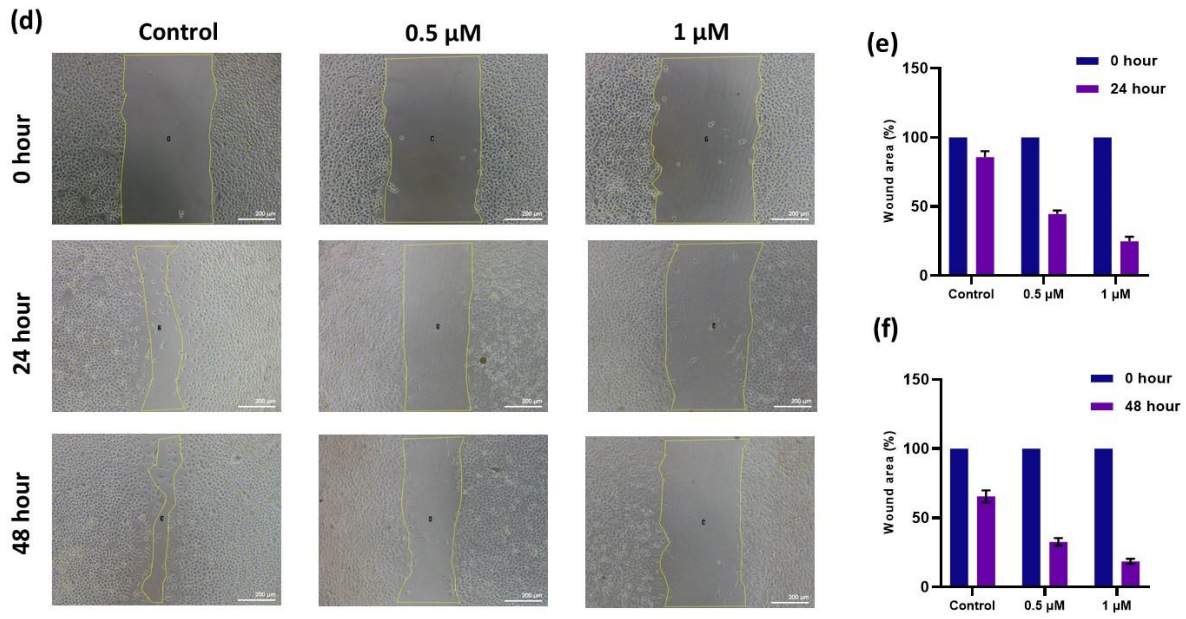

Figure 3.7: a) Inhibition of clonogenic potential of SiHa cells by prieurianin treatment at 0.5 µM and 1 µM b) graph showing decrease in number of colonies with prieurianin treatment compared to control c) Inhibtion of migratory potential of SiHa cells by prieurianin treatment d) graph representing wound area percentage at different time points. Results are represented as mean ± SD, **p < 0.01 as compared to control.

3.2.9. Expression studies of proteins involved in apoptosis

For a deep understanding of the molecular pathway through which prieurianin exerts its action, an analysis of major proteins involved in apoptosis was done using an apoptotic array membrane which holds about 43 target proteins. Protein isolation was performed in SiHa cells with prieurianin treated and control cells. As observed by the variation in expression, prieurianin activates the death receptor (DR) where death receptors (including

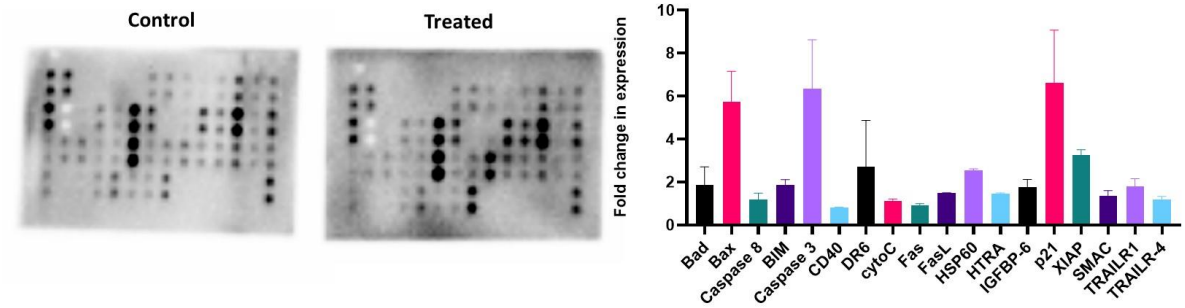

Figure 3.8: Apoptotic protein expression study in SiHa cells a) with and b) without treatment were analyzed using antibody array kit. c) Comparison of expression change in major proteins in prieurianin-treated cells with respect to control

TRAILR) are type I transmembrane proteins whose intracytoplasmic death domain (DD) is essential for signal transduction and apoptosis. Activation of death receptors tends to activate NF-KB which results in the activation of MAPK/JNK pathway. FasL, binding to the Fas forms a part of death receptor-mediated apoptosis where it activates the extrinsic mode of apoptotic pathway (21). This happens by the activation of procaspase 8 to caspase 8, which is the central part of the extrinsic pathway. This finally leads to the activation of executioner caspase 3 activation for apoptosis to occur. Simultaneously, prieurianin cause the upregulation of pro-apoptotic protein expression like Bad/bax that leads to the ROS generation (22,23). ROS generation causes the mitochondrial factors release including cytochrome c and conversion of bid to tbid. The formation of tBid results in the catalytic activation initiator procaspase 9, the key molecule in intrinsic pathway, to active caspase 9. This activation of caspase 9 also finally converges to the activation of caspase 3, altogether taking cell to its demolition phase (24). Prieurianin causes the over expression of p21 that regulates the cell cycle by inhibition of cyclin cdk complex, resulting in cell cycle arrest (Figure 3.8).

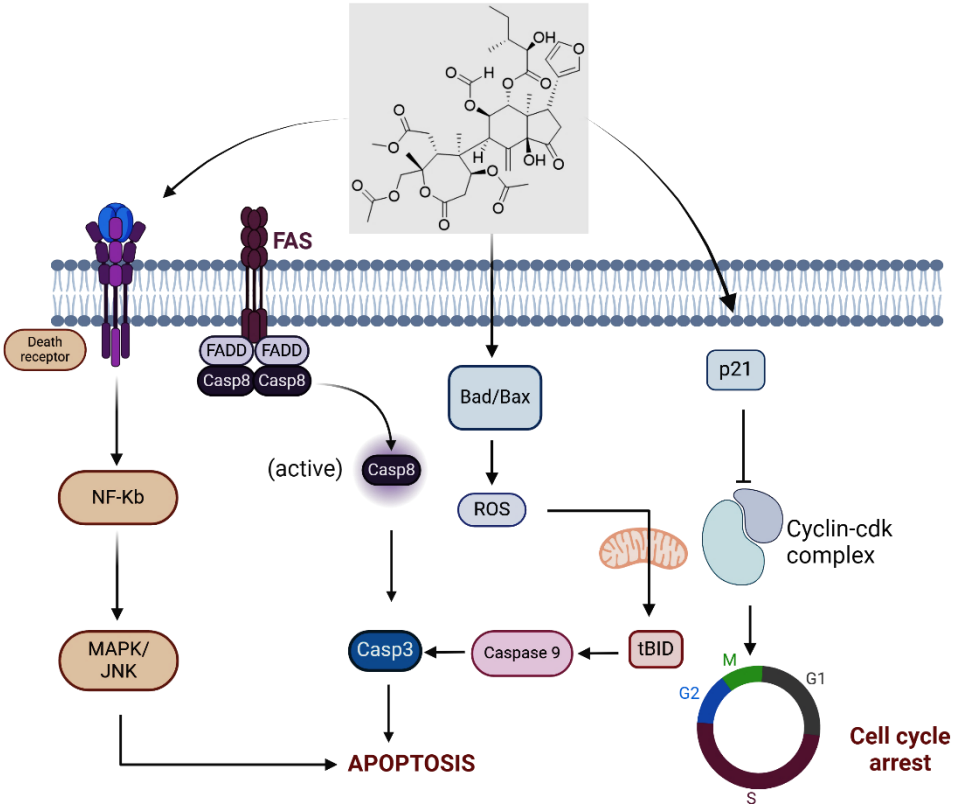

Scheme 1: Proposed mechanism of action of prieurianin

3.3 Materials and Methods

3.3.1. Cell Culture Procedures

The following human cancer cell lines were utilized in biological assays: HeLa and SiHa (cervical cancer), MDA-MB-231 (triple-negative breast cancer), A549 (non-small cell lung cancer), and PANC-1 (pancreatic cancer). These cell lines were sourced from the American Type Culture Collection (ATCC, USA) and the National Centre for Cell Science (India). Additionally, MCF-10A, a non-tumorigenic epithelial cell line, was obtained from Elabscience, USA. Cells were cultured in Dulbecco's Modified Eagle Medium (DMEM, Sigma), which was supplemented with 10% fetal bovine serum (FBS, Himedia) and 1% antibiotic-antimycotic solution (Himedia) to ensure optimal growth conditions. All cells were maintained at 37°C in a humidified incubator with 5% CO_2 to mimic physiological conditions. Cells were regularly monitored for contamination and passaged when they reached approximately 70-80% confluence to ensure consistent growth and experimental reproducibility.

3.3.2. Cell Proliferation Assay

To assess the impact of prieurianin on cell proliferation, cells were seeded in 96-well plates at a density of 8×10^3 cells per 100 µL of DMEM per well. The plates were incubated for 24 and 48 hours to allow cell attachment and initial proliferation. Prieurianin was added at concentrations of 5, 10, 20, 50, and 100 µM 24 hours post-seeding. Following incubation for 24 and 48 hours, 100 µL of MTT solution (0.5 mg/mL) was added to each well, and the plates were incubated at 37°C for 2-4 hours. The MTT solution was then removed, and the wells were washed with phosphate-buffered saline (PBS) to remove residual dye. To solubilize the formazan crystals formed by viable cells, 100 µL of dimethyl sulfoxide (DMSO) was added to each well, and the absorbance was measured at 570 nm using a Synergy H1 multimode plate reader (Biotek). The results were analyzed to determine the inhibitory effects of prieurianin on cell proliferation, and data were expressed as a percentage of control values.

3.3.3. Internalization Study Using SERS

Surface-enhanced Raman scattering (SERS) analysis was employed to study the internalization of prieurianin in SiHa cells. Cells were seeded onto glass-bottom chamber slides at a density of 25,000 cells per well and allowed to adhere for 24 hours. Cells were then treated with prieurianin at a concentration of 1 mM. Gold nanoparticles (40 nm in size) were used as the SERS substrate. SERS signals were collected using a 633 nm laser with a power of 5 mW and an integration time of 5 seconds. To obtain the SERS spectrum of the compound, 1 mM prieurianin in methanol was mixed with gold nanoparticles in a 2:8 ratio, and spectra were collected. For cellular analysis, treated and untreated SiHa cells were washed three times with PBS to remove excess compound, incubated with gold nanoparticles for 10 minutes, and subjected to SERS spectral analysis and imaging using a confocal Raman spectroscope (WITec, Germany) equipped with a 600 g/mm grating and a Peltier-cooled charge-coupled device (CCD) detector unit. SERS imaging was performed over a 100 × 100 µm area with 100 × 100 points per line and an integration time of 0.02 seconds per point. Data processing and analysis were conducted using the WITec Project 5.2 Plus software, which included background noise reduction and cosmic ray removal.

3.3.4. Apoptotic Assays

The apoptotic effects of prieurianin were examined using multiple assays. Live/dead staining was performed using the ethidium bromide-acridine orange dual-staining method. SiHa cells were treated with prieurianin, stained with the dye mixture, and visualized under a Nikon TS100 inverted microscope. Apoptotic and necrotic cells were distinguished based on their staining patterns. The annexin V apoptosis assay was carried out using the FITC Annexin V apoptosis detection kit (BD Pharmingen) according to the manufacturer's protocol. Cells were treated with prieurianin, stained with annexin V and propidium iodide, and analyzed using a flow cytometer. The percentage of early and late apoptotic cells was quantified to evaluate the pro-apoptotic potential of prieurianin.

3.3.5. Caspase Fluorometric Assay

The activation of caspases - key markers of apoptosis - was assessed using a fluorometric assay for caspases 3, 8, and 9. SiHa cells were seeded in 6-well plates at a density of 3×10^6 cells per well and treated with varying concentrations of prieurianin. Caspase activation was measured using a fluorometric kit (Abcam) following the manufacturer's instructions. Fluorescence intensity was recorded at an excitation wavelength of 400 nm and an emission

wavelength of 505 nm using a Synergy H1 multimode plate reader. The results were analyzed to determine the dose-dependent activation of caspases and the apoptotic potential of prieurianin.

3.3.6. Nucleic Acid Degradation and DNA Fragmentation Studies

DNA condensation and fragmentation were evaluated using Hoechst 33258 staining. SiHa cells were seeded in 96-well plates at a density of 7×10^3 cells per well, treated with prieurianin, and stained with Hoechst dye at a concentration of 1 µg/mL. Fluorescent microscopy was used to observe nuclear condensation and fragmentation, indicative of apoptotic cell death.

3.3.7. Cell Cycle Analysis

The effect of prieurianin on the cell cycle was analyzed using flow cytometry. Cells were treated with prieurianin and stained with propidium iodide using the BD Cycle Test Plus DNA kit (BD Pharmingen, cat. no. 340242). The distribution of cells across different phases of the cell cycle (G0/G1, S, and G2/M) was determined by flow cytometric analysis. Additionally, Western blotting was performed to examine the expression of cell cycle-regulatory proteins, including Cdk-2, cyclin A2, cyclin B1, and Cdc-25. Protein extracts were prepared from SiHa cells, quantified using the Pierce BCA Assay Kit (Pierce, cat. no. 23225), and resolved by SDS-PAGE. Proteins were transferred onto membranes, probed with specific antibodies, and detected using enhanced chemiluminescence (ECL). β-actin was used as a loading control for normalization.

3.3.8. Mitochondrial Membrane Potential Analysis

Changes in mitochondrial membrane potential were analyzed using the JC-1 assay (Sigma-Aldrich). SiHa cells were treated with prieurianin, stained with the JC-1 dye, and visualized under a Nikon TS100 inverted microscope. Healthy cells exhibited red fluorescence due to JC-1 aggregates, while apoptotic cells displayed green fluorescence due to the monomeric form of JC-1. The fluorescence shift was used to assess mitochondrial membrane depolarization as an indicator of early apoptosis.

3.3.9. Anti-Metastatic Studies

The anti-metastatic potential of prieurianin was evaluated using clonogenic and scratch wound assays. For clonogenic assays, cells were seeded at a density of 1×10^3 cells per well, treated with prieurianin at concentrations of 0.5 and 1 μM, and incubated for 9 days. Colonies were fixed with methanol, stained with 0.3% crystal violet, and counted manually. In scratch wound assays, cells were seeded in 6-well plates, and a scratch was created using a sterile pipette tip after 24 hours of incubation. Cells were treated with prieurianin, and wound closure was monitored at 0, 24, and 48 hours. Images were captured, and the percentage of wound closure was quantified using ImageJ software to assess the inhibitory effects of prieurianin on cell migration.

3.3.10. Apoptotic Protein Expression

Western blot analysis was conducted to examine the expression levels of key apoptotic proteins, including p53, Bax, Bcl-2, and cleaved caspase-3. SiHa cells treated with prieurianin were lysed, and protein extracts were prepared for analysis. Proteins were resolved by SDS-PAGE, transferred to membranes, and probed with specific primary and secondary antibodies. Bands were visualized using enhanced chemiluminescence detection using the ImageJ software. The expression levels were normalized to the β-actin loading control to ensure consistency in protein quantification. This analysis provided insights into the molecular mechanisms underlying the apoptotic effects of prieurianin.

3.3.11. Statistical Analysis

All experiments were conducted in triplicate, and data were expressed as mean ± standard deviation (SD). Statistical significance was determined using one-way analysis of variance (ANOVA), followed by Tukey's post hoc test for multiple comparisons. A p-value of less than 0.05 was considered statistically significant. GraphPad Prism software (version 8.0) was used for data analysis and graphical representations.

3.3.12. Quality Control

To ensure the validity and reproducibility of the findings, all experimental procedures were carried out under standardized laboratory conditions. Cell lines were authenticated using short tandem repeat (STR) profiling, and contamination was regularly checked using

mycoplasma testing kits. Reagents and media were prepared fresh or stored according to the manufacturer's guidelines, and instruments were calibrated periodically.

3.4. Conclusion

The present study provides a comprehensive evaluation of the anticancer potential of prieurianin, a limonoid, in cervical cancer cells (SiHa). This study elucidates prieurianin's apoptotic mechanisms, its impact on cancer cell proliferation, and its ability to suppress migration and metastasis, highlighting its role as a promising therapeutic agent against cervical cancer. Cytotoxicity analysis using the MTT assay demonstrated that prieurianin effectively inhibits the growth of cervical cancer cells (IC_{50} = 3.9 µM), while showing minimal toxicity towards normal WI-38 lung fibroblast cells. These findings indicate prieurianin's selective cytotoxicity, which is a critical criterion for its therapeutic application. Subsequent apoptotic evaluation using dual staining (acridine orange-ethidium bromide), APOPercentage, and annexin V/PI assays revealed concentration-dependent apoptotic cell death. Flow cytometric analysis confirmed a significant reduction in viable cell populations and progression to late apoptosis with prieurianin treatment, underscoring its ability to induce programmed cell death effectively. Mechanistic insights into prieurianin-induced apoptosis were obtained through caspase activation studies, where a marked activation of executioner caspase-3 and initiator caspases (caspase-8 and caspase-9) was observed. These results indicate the involvement of both extrinsic (death receptor-mediated) and intrinsic (mitochondrial) apoptotic pathways. Mitochondrial membrane depolarization studies (JC-1 assay) further validated prieurianin's role in triggering the intrinsic pathway, as evidenced by a loss of mitochondrial membrane potential and subsequent cytochrome c release. Additionally, prieurianin disrupted the cell cycle, as observed through cell cycle analysis, where treated cells showed significant accumulation in the sub-G0 phase, indicating DNA fragmentation and apoptotic progression. Further confirmation through Hoechst 33342 staining revealed chromatin condensation and nuclear fragmentation, hallmark features of apoptosis. Expression studies of apoptotic proteins using targeted arrays demonstrated prieurianin's ability to upregulate pro-apoptotic proteins (Bax, Bad) and activate death receptors (Fas, TNFR), while inhibiting anti-apoptotic signals, leading to the activation of caspase cascades. Importantly, prieurianin also induced p21 expression, which regulates cell cycle arrest by inhibiting cyclin-dependent kinase activity. In addition to its pro-apoptotic effects, prieurianin demonstrated anti-metastatic

properties by reducing clonogenic potential and suppressing cell migration, as confirmed by the colony formation and wound healing assays. This dual action, targeting both cancer cell survival and metastatic potential, underscores prieurianin's therapeutic versatility. In conclusion, the current study highlights prieurianin as a potent anticancer agent capable of inducing apoptosis through both intrinsic and extrinsic pathways, disrupting cell cycle progression, and inhibiting cancer cell migration and clonogenicity. By targeting multiple pathways simultaneously, prieurianin exhibits significant potential to overcome resistance mechanisms often observed in cancer therapies. Future studies involving *in vivo* evaluations, pharmacokinetics, and formulation development will be essential to establish prieurianin’s clinical efficacy and therapeutic index. These findings contribute to the growing body of evidence supporting limonoids as promising candidates in natural product-based drug development for the treatment of cervical and other aggressive cancers.

3.4 References

1. Durán-Peña MJ, Botubol-Ares JM, Collado IG, Hernandez-Galán R. Degraded limonoids: biologically active limonoid fragments re-enhancing interest in Meliaceae and Rutaceae sources. Vol. 22, Phytochemistry Reviews. 2023.
2. Roy A, Saraf S. Limonoids: overview of significant bioactive triterpenes distributed in plants kingdom. Biological and Pharmaceutical Bulletin. 2006;29(2):191-201.
3. Shi YS, Zhang Y, Li HT, Wu CH, El-Seedi HR, Ye WK, et al. Limonoids from Citrus: Chemistry, anti-tumor potential, and other bioactivities. Vol. 75, Journal of Functional Foods. Elsevier Ltd; 2020.
4. Olatunji TL, Odebunmi CA, Adetunji AE. Biological activities of limonoids in the Genus Khaya (Meliaceae): a review. Futur J Pharm Sci. 2021;7(1).
5. Tundis R, Loizzo MR, Menichini F. An Overview on Chemical Aspects and Potential Health Benefits of Limonoids and Their Derivatives. Vol. 54, Critical Reviews in Food Science and Nutrition. 2014. p. 225–50.
6. Chen Q, Ruan D, Shi J, Du D, Bian C. The multifaceted roles of natural products in mitochondrial dysfunction. Vol. 14, Frontiers in Pharmacology. 2023.
7. Yang Y, He PY, Zhang Y, Li N. Natural Products Targeting the Mitochondria in Cancers. Vol. 26, Molecules. 2021.

8. Hashem S, Ali TA, Akhtar S, Nisar S, Sageena G, Ali S, et al. Targeting cancer signaling pathways by natural products: Exploring promising anti-cancer agents. Vol. 150, Biomedicine and Pharmacotherapy. Elsevier Masson s.r.l.; 2022.
9. Manners GD. Citrus limonoids: Analysis, bioactivity, and biomedical prospects. Vol. 55, Journal of Agricultural and Food Chemistry. 2007. p. 8285–94.
10. Vergoten G, Bailly C. Insights into the Mechanism of Action of the Degraded Limonoid Prieurianin. Vol. 25, International Journal of Molecular Sciences. Multidisciplinary Digital Publishing Institute (MDPI); 2024.
11. Kablan A, Saunders RA, Szkudlarek-Mikho M, Chin AJB, Bosio RM, Fujii K, et al. Prieurianin Causes Weight Loss in Diet-Induced Obese Mice and Inhibits Adipogenesis in Cultured Preadipocytes. 2010.
12. Kumar P, Nagarajan A, Uchil PD. Analysis of cell viability by the MTT assay. Cold Spring Harb Protoc. 2018 Jun 1;2018(6):469–71.
13. Movasaghi Z, Rehman S, Rehman IU. Raman spectroscopy of biological tissues. Vol. 42, Applied Spectroscopy Reviews. 2007. p. 493–541.
14. Ciniglia C, Pinto G, Sansone C, Pollio A. Acridine orange/Ethidium bromide double staining test: A simple In-vitro assay to detect apoptosis induced by phenolic compounds in plant cells [Internet]. Vol. 26, International Allelopathy Foundation. 2010.
15. Miller E. Apoptosis Measurement by Annexin V Staining.
16. Mwale C, Sunaga T, Wang Y, Bwalya EC, Wijekoon HMS, Kim S, et al. In vitro chondrotoxicity of bupivacaine, levobupivacaine and ropivacaine and their effects on caspase activity in cultured canine articular chondrocytes. Journal of Veterinary Medical Science. 2023;85(4):515–22.
17. Crowley LC, Marfell BJ, Waterhouse NJ. Analyzing cell death by nuclear staining with Hoechst 33342. Cold Spring Harb Protoc. 2016;2016(9).
18. Priyadarsini RV, Murugan RS, Sripriya P, Karunagaran D, Nagini S. The neem limonoids azadirachtin and nimbolide induce cell cycle arrest and mitochondria-mediated apoptosis in human cervical cancer (HeLa) cells. Free Radic Res. 2010;44(6).
19. Zheng B, Meng J, Zhu Y, Ding M, Zhang Y, Zhou J. Melatonin enhances SIRT1 to ameliorate mitochondrial membrane damage by activating PDK1/Akt in granulosa cells of PCOS. J Ovarian Res. 2021 Dec 1;14(1).

20. Valsan A, Meenu MT, Murali VP, Malgija B, Joseph AG, Nisha P, et al. Exploration of Phaeanthine: A Bisbenzylisoquinoline Alkaloid Induces Anticancer Effect in Cervical Cancer Cells Involving Mitochondria-Mediated Apoptosis. ACS Omega. 2023 Apr 25;8(16):14799–813.
21. Mahdizadeh SJ, Thomas M, Eriksson LA. Reconstruction of the Fas-Based Death-Inducing Signaling Complex (DISC) Using a Protein-Protein Docking Meta-Approach. J Chem Inf Model. 2021 Jul 26;61(7):3543–58.
22. Aggarwal V, Tuli HS, Varol A, Thakral F, Yerer MB, Sak K, et al. Role of reactive oxygen species in cancer progression: Molecular mechanisms and recent advancements. Vol. 9, Biomolecules. 2019.
23. Dengler MA, Robin AY, Gibson L, Li MX, Sandow JJ, Iyer S, et al. BAX Activation: Mutations Near Its Proposed Non-canonical BH3 Binding Site Reveal Allosteric Changes Controlling Mitochondrial Association. Cell Rep. 2019 Apr 9;27(2):359-373.e6.
24. Peng Z, Gillissen B, Richter A, Sinnberg T, Schlaak MS, Eberle J. Enhanced Apoptosis and Loss of Cell Viability in Melanoma Cells by Combined Inhibition of ERK and Mcl-1 Is Related to Loss of Mitochondrial Membrane Potential, Caspase Activation and Upregulation of Proapoptotic Bcl-2 Proteins. Int J Mol Sci. 2023;24(5).

Chapter 4

Investigation of anti-metastatic and anti-angiogenic potential of niloticin and prieurianin

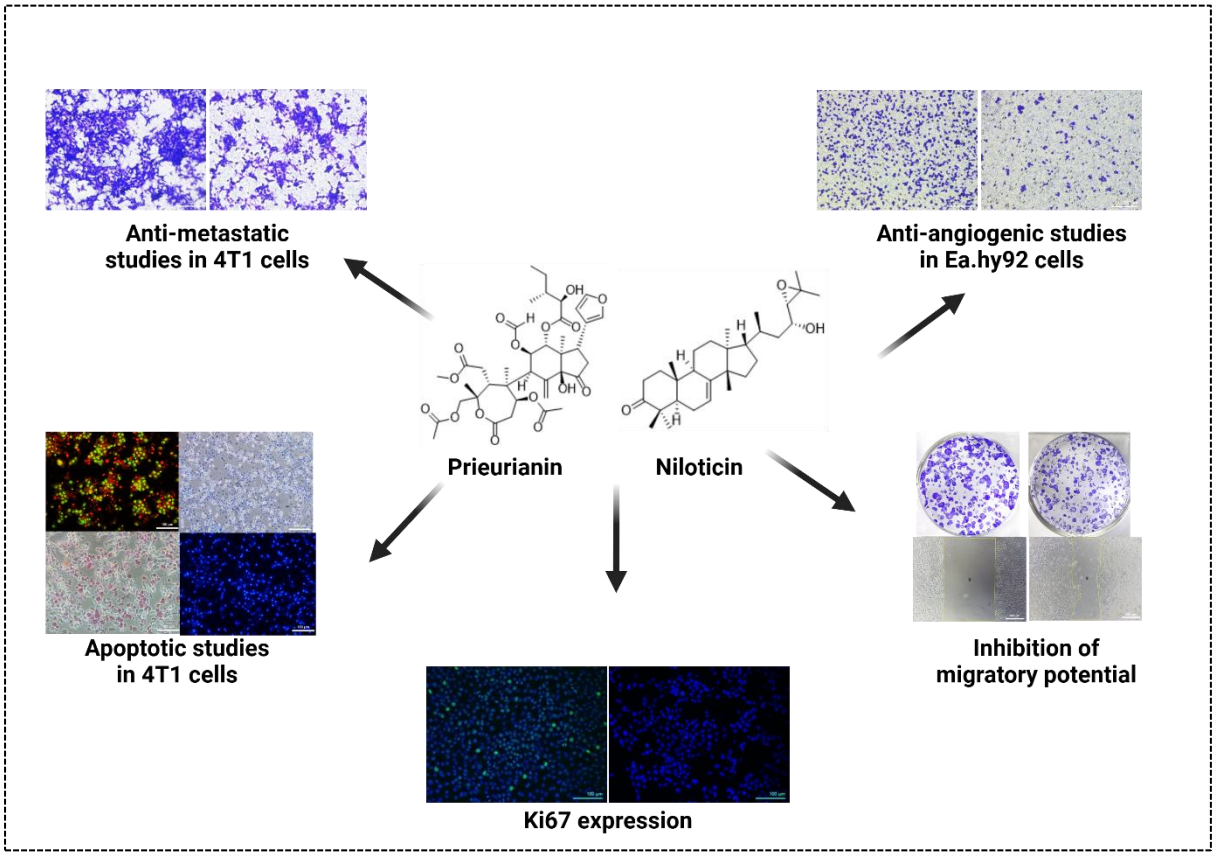

Abstract

Metastasis and angiogenesis are critical processes in cancer progression, contributing significantly to tumor proliferation and dissemination. This complementary study evaluates the anti-metastatic and anti-angiogenic potential of two natural compounds, prieurianin and niloticin, in 4T1 triple-negative breast cancer cells and Ea.hy926 endothelial cells. Cytotoxicity analysis in 4T1 cells revealed IC_{50} values of 13.1 µM and 5.9 µM for niloticin and prieurianin, respectively. Various assays, including live-dead, trypan blue, and eosin staining, confirmed the apoptotic effects of these compounds, with pronounced DNA condensation observed via Hoechst staining. Anti-proliferative properties were substantiated through Ki-67 immunofluorescence, with prieurianin exhibiting a three-fourths reduction in Ki-67 expression and niloticin showed a 50% reduction. Colony formation assays demonstrated significant inhibition of metastatic potential. In contrast,

scratch wound, cell adhesion, migration, and invasion assays further corroborated the anti-metastatic efficacy of both compounds where prieurianin exhibited superior inhibition. Additionally, anti-angiogenic studies in Ea.hy926 endothelial cells highlighted significant suppression of migratory and invasive behaviors, as demonstrated by wound healing and transwell invasion and migration assays. Together, these results underscore the promising dual anti-metastatic and anti-angiogenic effects of prieurianin and niloticin, paving the way for their anti-cancer therapeutic potential.

4.1 Introduction

Metastasis, the process by which cancer cells spread from their primary site to distant organs, represents the leading cause of cancer-related mortality. Approximately 90% of cancer deaths are attributable to metastatic progression, underscoring its significant impact on patient prognosis. Unlike primary tumors, metastatic lesions often exhibit distinct biological properties, complicating treatment strategies and necessitating a deeper understanding of the mechanisms underpinning this process. The metastatic cascade involves several stages, including local invasion, intravasation into the bloodstream, survival in circulation, extravasation, and colonization of distant tissues (1). Cancer cells must overcome numerous biological barriers, often exploiting host factors such as the immune system and extracellular matrix to facilitate their spread (2,3). Despite advances in oncology, effective strategies to specifically target and prevent metastasis remain limited, with most therapies primarily addressing tumor shrinkage rather than the dissemination and establishment of metastatic colonies. The development of anti-metastatic drugs is a challenging but crucial area of research. Traditional cancer treatments, including chemotherapy and targeted therapies, are often evaluated based on their ability to reduce primary tumor size rather than inhibit metastatic progression (4). This approach has contributed to a paucity of therapies specifically designed to target metastasis. However, recent efforts have begun to shift this paradigm by focusing on the unique biology of metastatic cells and their microenvironments. For instance, drugs targeting pre-metastatic niches, tumor dormancy, and immune evasion mechanisms are emerging as promising strategies. Examples include agents that inhibit epithelial-to-mesenchymal transition (EMT), disrupt tumor-stroma interactions or modulate the immune response to prevent metastatic outgrowth. Despite these advances, the translation of preclinical findings into effective clinical therapies remains a significant hurdle, with many candidates failing to demonstrate efficacy in advanced clinical trials (5,6).

Natural products have long served as a valuable source of therapeutic agents in oncology, offering a diverse array of bioactive compounds with unique mechanisms of action. These compounds, derived from plants, microorganisms, and marine organisms, have shown potential in modulating key processes involved in metastasis (7). For example, certain phytochemicals can inhibit EMT, reduce cancer cell invasiveness, or disrupt the formation of pre-metastatic niches by altering the tumor microenvironment. Additionally, natural products often exhibit multi-targeted effects, making them particularly suited to addressing the complexity of metastatic disease. Compounds such as curcumin, resveratrol, and betulinic acid have demonstrated anti-metastatic properties in preclinical models, highlighting the potential of natural products as a complementary approach to conventional therapies. Furthermore, the relative safety and availability of many natural compounds make them attractive candidates for long-term use in preventing metastasis or managing dormant cancer cells (8). In conclusion, metastasis remains a formidable challenge in oncology, driving the need for innovative therapeutic strategies. Anti-metastatic drugs hold immense promise but require a paradigm shift in drug development to focus on the unique characteristics of metastatic disease. Natural products, with their diverse bioactivities and historical success in drug discovery, represent a promising avenue for developing novel anti-metastatic agents. By integrating insights from metastatic biology with the potential of natural compounds, researchers can advance the fight against metastatic cancer and improve outcomes for patients worldwide (9,10).

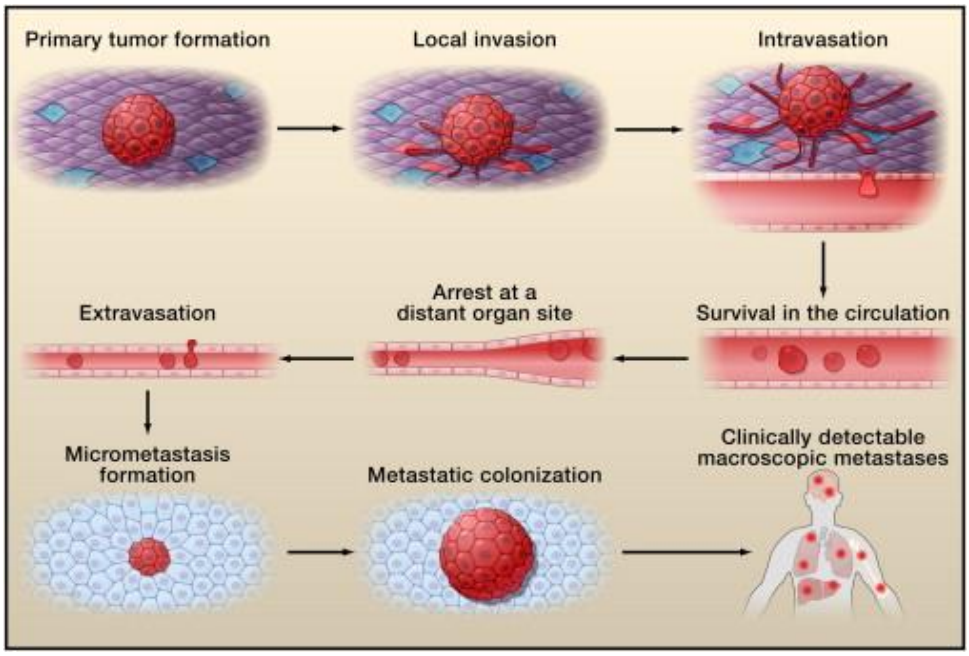

Figure 4.1. Metastasis Cascade, Cell, ISSN: 0092-8674, Vol: 147, Issue: 2, Page: 275-292

Angiogenesis, the process of forming new blood vessels from pre-existing vasculature, is a critical physiological mechanism involved in embryogenesis, wound healing, and tissue regeneration. However, its dysregulation plays a pivotal role in pathological conditions such as cancer, where uncontrolled angiogenesis supports tumor growth, invasion, and metastasis. The tumor microenvironment actively secretes pro-angiogenic factors, including vascular endothelial growth factor (VEGF) and fibroblast growth factor (FGF), which stimulate endothelial cell proliferation and migration (11). This neovascularization ensures a sustained supply of oxygen and nutrients to rapidly dividing cancer cells, thereby enabling their survival and progression. Despite its crucial role, tumor-associated angiogenesis often results in abnormal, leaky, and poorly structured blood vessels, contributing to hypoxia and therapeutic resistance. To counteract the detrimental effects of pathological angiogenesis, anti-angiogenic therapies have emerged as a cornerstone in cancer treatment. These therapies aim to inhibit the formation of new blood vessels or normalize aberrant vasculature within tumors. Anti-angiogenic agents are broadly categorized into two groups: direct inhibitors that target endothelial cells in growing vasculature and indirect inhibitors that suppress pro-angiogenic signaling pathways. Notable examples include monoclonal antibodies such as bevacizumab, which neutralizes VEGF, and tyrosine kinase inhibitors (TKIs) like sunitinib and sorafenib which disrupt intracellular signaling pathways critical for angiogenesis. Although these agents have demonstrated efficacy in slowing tumor growth, they are often associated with limitations such as transient responses, resistance mechanisms, and adverse side effects, including hypertension and impaired wound healing. Consequently, there is an ongoing need for innovative strategies that enhance the specificity and durability of anti-angiogenic therapies (12).

Angiogenesis is a multi-step process critical for the formation of new blood vessels from existing ones. It begins with hypoxia, a condition of low oxygen levels, which stabilizes Hypoxia-Inducible Factor-1 (HIF-1). This stabilization leads to the upregulation of pro-angiogenic factors such as Vascular Endothelial Growth Factor (VEGF), Epidermal Growth Factor (EGF), Fibroblast Growth Factor (FGF), and Insulin-like Growth Factor 1 (IGF-1). Among these, VEGF plays a pivotal role by binding to VEGFR2 on endothelial cells, initiating angiogenic signaling. The next step is proteolytic degradation, where hypoxia-induced signaling upregulates matrix metalloproteinases (MMPs) to degrade the basement membrane surrounding the endothelial cells. This degradation allows the

detachment of pericytes, the supportive cells of blood vessels, and facilitates the outward migration of endothelial cells.

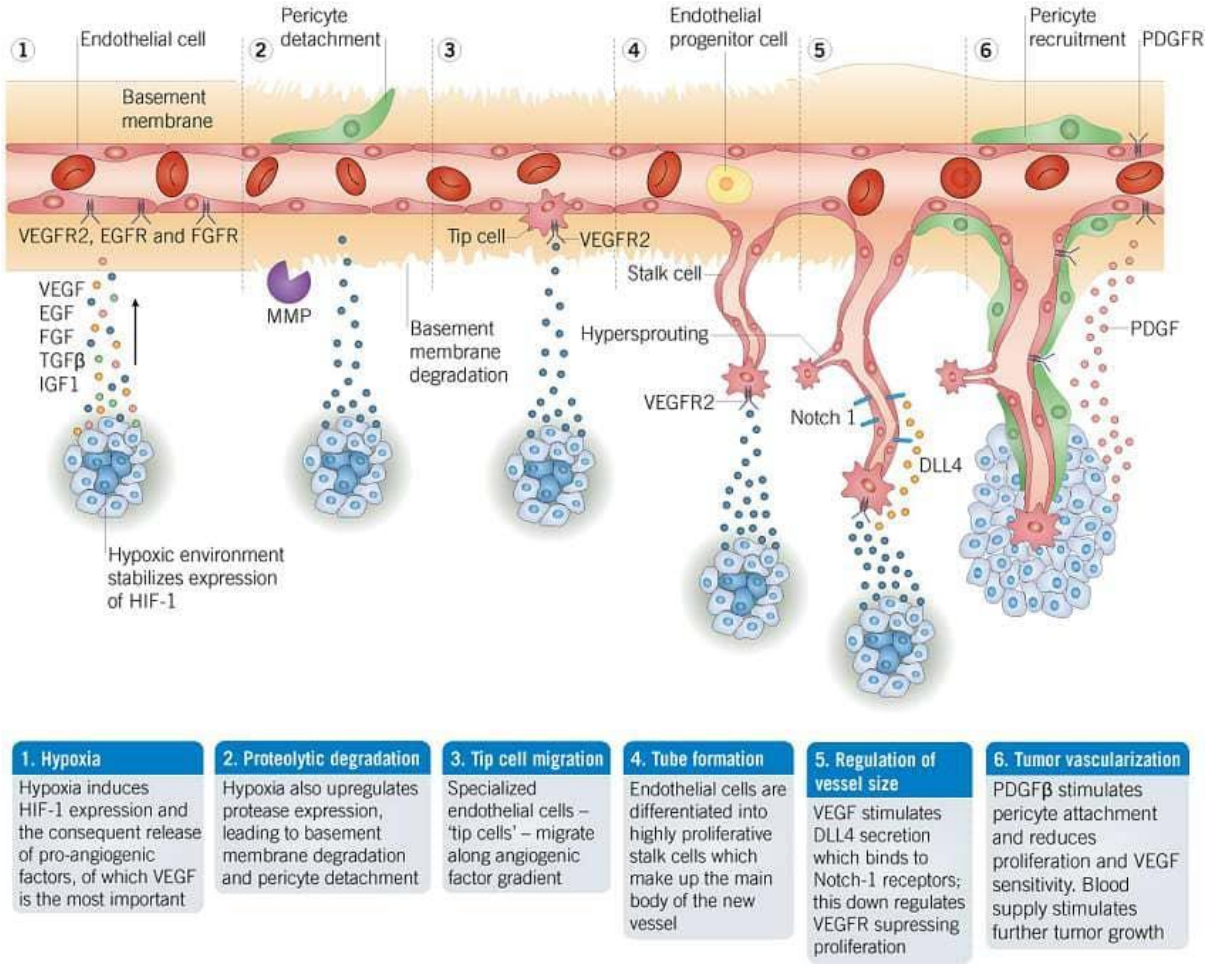

Figure 4.2. The process of angiogenesis. Credits: Tocris Bioscience

In the third stage, specific endothelial cells differentiate into tip cells, which leads the migration of the nascent vessel by extending filopodia toward the gradient of angiogenic factors. Behind the tip cells, stalk cells proliferate and elongate to form the structural body of the growing vessel, creating a tubular structure in the process. To regulate vessel size and prevent excessive branching, VEGF induces the expression of Delta-like ligand 4 (DLL4) in tip cells, which activates Notch1 receptors on adjacent stalk cells. This Notch signaling downregulates VEGF responsiveness in stalk cells, ensuring controlled vessel growth and proper size. The final stage is the maturation and stabilization of the newly formed vessels. Platelet-derived growth Factor-B (PDGF-B) recruits pericytes, which attach to the endothelial cells, providing structural support and reducing the vessels'

sensitivity to VEGF. This stabilization is particularly important in pathological conditions like tumor vascularization, where tumors exploit the new blood vessels for oxygen and nutrient supply to sustain their growth. Through this intricate sequence of steps, spanning hypoxia, basement membrane degradation, endothelial cell migration, tube formation, and vessel stabilization, angiogenesis ensures proper vascular remodeling in both physiological and pathological contexts. Its dual role in health and disease makes it a vital target for therapeutic interventions, especially in cancer treatment.

Natural products offer a promising avenue for the development of novel anti-angiogenic agents. Historically, compounds derived from natural sources have significantly contributed to drug discovery, particularly in oncology (13). These bioactive molecules exhibit diverse chemical structures and mechanisms of action, allowing them to target multiple pathways involved in angiogenesis. For example, curcumin, a polyphenolic compound derived from turmeric, has been shown to inhibit endothelial cell proliferation and VEGF expression. Similarly, resveratrol, found in grapes and red wine, exhibits anti-angiogenic activity by modulating hypoxia-inducible factor-1α (HIF-1α) and matrix metalloproteinases (MMPs). Marine-derived compounds, such as halichondrin and its derivatives, have also demonstrated the potential to disrupt angiogenic signaling. These natural products not only provide a rich reservoir of chemical diversity but also exhibit favorable safety profiles, making them attractive candidates for integration into existing therapeutic regimens. In conclusion, angiogenesis is a double-edged sword in cancer biology, essential for tumor survival yet offering a targetable vulnerability. Anti-angiogenic drugs have revolutionized cancer therapy, but challenges such as resistance and side effects necessitate the exploration of alternative approaches. Natural products, with their multifaceted mechanisms and historical success in drug discovery, represent a promising frontier in the quest for effective and sustainable anti-angiogenic therapies. By harnessing the potential of these compounds and integrating them with advanced drug delivery systems, researchers can pave the way for more targeted and less toxic cancer treatments.

4.2 Results and Discussion

4.2.1 Cytotoxicity analysis in 4T1 triple-negative breast cancer cells

In the previous chapters, anticancer mechanistic studies of niloticin and prieurianin were already demonstrated in HeLa and SiHa cells. Here, studies of these molecules are extended for their anti-metastatic potential in 4T1 murine model triple-negative breast cancer cells

(14,15). Before going to detailed studies, initially, cytotoxicity analysis of niloticin and prieurianin was done in 4T1 cells by MTT assay, where the IC_{50} values are found out to be 13.1 µM and 5.9 µM, respectively, at 24 hours of incubation. This shows the effect of niloticin and prieurainin in 4T1 cell proliferation (Figure 4.3).

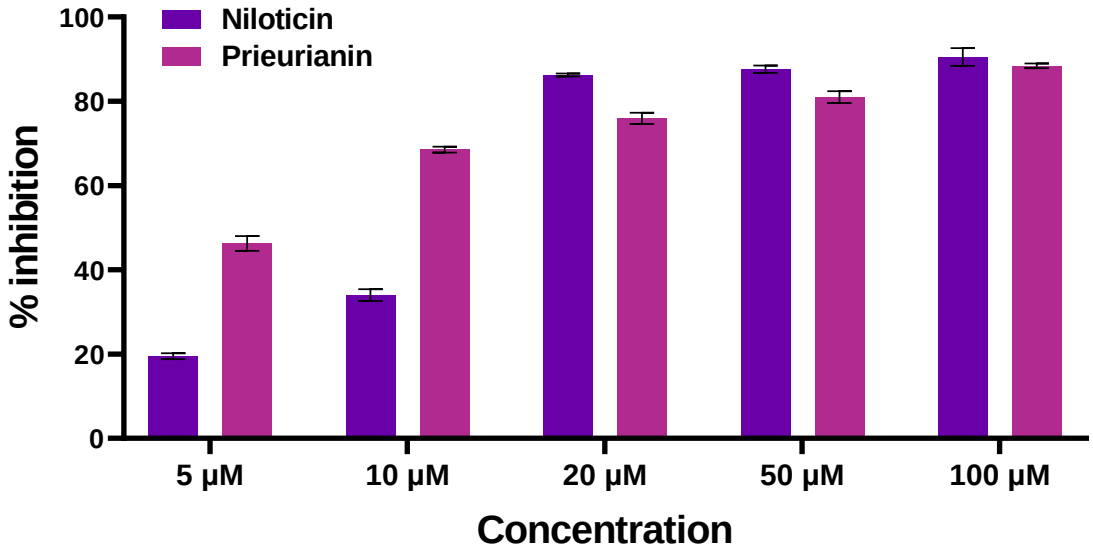

Figure 4.3. Comparative study of percentage inhibition of niloticin and prieurianin in 4T1 cells

4.2.2 Assays to reveal the cell death induced by niloticin and prieurianin

With the exploration of anti-metastatic potential of the molecule, the effect on cell death of 4T1 cells was also analyzed initially. First, a live-dead assay using acridine orange and ethidium bromide was performed, for niloticin at 10 µM and 13 µM concentrations and prieurianin at 3 µM and 5 µM. A variation in colouration from green to reddish orange was observed for control to niloticin and prieurianin-treated cells at 24 hours of incubation proving the membrane disruption. Further trypan blue staining was performed. Trypan blue is a stain used to quantify live cells by labeling dead cells exclusively. Because live cells have an intact cell membrane, trypan blue cannot penetrate the cell membrane of live cells and enter the cytoplasm. In a dead cell, trypan blue passes through the porous cell membrane and enters the cytoplasm. Under light microscopy analysis, only dead cells have a blue color (16). Here trypan blue stain was added to control and 4T1 cells treated with both compounds, where we could observe treated cells show a blue colouration and live cells exhibited a clear cytoplasm. Similarly, eosin staining was also performed to back these experiments (17). The cells were treated with the compounds and imaging was done. Here, we could find the pink colouration in treated cells where control cells omit the intake of

dye, which will be visible as colourless. With the help of these assays, it was confirmed that the niloticin and prieurianin have an effect in inducing cell death in 4T1 cells.

The DNA condensation as a result of apoptosis was also analysed using Hoescht staining (18), where Hoescht stain was added to niloticin and prieurianin-treated cells, and imaging using light microscopy was done. Here we could find highly intensified regions of condensed DNA regions, where apoptotic cells are more where control cells exhibit an even pattern (Figure 4.4, 4.5).

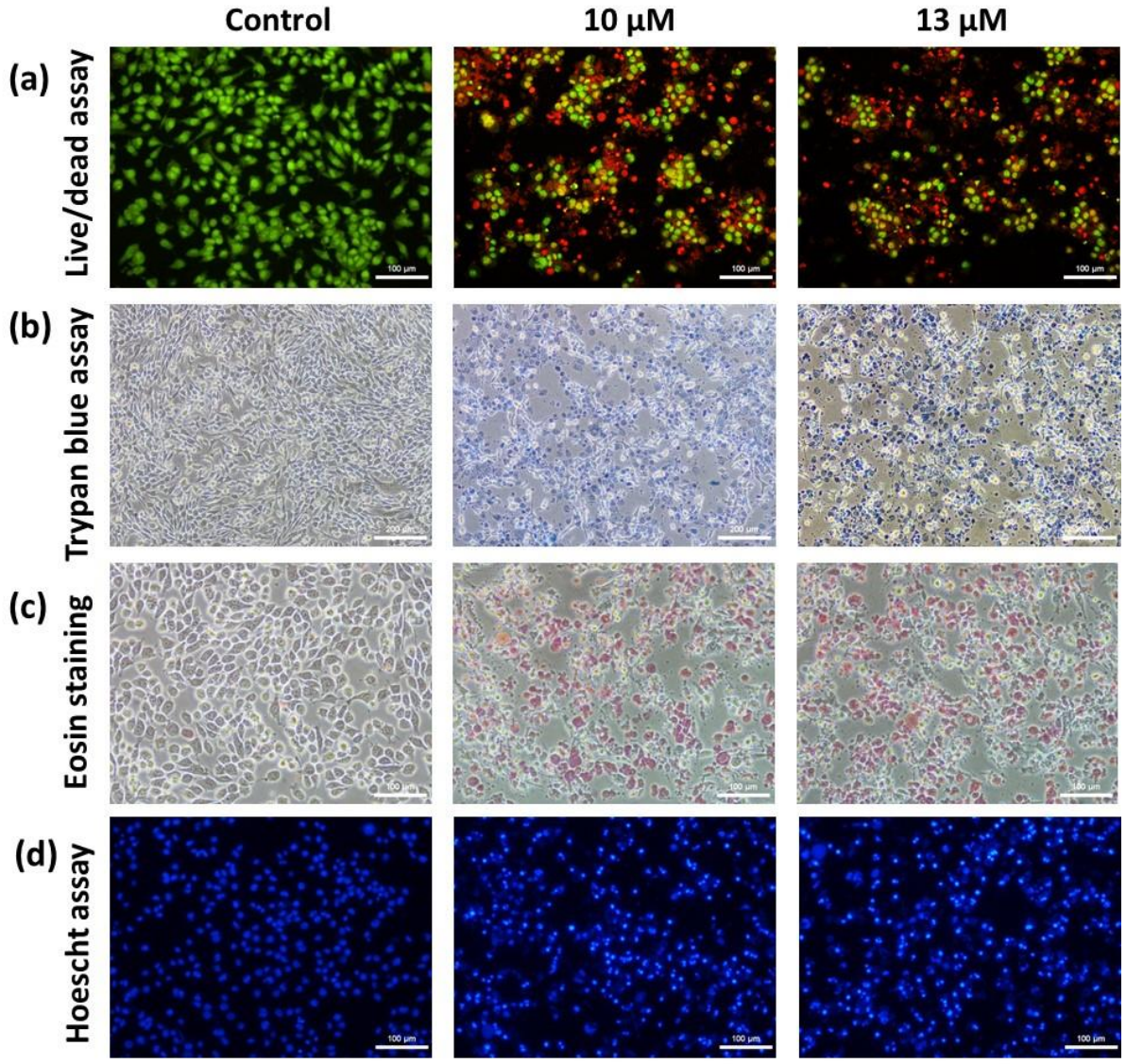

Figure 4.4. Cell death induced by niloticin (a) Live-dead dual staining. Green channel: emission wavelength (λ_{ex} = 450-490 nm), excitation wavelength (λ_{ex} = 520 nm) (b) Trypan blue assay (c) Eosin staining (d) Hoechst nuclear staining. Blue channel: emission wavelength (λ_{ex} = 361-389 nm), excitation wavelength (λ_{ex} = 430-490 nm). The scale bar indicates 100 µm.

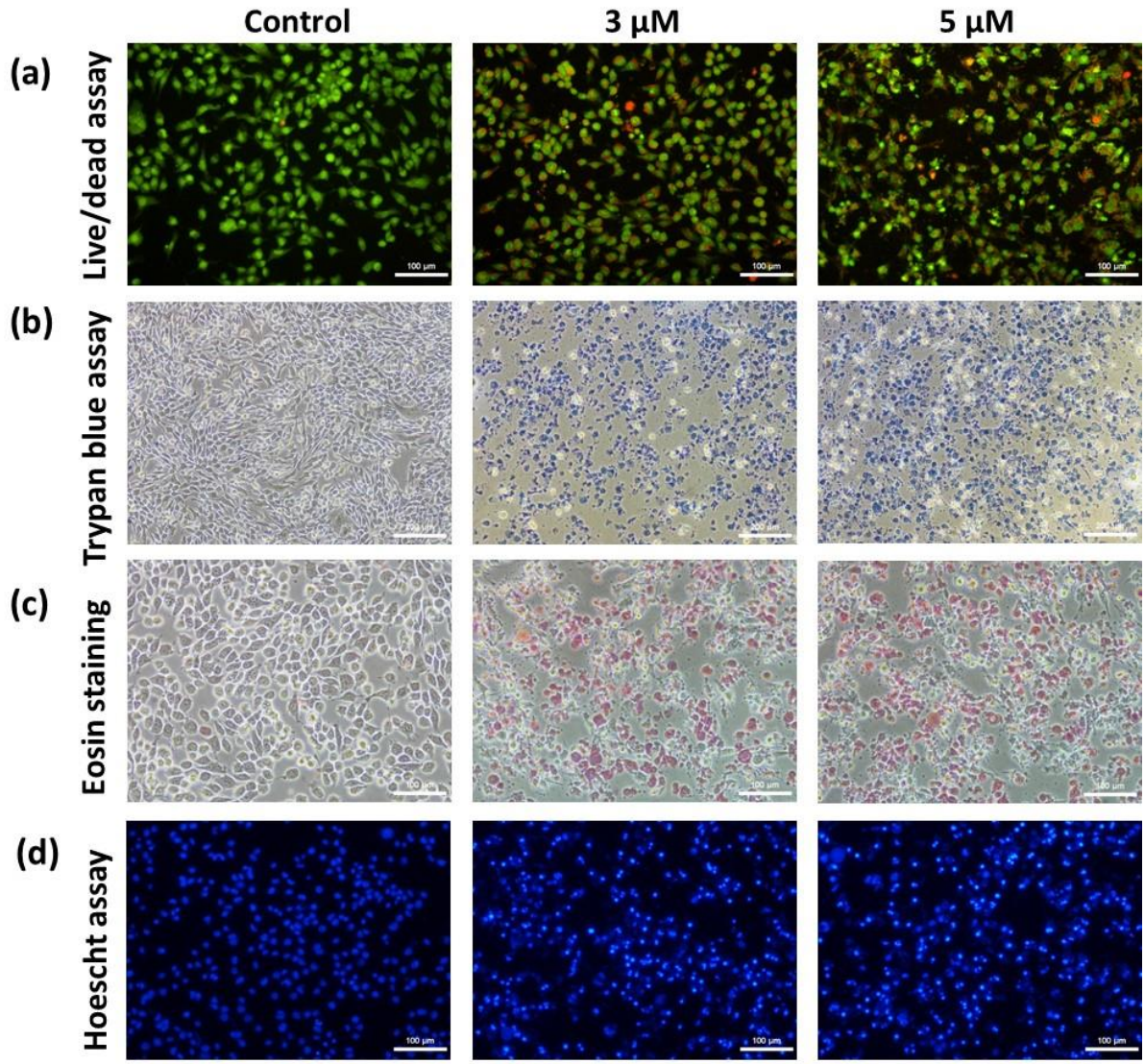

Figure 4.5. Cell death induced by prieurianin (a) Live-dead dual staining. Green channel: emission wavelength (λex = 450-490 nm), excitation wavelength (λex = 520 nm) (b) Trypan blue assay (c) Eosin staining (d) Hoechst nuclear staining. Blue channel: emission wavelength (λ_{ex} = 361-389 nm), excitation wavelength (λ_{ex} = 430-490 nm). The scale bar indicates 100 µm.

4.2.3 Immunofluorescence assay of KI67 in 4T1 cells

Nuclear antigen Ki-67 is widely accepted as a cell proliferation marker in both research and cancer diagnostic settings. Ki-67 protein has been widely used as a proliferation marker for human tumor cells for decades (19) . In recent studies, multiple molecular functions of this large protein have become better understood. Ki-67 has roles in both interphase and mitotic cells, and its cellular distribution dramatically changes during cell cycle progression. As Ki-67 is a major factor in actively dividing cells, it is important analyze the expression to check its metastatic potential. Here, concentration was selected for the

assay, where only 20% of cell death was observed. Niloticin was taken in 3 µM and 6 µM concentrations and prieurianin in 0.5 µM and 1 µM and treatment was done in 4T1 cells.

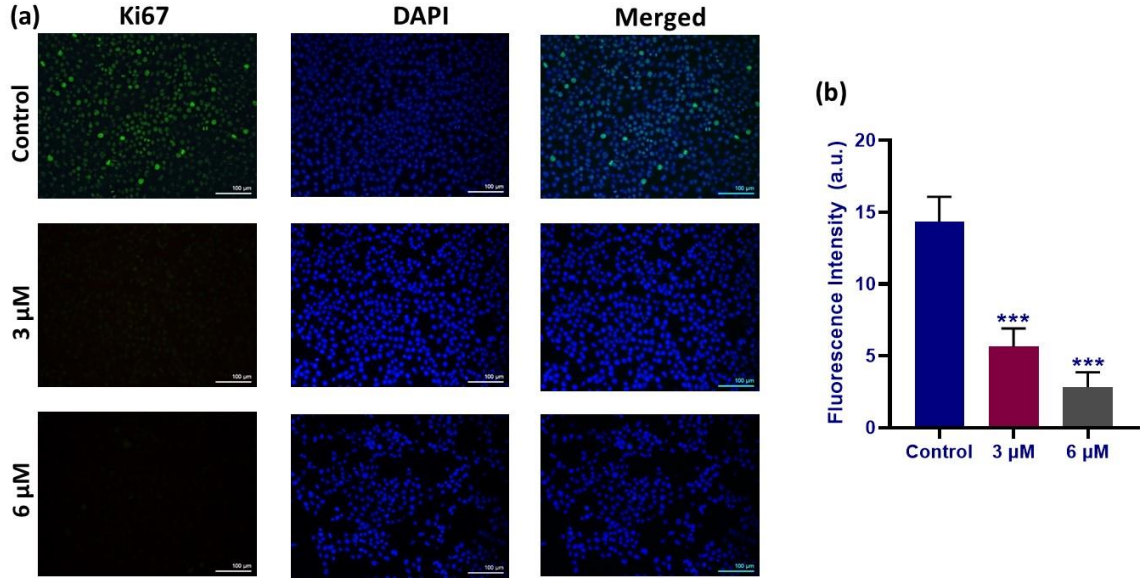

Figure 4.6. Analysis of Ki67 expression in 4T1 cells at 3 µM and 6 µM niloticin treatment f) graph showing fluorescent intensity of Ki67 expression of niloticin treated cells compared to control. Blue channel: emission wavelength (λex = 361-389 nm), excitation wavelength (λex = 430-490 nm). Results are represented as mean ± SD, **p < 0.01, ***p < 0.001 as compared to control.

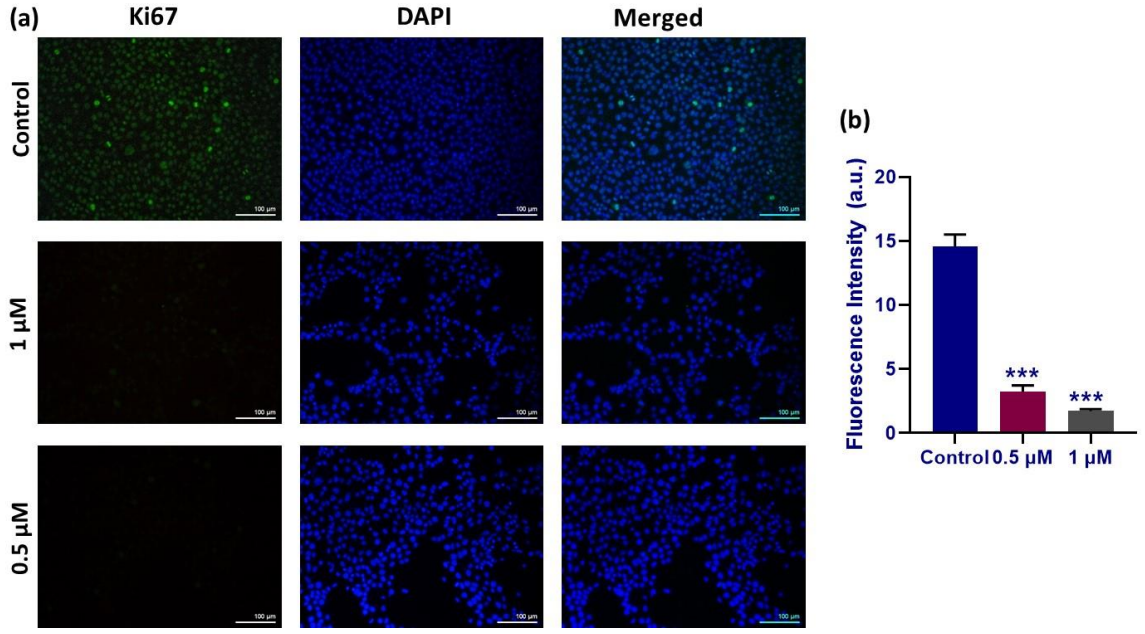

Figure 4.7. Analysis of Ki67 expression in 4T1 cells at 0.5 µM and 1 µM prieurianin treatment f) graph showing fluroscent intensity of Ki67 expression of prieurianin treated cells compared to control. Blue channel: emission wavelength (λ_{ex} = 361-389 nm), excitation wavelength (λ_{ex} = 430-490 nm). Results are represented as mean ± SD, **p < 0.01, ***p < 0.001 as compared to control.

After 24 hours of incubation, anti-Ki-67 antibody was added, followed by FITC conjugated secondary antibody. Visualization was done using DAPI staining using inverted light microscopy. From the results obtained, it is observed that expression of Ki-67 is higher in control, i.e. continuously dividing cells which tend to get decreased upon treatment of the compounds. In the case of niloticin, from the quantitative analysis, it was observed that the expression was reduced to half while prieurianin, after treatment, there was around a three-fourth reduction in the expression of Ki-67. The data obtained suggests a significant reduction in the proliferation potential of the 4T1 cells upon treatment with both the molecules, indicating reduced metastatic potential even in the low concentrations (Figure 4.6, 4.7).

4.2.4 Colony forming assay

As a next step, the effect in inhibition of metastasis and the ability of colonization inhibition has been studied using colony formation assay (20). 4T1 cells were seeded and niloticin (3 µM and 6 µM) and prieurianin (0.5 µM and 1 µM) is added, which were then incubated for around 8-9 days. After this period, visualization was done after fixing the cells and crystal violet staining under a light microscope. The images clearly explain the inhibition of colony forming ability of 4T1 cells by niloticin and prieurianin. In the case of niloticin, there was a reduction of cell number from around 1000 to 500 at 3 µM concentration that was further reduced to 250 at 6 µM concentration while prieurianin, after 8 days of incubation, the colony number has been reduced from 820 to 580 at 0.5 µM concentration and further to 370 at 1 µM concentration (Figure 4.8, 4.9).

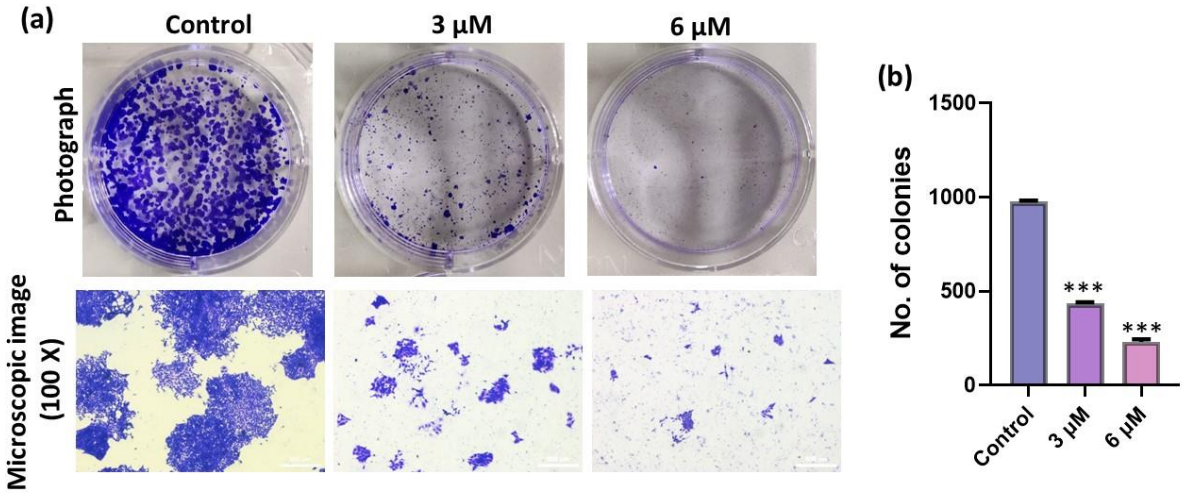

Figure 4.8. (a) Clonogenic assay of 4T1 assessed with the niloticin treatment. The scale bar indicates 200 µm. (b) graph showing number of the colonies during the colony forming assay. ***p < 0.001 compared to control.

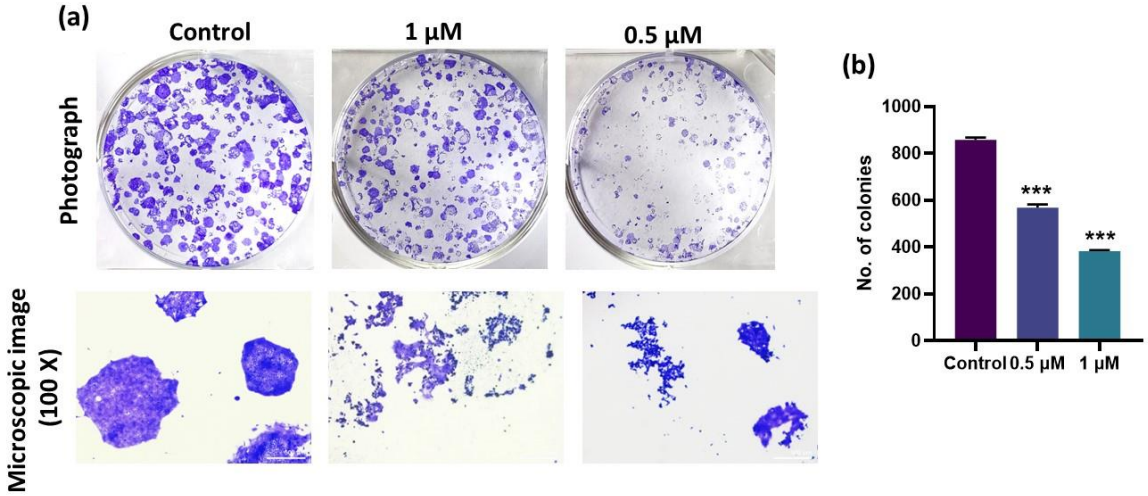

Figure 4.9. (a) Clonogenic assay of 4T1 assessed with the prieurianin treatment. The scale bar indicates 200 µm. (b) graph showing number of the colonies during the colony forming assay. Results are represented as mean ± SD, ***p < 0.001 compared to control.

4.2.5 Anti-metastatic potential evaluation of niloticin and prieurianin in 4T1 cells by scratch wound assay

The metastatic potential of 4T1 cells and anti-metastatic action exerted by niloticin and prieurianin were studied with the help of a wound healing assay. The analysis extends from zero hour to 24 and 48 hours, where the percentage of cell movement with comparison to zeroth hour is measured. Firstly, for niloticin the wound closure percentage for control has been reduced to 80% at 24 hours and the wound is almost completely closed after 48 hours (Figure 4.10). For prieurianin, in control cells after 24 hours, wound closure area has been reduced to 75% after 24 hours and to 48% after 48 hours of incubation (Figure 4.11).

4.2.6 Cell adhesion, invasion and migration assay

In cancer development and progression, invasion, and metastasis occur when tumor cells disseminate from the primary tumor spreading through the circulatory and lymptic systems, invade across the basement membranes and endothelial walls and finally colonize distant organs. Cell migration, invasion, and adhesion are pivotal steps in this process, hence its study and understanding are crucial to fight against the disease. The ability of cells to adhere, invade of extracellular matrix, and movement to other sites has been studied by

various assays (21–23) . The assays include cell adhesion assay, which reflects the number of cells that have been attached to matrigel, where matrigel-coated transwell cell culture inserts coated with matrigel mimics the extracellular matrix (ECM) after treatment with

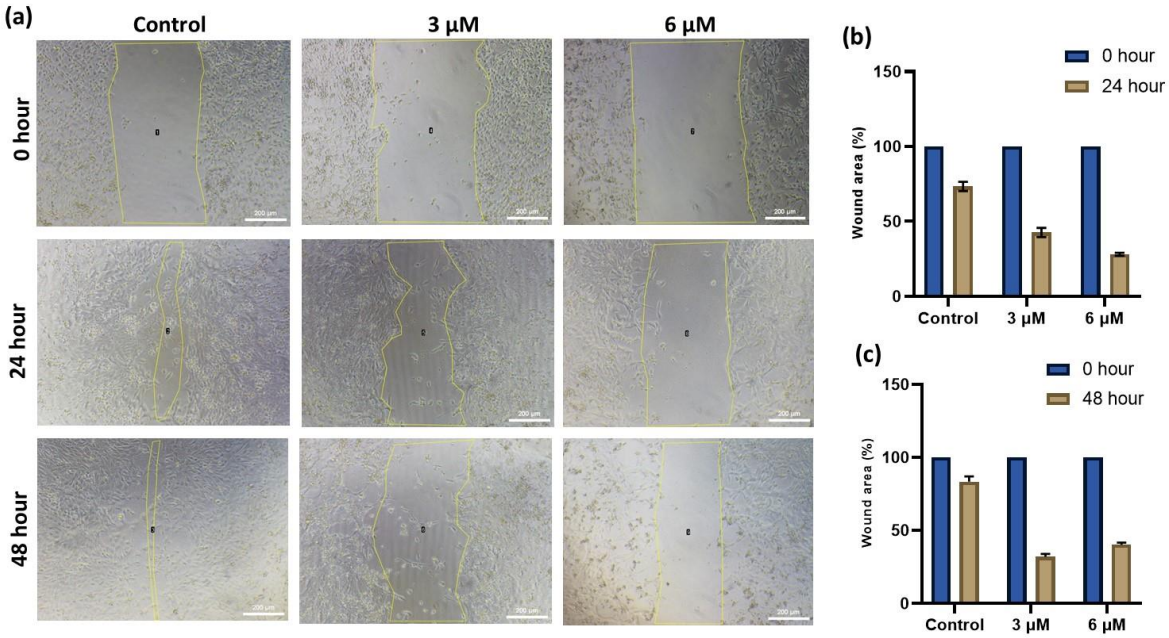

Figure 4.10. (a) Wound healing assay in 4T1 cells for 24 h and 48 h of incubation with niloticin, (b) and (c) % of wound area and wound closure changes with the treatment group at 24 and 48 hours (niloticin - 3 & 6 µM) compared with control

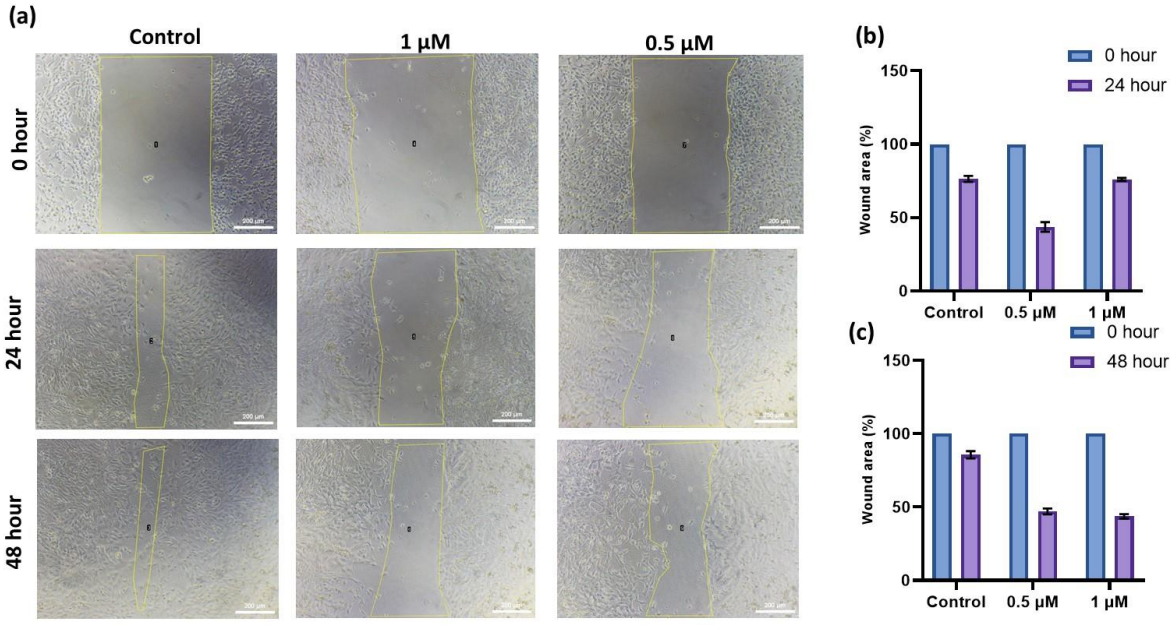

Figure 4.11. (a) Wound healing assay in 4T1 cells for 24 h and 48 h of incubation with prieurianin, (b) and (c) % of wound area and wound closure changes with the treatment group at 24 and 48 hours (prieurianin – 0.5 & 1 µM) compared with control

niloticin and prieurianin. Niloticin in 3 µM and 6 µM concentrations and prieurianin in 0.5 µM and 1 µM was added to 4T1 cells. Then, the treated cells were trypsinized and added to matrigel-coated transwell cell culture inserts. It was incubated for 8 hours and stained with crystal violet, and imaging under light microscopy was done. The cells were counted using ImageJ software where the number of cells attached is calculated. As observed, for niloticin, the number of cells attached gets reduced from 780 to 400 and further to 380 at different concentrations while prieurianin, numbers of cells that got adhered decreased from around 640 to 350 and around 200 at different concentrations (Figure 4.12a, 4.13a).

Next, the ability of cells to migrate against the transwell membrane has been studied by cell migration assay. Here, post-treated 4T1 cells were seeded to transwell cell culture inserts, and incubated for 8 hours. After that, wells were stained with crystal violet, and imaging was done. The results indicated a significant decrease in the number of cell that migrated against transwell membrane after treatment with niloticin and prieurianin compared with untreated ones. In the case of niloticin, the number of cells migrated through transewell membrane decreased from 1200 to around 250 in final concentration and for prieurianin, the cell number reduced from approximately 3000 to 1200 at final concentration (Figure 4.12b, 4.13b).

The invasive nature of cancer cells is another critical feature to promote angiogenesis. Here, the invasiveness of the cells was studied by cell invasion assay, making use of matrigel-coated cell culture inserts. Here, cells were pretreated with niloticin and prieurianin at different concentrations, which after 24 hours were seeded onto the wells and incubated for 7 to 8 hours. And the migration rate of treated and untreated cells was found out by staining with crystal violet imaging and finally counted using ImageJ software. As the results suggest, the number of cells attached comparing the control group was significantly decreased in both the treatment groups of niloticin and prieurianin. In case of niloticin, we could observe approximately 3 times decrease in the number of cells attached compared to the control while in the case of prieurianin, 2 times decrease was found (Figure 4.12c, 4.13c).

The findings demonstrate that both niloticin and prieurianin effectively reduce the adhesion, migration, and invasion of 4T1 cells in a dose-dependent manner. These results highlight their potential as therapeutic agents in inhibiting metastatic processes, which are critical for cancer progression. The significant reduction in cellular activities suggests that

these compounds can disrupt the interactions between cancer cells and the extracellular matrix, as well as their migratory and invasive capabilities. This underscores their promise in developing novel anti-metastatic strategies, paving the way for further preclinical and clinical investigations.

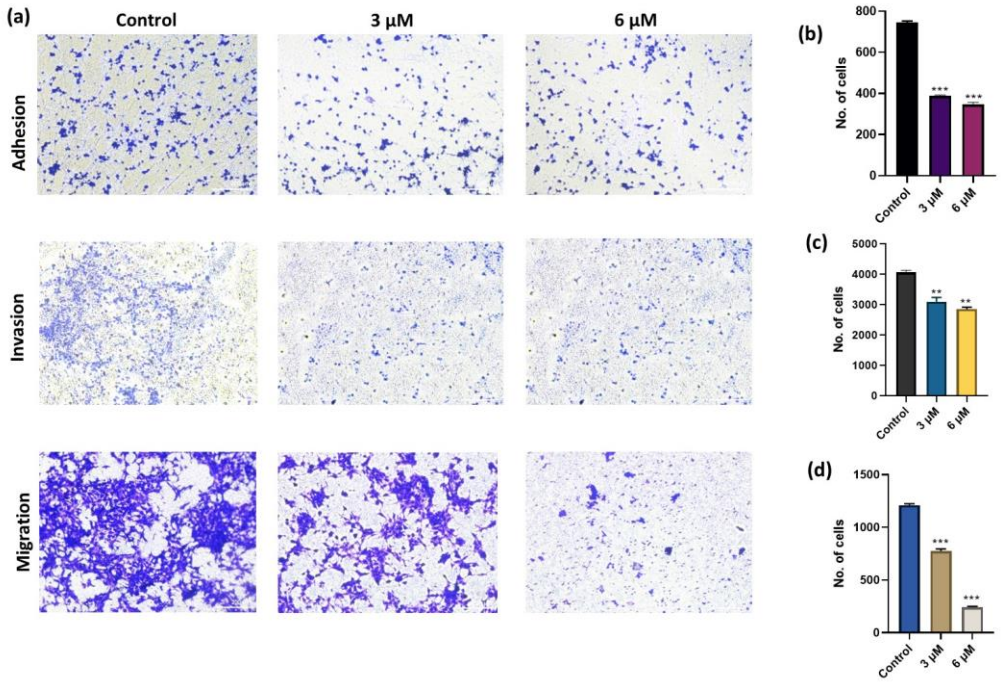

Figure 4.12. (a) cell adhesion assay and the number of adhered cells, migration assay of 4T1 cells using cell culture inserts and invasion assay of the 4T1 cells using matrigel coated transwell inserts for niloticin, (b) graph showing number of adhered cells (c) graph showing number of invaded cells (d) graph showing number of migrated cells through transwell membrane. The scale bar indicates 200 µm. Results are represented as mean ± SD, **p < 0.01, ***p < 0.001 compared to control.

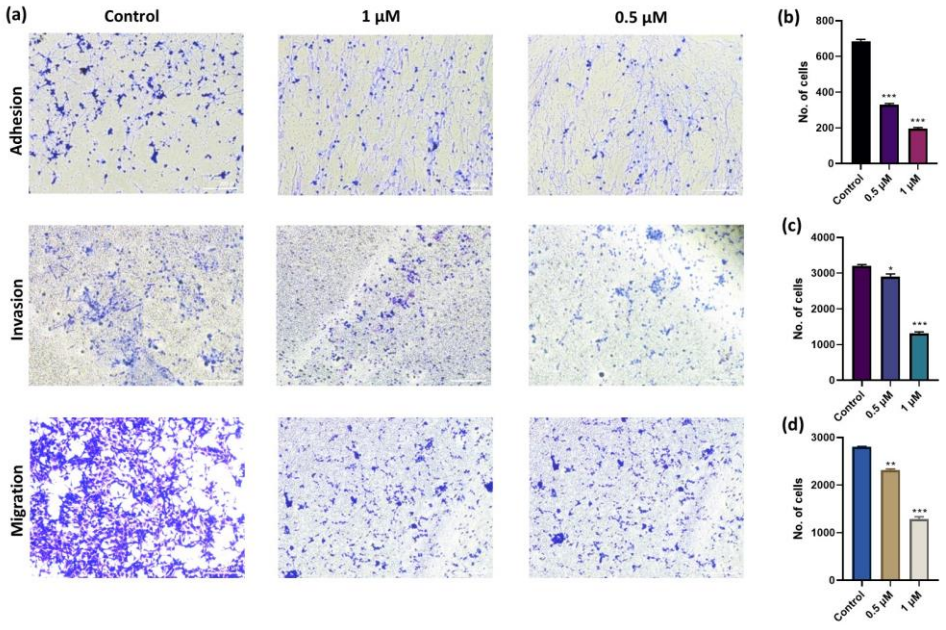

Figure 4.13. a) cell adhesion assay and the number of adhered cells, migration assay of 4T1 cells using cell culture inserts and invasion assay of the 4T1 cells using matrigel coated transwell inserts for prieurianin, (b) graph showing number of adhered cells (c) graph showing number of invaded cells (d) graph showing number of migrated cells through transwell membrane. The scale bar indicates 200 µm. Results are represented as mean ± SD, **p < 0.01, ***p < 0.001 compared to control.

Anti-angiogenic studies of niloticin and prieurianin in Ea.hy926 cells

Ea.hy926 is a human endothelial hybrid cell line. This human umbilical vein cell line, EA.hy926, was established by fusing primary human umbilical vein cells with a thioguanine-resistant clone of A549 by exposure to polyethylene glycol (PEG) (24). Here, a basic anti-angiogenic potential analysis of niloticin and prieurianin was done in Ea.hy926 cells.

4.2.7 Scratch wound assay in Ea.hy926 cells

Initially, a wound healing assay was performed and the migratory potential of the cells before and after treatment with the compounds were analyzed for 0 and 24 hours of incubation. Niloticin was treated at a concentration of 4 µM and prieurianin at a concentration of 0.8 µM. The results indicate that about 90% of wound area closure was seen in control cells after 24 hours of incubation. In the case of niloticin, approximately 40% of the area was only reduced and for prieurianin, only about 10% of the wound area was reduced after 24 hours of incubation (Figure 4.14). The results suggested the effect of niloticin and prieurianin in the movement of Ea.hy926 cells.

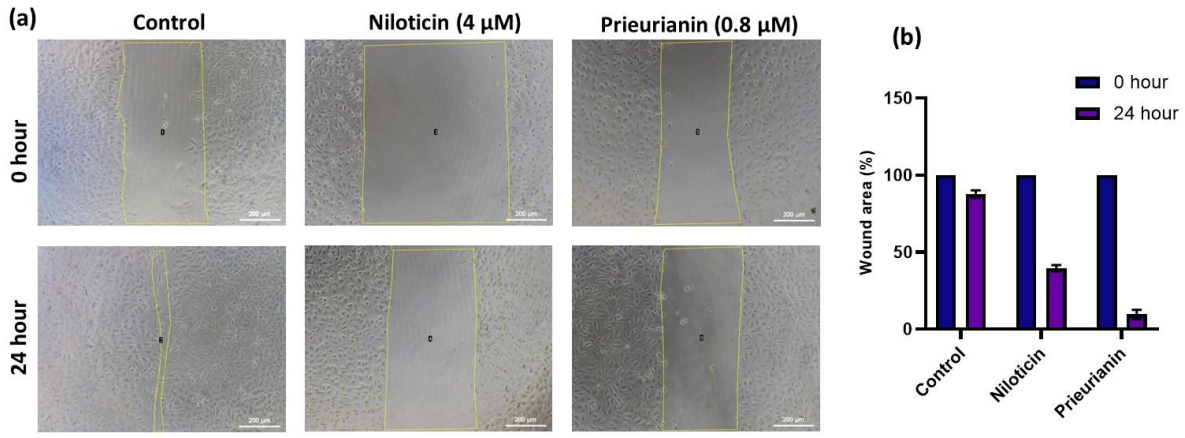

Figure 4.14. (a) Wound healing assay in Ea.hy926 cells for 24 of incubation with niloticin and prieurianin and (b) graph representing the wound area closure for both molecules at 24h.

4.2.8 Cell migration and invasion assays in Ea.hy926 cells

To assess the inhibition of the migratory potential of the molecules, cell migration assay was performed using transwell cell culture inserts. The Ea.hy926 cells were treated with niloticin (4 µM) and prieurianin (0.8 µM), and after 24 hours of incubation, the treated and untreated cells were added to transwell cell culture inserts. After 8 hours of incubation, the cell movement was visualized using crystal violet staining, and the results suggested that around half of the cells got migrated after the treatment with both molecules. Subsequently cell invasion assay was carried out, as the invasion of ECM by the cells is the crucial step in angiogenesis. Here, the treated cells were added into the transwell cell culture inserts coated with matrigel. After staining with crystal violet images were taken, and the invasive potential of Ea.hy926 cells was checked in cells with and without treatment. The results suggested that control group shows a better invasive nature while in treatment groups, the number of cells migrated has been reduced to half (Figure 4.15).

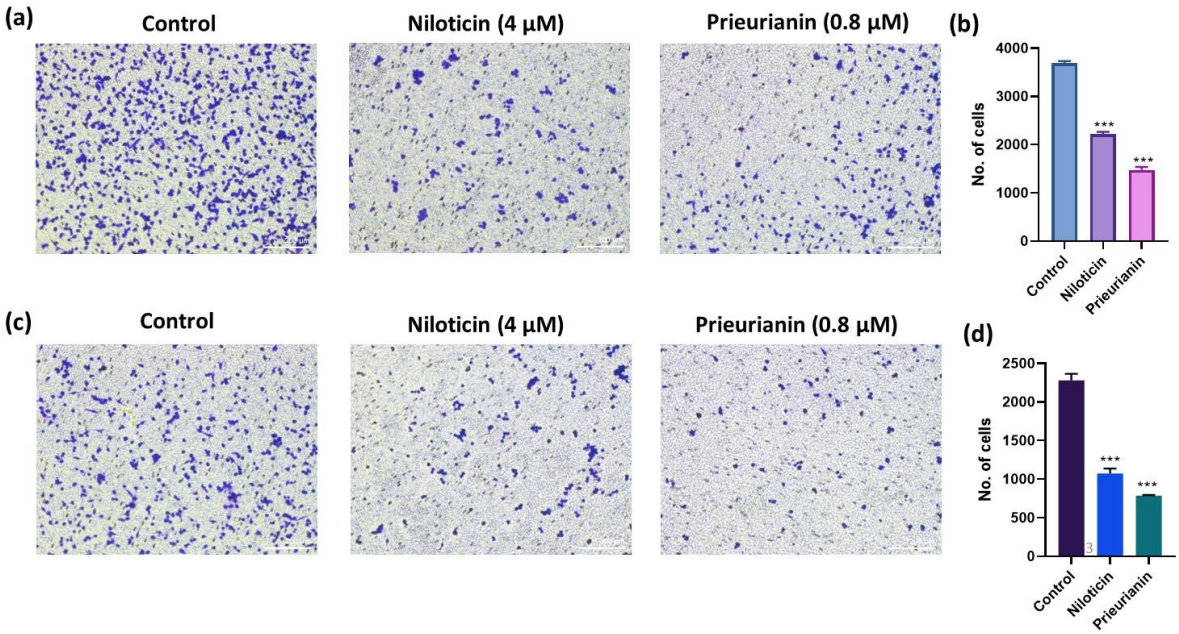

Figure 4.15. (a) Migration assay using cell culture inserts, with treatments with niloticin and prieurianin. The scale bar indicates 200 µm. (b) graph showing number of migrated cells compared with control, (c) invasion assay and (c) fold change in the invaded cells in the treatment with niloticin and prieurianin compared with control. The experiments were conducted in triplicates and the graphical value represents average ± SD, and *** indicates p value <0.001, considered as significant when compared to the control.

4.3 Materials and methods

4.3.1 Cell culture methods

The murine triple negative breast cancer cell, 4T1 was obtained from ATCC and maintained in RPMI, Sigma, and supplemented with 10% Fetal Bovine Serum (FBS, Himedia) and 1% antibiotic antimycotic solution 100X (with 10,000 units Penicillin, 10

mg Streptomycin and 25 µg Amphotericin B per mL in 0.9% normal saline-Himedia) and maintained at 5% CO_2 at 37°C in the incubator.

4.3.2 Cytotoxicity assays

The 4T1 cells were seeded in 96 well plate for 24 h and after the incubation compounds niloticin and prieurianin at different concentrations was added and incubated for 24 h. After the desired incubation time, MTT dissolved in HBSS was added to each well for 2-4 h and the formazan crystals were dissolved in 100 µL of DMSO by removing the MTT solution. The absorbance was measured at 570 nm in a multimode plate reader.

4.3.3 Apoptotic assays

The cells were seeded in 96 well plate, after 24 h of incubation, niloticin at two different concentrations (10 µM and 13 µM) and prieurianin (3 µM and 5 µM) were added. With 24 h incubation of the compound, live dead assay, trypan blue assay, eosin staining and Hoechst nuclear staining were performed by adding the specified dyes. And the images were taken in a fluorescent microscope. For live dead staining, acridine orange and ethidium bromide were added.

4.3.4 Immunofluorescence Assay for Ki67 Expression

Ki67 expression was analyzed in niloticin-treated cells via immunofluorescence. Cells were seeded at 7×10^3 per well in 96-well plates, treated with niloticin (3 µM and 6 µM) and prieurianin (0.5 µM and 1 µM), and stained for Ki67 after fixation and permeabilization. Secondary antibody staining and DAPI staining were performed, followed by imaging using the Nikon TS100 inverted fluorescent microscope.

4.3.5 Colony formation assay

Cells were seeded at a density of 1×10^3 cells per well in a 6-well plate. After 24 hours of incubation, compounds at two distinct concentrations, niloticin (3 µM and 6 µM) and prieurianin (0.5 µM and 1 µM) were introduced, and the cells were permitted to develop colonies over the subsequent 9 days. Following this incubation period, colonies were visualized through staining with 0.3% crystal violet for 10 minutes, followed by washing with PBS. Imaging was conducted using a Nikon-TS100 Inverted microscope, and the captured images were processed. Colony quantification was performed using Image J software. The survival fraction was computed utilizing the formula:

Plating efficiency (PE) = No. of colonies counted × 100/ No. of cells seeded

Surviving fraction (SF) = PE of treated sample × 100/ PE of control

4.3.6 Wound healing assay

Cells were seeded in a 96-well plate at a seeding density of 10 x 10^4 cells per well. Wounds were created in each well by carefully scratching with a 200 µL pipette tip. Various concentrations of compounds were then applied, and images were captured at regular intervals to monitor the wound healing progress. The treated group was subsequently compared to the untreated control to assess the impact of the compounds on the observed wound closure. The wound area was evaluated with the help of ImageJ software.

4.3.7 Adhesion, Migration and Invasion assays

In the cell adhesion assay, cells were initially seeded in a 6-well plate and allowed to incubate for 24 hours. After this incubation period, compounds were introduced, niloticin (3 µM and 6 µM) and prieurianin (0.5 µM and 1 µM). The following day, 48-well plates were coated with 100 µL of diluted matrigel. Once gelled, trypsinized cells from both the untreated and treated groups were added to the matrigel-coated wells and incubated for 4 hours. The cells were subsequently fixed using 70% methanol, stained with a 0.3% crystal violet solution, and images were captured for analysis. The transwell migration and invasion assays utilized cell culture inserts of 8.0 µm pore size. These inserts created a barrier between two distinct media compartments, where the lower portion contained either conditioned medium or serum-containing medium, and the inside of the insert housed cells in serum-free medium, separated by a porous membrane. In the invasion assay, the upper side of the insert was coated with diluted matrigel. Cells were introduced into the serum-free medium, and after 24 hours of incubation, they migrated through the pores towards the serum-containing medium. Following the specified incubation period, the inserts were fixed, stained, and subjected to image capture. Subsequent calculations were performed using Image J software.

4.4 Conclusion

Metastasis and angiogenesis remain formidable challenges in cancer therapy, requiring innovative approaches to mitigate their contributions to disease progression and mortality. In this study, prieurianin and niloticin demonstrated remarkable potential as dual anti-metastatic and anti-angiogenic agents in in vitro models of 4T1 triple-negative breast

cancer and Ea.hy926 endothelial cells. Cytotoxicity studies confirmed their efficacy in inhibiting cell proliferation, where prieurianin exhibited a more pronounced effect than niloticin. Apoptosis was validated through live-dead, trypan blue, eosin staining, and Hoechst staining assays, where the compounds induced significant DNA condensation and membrane disruption. The inhibition of Ki-67 expression further validated the suppression of cellular proliferation, with prieurianin achieving a substantial three-fourths reduction compared to niloticin's 50% reduction. The colony formation assays provided additional evidence of the compounds' anti-metastatic properties, showing dose-dependent reductions in colony numbers. Scratch wound assays demonstrated significant inhibition of cell migration, with prieurianin exhibiting superior wound closure prevention over niloticin. Cell adhesion, migration, and invasion assays further corroborated the compounds' ability to impede the metastatic cascade, particularly in suppressing interactions with the extracellular matrix. Invasion assays revealed a three-fold decrease in the invasive potential of niloticin-treated cells and a two-fold reduction in prieurianin-treated cells, underscoring their distinct inhibitory mechanisms. Anti-angiogenic evaluations in Ea.hy926 cells provided crucial insights into the compounds' ability to target endothelial cells, with prieurianin significantly reducing migratory and invasive capacities. The wound healing assay showed an almost complete inhibition of wound closure in prieurianin-treated cells, while niloticin also markedly restricted migration. Transwell migration and invasion assays further supported these findings, with both compounds halving the invasive potential of endothelial cells. In conclusion, prieurianin and niloticin exhibit complementary and potent anti-metastatic and anti-angiogenic activities, positioning them as promising candidates for therapeutic development. Their natural origin, multi-targeted mechanisms, and demonstrated efficacy highlight their potential in addressing the complex challenges of metastatic cancer. Further *in vivo* and clinical studies are warranted to validate these findings and explore their integration into existing treatment regimens, aiming to improve patient outcomes in metastatic cancer therapy.

4.5 References

1. Lambert AW, Pattabiraman DR, Weinberg RA. Emerging Biological Principles of Metastasis. Vol. 168, Cell. Cell Press; 2017. p. 670–91.
2. The pathogenesis of cancer.
3. Hanahan D, Weinberg RA. Hallmarks of cancer: The next generation. Vol. 144, Cell. 2011. p. 646–74.

4. Gandalovičová A, Rosel D, Fernandes M, Veselý P, Heneberg P, Čermák V, et al. Migrastatics—Anti-metastatic and Anti-invasion Drugs: Promises and Challenges. Vol. 3, Trends in Cancer. Cell Press; 2017. p. 391–406.
5. Steeg PS. Tumor metastasis: Mechanistic insights and clinical challenges. Vol. 12, Nature Medicine. 2006. p. 895–904.
6. Chaffer CL, Weinberg RA. A Perspective on Cancer Cell Metastasis [Internet].
7. Jiang YL, Liu ZP. Natural Products as Anti-Invasive and Anti-Metastatic Agents. Vol. 18, Current Medicinal Chemistry. 2011.
8. Chanvorachote P, Chamni S, Ninsontia C, Phiboonchaiyanan PP. Potential anti-metastasis natural compounds for lung cancer. Vol. 36, Anticancer Research. International Institute of Anticancer Research; 2016. p. 5707–17.
9. Massagué J, Obenauf AC. Metastatic colonization by circulating tumour cells. Vol. 529, Nature. Nature Publishing Group; 2016. p. 298–306.
10. Anderson RL, Balasas T, Callaghan J, Coombes RC, Evans J, Hall JA, et al. A framework for the development of effective anti-metastatic agents. Vol. 16, Nature Reviews Clinical Oncology. Nature Publishing Group; 2019. p. 185–204.
11. Ferrara N, Kerbel RS. Angiogenesis as a therapeutic target. Vol. 438, Nature. 2005. p. 967–74.
12. Carmeliet P, Jain RK. Molecular mechanisms and clinical applications of angiogenesis. Vol. 473, Nature. 2011. p. 298–307.
13. Khalid EB, Ayman ELMELK, Rahman H, Abdelkarim G, Najda A. Natural products against cancer angiogenesis. Vol. 37, Tumor Biology. Springer Science and Business Media B.V.; 2016. p. 14513–36.
14. Tao K, Fang M, Alroy J, Gary GG. Imagable 4T1 model for the study of late stage breast cancer. BMC Cancer. 2008 Aug 9;8.
15. Mouse 4T1 Breast Tumor Model. 2000.
16. Crowley LC, Marfell BJ, Christensen ME, Waterhouse NJ. Measuring cell death by trypan blue uptake and light microscopy. Cold Spring Harb Protoc. 2016 Jul 1;2016(7):643–6.
17. Fischer AH, Jacobson KA, Rose J, Zeller R. Hematoxylin and eosin staining of tissueand cell sections. Cold Spring Harb Protoc. 2008 May;3(5).
18. Crowley LC, Marfell BJ, Waterhouse NJ. Analyzing cell death by nuclear staining with Hoechst 33342. Cold Spring Harb Protoc. 2016;2016(9).

19. Li LT, Jiang G, Chen Q, Zheng JN. Predic Ki67 is a promising molecular target in the diagnosis of cancer (Review). Vol. 11, Molecular Medicine Reports. Spandidos Publications; 2015. p. 1566–72.
20. Franken NAP, Rodermond HM, Stap J, Haveman J, van Bree C. Clonogenic assay of cells in vitro. Nat Protoc. 2006 Dec;1(5):2315–9.
21. Kramer N, Walzl A, Unger C, Rosner M, Krupitza G, Hengstschläger M, et al. In vitro cell migration and invasion assays. Vol. 752, Mutation Research - Reviews in Mutation Research. 2013. p. 10–24.
22. Justus CR, Marie MA, Sanderlin EJ, Yang L V. Transwell In Vitro Cell Migration and Invasion Assays. In: Methods in Molecular Biology. Humana Press Inc.; 2023. p. 349–59.
23. Justus CR, Leffler N, Ruiz-Echevarria M, Yang L V. In vitro cell migration and invasion assays. Journal of Visualized Experiments. 2014 Jun 1;(88).
24. Lu H, Li X, Zhang J, Shi H, Zhu X, He X. Effects of cordycepin on HepG2 and EA.hy926 cells: Potential antiproliferative, antimetastatic and anti-angiogenic effects on hepatocellular carcinoma. Oncol Lett. 2014;7(5):1556–62.

ABSTRACT

Name of the Student: **Anuja Joseph G.**	Registration No.:**10BB19J39005**
Faculty of Study: **Biological Science**	Year of Submission: **2025**
AcSIR academic centre/CSIR Lab: **CSIR-NIIST, TVM, Kerala**	
Name of the Supervisor: **Dr. K. V. Radhakrishnan**	Co-supervisor: **Dr. Kaustabh Kumar Maiti**
Title of the thesis: **Exploring the Anticancer Potential of Niloticin and Prieurianin: Promising Phytochemicals from *Aphanamixis polystachya* (Wall.) R.Parker**	

Cancer is a multifaceted group of diseases characterized by uncontrolled cell growth, tissue invasion, and metastasis, and remains a leading cause of mortality worldwide. Current treatments are often limited by significant side effects and resistance, necessitating safer and more effective alternatives. Natural products, known for their structural diversity and bioactivity, provide a promising source for novel anticancer agents. This work investigates the therapeutic potential of bioactive compounds derived from *Aphanamixis polystachya*, a plant with diverse secondary metabolites, with a focus on their application in cervical and breast cancer treatment.

Chapter 1 introduces natural products as a cornerstone in drug discovery, emphasizing their role in developing safer and targeted cancer therapies. The pharmacological properties of *Aphanamixis polystachya* are explored, alongside an overview of cervical cancer, its global burden, and the limitations of conventional treatments. The potential of natural products to address these challenges is highlighted, forming the basis for the subsequent chapters.

Chapter 2 delves into the isolation and characterization of bioactive phytomolecules from *Aphanamixis polystachya,* identifying niloticin as a key compound with anticancer potential. Niloticin is evaluated for its apoptotic efficacy in HeLa cervical cancer cells, demonstrating selective toxicity toward cancer cells while sparing non-cancerous cells. Molecular studies reveal its ability to engage intrinsic and extrinsic apoptotic pathways through interactions with key apoptotic proteins. Its anti-metastatic properties are further confirmed via in vitro assays, positioning niloticin as a promising candidate for targeted anticancer therapy.

Chapter 3 shifts focus to prieurianin, another potent compound, which exhibits strong apoptotic activity in SiHa cervical cancer cells with an IC50 value of 3.9 µM. Various apoptosis assays validate its ability to trigger programmed cell death and arrest cell cycle progression. Prieurianin effectively engages both intrinsic and extrinsic apoptotic pathways and demonstrates anti-metastatic potential through scratch wound and colony formation assays, along with downregulation of the Ki-67 proliferation marker.

Chapter 4 presents a comparative evaluation of niloticin and prieurianin's anti-metastatic and anti-angiogenic effects in 4T1 triple-negative breast cancer cells and EaHy 926 endothelial cells. Both compounds inhibit cancer cell migration and invasion, as evidenced by colony formation and invasion assays, and downregulate key metastatic markers. Collectively, this study highlights the potential of *Aphanamixis polystachya*-derived phytomolecules as effective agents for targeted cancer therapy, paving the way for future research and development.

List of Publications

Emanating from the thesis

1. **Joseph AG,** Biji M, Murali VP, Sherin DR, Valsan A, Sukumaran VP, Radhakrishnan KV, Maiti KK. A comprehensive apoptotic assessment of niloticin in cervical cancer cells: a tirucallane-type triterpenoid from Aphanamixis polystachya (Wall.) Parker. RSC Medicinal Chemistry. 2024;15(10):3444-59. DOI: 10.1039/d4md90049a
2. **Joseph AG**, Biji, M, Murali, V. P, Radhakrishnan KV, Maiti KK. Exploring anticancer potential of prieurianin: a limonoid isolated from Aphanamixis polystachya (Wall.) Parker. (Manuscript under preparation)
3. **Joseph AG**, Biji, M, Murali, V. P., Radhakrishnan KV, Maiti KK. A comparative anti- metstatic and anti-angiogenic activities of niloticin and prieurianin, two potent anticancer phytoentities isolated from Aphanamixis polystachya (Wall.) Parker. (Manuscript under preparation)

Not related to thesis

1. Aswathy M, Banik K, Parama D, Sasikumar P, Harsha C, **Joseph AG**, Sherin DR, Thanathu MK, Kunnumakkara AB, Vasu RK. Exploring the cytotoxic effects of the extracts and bioactive triterpenoids from dillenia indica against oral squamous cell carcinoma: a scientific interpretation and validation of indigenous knowledge. ACS pharmacology & translational science. 2021 Mar 9;4(2):834-47 DOI: 10.1021/acsptsci.1c00011
2. Valsan A, Meenu MT, Murali VP, Malgija B, **Joseph AG**, Nisha P, Radhakrishnan KV, Maiti KK. Exploration of phaeanthine: A bisbenzylisoquinoline alkaloid induces anticancer effect in cervical cancer cells involving mitochondria-mediated apoptosis. ACS omega. 2023 Apr 10;8(16):14799-813. DOI: 10.1021/acsomega.3c01023
3. Vimalkumar PS, Sivadas N, Murali VP, Sherin DR, Murali M, **Joseph AG**, Radhakrishnan KV, Maiti KK. Exploring apoptotic induction of malabaricone A in triple-negative breast cancer cells: an acylphenol phyto-entity isolated from the

fruit rind of Myristica malabarica Lam. RSC Medicinal Chemistry. 2024. DOI: 10.1039/D4MD00391H

4. Subramanyan S, Karunakaran V, Deepika S, **Gracy AJ**, Sheeba V, Joseph K, Maiti KK, Varma RL, Radhakrishnan KV. Libocedroquinone: A Promising Anticancer Lead against Lung Cancer from Calocedrus Decurrens. Planta Medica International Open. 2022 Jun;9(01):e54-9. DOI: 10.1055/a-1699-8748
5. Subramanyan S, Deepika S, Ajith A, **Joseph Gracy A**, Dan M, Maiti KK, Varma RL, Radhakrishnan KV. Antiproliferative labdane diterpenes from the rhizomes of Hedychium flavescens Carey ex Roscoe. Chemical Biology & Drug Design. 2021 Oct;98(4):501-6. DOI: 10.1111/cbdd.13906
6. C. P. Irfana Jesin, V. R. Padma Priya, R. Kataria, V. Alisha, P. S. Vimalkumar, **A. G. Joseph**, G. C. Nandi, A One-Pot Tandem Synthesis of Sulfoximine-Based Urea From Organic Acid via Curtius Rearrangement . ChemistrySelect 2022, 7, e202202898. DOI: 10.1002/slct.202202898

Conference presentations

1. **Anuja Joseph G**., Biji M., K. V. Radhakrishnan and Kaustabh Kumar Maiti. Apoptosis induction in cervical cancer cells by Niloticin At 5th International Conference on Nutraceuticals and Chronic diseases (INCD 2022) held from 7-9 October 2022, at Department of Zoology, University of Delhi.
2. **Anuja Joseph G**, Greeshma Gopalan, K. V. Radhakrishnan. Investigation on phytochemical constituents & Antioxidant properties of Anethum graveolens Linn. At International Ayurveda Seminar held during March 12-19, 2021, organised in connection with the Fourth Global Ayurveda Festival- Virtual Conference & Expo.
3. **Anuja Joseph G.,** Greeshma Gopalan, Kavya Krishnamoorthy and radhakriishnan K.V. Phytochemical investigations on Anethum graveolens L. (dill) in the International virtual conference, Progress and Promises in Chemical Sciences (PPCS-2020) organized by Department of Chemistry, CHRIST (Deemed to be University), Bengaluru from 15 February 2020 to 15 March 2020.

Apoptosis Induction in Cervical Cancer Cells by the Limonoid, Niloticin

Joseph A.G.*, Biji M., Maiti K.K., Radhakrishnanan K.V.#

Chemical Sciences and Technology Division, CSIR-National Institute for Interdisciplinary Science and Technology (CSIR-NIIST), Thiruvananthapuram, Kerala; bAcademy of Scientific and Innovative Research, Ghaziabad, INDIA.

*Presenting Author: anujajosephg@gmail.com #Correspondence: radhu2005@gmail.com

Aphanamixis polystachya, comes under the family Meliaceae, is a valuable medicinal plant seen abundantly in India. Traditionally, the barks of *A. polystachya* is used in treatment of tumor, liver and spleen diseases. Limonoids are a major group of molecules present in this plant, which is well explored for its wide range of biological activities such as antiviral, anticancer, antifungal and antibacterial. The present study involves the exploration of anticancer potential of the niloticin, a limonoid isolated from the barks of *A. polystachya*. Preliminary antiproliferative studies were done in cervical cancer cell line HeLa by MTT assay, from which IC50 was found out to be 11.65 ± 0.02 μM at 24 hours of incubation. Further apoptotic potential of the molecule was studied by live dead assay, APOP assay, Hoescht staining, DNA fragmentation and annexin V-FITC flow cytometric analysis. Expression studies of cell cycle proteins shows downregulation of cdk1, cyclin A2, cyclin B1, proves the inhibition of proliferation of cancer cells upon treatment with niloticin. Caspase flurometric studies revealed the intrinsic mode of apoptosis in HeLa cells which is substantiated by the data from JC-1 mitochondrial membrane potential assay, in which the lower red/ green ratio indicates depolymerised mitochondrial membrane potential. The apoptotic potential of the molecule in Hela cells and its lesser toxicity in normal cells, attributes to the features of the compound to be developed as a potent drug against cervical cancer.

Investigation on phytochemical constituents & Antioxidant properties of *Anethum graveolens* Linn.

Anuja Joseph G., Greeshma Gopalan, Kavya Krishnamoorthy and Radhakrishnan K. V.*

Organic Chemistry Section, Chemical Sciences and Technology Division, National Institute for Interdisciplinary Science and Technology (CSIR), Trivandrum 695019, India

Email:radhu2005@gmail.com

Organic chemistry is an art executed science in which the isolation of bioactive compounds or molecules from natural resources makes it one of the most interesting and finest areas of modern chemistry. The key role played by plant-based systems in the healthcare of different cultures has been extensively documented and according to World Health Organization (WHO), approximately 65-80% of the world's population relies mainly on plant-derived traditional medicines for their primary health care. Medicinal plants have been used for centuries as remedies for human diseases. Treatments with the use of various plants have historically formed the basis of sophisticated traditional medicine, preceding the established scientific literature by thousands of years. Apiaceae (also known as Umbelliferaceae) family is an important natural resource that provides many useful products for food, spices, medicines, dyes, perfume and aesthetics. They comprise well-known and economically important plants such as angelica, anise, asafoetida, caraway, carrot, celery, chervil, coriander, cumin, dill, fennel, hemlock, lovage, cow parsley, parsley, parsnip, sea holly, giant hogweed and silphium. Among these, dill is widely used as a spice and also yields essential oil. The Ayurvedic uses of dill seeds are carminative, stomachic and diuretic. In these aspects, we carried out a detailed phytochemical investigation on dill seeds and 23 compounds were isolated. All the compounds were characterised using different NMR and HR-MS techniques.

Keywords: *Anethum graveolens*, GCMS

Phytochemical investigations on *Anethum graveolens* L. (dill)

Anuja Joseph G., Greeshma Gopalan, Kavya Krishnamoorthy and Radhakrishnan K. V.*

Organic Chemistry Section, Chemical Sciences and Technology Division, National Institute for Interdisciplinary Science and Technology (CSIR), Trivandrum 695019, India

Email:radhu2005@gmail.com

Organic chemistry is an art executed science in which the isolation of bioactive compounds or molecules from natural resources makes it one of the most interesting and finest areas of modern chemistry. The key role played by plant-based systems in the healthcare of different cultures has been extensively documented and according to World Health Organization (WHO), approximately 65-80% of the world's population relies mainly on plant-derived traditional medicines for their primary health care. Medicinal plants have been used for centuries as remedies for human diseases. Treatments with the use of various plants have historically formed the basis of sophisticated traditional medicine, preceding the established scientific literature by thousands of years. Apiaceae (also known as Umbelliferaceae) family is an important natural resource that provides many useful products for food, spices, medicines, dyes, perfume and aesthetics. They comprise well-known and economically important plants such as angelica, anise, asafoetida, caraway, carrot, celery, chervil, coriander, cumin, dill, fennel, hemlock, lovage, cow parsley, parsley, parsnip, sea holly, giant hogweed and silphium. Among these, dill is widely used as a spice and also yields essential oil. The Ayurvedic uses of dill seeds are carminative, stomachic and diuretic. In these aspects, we carried out a detailed phytochemical investigation on dill seeds and 23 compounds were isolated. All the compounds were characterised using different NMR and HR-MS techniques.

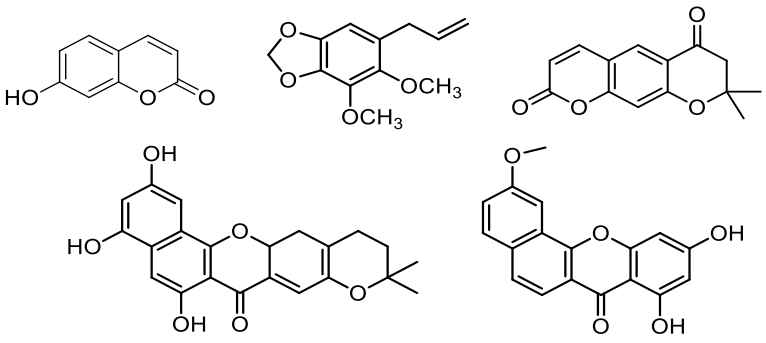

Keywords: *Anethum graveolens*, GCMS

RSC Medicinal Chemistry

ROYAL SOCIETY OF CHEMISTRY

CORRECTION

Cite this: *RSC Med. Chem.*, 2024, **15**, 4223

Correction: A comprehensive apoptotic assessment of niloticin in cervical cancer cells: a tirucallane-type triterpenoid from *Aphanamixis polystachya* (Wall.) Parker

Anuja Gracy Joseph,[ab] Mohanan Biji,[ab] Vishnu Priya Murali,[a] Daisy R. Sherin,[c] Alisha Valsan,[ab] Vimalkumar P. Sukumaran,[ab] Kokkuvayil Vasu Radhakrishnan*[ab] and Kaustabh Kumar Maiti*[ab]

DOI: 10.1039/d4md90049a

rsc.li/medchem

Correction for 'A comprehensive apoptotic assessment of niloticin in cervical cancer cells: a tirucallane-type triterpenoid from *Aphanamixis polystachya* (Wall.) Parker' by Anuja Gracy Joseph *et al.*, *RSC Med. Chem.*, 2024, **15**, 3444–3459, https://doi.org/10.1039/D4MD00318G.

The authors regret the omission of one of the affiliations for authors Kokkuvayil Vasu Radhakrishnan and Kaustabh Kumar Maiti from the original manuscript. The corrected list of authors and affiliations for this paper is shown above.

The Royal Society of Chemistry apologises for these errors and any consequent inconvenience to authors and readers.

[a] *Chemical Sciences and Technology Division (CSTD), Organic Chemistry Section, CSIR-National Institute for Interdisciplinary Science and Technology (CSIR-NIIST), Industrial Estate, Thiruvananthapuram 695019, India. E-mail: radhu2005@gmail.com, kkmaiti@niist.res.in*

[b] *Academy of Scientific and Innovative Research (AcSIR), Ghaziabad 201002, India*

[c] *School of Digital Sciences, Kerala University of Digital Sciences, Innovation and Technology, Thiruvananthapuram-695317, India*

RSC Medicinal Chemistry

ROYAL SOCIETY OF CHEMISTRY

RESEARCH ARTICLE

View Article Online
View Journal

Cite this: DOI: 10.1039/d4md00318g

A comprehensive apoptotic assessment of niloticin in cervical cancer cells: a tirucallane-type triterpenoid from *Aphanamixis polystachya* (Wall.) Parker†

Anuja Gracy Joseph,[ab] Mohanan Biji,[ab] Vishnu Priya Murali,[a] Daisy R. Sherin,[c] Alisha Valsan,[ab] Vimalkumar P. Sukumaran,[ab] Kokkuvayil Vasu Radhakrishnan *[a] and Kaustabh Kumar Maiti *[a]

Pharmacologically active small organic molecules derived from natural resources are prominent drug candidates due to their inherent structural diversity. Herein, we explored one such bioactive molecule, niloticin, which is a tirucallane-type triterpenoid isolated from the stem barks of *Aphanamixis polystachya* (Wall.) Parker. After initial screening with other isolated compounds from the same plant, niloticin demonstrated selective cytotoxicity against cervical cancer cells (HeLa) with an IC_{50} value of 11.64 μM. Whereas the compound exhibited minimal cytotoxicity in normal epithelial cell line MCF-10A, with an IC_{50} value of 83.31 μM. Subsequently, *in silico* molecular docking studies of niloticin based on key apoptotic proteins such as p53, Fas, FasL, and TNF β revealed striking binding affinity, reflecting docking scores of −7.2, −7.1, −6.8, and −7.2. Thus, the binding stability was evaluated through molecular dynamic simulation. In a downstream process, the apoptotic capability of niloticin was effectively validated through *in vitro* fluorimetric assays, encompassing nuclear fragmentation. Additionally, an insightful approach involving surface-enhanced Raman spectroscopy (SERS) re-establishes the occurrence of DNA cleavage during cellular apoptosis. Furthermore, niloticin was observed to induce apoptosis through both intrinsic and extrinsic pathways. This was evidenced by the upregulation of upstream regulatory molecules such as CD40 and TNF, which facilitate the activation of caspase 8. Concurrently, niloticin-induced p53 activation augmented the expression of proapoptotic proteins Bax and Bcl-2 and downregulation of IAPs, leading to the release of cytochrome C and subsequent activation of caspase 9. Therefore, the reflection of mitochondrial-mediated apoptosis is in good agreement with molecular docking studies. Furthermore, the anti-metastatic potential was evidenced by wound area closure and Ki67 expression patterns. This pivotal *in vitro* assessment confirms the possibility of niloticin being a potent anti-cancer drug candidate, and to the best of our knowledge, this is the first comprehensive anticancer assessment of niloticin in HeLa cells.

Received 4th May 2024,
Accepted 1st August 2024

DOI: 10.1039/d4md00318g

rsc.li/medchem

Introduction

Throughout history, humans have leveraged the therapeutic potential of nature, which provides a vast repository of bioactive compounds. Nature is often esteemed as the quintessential healer, with its components playing a critical role in managing numerous chronic diseases. Medicinal plants have been integral to healthcare from ancient traditional medicine to contemporary medical systems owing to their remarkable efficacy, safety, and cost-effectiveness. The extracts and isolated compounds from medicinal plants are preferred treatments for a variety of ailments. The relevance of natural product-based drug discovery persists as some of these compounds are indispensable even in the era of modern synthetic medicines due to their diverse physicochemical properties, including high bioactivity, biocompatibility, and bioavailability.[1,2] Although many modern therapeutic interventions have been practiced in recent decades, cancer continues to be a leading cause of

[a] CSIR-National Institute for Interdisciplinary Science and Technology (CSIR-NIIST), Chemical Sciences and Technology Division (CSTD), Organic Chemistry Section, Industrial Estate, Thiruvananthapuram 695019, India. E-mail: radhu2005@gmail.com, kkmaiti@niist.res.in
[b] Academy of Scientific and Innovative Research (AcSIR), Ghaziabad 201002, India
[c] School of Digital Sciences, Kerala University of Digital Sciences, Innovation and Technology, Thiruvananthapuram-695317, India

† Electronic supplementary information (ESI) available: The extraction and isolation procedure, characterization, preliminary cytotoxic evaluation of extracts, and molecular docking are discussed. See DOI: https://doi.org/10.1039/d4md00318g

death worldwide. Intensive research aims to discover a cure for this lethal affliction as existing treatments such as chemotherapy, radiation, and surgery pose risks to healthy cells and tissues. The escalating cancer incidence highlights the pressing need for an effective and affordable treatment with minimal side effects. In addition to the challenges associated with the disease itself, the development of chemoresistance has emerged as a major concern.[3–5] Within the spectrum of malignancies, cervical cancer holds the fourth position in terms of incidence, emerging as the predominant cause of mortality among women.[6] In this preview, natural products exert their actions by regulating multiple signaling pathways involved in cell growth and apoptosis, consequently impeding cancer cell progression and possessing immune activation, which results in tumor cell death.[7,8] Currently, there is a growing interest in the search for naturally occurring active molecules with high immunomodulation for cancer treatment.[9,10]

Aphanamixis polystachya (Wall.) Parker, also known as Amoora rohituka, a member of the Meliaceae family, is distinguished for its extensive medicinal properties.[11] Owing to its therapeutic potential, this plant has traditionally been used to address various health issues, including spleen and liver diseases, abdominal problems, tumors, eye disorders, rheumatoid arthritis, ulcers, and jaundice.[12,13] It exhibits pharmacological properties, such as antibacterial, antifungal, and insecticidal activities.[14] Furthermore, it possesses CNS depressant, analgesic, and clot lysis properties.[15] The ethyl acetate fraction of *A. polystachya* has demonstrated its ability to safeguard bone marrow cells against chromosomal abnormalities induced by gamma radiation in Swiss albino mice. This finding suggests potential applications in radiation therapy for cancer treatment.[16] Niloticin, a tirucallane-type triterpenoid isolated from *A. polystachya*, has demonstrated significant biological activities. One of the promising reported activities of niloticin is its ability to inhibit osteoclastogenesis by suppression of the RANKL-induced activation of the AKT, MAPK and NF-κB signaling pathways.[17] Niloticin functions as an antagonist of myeloid differentiation factor-2 (MD-2) and possesses anti-inflammatory activity.[18] The literature also hints at the insecticidal properties of niloticin, which is considered a prominent feature of this compound. Additionally, anti-plasmodial and anti-respiratory syncytial virus (RSV) activities have been reported for niloticin.[19,20] The cytotoxicity of niloticin is identified in several cancer cell lines, including gastric (BGC-823, KE-97), liver (Huh-7), breast (MDA), prostate (PC3, LNCaP), fibrosarcoma (HT-1080), and hepatoma (Hep3B).[21–24] However, comprehensive anti-cancer studies specifically targeting cervical cancer cell proliferation have not been reported, which constitutes a primary focus of the current investigation.

Considering these facets, our objective is to meticulously investigate the anticancer properties of the phytomolecule niloticin against cervical cancer, which is prevalent in the female reproductive system. In this process, the extraction and isolation of the desired phytomolecules have been carried out from the stem bark of *Aphanamixis polystachya*. The antiproliferative effect of the acetone extract was evaluated in cervical cancer (HeLa) cells, which demonstrates significant activity. Hence, we extended our studies with the isolation of key phytomolecules from acetone extract. The isolation yielded five distinct phytomolecules, falling into the category of tirucallane-type triterpenoids, which are characteristic of plants within the meliaceae family. The anticancer potential of the isolated compounds was then scrutinized in HeLa cells, resulting in niloticin being the most potent among them. This eventually led us to focus on the triterpenoid compound, niloticin, for an in-depth anticancer profiling investigation. *In silico* screening of niloticin with major protein targets of the apoptotic pathway show reasonably good binding affinity with key proteins involved in the signaling cascade, including p53, Fas receptor, Fas L, Bax, CDK2, BCL2 and TNF β. Therefore, to complement the *in silico* results, an *in vitro* downstream assessment was carried out to elucidate the apoptotic mechanisms by which niloticin operates, employing a variety of cell-based assays and analyzed DNA fragmentation by agarose gel electrophoresis, which was fully complemented by surface-enhanced Raman scattering (SERS) as an ultrasensitive spectroscopic modality. Furthermore, niloticin exerts its anti-proliferative potential by sub-G0 cell cycle arrest, confirmed by cell cycle assay and expression analysis of cell cycle regulatory proteins. To evaluate the apoptotic pathway, the expression of caspases was analyzed by fluorometric assays. Interestingly, it was observed that the niloticin followed both extrinsic and intrinsic modes of apoptosis, which is well supported by the molecular docking and protein expression studies of the involved key factors. Additionally, wound healing properties and the ability of clonogenic inhibition were evaluated, aiming to establish the anti-metastatic potential of niloticin backed by the expression analysis of Ki67 by immunofluorescence study. Finally, the pathway of the molecule's action was well confirmed by examining the expression of signaling proteins, thus solidifying niloticin's potential for further studies as a promising hit compound against cervical cancer. To date, this is the first detailed investigation of the anticancer potential of niloticin in cervical cancer using the HeLa cell line (Scheme 1).

Results and discussion

Extraction, isolation, and characterization of phyto entities from *Aphanamixis polystachya*

The acetone extract of the bark of *Aphanamixis polystachya* (Wall.) Parker was prepared by percolation, and its antiproliferative potential was primarily checked in HeLa (cervical cancer) cells using the MTT (3-(4,5-dimethylthiazol-2-yl)-2,5-diphenyl-2*H*-tetrazolium bromide) assay (Fig. S1, Table S1†), with IC_{50} values of 39.96 and 17.18 μg mL^{-1} at 24 and 48 hours of incubation, respectively. This led to the

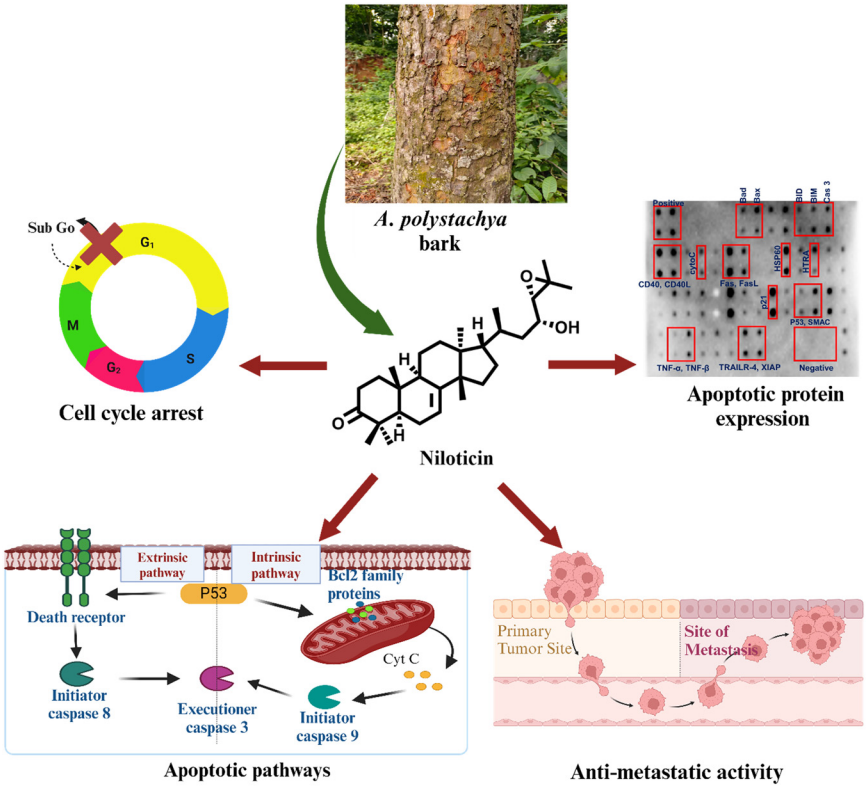

Scheme 1 Cell death induced by niloticin through intrinsic and extrinsic modes of apoptosis.

isolation and purification of phytomolecules from the acetone extract. The acetone extract, subjected to repeated column chromatographic separation, yielded five distinct molecules: niloticin (15 mg), bourjotinolone B (32 mg), piscidinol A (10 mg), 24-*epi*-piscidinol A (21 mg), and hispidol B (18 mg) (Fig. 1a–e). All molecules belong to tirucallane type-triterpenoid, and were characterized by 1D NMR, 2D NMR and HRMS, which were in accordance with the reported data (Fig. S3–S340†).[25–28]

Preliminary cytotoxic screening of isolated phytomolecules

A preliminary cytotoxic analysis of tirucallane type-triterpenoid against cervical cancer cells was conducted using the MTT assay in HeLa cells at concentrations ranging from 5 to 100 μM, and the IC_{50} values are shown in Fig. 1g. Among the phytomolecules, niloticin was found to be the most potent with an IC_{50} value of 11.64 μM at an incubation period of 24 hours. To check its anticancer potential in other cancer cells, we specifically conducted the MTT assay of niloticin on A549 (lung), PANC-1 (pancreatic), and MDA-MB-231 (breast) cancer cell lines by keeping the same concentrations of niloticin as in HeLa cells. The minimal inhibitory concentration (IC_{50}) was determined, which turned out to be 30.6 μM (A549), 16.5 μM (PANC-1) and 23.9 μM (MDA-MB-231), respectively, at 24 hours of incubation. This infers that niloticin is most active against cervical cancer (HeLa cell line) (Fig. 1i). As a better cytotoxicity was observed in HeLa cells, we also evaluated the activity of niloticin in SiHa (squamous cell carcinoma) with an IC_{50} value of 16.23 μM, which further proved the anti-proliferative potential of niloticin in cervical cancer cells. Since niloticin exhibited a pronounced inhibitory potential against the cervical cancer cell line, we evaluated its potential in MCF 10A, a non-tumorigenic epithelial cell line, and the observed IC_{50} was approximately 83.31 μM. This finding of the selective anti-cancer potential of niloticin urges us to conduct an in-depth apoptotic assessment on HeLa cells.

Computational screening of niloticin

In the pursuit of understanding the pharmacokinetic properties of niloticin, our initial evaluations revealed promising characteristics. Niloticin exhibited high human intestinal absorption, accompanied by a favorable lipophilicity with an iLOGP value of 4.58. Furthermore, the absence of PAINS (pan assay interference compounds) was confirmed (Fig. S42†). To elucidate the intricate interactions between niloticin and key signaling proteins within the apoptotic pathway of cervical cancer, we conducted comprehensive molecular docking simulations. Seven pivotal proteins in the pathway were selected for this study: p53 (PDB ID: 1TUP), Fas receptor (PDB ID: 3EZQ), Fas L (PDB ID: 5L19), Bax (PDB ID: 6EB6), CDK2 (PDB ID: 2UZE), BCL2 (PDB ID: 6O0K), and TNF β (PDB ID: 1TNR). Notably, docking scores below −6.5 were observed, indicating robust

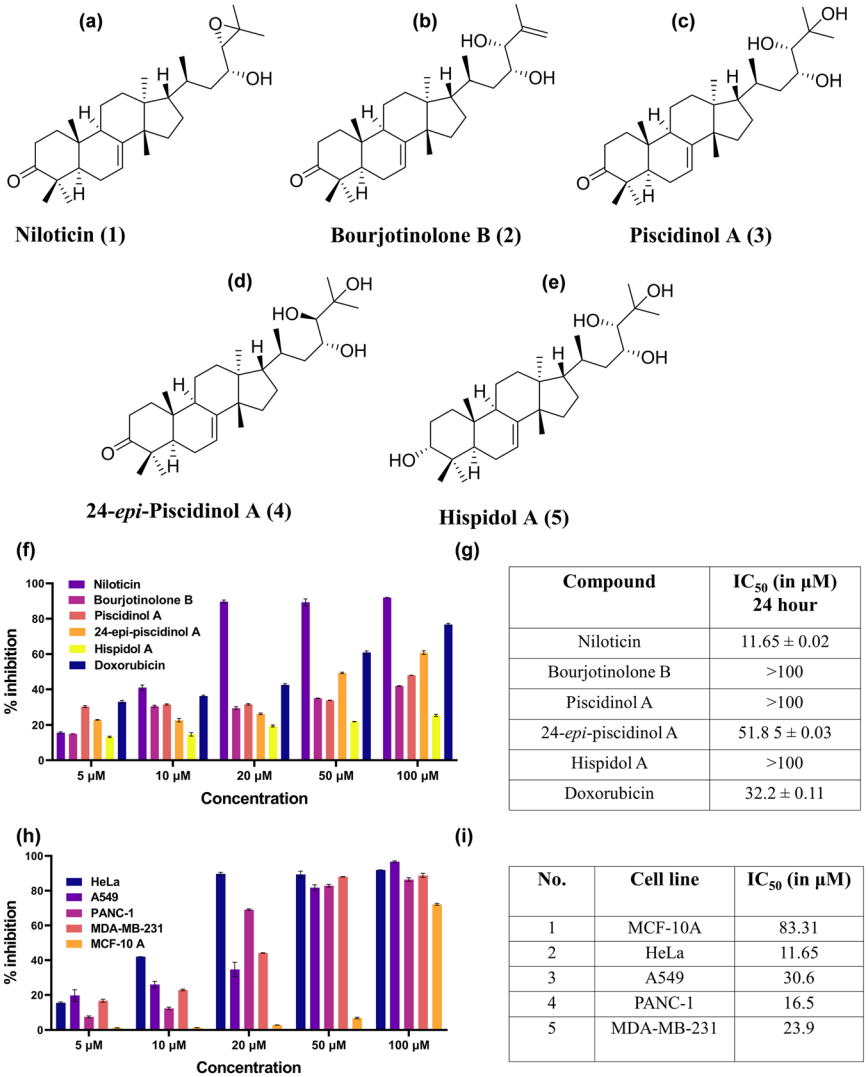

Compound	IC_{50} (in µM) 24 hour
Niloticin	11.65 ± 0.02
Bourjotinolone B	>100
Piscidinol A	>100
24-*epi*-piscidinol A	51.8 5 ± 0.03
Hispidol A	>100
Doxorubicin	32.2 ± 0.11

No.	Cell line	IC_{50} (in µM)
1	MCF-10A	83.31
2	HeLa	11.65
3	A549	30.6
4	PANC-1	16.5
5	MDA-MB-231	23.9

Fig. 1 Structure of a) niloticin, b) bourjotinolone, c) piscidinol A, d) 24-*epi*-piscidinol, and e) hispidol A. f) Graph showing the percentage toxicity of isolated molecules in HeLa cells, g) and their corresponding IC_{50} values. h) Comparative study of the percentage inhibition of niloticin in different cancer cell lines, i) and their IC_{50} values using the MTT assay.

interactions between niloticin and these proteins (Table S2†) (Fig. 2a–g).

Our analysis revealed the strong binding of niloticin with each protein, as evidenced by docking scores ranging from −6.8 to −9.0 kcal mol^{-1}. For instance, with the tumor suppressor protein p53 (PDB ID: 1TUP), niloticin formed hydrogen bonds and hydrophobic interactions with residues such as ASN 263, GLY 262, and GLU 258, resulting in a docking score of −7.2 kcal mol^{-1}. Similarly, interactions with the Fas receptor (PDB ID: 3EZQ) and Fas L (PDB ID: 5L19) yielded scores of −7.1 and −6.8 kcal mol^{-1}, respectively, involving crucial residues such as GLY 247, PHE 248, and ARG 144. Moreover, niloticin demonstrated high affinity for proteins like Bax (PDB ID: 6EB6), CDK2 (PDB ID: 2UZE), BCL2 (PDB ID: 6O0K), and TNF β (PDB ID: 1TNR),[29–34] with docking scores of −7.7, −7.2, −9.0, and −7.2 kcal mol^{-1}, respectively. These findings underscore the efficacy of niloticin as a promising therapeutic agent in cervical cancer treatment, warranting further investigation into its mechanistic pathways and clinical applications.

Molecular dynamics simulation of protein–niloticin complex

Subsequently, the exploration of niloticin's interactions with the selected proteins delved even deeper through extensive molecular dynamics simulations. These simulations, conducted using the OPLS-2005 force field, extended over a meticulous time frame of 100 nanoseconds. The root mean square deviation (RMSD) plot emerged as a crucial analytical tool in this phase. This plot not only provided insights into the structural dynamics, but also served as a robust indicator of the stability exhibited by both the individual proteins and their respective complexes with niloticin. Remarkably, the RMSD analysis revealed that, throughout the simulation period, the proteins and their complexes maintained structural integrity, demonstrating a maximum RMSD value of 3.5 Å (Fig. 2h).

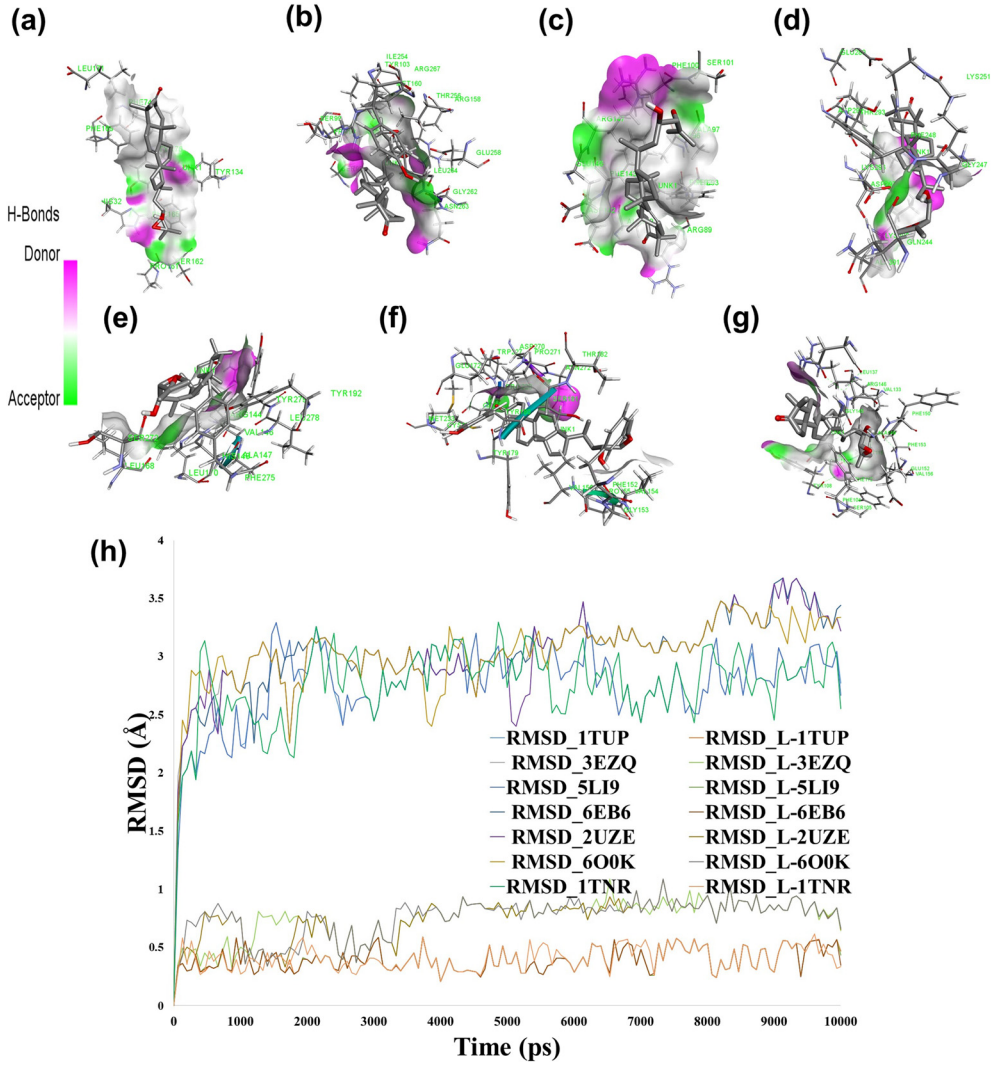

Fig. 2 3-D interaction of niloticin with a) TNF β, b) P53, c) Bax, d) Fas receptor, e) FasL, f) CDK2, and g) BCL2. h) RMSD plot of niloticin with different proteins.

This meticulous assessment of structural fluctuations underscores the resilience of the protein–niloticin complexes, affirming the sustained stability of the binding interactions. The limited deviation observed in the RMSD values accentuates the consistency and endurance of the strong molecular bonds between niloticin and the crucial proteins in the apoptotic pathway. This substantiates the premise that niloticin's impact extends beyond mere binding affinity, indicating a profound and enduring influence on the structural stability of the targeted proteins, further fortifying its potential as a key player in inducing apoptosis in human cervical cancer cells.

Apoptotic evaluation of niloticin

Various apoptotic assays were employed to assess the cell death mechanisms triggered by niloticin in HeLa cells. Firstly, we used acridine orange (AO) and ethidium bromide (EB) DNA-binding dyes as a dual staining method, which differentially labeled viable and dead cells, and observed the signals through fluorescence microscopy with a FITC filter. Considering the IC_{50} of niloticin, the apoptotic induction was conducted at two different concentrations (7 μM and 11 μM). The control cells, without niloticin treatment, were stained green as AO can penetrate the intact cell membrane of the viable cells, while the membrane-impermeant dye EB cannot. In contrast, niloticin-treated cells were stained reddish-orange because EB only enters cells with compromised membranes, binds to DNA, and exhibits a red fluorescence, indicating an early or late apoptotic stage of the cell, as shown in Fig. 3a. Furthermore, to confirm the changes in the cellular membrane due to apoptosis induction, we employed a non-fluorescent imaging method using the APOPercentage assay. In this assay, the dye enters cells with impaired membranes, staining them pink, while non-apoptotic cells remain unstained.[35] The current data align with the findings of the apoptotic potential of niloticin on HeLa

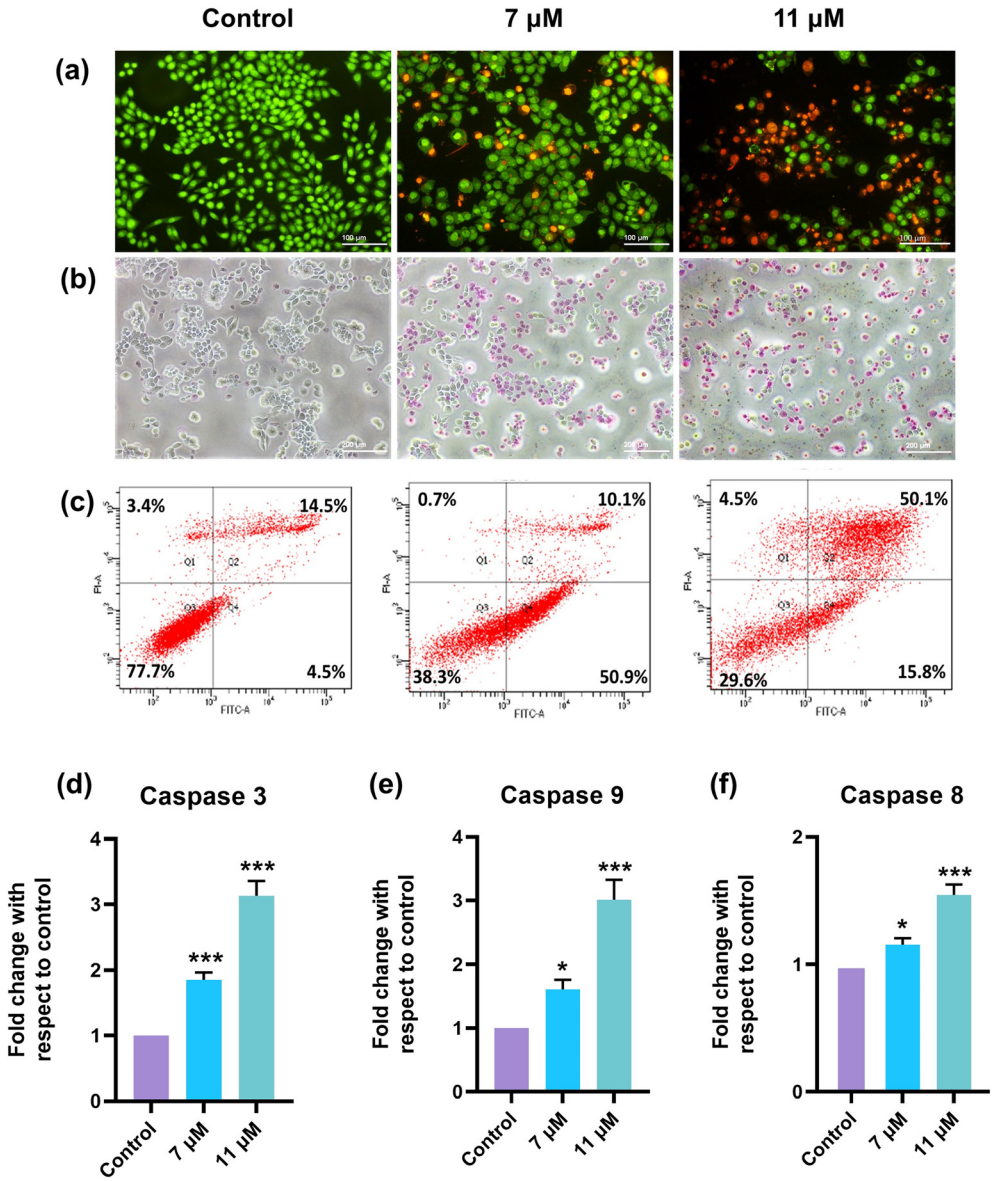

Fig. 3 Induction of apoptosis in HeLa cells by niloticin analysed in different concentrations of 7 and 11 μM by a) Acidine orange ethidium bromide dual staining method, b) APOP assay, c) annexin V apoptosis assay by FACS, and c) caspase expression analysis by fluorometric method. Major caspases, such as d) caspase-3, e) caspase-9 and f) caspase-8, involved in apoptotic pathways were checked and it was observed that all 3 caspases show a fold increase in its fluorescence intensity with respect to control. Results are represented as mean ± SD, $*p < 0.05$, $**p < 0.01$, $***p < 0.001$ compared to the control.

cells, *i.e.*, niloticin-treated cells were stained pink, with the intensity of the color increasing at higher concentrations. Meanwhile, control cells remained unstained, as observed under the microscope (Fig. 3b). The exposure of phosphatidylserine enhances the identification of apoptotic cells, and annexin V exhibits specific binding to this phospholipid, distinguishing apoptotic cells within a cellular population. This property is leveraged to confirm the apoptotic potential of niloticin in HeLa cells using the annexin V apoptosis assay. The quantification of cells labeled with annexin V-FITC and PI found in various quadrants (Q1, Q2, Q3, Q4) in the data obtained serves as a comprehensive indicator of cells at various phases. FITC and PI negative live cells are found in Q3, with a decrease from 77.7% in control to 38.3% and 29.6% in 7 and 11 μM niloticin treatment, respectively. The lowest cell population in Q1 of the treated cells (0.7% and 4.5%) indicates that the cells have undergone necrotic cell death. In Q4, 50.9% of annexin V-labelled cells were found in the 7 μM treatment group, indicating an early apoptotic stage and a noteworthy increase in the percentage of annexin V-FITC and PI-positive cells in Q3, rising from 14.5% in the control group to 49.2% in the niloticin-treated cells, effectively indicates that the cells are in the late apoptotic stage. This shift is evident in the flow cytometry data, highlighting the impact of niloticin on apoptosis, as shown in Fig. 3c.

Investigation of caspase-mediated apoptosis

Programmed cell death is largely orchestrated by the involvement of caspases, a distinct family of cysteine proteases. These caspases typically exist as inactive zymogens, undergoing a cascade of catalytic activation during apoptosis.[36] To assess the activation profile of caspases, a fluorescence-based assay was employed, where the intensity of fluorescence indicates the expression of different caspases. The apoptotic pathway may follow the extrinsic or intrinsic pathway, and can be differentiated by examining the expression of various initiator caspases. In this study, we investigated the activation of caspase 3, an executioner caspase crucial for both the extrinsic and intrinsic modes of the apoptotic pathway. The cells were thus treated with niloticin (7 and 11 μM). Compared to the control, we observed a threefold increase in the expression of caspase 3, confirming the induction of apoptosis (Fig. 3d). We also examined the activation of the caspases associated with the initiation of apoptosis induced by niloticin. For that, we looked at the expression of caspase 8 and caspase 9, which are significant factors of the extrinsic and intrinsic pathways. Interestingly, the expression of both caspase 8 and caspase 9 was found to be increased, confirming that niloticin acts through both extrinsic and intrinsic pathways of apoptosis (Fig. 3e and f). From reviewing the literature, it is observed that certain natural compounds falling within the terpenoids category (nimbolide in MCF-7 breast cancer cells, hyperforin in glioblastoma, and carnosic acid in PC-3 prostate carcinoma cells) exhibit similar patterns of execution for both apoptotic pathways.[37–39]

Evaluation of apoptosis by nuclear condensation and DNA fragmentation using fluorometric and SERS analysis

A hallmark of apoptotic events is DNA condensation, whereas the nuclei of unaffected cells retain a spherical shape with evenly distributed DNA. This feature can be utilized to illustrate the apoptotic potential of a compound using DNA-binding dyes. In this context, Hoechst 33342 staining is employed, which permeates both live and apoptotic cells, and selectively binds to adenine–thymine-rich regions of DNA in the minor groove.[40] Fluorescence can be observed in both normal and condensed DNA, but with a higher intensity in the condensed DNA. Fragmentation can also be effectively detected. In our experiment, niloticin-treated (7 μM and 11 μM) HeLa cells were stained with Hoescht 33342, and analyzed using fluorescent light microscopy. The images revealed a higher number of cells with condensed nucleic acids at varying concentrations, confirming apoptosis, while the DNA in healthy cells retains its spherical shape (Fig. 4a). During the apoptotic process, the cytogenic damage is characterized by DNA fragmentation. Endonucleases cleave the DNA into

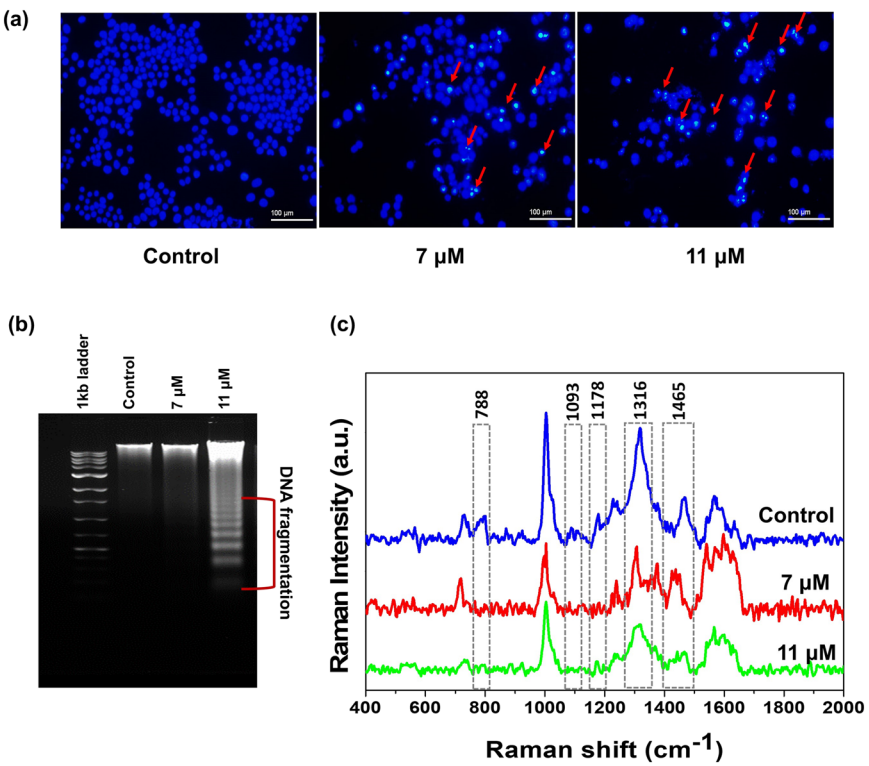

Fig. 4 Nucleic acid condensation in HeLa cells upon treatment with niloticin is proved by a) Hoescht staining method, where the condensed DNA will give an intense coloration compared to the untreated DNA, b) analysing the DNA laddering pattern in both control and treated cells, in which exonucleases act on niloticin-treated cells, giving a laddering pattern analysed by agarose gel electrophoresis, and c) SERS analysis of the DNA laddering.

internucleosomal fragments, which are indeed considered specific markers of apoptosis.[41] This fragmentation pattern can be visualized through DNA laddering using agarose gel electrophoresis. Niloticin in 7 and 11 μM doses were used to treat HeLa cells. DNA isolation was performed for both control and treated cells, which was further subjected to agarose gel electrophoresis (0.8%). The fragmented DNA was visualized as stained nucleic acids using ethidium bromide (Fig. 4b). The results exhibit a distinct laddering pattern in higher concentrations of niloticin-treated cells compared to control cells, demonstrating the strong apoptotic potential of the molecule. For further confirmation of the DNA fragmentation induced by niloticin treatment, surface-enhanced Raman spectroscopic (SERS) analysis of the DNA samples from the control cells and treated cells was conducted using the 633 nm laser of a confocal Raman microscope and colloidal gold nanoparticles (AuNPs: 40–45 nm) as the SERS substrate. The enhanced Raman spectra derived from these samples showed significant differences in the pattern, especially the diminished peaks of the phosphodiester linkage and O–P–O stretching vibrations (785 cm^{-1} and 1093 cm^{-1}). Moreover, the decreased intensity for the peaks of cytosine and guanine and the DNA ring breathing mode (1178 cm^{-1}, 1316 cm^{-1}, respectively) was also evident. As compared to the control, an enhanced peak at 1420 to 1440 cm^{-1} showing CH-deformation and a less intense peak for the deoxyribose vibration (1460–65 cm^{-1}) was also noticed in the DNA isolated from the treated cells (Fig. 4c).[42]

Apoptotic assessment based on cell cycle regulation

Genomic level mutations associated with cancer interfere with normal cell cycle mechanisms, compromising cell division control and resulting in the uncontrolled progression of cells.[43] The effect of the drug should reestablish the cell cycle checkpoint regulation that was mutated or direct it toward apoptosis by halting the cell division. To unveil the mechanistic action of niloticin in HeLa cells, the retardation in the progression of the cell cycle is confirmed *via* cell cycle assay by flow cytometric analysis. The assay uses propidium iodide, a fluorescent nucleic acid dye that can enter the apoptotic cells or those in the last stages of apoptosis. This stains the DNA and gives the exact number of cell populations at different phases of the cell cycle. In the experiment, most of the cells were found in the S and G2 phases in the control. Conversely, upon treatment, the maximum cell population was restricted to the sub-G0 phase. Initially, the sub-G0 population of cells without treatment were 7.6%, which in fact increased to 25.6% at 7 μM and further to 39.5% at 11 μM concentrations of niloticin (Fig. 5a). The data confirm the cell cycle arrest at the sub-G0 phase during the advancement of the cell cycle as the percentage of cells decreased in the G0/G1, S, and G2/M phases by the effect of niloticin. Cdk-2 is a key cell cycle regulator,

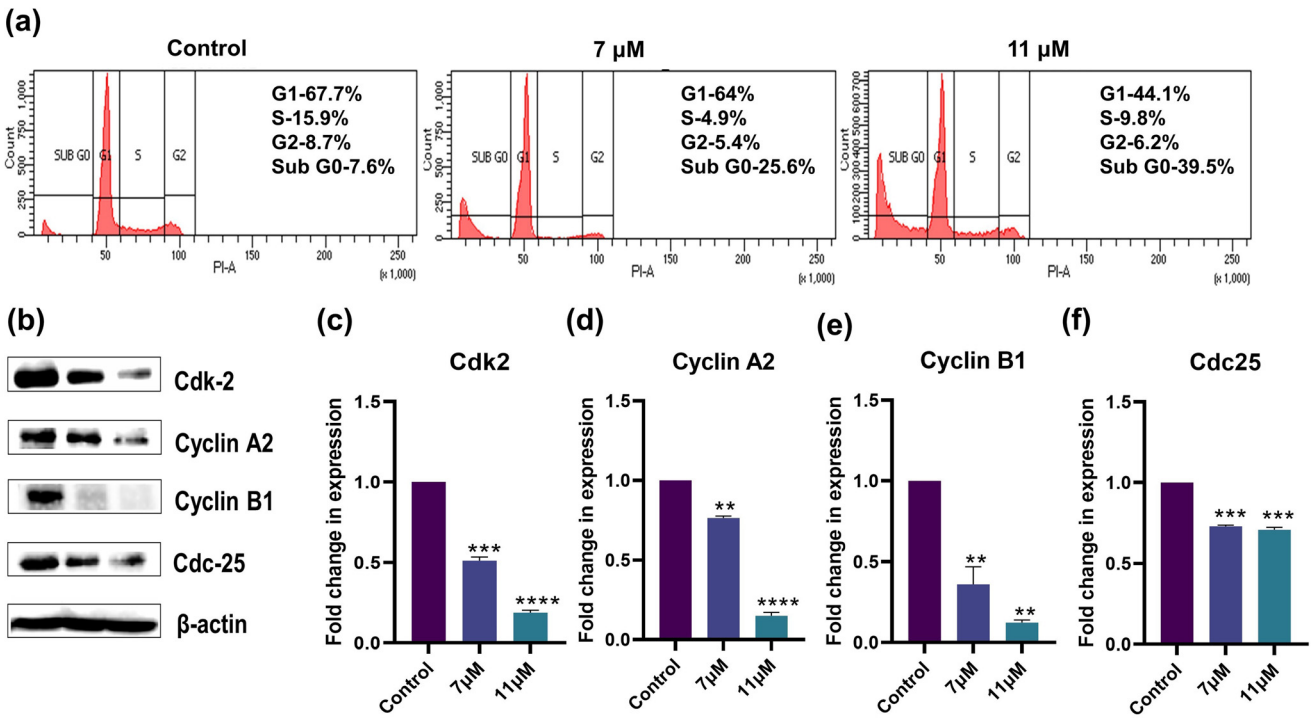

Fig. 5 Cell cycle pattern change analysis and study of the expression change in cell cycle regulatory proteins upon induction by niloticin in HeLa cells by a) Western blot of Cdk-2, cyclin A2, cyclin B1, and cdc-25, some of the major proteins in cell cycle regulation. b) Graph representing the fold change in the expression of Cdk-2, c) cyclin A2, d) cyclin B1, and e) Cdc25 in comparison with β-actin. f) Cell cycle assay using PI staining done by FACS, which confirms the sub-G0 phase arrest with a higher cell population. Results are represented as mean ± SD, $^{**}p < 0.01$, $^{***}p < 0.001$ compared to the control.

which has an important role in G1/S and G2/M transitions.[44] Cyclin A2, essential in the activation of kinases, interacts with Cdk-2 in the G1/S checkpoint. Cyclin B1 aids cells in entering a mitotic phase, where cyclin B1–cdk2 phosphorylates many proteins for cell cycle progression.[45,46] Cdc-25 promotes dephosphorylation in cdks, which is important in the progression of the cell cycle. Western blot analysis of the mentioned cell cycle proteins shows a downregulation in their expression on treatment with the compound, further affirming the cell cycle arrest by niloticin (Fig. 5b–f).

Apoptotic induction through mitochondrial membrane potential

Maintenance of a stable mitochondrial membrane potential is imperative for normal cell functioning. Sustained perturbation in the transmembrane potential eventually causes severe effects on the viability of cells. The dysfunction of the mitochondrial membrane appears to induce apoptosis, where activated caspases specifically target permeabilized mitochondria. This leads to the disturbance of electron transport and the subsequent loss of the mitochondrial transmembrane potential. JC-1 dye is a cationic dye that is lipophilic in nature and can enter mitochondria. It forms J-aggregates that are reversible complexes, exhibiting red fluorescence in cells with a normal transmembrane potential. On the other hand, due to less negativity in apoptotic cells, the JC-1 dye enters at a lower concentration, where aggregates cannot be formed. Thus, the JC-1 dye retains its green fluorescence. Here, to disclose the effect of niloticin in mitochondrial functioning, the cells are induced by the compound for 24 hours. Afterwards, the JC-1 dye is added, which forms aggregates in untreated ones. In contrast, it remains as a monomer in cells where mitochondrial depolarization occurred upon treatment with niloticin (Fig. 6a). Therefore, the data clearly express the increase in green fluorescence resulting from the action of the compound as mitochondrial dysfunction occurs, which substantiates the involvement of the intrinsic (mitochondrial-mediated) mode of apoptosis.

Inhibition of metastatic potential by niloticin

Firstly, the inhibition of clonogenic potential by niloticin in HeLa cells was assessed. The study investigates the capacity of an individual cell to develop into a colony, employing the cell survival assay to assess the reproductive potential of cells for unrestricted division and colony formation.[47] The conventional colony formation assay was conducted to evaluate the suppressive effect of niloticin on the ability to form colonies. Niloticin was introduced to HeLa cells at concentrations of 3 and 6 μM, and the quantification of colonies formed was carried out using ImageJ software. The data demonstrated a noticeable decline in the colony-forming capability of Hela cells in a dose-dependent fashion from a total count of 639 in the control cells to 424 in 3 μM and 397 at 6 μM niloticin induction (Fig. 7a). The ability of the cancer cells to migrate and establish themselves in distant organs, a pivotal step in the process of metastasis, serves as the foundation for this phenomenon. This is typically assessed by examining cell movement by scratch wound assay. The assay operates on the principle that when a wound is intentionally created in a layer of cells, these cells naturally migrate to restore cell-to-cell contact. In the experiment, niloticin was treated at the concentrations of 3 and 6 μM, and then examined for 0, 24, and 48 hours of incubation. The percentage of wound closure is calculated using ImageJ software. The data clearly indicate that the percentage of wound closure is significantly high in the control compared to that in the niloticin-treated cells (Fig. 7c and d).

Immunofluorescence assay of Ki67

The expression of Ki67, a proliferation marker, may be utilized in cancer diagnostics.[48] Here, we determined the anti-metastatic potential of niloticin by evaluating the

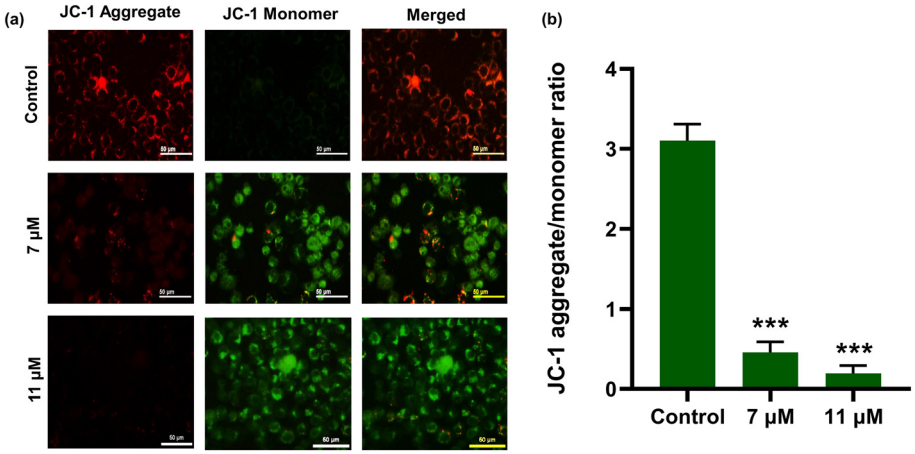

Fig. 6 a) Analysis of the change in the mitochondrial membrane potential is done by JC-1 assay in HeLa cells after induction with Niloticin. b) Graph showing the decrease in the JC-1 aggregate-to-monomer ratio with respect to the control. Results are represented as mean ± SD, ***$p <$ 0.001 is considered to be significant as compared to the control. Scale bar corresponds to 50 μm.

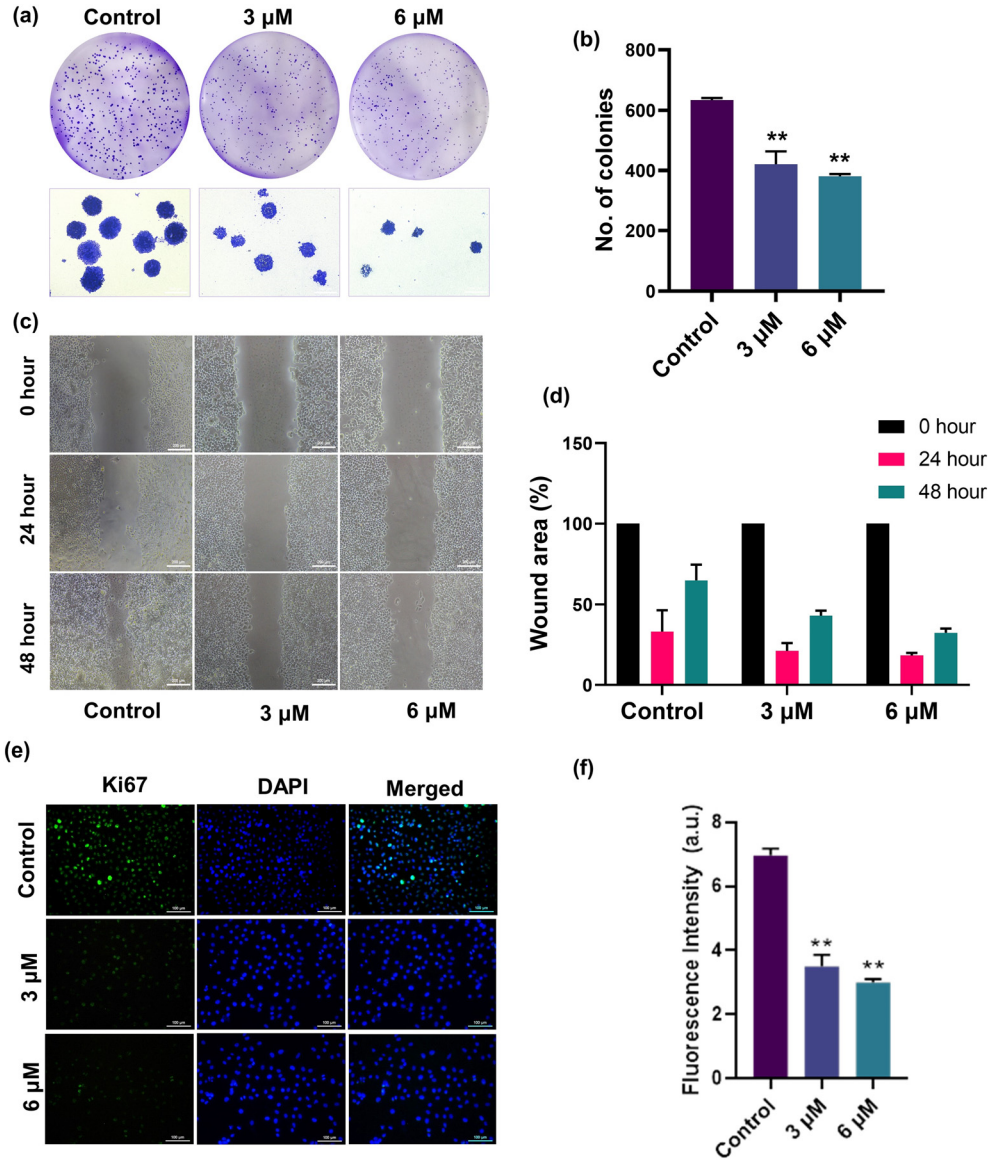

Fig. 7 a) Inhibition of the clonogenic potential of HeLa cells by niloticin treatment at 3 μM and 6 μM. b) Graph showing the decrease in the number of colonies with niloticin treatment compared to the control. c) Inhibition of the migratory potential of HeLa cells by niloticin treatment. d) Graph representing the wound area percentage at different time points. e) Analysis of Ki67 expression in HeLa cells at 3 μM and 6 μM niloticin treatment. f) Graph showing the fluorescence intensity of Ki67 expression of niloticin-treated cells compared to the control. Results are represented as mean ± SD, $^{**}p < 0.01$ as compared to the control.

expression of Ki67 in HeLa cells *via* immunofluorescence assay. Niloticin was treated at two different concentrations, and the DAPI staining was analyzed using a fluorescence microscope. The images clearly showed the downregulated expression of Ki67 in treated cells upon increasing concentration. Meanwhile, a higher expression was observed in the control cells.

Modulation of various protein expressions involved in apoptosis

Elucidation of the underlying mechanism of action of phytomolecule emphasizes the recognition of molecular targets that could be exploited for designing efficient therapeutic entities. The mechanistic route of action of niloticin may follow any of the cell death signaling pathways, which is unraveled by identifying the upregulation and downregulation of key proteins involved in apoptosis. Herein, the expression of a broad range of proteins were analyzed using a human apoptotic array membrane, which encompasses 43 major target proteins (Fig. 8a–c). HSP60 accumulates in the cytosol to induce various signals, conferring its action to either cell death or cell survival mechanisms. In the case of apoptosis, it leads to the maturation and activation of caspase 3.[49] The nuclear transcription factor, p53 is proapoptotic in function. In

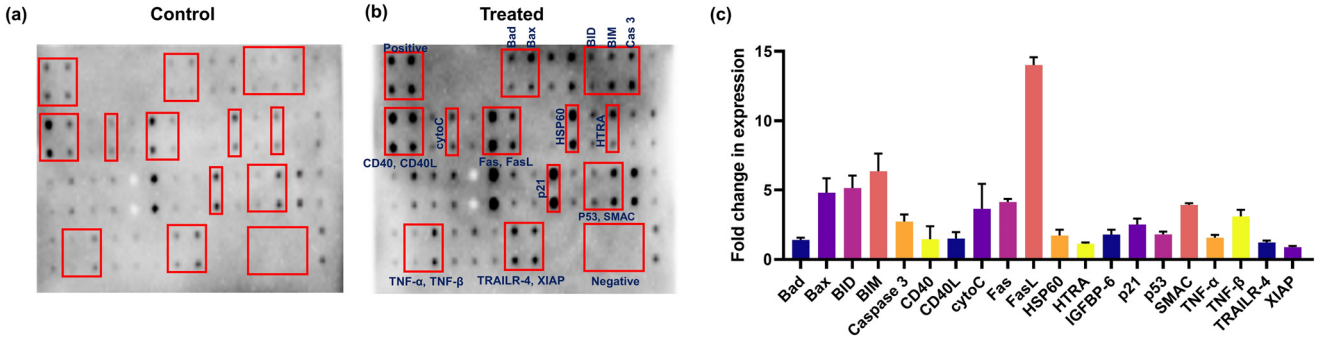

Fig. 8 Apoptotic protein expression study in HeLa cells a) with and b) without treatment were analyzed using an antibody array kit. c) Comparison of the expression change in major proteins in niloticin-treated cells with respect to the control.

response to various stresses, it is induced to exert its proapoptotic properties.[50] CD40 is a TNFR family member. Upon some signals, CD40 can exert a wide range of cellular responses. Here, the induction of niloticin results in the binding of CD40 to its ligand CD40L, which eventually results in the enzymatic maturation of caspase 8 and caspase 3. TNF, a pro-inflammatory cytokine, simultaneously activates cell survival and cell death mechanisms, and is the most potent inducer of apoptosis. By the action of niloticin, TNF is activated by CD40/CD40L, which is the upstream regulatory molecule.[51] The binding of TNF to its TNFR induces apoptosis. Specifically, the extrinsic mode of apoptosis is executed by the death receptor TRAILR and the continued signaling to the activation of caspases for the execution of apoptosis. p53 activation enhances cell cycle arrest, either by facilitating DNA repair or routing it to apoptosis. In the present study, the induction of niloticin effectively increases the expression of p53, which could be considered as the root of a further signaling pathway, as they directly regulate a broad range of target genes. Fas induces apoptosis by the cross-linking of its own receptor, FasL. It is already known that the upregulation of the Fas receptor in stimuli to any cell death signal is p53-dependent. So, the p53 upregulation by niloticin directly induces the binding of Fas to FasL,which could be observed from the intensity of expression. Increased expression of Fas/FasL enables catalytic activation of the initiator caspase-8, which is the key factor in the extrinsic mode of apoptosis. Likewise, activation of p53 also results in Bad/Bax pro-apoptotic protein expression. This further activates Bid, which is a Bcl-2 family member protein that aids in apoptosis in its truncated form, tBid. This activates Smac, a mitochondrial protein released during cellular apoptosis, counteracts inhibitory factors (IAPs), and promotes apoptosis progression. It is already reported that the export of smac to cytosol occurs in response to the induction of cytotoxic drugs. Along with SMAC activation, HTRA (a mitochondrial factor) gets released upon an apoptotic trigger from mitochondria into the cytosol. HTRA then interacts with IAPs, which enables the caspase to be free from its inhibition.[52] Cytochrome c is usually located in the inter-cristae spaces in mitochondria, which gets exported to cytosol when apoptotic signals permeabilize the mitochondrial membrane. In the cytosol, cyt c tends to activate Apaf-1, a requisite for the proteolytic activation of caspase-9, which is the critical initiator of caspase involved in the intrinsic mode of apoptosis. This is well supported by the expression analysis of cytochrome c and caspase 9. The direct p53 activation of caspase-8 and mitochondrial-mediated caspase 9 activation substantiates the concluded mode of extrinsic and intrinsic pathways of niloticin action in HeLa cells. This proteolytic maturation of caspase 8 and 9 finally results in the activation of caspase-3, the executional caspase that finally takes the cell to its demolition phase. p53 also activates p21, a key protein involved in cell cycle regulation that interacts with cyclin–cdk complexes and induces cell cycle arrest in niloticin-treated cells. The expression analysis of apoptotic proteins establishes a signaling pathway of action, and provides strong evidence for niloticin to be developed as a potent anticancer agent (Fig. 9).

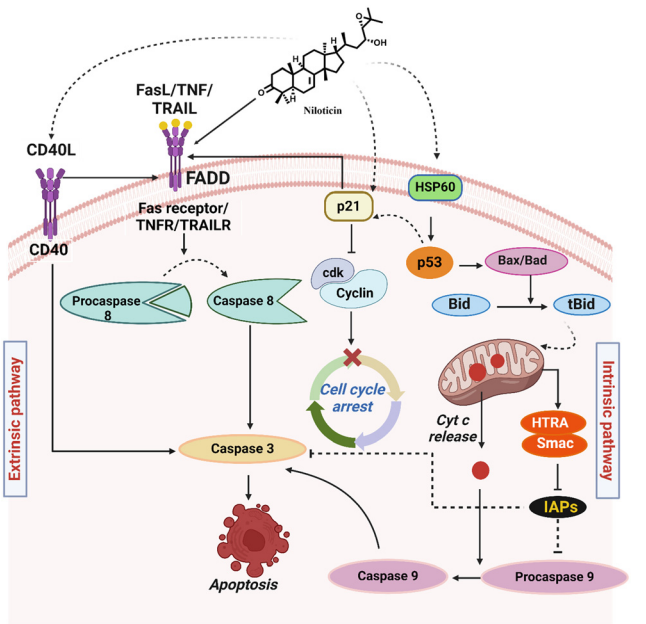

Fig. 9 Proposed mechanism of action of niloticin.

Conclusion

In summary, we have evaluated a detailed anticancer profiling of the tirucallane-type triterpenoid, niloticin, which exhibited the highest anticancer properties among the other four isolated triterpenoids from the stem barks of *Aphanamixis polystachya* against cervical cancer cells. The primary cytotoxicity assessment of niloticin was carried out in various cancer cell lines. The cervical cancer HeLa cells turned out to have an impressive IC_{50} value of 11 μM after 24 hours of treatment, which was adequate for apoptotic induction in HeLa cells. Molecular docking studies with major protein targets (such as TNF, Fas, p53, and caspases) exhibit reasonably high binding affinity with niloticin, as evidenced by docking scores ranging from −6.8 to −9.0 kcal mol^{-1}. The binding stability was further evaluated through molecular dynamic simulation. To complement the *in silico* studies, downstream *in vitro* cell-based assays were employed including annexin V assay by flow cytometric analysis for validating the apoptotic potential of niloticin. In a subsequent apoptotic evaluation, DNA condensation was evident by Hoechst staining and DNA laddering supported the apoptotic potential of niloticin in HeLa cells. The SERS fingerprint analysis in the treated cells enabled the tracking of cellular DNA breakage as a complementary assessment, which was fully complemented by the DNA laddering experiment. The cell cycle analysis indicated the arrest at the sub-G0 phase. The halt in cell cycle progression was determined by the analysis of the proteins involved, which finally takes the cell into apoptosis. Another interesting fact is the involvement of both extrinsic and intrinsic modes of apoptosis induced by niloticin, analyzed by the substantial expression of caspase 3, 9, and 8. The expression of major regulatory proteins involved in the apoptosis cascade is evident in the protein dot-blot assay. Finally, the modulation in the signaling pathways involved in the cancer was studied by analyzing the different proteins involved. The activation of p53 by the induction of niloticin was the key step. p53 induced the binding of FasL to the Fas receptor, resulting in the activation of the initiator caspase 8, a prominent factor of the extrinsic pathway of apoptosis. The activation of p53 also upregulates the expression of proapoptotic proteins Bad/Bax, and further activates Bid, SMAC and HTRA, which results in the export of cytochrome c from the nucleus to cytosol. Cytochrome c then activates Apaf-1, which is a requisite for the activation of caspase 9, the key factor in the intrinsic pathway of apoptosis. Both the extrinsic and intrinsic modes finally conclude in the catalytic activation of caspase-3, taking the cell to its demolition phase. Further evaluation of niloticin in its ability to inhibit colony formation and wound healing property reflected its anti-metastatic potential. Niloticin exerting its effect in the downregulation of the proliferative marker Ki67 by immunofluorescence assay further proves its capability as an anti-metastatic potential agent. We envisaged that the naturally occurring niloticin would become a successful blueprint to generate a potential anticancer hit compound for pre-clinical studies against the efficacious management of cervical cancer.

Materials and methods

General experimental procedures and chemicals

All of the solvents were used without further purification, and were of the highest available grade. Column chromatography was performed with silica gel (100–200 mesh; Merck, Darmstadt, Germany). TLC was carried out on Merck 60 F_{254} silica gel plates, detecting phytomolecules under UV light or by heating after spraying samples with a *p*-anisaldehyde–sulfuric acid mixture. NMR spectra were obtained from a Bruker Avance 500 MHz instrument with $CDCl_3$ and CD_3OD as the solvent, and chemical shifts were expressed in δ (ppm) relative to the TMS. The HR-ESI-MS spectrum was recorded at 60 000 revolutions using a Thermo Scientific Exactive mass spectrometer, and the purity of the tirucallane-type triterpenoids was analyzed by a Waters Arc analytical HPLC instrument.

Plant material collection. The stem barks of *A. polystachya* were collected from Parassala, Kerala (8.34780° N and 77.1410° E), Kerala, India in April 2017. The plant material was deposited at the Department of Botany, University of Kerala, Thiruvananthapuram (voucher number 2018-06-05).

Isolation and characterization of compounds from *A. polystachya*. About 1.0 kg of the dried stem bark was powdered mechanically and subjected to extraction with acetone at room temperature (3 L × 3 days). Following filtration, the extract was concentrated under reduced pressure using a rotary evaporator, resulting in an approximate yield of 20 g for the acetone extract. The acetone extract was subjected to silica gel column chromatographic separation and eluted with a mixture of petroleum ether/ethyl acetate from 100 : 0 v/v to 0 : 100 v/v. Twenty-two fractions (1–22) were obtained. Fractions 5–7 were applied to a silica gel column and eluted with a mixture of petroleum ether/ethyl acetate from 9 : 1 v/v to 4 : 1 v/v, affording compounds 1 (15 mg) and 2 (32 mg). Compounds 3 (10 mg), and 4 (21 mg) were isolated from fractions 8–15 through a silica gel column with petroleum ether/ethyl acetate from 4 : 1 v/v to 7 : 3 v/v. The purification of fractions 16–19 yielded compounds 5 (18 mg) *via* silica gel column with petroleum ether/ethyl acetate from 7 : 3 v/v to 3 : 2 v/v. The structures of the phytochemicals were analysed through 1D and 2D NMR, HR-ESI-MS analysis, and comparison with the literature report. The purity of the compounds was checked by a Waters Arc analytical HPLC instrument, and the chromatograms are shown in the ESI† (Fig. S9, S18 and S40).

Cell culture methods. HeLa (human cervical cancer) cell line and the triple-negative human breast cancer cell line MDA-MB-231 were purchased from American Type Culture Collection (ATCC, USA). The A549 (human non-small cell lung) cancer cell line and the human pancreatic cell line PANC-1 were procured from National Centre for Cell Science (NCCS, Pune). The MCF-10A, (normal breast epithelial) cell

line was obtained from Elabscience, USA. The HeLa, A549, PANC-1, and MDA-MB-231 cells were maintained in Dulbecco's modified Eagle medium (DMEM, sigma) with a supplement of 10% fetal bovine serum (FBS, himedia), 1% antibiotic antimycotic solution (Himedia). MCF-10A cells were grown in mammary epithelial cell growth medium (MEGM, Lonza) with 5% horse serum, and all the cells were maintained in 5% CO_2 at 37 °C culture conditions.

Cell proliferation assay. A seeding density of 8×10^3 cells per 100 μL of DMEM media was added to 96-well plates for 24 and 48 hour proliferation studies. Niloticin at different concentrations (5 μM, 10 μM, 20 μM, 50 μM, 100 μM) were added to the plates after 24 hours of incubation. After 24 and 48 hours of incubation with the compound, 100 μL of MTT (3-[4,5-dimethylthiazole-2-yl]-2,5-diphenyltetrazolium bromide) at a concentration of 0.5 mg mL^{-1} in Hanks balanced salt solution (HBSS) was added to each well after removing the spent medium and washing with PBS, and then incubated at 37 °C for 2–4 hours under dark conditions. Then, the MTT solution was removed, and the sample was again washed with PBS. Finally, 100 μL of DMSO was added to each well for dissolving the formazan crystals. The conversion of the yellow-coloured MTT to a violet color was observed, and the absorbance was measured using a multimode plate reader (Synergy H1, Biotek) at 570 nm.

Molecular simulations. Initial pharmacokinetic parameters of niloticin were assessed using the SwissADME online tool.[53] This tool provides valuable insights into the drug-likeness, human intestinal absorption, and lipophilicity. Molecular docking studies were conducted to elucidate the binding interactions between niloticin and key proteins involved in the apoptotic pathway. AutoDock Vina was employed for the docking simulations, utilizing the crystal structures of selected proteins from RCSB PDB – p53 (1TUP), Fas receptor (3EZQ), FasL (5L19), Bax (6EB6), CDK2 (2UZE), BCL2 (6O0K), and TNF β (1TNR). The docking score was used to screen the interactions.[54] Docking simulations were visualized and analyzed using UCSF Chimera version 1.16.[55] This molecular visualization software facilitated a comprehensive examination of the binding orientations and interactions between niloticin and the target proteins. The stability and dynamic behavior of the seven protein–niloticin complexes were further investigated through molecular dynamics simulations. Desmond, a component of the Schrödinger suite, was employed for these simulations, extending over 100 nanoseconds.[56] The root mean square deviation (RMSD) analysis was carried out to assess the structural stability of the complexes.

Apoptotic assays. The apoptotic potential of the compound was checked by live dead assay using the ethidium bromide-acridine orange dual staining method and APO percentage assay, which distinguishes live cells from those that have undergone apoptosis. The imaging was performed by the Nikon-TS100 inverted microscope. An annexin V apoptosis assay was performed by using the FITC annexin V apoptosis detection kit (BD Pharmingen), following the assay protocol mentioned. Here, the cells were stained with annexin V and propidium iodide, and the number of apoptotic cells can be determined *via* flow cytometric analysis.

Caspase fluorometric assay. The activation of caspases, being a major feature of apoptosis, is studied using the caspase fluorometric assay for caspase 3, 9 and 8. A cell density of 3×10^6 was seeded on 6-well plates, and apoptosis induction was done by treatment of HeLa cells with niloticin at different concentrations. The assay was carried out following the exact protocol given in the fluorometric assay kit (Abcam). The fluorescence intensity was measured using a multimode plate reader (Synergy H1, Biotek) at an excitation wavelength of 400 nm and emission at 505 nm. This was followed for all three caspases.

Nucleic acid degradation and DNA fragmentation studies. DNA condensation was analysed using Hoescht staining. A cell density of 7×10^3 was seeded on 96-well plate. After 24 hours of treatment with the compound, Hoescht stain (1 μg mL^{-1}) in PBS was added and imaging was performed under a DAPI filter of the Nikon-TS100 inverted microscope. Cells that had undergone apoptosis followed a laddering pattern while running in agarose gel. DNA isolation was done in HeLa cells after treatment with the compound for different concentrations using the Geneaid genomic DNA mini kit (Geneaid, cat. no. GB100), following the given protocol. The concentration of isolated DNA was analysed using the nanodrop method, and it was further normalised. The DNA was run in 0.8% agarose at 80 V and imaging was done using Chemidoc (Biorad). The DNA fragmentation pattern was then confirmed by Raman analysis. Gold nanoparticles of size 40–45 nm were used as SERS substrate that was mixed with the DNA sample in a 8 : 2 ratio. After 10 minutes of incubation, the SERS spectrum was analysed using the WITec Raman microscope (WITec, Inc., Germany) with 600 g mm^{-1} grating and Peltier CCD detector unit. Nanoparticle-mixed samples were excited with a 633 nm laser having 5 mW power. Spectral analysis was performed with a resolution of 3 cm^{-1} and 3 spectral accumulations with 5 s integration time.

Cell cycle analysis. The cell cycle arrest by the niloticin induction effect was studied using a cell cycle assay *via* flow cytometric analysis with the BD cycle test plus DNA kit (BD Pharmingen, cat. no. 340242). It uses propidium iodide staining, which can enter apoptotic cells and stain DNA, giving the cell population at different cell cycle phases *via* flow cytometric analysis. The expression of proteins involved in cell cycle regulation was studied using western blotting with the standard procedure. The protein isolation from HeLa cells in both treated and non-treated cells was done, and protein quantification was performed using the BCA assay kit (Pierce BCA Assay Kit cat no. 23225). The normalised SDS-PAGE was performed for the separation of proteins in the sample, followed by the transfer to the PVDF membrane. Blocking with 5% skim milk was performed, and membranes were incubated with respective primary antibodies (Cell Signaling Technology, USA) for 18 hours at 4

°C. After the secondary antibody (HRP conjugated) incubation, chemiluminescence was detected with (Takara Western BloT Hyper HRP Substrate) for Cdk-2, cyclin A2, cyclin B1 and Cdc-25, along with beta actin as the loading control using the Chemidoc imaging system (Biorad).

Mitochondrial membrane potential analysis. The alteration in the mitochondrial membrane potential was analysed by JC-1 assay using JC-1 (5,5,6,6′-tetrachloro-1,1′,3,3′-tetraethylbenzimi-dazoylcarbocyanine iodide) dye (Sigma Aldrich), which is a cationic dye normally exhibiting green fluorescence. In cells that have undergone apoptosis, this dye will aggregate and gives a red fluorescence, which can be observed *via* imaging using Nikon-TS100 inverted microscope with an FITC filter.

Anti-metastatic studies. The antimetastatic potential of niloticin was checked using the clonogenic assay, where a cell density of 1×10^3 cells was seeded into 6-well plate. Once the cells attained morphology, the niloticin was treated in 3 μM and 6 μM concentrations and incubated for another 9 days at 37 °C, allowing the cells to grow into colonies. After that, the cells were fixed with 70% methanol, followed by 0.3% crystal violet staining for visualization. Subsequently, the cells were washed with PBS. Imaging was done using the Nikon-TS100 inverted microscope and further processing was done using ImageJ software. For the scratch wound assay, cells were seeded into 96-well plates. After 24 hours, when a monolayer of cells was formed, a vertical scratch was made using a 200 μL tip and washed with PBS. The compound was added in two different concentrations, and non-treated cells were taken as control. Cells were then monitored for its movement to heal the wound, and images were taken after a period of 0, 24 and 48 hours incubation using the Nikon-TS100 inverted microscope. The area of wound closure was analysed using ImageJ software.

Immunofluorescence assay of Ki67. The anti-metastatic potential of niloticin was further studied by analysis of the expression of Ki67 *via* immunofluorescence assay. A cell density of 7×10^3 was seeded to a 96-well plate, and niloticin was treated at two different concentrations. After 24 hours of incubation, cells were washed with PBS and fixed by 4% paraformaldehyde for 15–30 min at 37 °C. After that, the cells were treated with 0.1% Triton-X for 10 min. Cells were again washed with PBS and blocking was performed using 5% BSA in PBST for 1 hour. Again, washing with PBST was performed 3 times with 5 minutes interval. Then, the primary antibody for Ki67 was added and incubated overnight. After that, the secondary antibody was added, followed by DAPI staining, and images were visualized and captured using the Nikon-TS100 inverted fluorescent microscope.

Apoptotic protein expression. The expression of proteins that play a central role in apoptosis was determined by the human apoptotic antibody array membrane (Abcam). The experiment was conducted, strictly following the manufacturer's protocol. HeLa cells were seeded and treated with niloticin, followed by protein isolation, as outlined in the given protocol. A final volume of 1.2 ml of sample was used for analysis, as per the instruction. Imaging was done with the help of chemidoc (Biorad). Further analysis and densitometric data were obtained with the help of ImageJ software.

Abbreviations

TNF	Tumor necrosis factor
SERS	Surface-enhanced Raman spectroscopy
CD40	Cluster of differentiation 40
IAPs	Inhibitor of apoptosis proteins
Bax	Bcl-2-associated X protein
Cdk2	Cyclin-dependent kinase 2
MTT	(3-(4,5-Dimethylthiazol-2-yl)-2,5-diphenyl-2*H*-tetrazolium bromide)
FITC	Fluorescein isothiocyanate
FACS	Fluorescence-activated cell sorting
Cdc25	Cell division cycle 25
JC-1	5,5,6,6′-Tetrachloro-1,1′,3,3′-tetraethylbenzimi-dazoylcarbocyanine iodide
HSP60	Heat shock protein 60
TRAILR	TNF-related apoptosis-inducing ligand receptor
Bcl-2	B cell lymphoma-2
Bax	Bcl-2-associated X protein
Bid	Bcl-2 interacting domain
Smac	Second mitochondria-derived activator of caspase
Apaf-1	Apoptotic protease activating factor-1
FBS	Fetal bovine serum
NMR	Nuclear magnetic resonance
HRMS	High-resolution electrospray ionization mass spectrometry
PBS	Phosphate buffer saline
DMSO	Dimethyl sulfoxide
PI	Propidium iodide

Data availability

The data supporting this article have been included as part of the ESI.†

Author contributions

Anuja Gracy Joseph: experimentation, data collection, drafting, editing; Mohanan Biji: experimentation, data collection; Vishnu Priya Murali: experimentation, data collection; Daisy R. Sherin: molecular docking studies; Alisha Valsan: experimentation, drafting; Vimalkumar P. Sukumaran: experimentation; Kokkuvayil Vasu Radhakrishnan: conceptualization, editing; Kaustabh Kumar Maiti: supervision, editing.

Conflicts of interest

The authors declare no competing financial interest.

Acknowledgements

K. K. M. thanks the Council of Scientific and Industrial Research (CSIR), Govt. of India and Indian Council of Medical Research (ICMR), Govt. of India (No. 5/4-5/3/01/DHR/NEURO/2020-NCD-I) & (EM/IG/Dev.Res/2003-0001476) for research funding. AcSIR Ph.D. students A. G. J., V. K. N., M. B. and A. V. acknowledge CSIR for financial assistance through research fellowships. V. P. M. acknowledges the DHR Young Scientist Program (R.12014/22/2021) for funding. We acknowledge Dr. Rakesh K. V. and Dr. Ashalatha S. Nair for the plant material collection.

References

1 C. E. Halim, S. L. Xinjing, L. Fan, J. B. Vitarbo, F. Arfuso, C. H. Tan, A. S. Narula, A. P. Kumar, G. Sethi and K. S. Ahn, *Pharmacol. Res.*, 2019, **147**, 104327.
2 A. H. Rahmani, M. A. Al Zohairy, S. M. Aly and M. A. Khan, *BioMed Res. Int.*, 2014, **2014**, 1–15.
3 B. L. Sailo, K. Banik, S. Girisa, D. Bordoloi, L. Fan, C. E. Halim, H. Wang, A. P. Kumar, D. Zheng, X. Mao, G. Sethi and A. B. Kunnumakkara, *Cancers*, 2019, **11**, 246.
4 K. Banik, A. M. Ranaware, V. Deshpande, S. P. Nalawade, G. Padmavathi, D. Bordoloi, B. L. Sailo, M. K. Shanmugam, L. Fan, F. Arfuso, G. Sethi and A. B. Kunnumakkara, *Pharmacol. Res.*, 2019, **144**, 192–209.
5 M. A. Zaimy, N. Saffarzadeh, A. Mohammadi, H. Pourghadamyari, P. Izadi, A. Sarli, L. K. Moghaddam, S. R. Paschepari, H. Azizi, S. Torkamandi and J. Tavakkoly-Bazzaz, *Cancer Gene Ther.*, 2017, **24**, 233–243.
6 A. Valsan, M. T. Meenu, V. P. Murali, B. Malgija, A. G. Joseph, P. Nisha, K. V. Radhakrishnan and K. K. Maiti, Exploration of Phaeanthine: A Bisbenzylisoquinoline Alkaloid Induces Anticancer Effect in Cervical Cancer Cells Involving Mitochondria-Mediated Apoptosis, *ACS Omega*, 2023, **8**(16), 14799–14813, DOI: **10.1021/acsomega.3c01023**.
7 S. K. L. Ong, M. K. Shanmugam, L. Fan, S. E. Fraser, F. Arfuso, K. S. Ahn, G. Sethi and A. Bishayee, *Cancers*, 2019, **11**, 611.
8 S. Hashem, T. A. Ali, S. Akhtar, S. Nisar, G. Sageena, S. Ali, S. Al-Mannai, L. Therachiyil, R. Mir, I. Elfaki, M. M. Mir, F. Jamal, T. Masoodi, S. Uddin, M. Singh, M. Haris, M. Macha and A. A. Bhat, *Biomed. Pharmacother.*, 2022, **150**, 113054.
9 G. Nuzzo, G. Senese, C. Gallo, F. Albiani, L. Romano, G. D'ippolito, E. Manzo and A. Fontana, *Mar. Drugs*, 2022, **20**, 386.
10 S. I. A. Mohamed, I. Jantan and M. A. Haque, Naturally Occurring Immunomodulators with Antitumor Activity: An Insight on Their Mechanisms of Action, *Int. Immunopharmacol.*, 2017, 291–304, DOI: **10.1016/j.intimp.2017.07.010**.
11 A. V. Krishnaraju, C. V. Rao, T. V. N. Rao, K. N. Reddy and G. Trimurtulu, *Am. J. Infect. Dis.*, 2009, **5**, 60–67.
12 S. K. Sadhu, P. Phattanawasin, M. S. K. Choudhuri, T. Ohtsuki and M. Ishibashi, *J. Nat. Med.*, 2006, **60**, 258–260.
13 A. P. Mishra, S. Saklani, S. Chandra, A. Mathur, L. Milella and P. Tiwari, *World J. Pharm. Pharm. Sci.*, 2014, **3**, 2242–2252.
14 M. S. Hossain, M. Islam, I. Jahan and M. K. Hasan, *Phytomed. Plus*, 2023, **3**, 100448.
15 M. M. Hossain, J. Biva, R. Jahangir, M. Mynol and I. Vhuiyan, Central Nervous System Depressant and Analgesic Activity of Aphanamixis Polystachya (Wall.) Parker Leaf Extract in Mice, *Afr. J. Pharm. Pharmacol.*, 2009, **3**(5), 282–286.
16 J. C. Ganesh and V. A. Venkatesha, *Int. J. Radiat. Biol.*, 2006, **82**, 197–209.
17 H. Xu, Y. Jia, J. Li, X. Huang, L. Jiang, T. Xiang, Y. Xie, X. Yang, T. Liu, Z. Xiang and J. Sheng, *Biomed. Pharmacother.*, 2022, **149**, 112902.
18 G. Chen, C. Liu, M. Zhang, X. Wang and Y. Xu, *Int. J. Immunopathol. Pharmacol.*, 2022, **36**, 039463202211330.
19 A. D. Reegan, A. Stalin, M. G. Paulraj, K. Balakrishna, S. Ignacimuthu and N. A. Al-Dhabi, *Med. Chem. Res.*, 2016, **25**, 1411–1419.
20 A. D. Reegan, M. R. Gandhi, M. G. Paulraj, K. Balakrishna and S. Ignacimuthu, *Acta Trop.*, 2014, **139**, 67–76.
21 Z. L. Hong, J. Xiong, S. B. Wu, J. J. Zhu, J. L. Hong, Y. Zhao, G. Xia and J. F. Hu, *Phytochemistry*, 2013, **86**, 159–167.
22 C. Yan, Y. D. Zhang, X. H. Wang, S. D. Geng, T. Y. Wang, M. Sun, W. Liang, W. Q. Zhang, X. D. Zhang and H. Luo, *Fitoterapia*, 2016, **113**, 132–138.
23 W. Y. Zhao, J. J. Chen, C. X. Zou, Y. Y. Zhang, G. D. Yao, X. B. Wang, X. X. Huang, B. Lin and S. J. Song, *Bioorg. Chem.*, 2019, **84**, 309–318.
24 K. Miyake, Y. Tezuka, S. Awale, F. Li and S. Kadota, *Nat. Prod. Commun.*, 2010, **5**, 1934578X1000500.
25 R. Su, M. Kim, H. Kawaguchi, T. Yamamoto, K. Goto, T. Taga, Y. Miwa, M. Kozuka and S. Takahashi, Triterpenoids from the Fruits of Phellodendron Chinese SCHNEID.: The Stereostructure of Niloticin, *Chem. Pharm. Bull.*, 1990, **38**(6), 1616–1619.
26 X.-N. Wang, C.-Q. Fan, S. Yin, L.-P. Lin, J. Ding and J.-M. Yue, *Cytotoxic Terpenoids from Turraea Pubescens*, 2008.
27 J. D. Mcchesney, J. Dou, R. D. Sindelar, D. K. Goins, L. A. Walker and R. D. Rogers, *Tirucallane-Type Triterpenoids: Nmr and X-Ray Diffraction Analyses of 24-Epi-Piscidinol A and Piscidinol A*, 1997, vol. 27.
28 S. D. Jolad, J. J. Hoffmann, H. K. Schram and J. R. Cole, Constituents of Trichilia Hispida (Meliaceae). 4. Hispidols A and B, Two New Tirucallane Triterpenoids, *J. Org. Chem.*, 1981, **46**, 4085–4088.
29 S. J. Mahdizadeh, M. Thomas and L. A. Eriksson, Reconstruction of the Fas-Based Death-Inducing Signaling Complex (DISC) Using a Protein-Protein Docking Meta-Approach, *J. Chem. Inf. Model.*, 2021, **61**(7), 3543–3558, DOI: **10.1021/acs.jcim.1c00301**.

30 T. K. Khatal and G. U. Chaturbhuj, Computational Analysis of the Binding Site(s) of TNF β-TNFR1 Complex: Implications for Designing Novel Anticancer Agents, *Clin. Cancer Drugs*, 2018, **5**(2), 94–104, DOI: **10.2174/2212697x06666181126111445**.

31 M. A. Dengler, A. Y. Robin, L. Gibson, M. X. Li, J. J. Sandow, S. Iyer, A. I. Webb, D. Westphal, G. Dewson and J. M. Adams, BAX Activation: Mutations Near Its Proposed Non-Canonical BH3 Binding Site Reveal Allosteric Changes Controlling Mitochondrial Association, *Cell Rep.*, 2019, **27**(2), 359–373.e6, DOI: **10.1016/j.celrep.2019.03.040**.

32 A. Tondar, S. Sánchez-Herrero, A. K. Bepari, A. Bahmani, L. Calvet Liñán and D. Hervás-Marín, *Biomolecules*, 2024, **14**, 544.

33 W. Liu, U. Ramagopal, H. Cheng, J. B. Bonanno, R. Toro, R. Bhosle, C. Zhan and S. C. Almo, Crystal Structure of the Complex of Human FasL and Its Decoy Receptor DcR3, *Structure*, 2016, **24**(11), 2016–2023, DOI: **10.1016/j.str.2016.09.009**.

34 A. P. D. Nurhayati, A. Rihandoko, A. Fadlan, S. S. Ghaissani, N. Jadid and E. Setiawan, Anti-Cancer Potency by Induced Apoptosis by Molecular Docking P53, Caspase, Cyclin D1, Cytotoxicity Analysis and Phagocytosis Activity of Trisindoline 1,3 and 4, *Saudi Pharm. J.*, 2022, **30**(9), 1345–1359, DOI: **10.1016/j.jsps.2022.06.012**.

35 L. Guang-Yu, B. Fan and Y. C. Zheng, *Biomed. Environ. Sci.*, 2010, **23**, 371–377.

36 Y. Shi, *Protein Sci.*, 2004, **13**, 1979–1987.

37 P. Elumalai, D. N. Gunadharini, K. Senthilkumar, S. Banudevi, R. Arunkumar, C. S. Benson, G. Sharmila and J. Arunakaran, *Toxicol. Lett.*, 2012, **215**, 131–142.

38 F. Hsu, W. Chen, C. Wu and J. Chung, *Environ. Toxicol.*, 2020, **35**, 1058–1069.

39 S. Kar, S. Palit, W. B. Ball and P. K. Das, *Apoptosis*, 2012, **17**, 735–747.

40 L. C. Crowley, B. J. Marfell and N. J. Waterhouse, *Cold Spring Harb. Protoc.*, 2016, **2016**, prot087205, DOI: **10.1101/pdb.prot087205**.

41 P. Majtnerová and T. Roušar, An Overview of Apoptosis Assays Detecting DNA Fragmentation, *Molecular Biology Reports*, Springer Netherlands, October 1, 2018, pp. 1469–1478, DOI: **10.1007/s11033-018-4258-9**.

42 Z. Movasaghi, S. Rehman and I. U. Rehman, Raman Spectroscopy of Biological Tissues, *Appl. Spectrosc. Rev.*, 2007, 493–541, DOI: **10.1080/05704920701551530**.

43 H. K. Matthews, C. Bertoli and R. A. M. de Bruin, Cell Cycle Control in Cancer, *Nat. Rev. Mol. Cell Biol.*, 2022, 74–88, DOI: **10.1038/s41580-021-00404-3**.

44 K. Bačević, G. Lossaint, T. N. Achour, V. Georget, D. Fisher and V. Dulić, *Sci. Rep.*, 2017, **7**, 13429.

45 A. Loukil, Cyclin A2: At the Crossroads of Cell Cycle and Cell Invasion, *World J. Biol. Chem.*, 2015, **6**(4), 346, DOI: **10.4331/wjbc.v6.i4.346**.

46 B. Strauss, A. Harrison, P. A. Coelho, K. Yata, M. Zernicka-Goetz and J. Pines, *J. Cell Biol.*, 2018, **217**, 179–193.

47 N. A. P. Franken, H. M. Rodermond, J. Stap, J. Haveman and C. van Bree, Clonogenic Assay of Cells in Vitro, *Nat. Protoc.*, 2006, **1**(5), 2315–2319, DOI: **10.1038/nprot.2006.339**.

48 L. T. Li, G. Jiang, Q. Chen and J. N. Zheng, Predic Ki67 Is a Promising Molecular Target in the Diagnosis of Cancer (Review), *Mol. Med. Rep.*, 2015, 1566–1572, DOI: **10.3892/mmr.2014.2914**.

49 D. Chandra, G. Choy and D. G. Tang, *J. Biol. Chem.*, 2007, **282**, 31289–31301.

50 Y. Shen and E. White, *P53-Dependent Apoptosis Pathways*, 2001.

51 J. S. Arya, M. M. Joseph, D. R. Sherin, J. B. Nair, T. K. Manojkumar and K. K. Maiti, Exploring Mitochondria-Mediated Intrinsic Apoptosis by New Phytochemical Entities: An Explicit Observation of Cytochrome c Dynamics on Lung and Melanoma Cancer Cells, *J. Med. Chem.*, 2019, **62**(17), 8311–8329, DOI: **10.1021/acs.jmedchem.9b01098**.

52 G. Van Loo, X. Saelens, M. Van Gurp, M. MacFarlane, S. J. Martin and P. Vandenabeele, *Cell Death Differ.*, 2002, **9**, 1031–1042.

53 A. Daina, O. Michielin and V. Zoete, *Sci. Rep.*, 2017, **7**, 42717.

54 O. Trott and A. J. Olson, AutoDock Vina: Improving the Speed and Accuracy of Docking with a New Scoring Function, Efficient Optimization, and Multithreading, *J. Comput. Chem.*, 2010, **31**(2), 455–461, DOI: **10.1002/jcc.21334**.

55 E. F. Pettersen, T. D. Goddard, C. C. Huang, G. S. Couch, D. M. Greenblatt, E. C. Meng and T. E. Ferrin, UCSF Chimera – A Visualization System for Exploratory Research and Analysis, *J. Comput. Chem.*, 2004, **25**(13), 1605–1612, DOI: **10.1002/jcc.20084**.

56 K. J. Bowers, E. Chow, H. Xu, R. O. Dror, M. P. Eastwood, B. A. Gregersen, J. L. Klepeis, I. Kolossvary, M. A. Moraes, F. D. Sacerdoti and J. K. Salmon, *Proceedings of the 2006 ACM/IEEE Conference on Supercomputing*, Florida, 2006.

